DOCTOR OF PHILOSOPHY

A(1-42) induced metabolic effects in a stem cell derived neuron and astrocyte network.

Marta Tarczyluk

2013

Aston University

Aβ(1-42) induced metabolic effects in a stem cell derived neuron and astrocyte network.

Marta Anna Tarczyluk

Doctor of Philosophy

March 2013

Aston University

Aβ(1-42) induced metabolic effects in a stem cell derived neuron and astrocyte network.

Marta Anna Tarczyluk

Doctor of Philosophy

March 2013

Thesis summary

Alzheimer's Disease (AD) is the most common form of dementia currently affecting more than 35 million people worldwide. Hypometabolism is a major feature of AD and appears decades before cognitive decline and pathological lesions. This has a detrimental impact on the brain which has a high energy demand.

Current models of AD fail to mimic all the features of the disease, which has an impact on the development of new therapies. Human stem cell derived models of the brain have attracted a lot of attention in recent years as a tool to study neurodegenerative diseases.

In this thesis, neurons and astrocytes derived from the human embryonal carcinoma cell line (NT2/D1) were utilised to determine the metabolic coupling between neurons and astrocytes with regards to responses to hypoglycaemia, neuromodulators and increase in neuronal activity.

This model was then used to investigate the effects of Aβ(1-42) on the metabolism of these NT2-derived co-cultures as well as pure astrocytes. Additionally primary cortical mixed neuronal and glial cultures were utilised to compare this model to a widely accepted *in vitro* model used in Alzheimer's disease research.
Co-cultures were found to respond to Aβ(1-42) in similar way to human and *in vivo* models. Hypometabolism was characterised by changes in glucose metabolism, as well as lactate, pyruvate and glycogen. This led to a significant decrease in ATP and the ratio of NAD^+/NADH. These results together with an increase in calcium oscillations and a decrease in GSH/GSSG ratio, suggests Aβ-induces metabolic and oxidative stress. This situation could have detrimental effects in the brain which has a high energy demand, especially in terms of memory formation and antioxidant capacity.

Key words: Alzheimer's Disease, ANLS, astrocytes, hypometabolism, stem cells

Acknowledgements

I would especially like to thank my supervisor Dr. Eric Hill for his time, sharing his passion for science and his friendship that helped make my PhD an amazing journey. His advice and optimism were invaluable. Special thanks to Dr. Dave Nagel and Erin Tse for friendship, advice, and numerous supportive conversations over coffee. Thanks also to Professor Mike Coleman and Dr. Rhein Parri for their help, guidance, and expertise. I also wish to thank my best friend Jono Sheard for his support, advice and listening for hours to complaints about unsuccessful western blots.

I would like to thank my partner Hayden from the bottom of my heart, for his constant love and support. Thank you for your love of food, your understanding and for spontaneous weekends in Wales when things were tough and I needed to see the sea.

I will be forever thankful to my amazing family for their love and inspiration. My brother who listens to me and who like me understands the good and the bad sides of living so far from home; my aunt who always encouraged my passion for biology and research. And above all, I would like to thank my parents for working so hard to support me and for their continual motivation that has allowed me to reach for my dreams. Thank you.

List of contents

List of figures

Abbreviations

Aβ	Amyloid beta
ABAD	Abeta-binding alcohol dehydrogenase
AD	Alzheimer's disease
AFM	Atomic force microscopy
AICD	Amyloid precursor protein intracellular domain
αKGDH	α-ketoglutarate dehydrogenase
AMPA	2-amino-3-(3-hydroxy-5-methyl-isoxazol-4-yl) propanoic acid
ANLS	Astrocyte-neuron lactate shuttle
APLP	Amyloid precursor-like protein
APOE	Apolipoprotein E
APP	Amyloid precursor protein
ATP	Adenosine-5'-triphosphate
BACE1	β-site APP cleaving enzyme-1
BACE1	β-site APP cleaving enzyme-2
CNS	Central nervous system
CSF	Cerebrospinal fluid
CypD	Cyclophilin D
COX	Cytochrome c oxidase

DTNB	5,5'-dithiobis-(2-nitrobenzoic acid)
ETC	Electron transport chain
ER	Endoplasmic reticulum
FAD	Familial Alzheimer's disease
G-6-P	Glucose 6-phosphate
GFAP	Glial fibrillary acidic protein
GLAST	Glutamate–aspartate transporter
GLT-1	Glial glutamate transporter
GLUT	Glucose transporter
GSSG	Glutathione disulfide
GSH	Glutathione
GSK-3	Glycogen synthase kinase 3
hESC	Human embryonic stem cell
HFIP	Hexafluoroisopropanol
IDE	Insulin degrading enzyme
iPSC	Induced pluripotent stem cells
LDH	Lactate dehydrogenase
LOAD	Late-onset Alzheimer's disease
LTP	Long-term potentiation
MCI	Mild cognitive impairement

MCT	Monocarboxylate transporter
mtDNA	Mitochondrial DNA
MPTP	Mitochondrial permeability transition pore
NAD$^+$	Nicotinamide adenine dinucleotide
NADH	Reduced nicotinamide adenine dinucleotide
NADP$^+$	Nicotinamide adenine dinucleotide phosphate
NADPH	Reduced nicotinamide adenine dinucleotide phosphate
NEP	Neprilysin
NFT	Neurofibrillary tangles
NMDA	N-methyl-D-aspartate
PDH	Pyruvate dehydrogenase
PET	Positron emission tomography
PP1	Phosphoprotein phosphatase 1
PS1/2	Presenilin 1/2
ROS	Reactive oxygen species
SDS	Sodium dodecyl sulfate
SSA	Sulfosalicylic acid
TBOA	DL-*threo*-β-Benzyloxyaspartic acid
TCA	Tricarboxylic acid cycle
TGN	Trans-Golgi network

ThT   Thioflavin T

Chapter 1: Introduction

1.1   The overview/prevalence of Alzheimer's Disease

Alzheimer's disease (AD) is a neurodegenerative disease and is the most common form of late-life functional mental deterioration in humans. According to the World Alzheimer's Report currently more than 35 million people live with Alzheimer's disease globally, as well as other types of dementia. These numbers are predicted to double every 20 years, reaching 65.7 million in 2030 and 115.4 million in 2050 (International, 2009).

1.2   Symptoms and pathology

Symptoms of AD include progressive memory loss, impaired cognitive function, decline in language function, changes in behaviour that includes agitation, aggression, paranoia, delusion and apathy (Selkoe, 2001).

These symptoms are associated with the presence of two types of lesions in the brain, neurofibrillary tangles (NFTs) and amyloid (neuritic) plaques. NFTs are composed of tau protein, which are localized within neurons and were discovered in the early investigations of the disease by silver staining. Amyloid plaques are extracellular depositions of fibrillar amyloid-beta (Aβ) and were discovered by the use of Congo Red dye (Puchtler et al., 1962). However, in recent years it has become clear that amyloid plaques and neurofibrillary tangles are only 'tombstones' marking the site of neuronal death (Selkoe, 2001).

Alzheimer's disease, unlike other neurodegenerative diseases such as Parkinson's disease, does not affect a single transmitter class and is highly heterogeneous (Selkoe, 2001). Some studies suggest that Aβ deposition drives tau aggregation

17

(Gotz et al., 2001). The accumulation of both tau and Aβ results in oxidative stress and inflammation which in turn cause energetic failure and synaptic dysfunction (Querfurth and LaFerla, 2010). Furthermore, increased oxidative stress, impaired protein-folding, together with a deficiency in clearance of damaged proteins, combine to increase the accumulation of amyloid and tau proteins (Hoozemans et al., 2009, López Salon et al., 2000).

1.2.1 Neuritic plaques

Neuritic plaques or amyloid plaques are one of the two pathologic lesions found in postmortem brains of Alzheimer's patients and are composed of fibrillar Aβ (Glenner and Wong, 1984).

Amyloid plaques are associated with dystrophic neurites which are found within the plaque and around it. Dystrophic neurites are characterized by the presence of enlarged lysosomes, multiple mitochondria and paired helical filaments (Selkoe, 2001). Plaques are also surrounded by other types of cells such as astrocytes and microglia. Both types of cells express markers characteristic for their activation i.e. CD45 and HLA-DR for microglia and a dramatic increase in glial fibrillary acidic protein (GFAP) for astrocytes. Microglia are usually found close to the amyloid core while astrocytes often surround the plaque, with some of the processes extending towards the core of the plaque (Nagele et al., 2004). The length of time it takes to accumulate Aβ(1-42) and form plaques in AD brains is unknown, but they are thought to form gradually over months or years (Nagele et al., 2004).

The neuritic plaques are mainly composed of A(β1-42) which is a slightly longer and more hydrophobic and therefore prone to aggregation (Snyder et al., 1994). The size

of the plaque varies widely from 10 to 120 μm in diameter (Selkoe, 2001). Aβ and its aggregation will be further discussed in chapter 2.

1.2.2 Neurofibrillary tangles

Neurofibrillary tangles (NFTs), the intracellular aggregates that occur in AD and other neurodegenerative diseases termed tauopathies, are formed by paired helical filaments (PHFs) (Kurt et al., 1997). The major component of PHFs was identified in the 1980's as the microtubule-associated protein tau (Grundke-Iqbal et al., 1986). Normally tau is a soluble and abundant protein in axons and is involved in stabilization of microtubules and vesicle transport. However, in Alzheimer's Disease, tau is hyperphosphorylated which makes the protein insoluble and prone to self-association (Grundke-Iqbal et al., 1986). Additionally, hyperphosphorylation of tau leads to a decrease in the binding of tau to microtubules. The degree of tau phosphorylation depends on the balance between the activities of protein kinases and phosphatases. The abnormal tau hyperphosphorylation seen in AD could be cause by either an upregulation of tau kinases or a downregulation of tau phosphatases. Tau kinases include glycogen synthase kinase-3 (GSK-3), mitogen activated protein kinase (MAPK), cyclin-dependent kinase 5 (CDK5), protein kinase C (PKC), Jun N-terminal kinases or calcium/calmodulin-dependent protein kinase (CaMKII). Tau phosphatases include protein phosphatase-1 (PP-1), protein phosphatase-2 (PP-2) and protein phosphatase-5 (PP-5) (Huang and Jiang, 2009). It is unclear whether there is an association between Aβ and hyperphosphorylated tau. However, there is a growing body of evidence that Aβ can interact with tau and accelerate formation of NFTs as well as induce its hyperphosphorylation. Aβ has been shown to induce activation of both GSK-3 isosymes. As GSK-3β is one of the tau kinases, thus its activation can lead to hypephosphorylation of tau (Kremer et al., 2011).

However, it has also been found that tau deficiency prevents Aβ-induced cognitive defects (Shipton et al., 2011). In addition, tau appears to be necessary for amyloid to disrupt axonal transport *in vitro* (Vossel et al., 2010). However, the relationship between Aβ and tau in onset and progression of Alzheimer's Disease requires further investigation.

1.3   APP processing

The 37-43 amino acid amyloid-beta (Aβ) peptide is derived from Amyloid Precursor Protein (APP) by sequential proteolytic cleavage in a physiologically normal pathway (Shoji et al., 1992, Haass et al., 1993a). APP comprises a heterogeneous group of type I membrane glycoproteins which are ubiquitously expressed. This heterogeneous group arises from alternative splicing, yielding three major isoforms of 695, 751 and 770 residues. These isoforms are also post-translationally modified to include N- and O-linked glycosylation, phosphorylation, sulphation and complex proteolysis (Weidemann et al., 1989, Hung and Selkoe, 1994). Isoforms of 751 and 770 residues are widely expressed in non-neuronal cells as well as neurons. However, neuronal cells express higher levels of the 695 amino acids isoform which are expressed at a low level in non-neuronal cells (Haass et al., 1991). The 751 and 770 isoforms contain an additional exon which codes for 56-amino acid motif homologous to the Kunitz-type serine protease inhibitors (KPI). Isoforms such as 751/770 are found in human platelets and can act as inhibitors of factor XIa which is a serine protease in the coagulation pathway (Smith et al., 1990). APP is highly conserved and found in all mammals and is a member of a larger gene family, the amyloid precursor-like proteins (APLPs) (Slunt et al., 1994).

APP is a membrane protein with an amino terminus orientated to the lumen/extracellular space and its carboxyl terminus within the cytosol (Dyrks et al.,

1988). APP has been shown to be initially targeted into the secretory pathway; however, it is processed proteolytically at other sites within the cell (Weidemann et al., 1989). APP can be processed by three proteases called α-, β- and γ-secretases (Haass, 2004) during two processing pathways: the amyloidogenic pathway and the non-amyloidogenic pathway (Fig. 1.1). Non-amyloidogenic processing of APP involves γ-secretase and α-secretase which cleaves approximately in the middle of the Aβ sequence thus abolishing its production (Nunan and Small, 2000). This cleavage generates the truncated carboxy-terminal fragment (C83), which lacks the amino-terminal region of Aβ. Subsequent processing within a membrane by γ-secretase produces a peptide called p3 (Haass et al., 1993b) as well as APP intracellular domain (AICD) (Gu et al., 2001) which is released into the cytosol. AICD has been found to have a function in nuclear signaling (von Rotz et al., 2004) (Fig. 1.1).

Aβ is generated via the amyloidogenic pathway by the consecutive action of β- and γ-secretases (Haass, 2004) (Fig. 1.1). The main β-secretase in the human brain is β-site APP cleaving enzyme (BACE) 1, which cleaves full length APP at Asp1 of the amyloid beta sequence (Nunan and Small, 2000). The cleavage of APP by BACE1 leads to shedding of the APP ectodomain (sAPPβ) and generation of a C-terminus fragment, C99 which is sequentially cleaved by γ- secretase. The latter cleavage occurs within the hydrophobic environment of cell membranes. The γ- secretase cleavage of C99 fragment results in the formation of the Amyloid Precursor Protein Intracellular Domain (AICD) fragment and two Aβ variants, either 40 or 42 amino acids in length (Cole and Vassar, 2007). These are released to extracellular fluids such as plasma or cerebrospinal fluid (CSF) (Seubert et al., 1992) (Fig. 1.1).

21

Aston University

Illustration removed for copyright restrictions

Figure 1.1   APP processing via non-amyloidogenic and amyloidogenic pathway. Diagram reproduced from Debby Van Dam & Peter Paul De Deyn (2006)

1.3.1   β-secretase

Following its identification, β-secretase was given several different names including memapsin, aspartyl protease 2 or BACE1 (β-site APP cleaving enzyme-1) (Vassar et al., 1999). BACE1 is a membrane-bound aspartyl protease which has its active site in the lumen/extracellular space (Hong et al., 2000). In addition to BACE1, a homologous protease, BACE2 has been identified (Cole and Vassar, 2007). BACE2 does not play a role in the amyloidogenic pathway and has been shown to have an anti-amylodogenic activity in non-neuronal cells (Farzan et al., 2000).

BACE1 is ubiquitously expressed, with the highest levels found in the brain and pancreas. BACE1 mRNA levels are highest in neurons but this enzyme is also found at lower levels in glia (Cole and Vassar, 2007). The physiological function of BACE1 is not well understood. High expression of BACE1 postnatally (Willem et al., 2006) has been found to be related to myelination (a process which occurs after birth). It has been shown that BACE1 knockout mice demonstrate a significant hypomyelination (Willem et al., 2006). Other physiological roles of BACE1 such as regulation of voltage-dependent sodium channels are currently under investigation (Kim et al., 2007).

BACE1 is translocated into the endoplasmic reticulum (ER) as an immature pro-enzyme. During maturation it undergoes post-translational modifications which include N-glycosylation and palmitoylation (Capell et al., 2000). Once the pro-peptide is removed from the immature BACE1, it reaches the PM and is enriched in lipid rafts (Riddell et al., 2001). BACE1 is then internalized and is recycled to trans-Golgi network (TGN) via endosomes (Walter et al., 2001). As an aspartyl protease, BACE1 has an acidic pH optimum and has optimal activity at about 4.5. This limits localization of BACE1 activity to acidic compartments of the secretory pathway (Cole

23

and Vassar, 2007). Additionally, BACE1 can cleave APP within late Golgi compartments (Haass et al., 2012).

1.3.2   γ-secretase

γ-secretase mediated cleavage of APP occurs within the transmembrane domain (TMD). γ-secretase is a protease complex and consists of four core components – endoproteolyzed presenilin (a heterodimer of N- and C-terminal fragments), nicastrin (NCT), anterior pharynx defective (APH)-1α or APH-1β and the PS enhancer (PEN)-2. PS1 and PS2 contain two critical aspartyl residues which form a catalytic subunit of γ-secretase (Wolfe et al., 1999).

 All four of these components are necessary for full γ-secretase activity (Edbauer et al., 2003) however, little is known about NCT, APH-1 and PEN-2 function. NCT is thought to act as a substrate-binding receptor of γ-secretase (Shah et al., 2005) and PEN-2 is involved in PS endoproteolysis and stabilization (Prokop et al., 2004). Very little is currently known about APH-1 function.

The processing of APP by γ-secretase involves multiple steps. It has been shown that γ-secretase substrates are cleaved several times within their transmembrane domains. Cleavages at ε-, ζ-, and γ-sites have been described (Sastre et al., 2001, Weidemann et al., 2002). Additionally, the final γ-cleavage can occur at different sites, between 37 and 43 amino acids of the Aβ sequence. This produces Aβ proteins that differ in length and are more prone to aggregation and toxicity such as Aβ(1-42) (Haass and Selkoe, 2007).

γ-Secretase has been found to cleave APP at the plasma membrane (PM) as well as in endosomal/lysosomal system (Pasternak et al., 2004, Kaether et al., 2006).

However, it has been shown the ε-cleavage differs in endosomes and PM (Fukumori et al., 2006), possibly due to different pH or lipid composition. Due to the complex morphology of neurons, little is known about subcellular site of γ-secretase processing (Haass et al., 2012). γ-secretase is present in synapses and distal axons (Frykman et al., 2010) but the precise site of processing by both β-, and γ-secretases has yet to be determined.

1.3.3 α-secretase

Anti-amyloidogenic processing of Aβ involves cleavage by proteases called α-secretases. This enzyme cleaves within Aβ domain, between Lys16 and Leu17 residues (Wang et al., 1991). This cleavage produces large APP amino-terminal domain (sAPPα) and C83. α-secretases are plasma membrane (PM)-bound proteases (Sisodia, 1992) and include several zinc metalloproteinases such as ADAM9, ADAM10, TACE/ADAM17 and ADAM19 (Allinson et al., 2003). However, studies suggest that in neurons the main α-seretase is ADAM10 (Kuhn et al., 2010) and its expression has been found throughout the cortex and hippocampus (Marcinkiewicz and Seidah, 2000). Other substrates for α-secretase include Notch receptors, tumor necrosis factor α, cadherins and IL-6 receptor. Due to the wide variety of α-secretase substrates cleavage is considered to be sequence independent and depends upon the proteins α-helical conformation as well as the distance of the hydrolyzed bond from the membrane (Sisodia, 1992).

In neurons the predominant pathway for processing of APP appears to be the amyloidogenic pathway due to higher expression of BACE1, whilst in other cells the non-amyloidogenic pathway dominates (Haass et al., 2012). However, neuronal overexpression of ADAM10 reduces amyloidogenic processing of APP and Aβ production (Postina et al., 2004).

APP processing via amyloidogenic or anti-amyloidogenic pathways can be modulated by activation of receptors such as serotonin/5-hydroxytrypamine (5-HT4) receptor, metabotropic glutamate receptors as well as muscarinic acetylocholine receptors (Allinson et al., 2003). Signalling downstream of these receptors regulates sAPPα and Aβ secretion via intermediates that include protein kinase C, inositol 1,4,5-triphosphate and cytosolic calcium (Allinson et al., 2003).

1.4   Biosynthesis and trafficking

APP undergoes post-translational modifications during its transit from the ER to PM. However, only a small number of APP molecules reach the PM (~10%), whilst the majority localizes to the Golgi apparatus and trans-Golgi network (TGN) (Haass et al., 2012). Once APP reaches the PM it can be processed by α- and γ-secretases. APP that is not cleaved immediately, is internalized as it contains "YENPTY" internalization motif near its carboxy-terminal region (Lai et al., 1995). Once internalized, APP is delivered to endosomes (Haass et al., 2012).

It has been shown that in non-neuronal polarized cells APP is targeted to the basolateral side of the cell (Haass et al., 1994). Secretases are also differentially sorted, with BACE1 being targeted to the apical surface (Capell et al., 2002) and ADAM10 being targeted basolaterally (Wild-Bode et al., 2006). γ-secretase has been found on both apical and basolateral surfaces (Capell et al., 2002). This suggests that Aβ generation is markedly reduced in polarized cells (Capell et al., 2002). However, it has been found that the Swedish mutation that occurs just before BACE1 cleavage site (Fig. 1.2) affects the sorting of APP. The Swedish mutant version of APP when expressed in the polarized MDCK cell line was sorted to the apical surface, increasing both sAPPβ and Aβ generation (De Strooper et al., 1995).

Neuronal cells are highly polarized into soma, axons and dendrites and each of these compartments has different physiological functions (Haass et al., 2012). A complex system of microtubules, kinesin and dynein motor proteins and sorting signals ensures a highly controlled delivery of specific proteins to different compartments in neurons (Haass et al., 2012) and disturbances in this system has been previously linked to AD (Morfini et al., 2009).

Polarized trafficking of APP in neurons is poorly understood. In the soma the trafficking of APP appears to be similar as in nonneuronal cells. APP is transported from ER to Golgi and then to the TGN. However, once APP leaves the TGN it is then transported to axons and dendrites in post-Golgi transport vesicles (Kins et al., 2006). This delivery relies upon the use of the fast axonal transport system (Koo et al., 1990). In contrast to non-neuronal cells, in neurons the basolateral sorting signal in APP sequence appear to have no known function.

1.5   Genetics of familial Alzheimer's Disease

Investigation into the inherited forms of AD has provided insights into the processes and genes associated with this disease. AD is inherited in the autosomal dominant fashion and accounts for about 5-10% of all AD cases (Selkoe, 2001). However, it is believed that the majority of sporadic AD patients have genetic determinants which could predispose them to the disease as opposed to directly causing it. Very often these two forms of AD are indistinguishable from each other, except for the earlier onset of the diseases in the familial AD. Presently, inherited alterations in four genes have been credibly linked to increases in the production and/or the cerebral deposition of the Aβ peptides - APP, PS1, PS2 and ApoE (Selkoe, 2001).

Families carrying missense mutations in the APP gene generally have an early onset of the disease before the age of 65. Some missense mutations in APP affect cleavage sites and are located either immediately before the β-secretase site, or just after the α-secretase or γ-secretase cleavage sites (Fig. 1.2). Mutations at the amino terminus of the Aβ region that affect the β-secretase site (such as the Swedish mutation) increase the production of Aβ(1-42) and Aβ(1-40) by favoring cleavage by β-secretase as opposed to α-secretase (Citron et al., 1992). Mutations affecting the γ-secretase site (located just beyond the carboxyl terminus of Aβ) such as Austrian, Iranian, London or Florida mutations selectively enhance the production of Aβ species ending at residue 42 which aggregate more rapidly (Selkoe, 2001). Mutations such as Arctic (Nilsberth et al., 2001) or Dutch (Levy et al., 1990) which are found in mid region (Fig. 1.2), affect the sequence of Aβ and were found to change its structure, and thus increase its aggregation (Haass et al., 2012).

Missense mutations in the presenilin genes are the most common cause of familial AD. They cause the earliest and most aggressive forms of AD with early symptoms showing at the age of 50 and death of patients in their 60s. Presently 75 missense mutations have been identified in the presenilin1 gene which is located on chromosome 14, while only 3 in presenilin-2 gene on chromosome 1 (Selkoe, 2001). Mutations in the presenilins leads to a 1.5 – 3-fold increase in the number of plaques compared to sporadic cases of AD (Lemere et al., 1996).

e4 allele of apolipoprotein E (ApoE4) was discovered in human cerebrospinal fluid as a protein that binds immobilized Aβ peptides. The inheritance of one or two e4 alleles of ApoE increases the probability of developing AD and results in an earlier mean age of onset than in subjects carrying e2 and or e3 alleles (Corder et al., 1993). The mechanism by which ApoE4 interacts with Aβ is not known. It is possible that this

isoform somehow enhances the deposition of Aβ or affects its clearance leading to increased numbers of plaques in the brain (Castellano et al., 2011).

1.6   Risk factors for late onset Alzheimer's Disease and treatments

The primary risk factor for Alzheimer's disease and most forms of dementia is advanced age. After the age of 65 the prevalence of disease doubles every five years (International, 2009).

Late-onset Alzheimer's disease (LOAD) is also associated with genetic factors. One of the biggest genetic factors discovered is the ApoE4, where one allele results in a 2.5-fold increase in risk, whilst two alleles cause a 16-fold increase.

Results from four large genome-wide association studies (GWAS) have discovered nine novel loci associated with the late-onset form of the disease. These include clusterin (CLU), phosphatidylinositol-binding clathrin assembly protein (PICALM), complement receptor 1 (CR1), bridging integrator 1 (BIN1), ATP-binding cassette transporter (ABCA7), membrane-spanning 4-domains subfamily A (MS4A cluster), CD2-associated protein (CD2AP), sialic acid-binding immunoglobulin-like lectin (CD33) and ephrin receptor A1 (EPHA1) (Harold et al., 2009, Lambert et al., 2009, Seshadri et al., 2010, Naj et al., 2011, Hollingworth et al., 2012). These ten genes have been found to be associated with three biological pathways, which include; immune system function (CLU, CR1, ABCA7, MS4A cluster, CD33, EPHA1), cholesterol metabolism (APOE, CLU, ABCA7) and synaptic dysfunction and cell membrane processes (PICALM, BIN1, CD33, CD2AP, EPHA1) (Morgan, 2011).

Aston University

Illustration removed for copyright restrictions

Figure 1.2 Representative APP mutations. Reproduced from Debby Van Dam & Peter Paul De Deyn (2006)

In addition to genetic factors, some epidemiological studies also suggest that environmental factors such as education or head injury may also be involved in the onset of Alzheimer's Disease (International, 2009).

No treatments are currently available that could cure, or slow down or prevent the progressive course of dementia. Treatments available are at best partially effective, as they can only ameliorate the symptoms of the disease to some extent (International, 2009). The scarcity of effective treatments could be due in part to lack of realistic or relevant models of the disease which translate into a limited understanding of the cellular processes that are at the root of the early stages of the disease.

1.7   Mitoenergetics and oxidative stress in Alzheimer's Disease

Decreased brain metabolism is a feature of AD that is present before the onset of clinical symptoms and cognitive decline. Emerging evidence from studies on mitochondrial function, demonstrate changes in activities of enzymes involved in oxidative phosphorylation and TCA cycle in AD. In addition, mutations in mtDNA and changes in morphology of mitochondria may be responsible for the apparent hypometabolism and oxidative stress that is seen in the brains of AD individuals.

1.7.1   Mitochondria

Mitochondria are essential in many cellular processes, which include energy metabolism, oxidation of fatty acids, calcium homeostasis, apoptosis and cell signalling (Anandatheerthavarada and Devi, 2007). As neurons have a high-energy demand, mitochondria are crucial for their functioning, especially at the synapses. Synapses are enriched with mitochondria and by producing ATP and sustaining

31

calcium homeostasis play an important role in neurotransmission (Anandatheerthavarada and Devi, 2007).

1.7.2 Intracellular Aβ

Many studies have focused on the intracellular Aβ and have revealed that the majority of intracellular Aβ is the 1-42 form (Gouras et al., 2000), which is mainly produced within membranes such as the plasma membrane (Kaether et al., 2006), the secretory pathway (Khvotchev and Sudhof, 2004) or endosomal compartments (Pasternak et al., 2004). However, due to the orientation of APP and the secretases involved in its cleavage it has been difficult to explain the presence of Aβ in the cytosol. Some studies have shown that Aβ integrates into lipid membranes (Arispe et al., 1993) which can lead to a loss of membrane integrity in endosomal compartments and the subsequent leakage of Aβ into the cytosol (Yang et al., 1998).

1.7.3 Mitochondria in AD

In early AD, Aβ induces oxidative stress which is associated with mitochondrial dysfunction (Manczak et al., 2006). Both APP and Aβ have been found within mitochondrial membranes where they can block transport of nuclear-encoded proteins. Aβ has also been shown to affect the electron-transport chain (ETC) but it also binds to mitochondrial proteins ultimately causing an increase in ROS production and mitochondrial damage (Reddy and Beal, 2008). It has been suggested that mitochondrial dysfunction, low ATP production and oxidative damage at the synapses leads to cognitive decline in AD patients (Reddy and Beal, 2008).

1.7.4 Aβ and APP inside mitochondrial membranes and matrix

Mitochondria require a large number of proteins for physiological functioning and unlike other organelles, contain their own genome. Mitochondrial DNA (mtDNA) only codes for 13 polypeptides which are a part of the ETC (Anandatheerthavarada and Devi, 2007). Hence, mitochondria depend upon proteins encoded by the nuclear genome. It has been shown that about 1500 nuclear-encoded polypeptides are transported into mitochondria under normal, physiological conditions (Gabaldon and Huynen, 2004). This transport is tightly regulated and in most cases requires functional outer and inner-membrane import channels (Anandatheerthavarada and Devi, 2007).

An important feature of the proteins that are targeted to mitochondria, is that they need to be in an unfolded conformation for the translocation to occur. Translocation of proteins to inner membrane and matrix also requires ATP and functional mitochondrial membrane potential (Anandatheerthavarada and Devi, 2007).

Many studies have shown the presence of APP and Aβ within mitochondrial membranes (Anandatheerthavarada et al., 2003, Devi et al., 2006, Manczak et al., 2006). Anandatheerthavarada *et al.* (2003) used *in vitro* mitochondrial-import and *in vivo* neuronal-expression studies to first demonstrate that both endogenous and ectopically expressed wild-type and Swedish APP695 localize to the plasma membrane and mitochondria of human HCN-1A neurons. Additionally, it was shown that the mitochondrial APP is orientated so that the NH_2-terminal faces inside the mitochondria while COOH-terminal faces the cytosol and that APP is in contact with mitochondrial inner and outer translocase proteins. In the same study, the authors demonstrated that the acidic domain (sequence 220–290 of APP) causes transmembrane arrest with the 73-kD portion of COOH-terminal facing the

cytoplasmic side. Subsequent studies have confirmed this orientation of mitochondrial APP (Park et al., 2006).

A study on human brain tissue has also shown a significant increase in full-length and C-terminal truncated (lacking Aβ domain) APP accumulation in the mitochondria of AD patients in comparison with aged-matched controls (Devi et al., 2006). Similarly Aβ has also been found inside mitochondria in neuronal cultures (Manczak et al., 2006), transgenic mice (Caspersen et al., 2005, Manczak et al., 2006) and human AD brains (Lustbader et al., 2004).

APP arrest across mitochondrial import channels leads to inhibition of the transport of nuclear-encoded cytochrome *c* oxidase subunits IV and Vb. These findings were associated with a decrease in cytochrome *c* oxidase activity as well as increased levels of H_2O_2. (Devi et al., 2006). These results were also in line with previous *in vitro* studies on HCN neuronal cells, where accumulation of APP695 in mitochondria was linked to a decrease in mitochondrial membrane potential, ATP levels and mitochondrial cytochrome *c* oxidase activity.

It is still unclear whether Aβ accumulates inside the mitochondrial matrix or exclusively in the membrane compartments (Muirhead et al., 2010). Walls *et al.* (2012) have shown that Aβ may be associated with the matrix as it co-localized with matrix chaperone Hsp60. Aβ has also been found to interact with other mitochondrial matrix proteins such as Abeta-binding alcohol dehydrogenase (ABAD) which suggest its localization in the matrix (Lustbader et al., 2004). However, Aβ has not been detected in the mitochondrial matrix on its own. One of the possible explanations could be the presence of mitochondrial proteinases which could degrade Aβ such as PreP or IDE (Qiu et al., 1998, Falkevall et al., 2006). Other studies also found that in

rats, mitochondrial Aβ is transported via the translocase of the outer membrane (TOM) and localizes in the mitochondrial cristae (Hansson Petersen et al., 2008).

It is also not understood whether Aβ is produced locally in mitochondria or imported from the cytosol. At present evidence supports both possibilities (for review see (Muirhead et al., 2010) and requires further investigation.

To summarize, mutant APP and/or Aβ can enter mitochondria and interact with mitochondrial proteins, disrupt ETC, increase ROS production and inhibit generation of ATP (Reddy and Beal, 2008).

1.7.5 Aβ interactions with mitochondrial proteins

The most well characterized protein interacting with Aβ in mitochondria is Abeta-binding alcohol dehydrogenase (ABAD). This protein has been previously found in ER and mitochondria and is expressed in all tissue types (Yan et al., 1997). ABAD is an enzyme which catalyzes reduction of aldehydes and ketones as well as the oxidation of alcohols and has a wide range of diverse substrates (Muirhead et al., 2010). In mitochondria, it is believed to have a function in energy production and homeostasis, particularly during the third step of beta-oxidation of fatty acids (He et al., 1998). This makes ABAD important during glucose deficiency, where there is a need for other energy sources (Du Yan et al., 2000). ABAD was also found to protect against neurodegeneration in mouse models of ischaemic stress (Du Yan et al., 2000) or from the loss of dopaminergic neurons in mice treated with MPTP (Tieu et al., 2004).

Both Aβ(1-42) and Aβ(1-40) have been found to interact with ABAD (Lustbader et al., 2004) and inhibit its activity (Yan et al., 1999) and it has been demonstrated that the residues 13-22 of Aβ are critical for this inhibition (Oppermann et al., 1999). Inhibition

of ABAD requires micromolar concentrations of Aβ even though binding occurs at nanomolar concentrations (Yan et al., 1997). This suggests that aggregation of Aβ might be an important aspect of inhibition. However, the cytotoxic effects of Aβ are not simply a result of ABAD inhibition. Overexpression of ABAD in its inactive form in the presence of Aβ did not increase its toxicity in comparison to Aβ alone (Yan et al., 1999). This suggests a downstream effect mediated by the active enzyme, which is bound to Aβ (Yan et al., 1999). This hypothesis has been supported by studies on overexpression of ABAD and Aβ, which resulted in increased DNA fragmentation and apoptosis (Yan et al., 1997, Yan et al., 1999) as well as increased levels of hydrogen peroxide, decreased mitochondrial function, decreased glucose utilization and ATP production and ultimately cell death (Takuma et al., 2005). In addition, inhibition of ABAD-Aβ binding has also been found to protect against mitochondrial dysfunction and improve spatial memory (Yao et al., 2011).

A second protein that binds to Aβ in mitochondria is cyclophilin D (CypD). It is a peptidylprolyl isomerase F that is found in mitochondria where it can translocate to the inner mitochondrial membrane during opening of the mPTP (mitochondrial permeability transition pore) during oxidative stress (Connern and Halestrap, 1994). mPTP has been shown to play a central role in both necrotic and apoptotic cell death (Leung and Halestrap, 2008) and some studies have demonstrated that CypD deficiency protects against Ca^{2+} and oxidative stress induced cell death (Schinzel et al., 2005).

CypD has been found to bind Aβ with Aβ(1-42) with greater affinity than Aβ(1-40) and increased levels of CypD have been reported in AD brains (Du et al., 2008). The interaction of Aβ and CypD leads to an increase in ROS production, which in turn induces translocation of CypD to the inner mitochondrial membrane and mPTP opening and cell death (Du et al., 2008). CypD deficiency in AD transgenic mice

protects against Aβ and oxidative stress-induced death and improves learning and memory (Du et al., 2008).

1.7.6   Mitochondrial bioenergetics in AD

There is increasing evidence suggesting that mitochondrial bioenergetics and brain metabolism affect processing of APP (Gabuzda et al., 1994, Gasparini et al., 1997). One of the functions of mitochondria is the oxidation of reduced NADH to NAD^+. This process is important in other bioenergetics pathways such as glycolysis which require NAD^+ (Selfridge et al., 2013). NADH is produced during glycolysis, the TCA cycle and other reactions is oxidized by complex I through electron donation. Additionally, the malate-aspartate shuttle transfers NAD^+ reducing agents into mitochondria. A number of studies have demonstrated that during mitochondrial dysfunction the ratio of NAD^+/NADH decreases (Braidy et al., 2011, Stefanatos and Sanz, 2011).

NAD^+ is utilized or plays an important role in the activation of many enzymes including sirtuins. The role of sirtuins in neuroprotection and longevity has been intensively studied and they have been considered as a therapeutic targets in AD (Lombard et al., 2011, Zhang et al., 2011). Sirtuin 1 has been found to have a role in APP processing. It upregulates expression of ADAM10, which encodes α-secretase, and co-activates the retinoic acid receptor β (RARβ), which is a regulator of ADAM10 transcription (Donmez et al., 2010). It has also been shown that in AD mice overexpressing SIRT1 there is a reduction in amyloid plaque and Aβ(1-42) burden as well as increased levels of α-secretase . On the other hand deletion of SIRT1 results in increased mortality at 3-5 months of age. It has been concluded that by decreasing the NAD^+/NADH ratio and reducing the amount of NAD^+ available to sirtuin 1,

mitochondrial dysfunction could lead to decreased levels of α-secretase and allow β-secretase cleavage and production of Aβ(1-42) (Selfridge et al., 2013).

The electron transport chain (ETC) is located in the inner mitochondrial membrane and is made up of five complexes (I-V). These complexes consist of multiple subunits and all contain subunits encoded by nuclear and mtDNA, with the exception of complex II which is only encoded in the nuclear genome (Tomitsuka et al., 2003). All five complexes show impairment in AD patients (Mao and Reddy, 2011). Parker *et al.* (1990) demonstrated a reduction in the activity of in cytochrome *c* oxidase (COX, complex IV) in platelets from AD patients, which was later confirmed in AD brains (Kish et al., 1992). Since then, COX activity has been shown to be systematically reduced in AD (Curti et al., 1997, Wong-Riley et al., 1997, Bosetti et al., 2002). However, it is still unclear whether a decrease in COX activity is a result of a genetic mutation or toxic insults such as Aβ (Selfridge et al., 2013).

Cytochrome *c* oxidase has 13 subunits, 10 of which are encoded in the nuclear genome and 3 by mtDNA. Swerdlow *et al.* (1997) used a cybrid approach to investigate the mtDNA effect. They isolated platelets from AD patients and controls and fused them with human NT2 cells, which were initially depleted of their endogenous mtDNA. This study revealed a decrease in the activity of COX and mitochondrial membrane potential, as well as an increase in free radicals and oxidative stress and activation of apoptosis pathways. Since then other studies using cybrid lines with mitochondria from AD patients have shown similar results (Khan et al., 2000, Cardoso et al., 2004).

COX inhibition has been shown to reduce non-amyloidogenic APP processing (Gabuzda et al., 1994, Gasparini et al., 1997) by preventing α-secretase cleavage and allowing β-secretase action. Free radicals have been found to further activate β-

secretase. However, results from studies on transgenic AD mice expressing mutant APP and presenilin 1, but lacking COX in neurons, have shown significantly fewer amyloid plaques, reduction in Aβ(1-42) levels and reduced oxidative stress (Fukui et al., 2007). This suggests that COX impairment may not be responsible for Aβ accumulation in AD brain.

Interestingly, a study on APOE4 carriers demonstrated lower COX activity which was low even in the absence of fibrillar Aβ suggesting that either a reduction in COX activity appears early in the disease or that mtDNA contributes to it.

The changes in metabolism associated with Alzheimer's Disease are discussed in further detail in section 4.1

1.7.7 Ageing and mitochondria

Ageing is considered the primary risk factor for AD. Mitochondria have long been thought to contribute to ageing via the accumulation of mutations in mtDNA and an increased production of ROS (Lin and Beal, 2006).

Ageing phenotypes have been linked to mtDNA changes and tissues from aged individuals have been shown to have lower respiratory function (Kujoth et al., 2006). An increase in the number of point mutations and deletions has also been found in cells from aged individuals and evidence has shown that 8-hydroxy-2-deoxyguanosine (damaged DNA) is also increased (Kujoth et al., 2006). It has been suggested that mutations in mtDNA that are involved in ageing phenotypes could also contribute to AD (Reddy and Beal, 2008).

Age related changes in mitochondria include a decline in ETC function. The activity of complex I and IV decreases whilst complex II is preserved (Navarro and Boveris, 2007). In addition, mitochondrial mass also appears to be affected (Barrientos et al., 1997) and oxidative stress markers such as protein carbonylation, lipid oxidation and mtDNA oxidation increase (Boveris and Navarro, 2008). Oxidation of mtDNA makes it very susceptible to mutation as oxidized bases can be misread during replication (Ozawa, 1997). Oxidative stress could be a major contributor to the high mutation rate of mtDNA which is 10 times the rate of that observed in nuclear DNA (Mecocci et al., 1993).

Mitochondrial function and dynamics change with advancing age. These changes affect bioenergetics and metabolism which in turn increase Aβ production and thus contribute to the development of AD.

1.7.8 mtDNA in AD

Studies on ageing and mitochondrial function have led to the mitochondrial cascade hypothesis of sporadic Alzheimer's Disease (Swerdlow and Khan, 2004). It proposes that a person's genes determine mitochondrial function and durability, which in turn determine how mitochondrial functions change with age and as a result initiate AD (Swerdlow and Khan, 2004). As this hypothesis is based on inheritance of mutations, the possibility that maternally inherited mtDNA may influence AD has been investigated. However, the results are not conclusive. Some studies have shown that there is no evidence of maternally-inherited AD risk factor or that it is in fact paternally-inherited (Ehrenkrantz et al., 1999). Whereas other studies however have demonstrated a strong link between maternal inheritance and AD risk (Edland et al., 1996). One particular study investigating COX activity in subjects with an AD-affected mother, found a 30% decrease in COX activity in comparison to patients with an AD-

affected father or no history of the disease (Mosconi et al., 2011). Unfortunately, these studies cannot directly prove that mtDNA is a risk factor, although they indicate that it should be further investigated (Selfridge et al., 2013).

1.7.9 Oxidative stress in AD

The brain is especially sensitive to oxidative damage due to its high lipid content and high oxygen metabolism as well as low antioxidant defences (Floyd, 1999). Oxidative damage has been found to occur early in AD before Aβ depositions and plaque pathology appear (Nunomura et al., 2001). Several studies have demonstrated oxidized RNA, nuclear and mtDNA, lipids and proteins in brains of AD patients (Mecocci et al., 1994, Sayre et al., 1997, Nunomura et al., 1999). The mechanisms underlying the increase in ROS production have been extensively studied and are explained in more detail in section 4.1. Oxidative stress was also shown to increase the expression of β-secretase and in turn production of Aβ(1-42) by activation of c-Jun N-terminal kinase (JNK) and p38 mitogen-activated protein kinase (MAPK) (Tamagno et al., 2005) as well as increase tau phosphorylation through activation of glycogen synthase kinase 3 (GSK-3) (Lovell et al., 2004). Further investigations have shown that activation of JNK leads to upregulation of APP, BACE1 and presenilin 1 through demethylation of their promoters and histone deacetylation (Guo et al., 2011).

1.8 Animal models of AD

Alzheimer's disease is unique to humans. However, it is very difficult to study the disease in patients as we do not understand how or when the disease starts. To overcome this, a wide range of animal models of the condition has been developed and used to study its mechanisms and progression and to develop treatments. Such

models of AD can be broadly split into three types: natural, genetic and interventional models (Laurijssens et al., 2012).

Natural models include polar bears, dogs, cats, goats, sheep and some of the non-human primates such as mouse lemurs or rhesus monkeys. These animals spontaneously develop some of the pathology related to AD (Van Dam and De Deyn, 2011). For example, dogs have recently been used as AD model due to the similarity in canine and human brain ageing. An additional advantage, is the fact that the Aβ sequence is conserved between dogs and humans (Johnstone et al., 1991). Dogs have been shown to develop Aβ and diffusible plaque depositions and the extent of the Aβ depositions correlates with cognitive impairment (Laurijssens et al., 2012).

Progress in the understanding of the genetic factors that contribute or cause AD have resulted in many attempts to develop animal models that overexpress genes, which are involved in the familial forms of AD. Transgenic (tg) mouse models are widely used to study AD and remain the model of choice for numerous studies (Duff and Suleman, 2004). Mice have been extensively used as transgenic models and have had an important influence on our understanding of mechanisms involved in Aβ production, deposition and clearance. Rodent models have been of a great value for studying the disease and mice are relatively easy and cheap to maintain, have short life spans and are easy to manipulate genetically. However, their life span makes the relevance of the model to diseases of ageing questionable.

In addition, the development of human AD may not be faithfully reflected in the mouse models as mice overexpressing APP were found to develop plaques if the level of APP is 8-fold over the normal APP level. In comparison, humans with only a 50 per cent increase in APP (individuals with Down syndrome that have three copies

of APP gene) have a very rapid progression of the disease (Duff and Suleman, 2004).

Due to the complexity of the disease it has been difficult to create an ideal mouse model which mimics all aspect of the pathology of the human disease. Mouse models fail to convincingly demonstrate the neuropathological hallmarks of AD (Dodart et al., 2002a). Mutant animals either develop plaques (APP or PS mice mutants) but no tangles, whereas tau mutants show the presence of tangles but no plaques. Several laboratories have created double APP/PS tg mice which showed accelerated neuropathology but still have not demonstrated the multiple characteristics of AD (Duff and Suleman, 2004). A triple transgenic mouse (APP/PS/Tau) was created by Oddo *et al.* (2003). This model develops extracellular plaques as well as neurofibrillary tangles and demonstrates impaired synaptic plasticity. This model has been successfully used in studies on inflammation, oxidative stress and mitochondrial function in AD (Laurijssens et al., 2012). Nevertheless the progressive loss of neurons in hippocampus and specific cortical regions is not present in many of the transgenic models, which is a major limitation of these models.

Another genetic model often used in studies of AD is *Drosophila melongaster.* This fruit-fly has a well organised brain and despite the differences in anatomical organisation to human brain, it has a similar basic cell biology (Sang and Jackson, 2005). However a major limitation is that hippocampal functions that are impaired early in the AD cannot be studied in invertebrates.

Interventional animal models are based on the introduction of substances into the brain or the induction of lesions in specific brain regions (Laurijssens et al., 2012). These models involve introduction of Aβ peptide into the brain of e.g. rat (Nakamura

et al., 2001) or rhesus monkey (Li et al., 2010). However, despite the fact that some of the clinical symptoms can be induced in animals, these models lack resemblance to AD pathology (Duyckaerts et al., 2008).

1.9   *In vitro* models of AD

In addition to difficulties in modelling the changes described above in patients as well as *in vivo*, *in vitro* models often lack the complexity to efficiently recapitulate the interactions between brain cells during disease. Such models should at minimum be human and be able to produce both neurons and astrocytes individually as well as in co-culture. Both cell types should be functional, demonstrating activities such as action potential firing as well as responses to both neurotransmitters and gliotransmitters and should demonstrate the metabolic coupling that is hypothesised to occur in the brain.

Currently many *in vitro* cell culture systems are used for research and these include primary cultures of dissociated or reaggregated neurons and glia, clonal cell culture lines and stem cells.

1.9.1   Transformed cells

Transformed cells are continuous cell lines which are derived from neuroblastomas, gliomas and pheochromocytomas. Transformed cell lines usually have a life span of about 50 divisions, however some have been immortalized. The major advantages of transformed cells include their homogeneity and the ease with which they are grown and maintained in the laboratory. However, as these cells are derived from neoplastic tissue, they are abnormal and as such their similarity to *in vivo* phenotypes is questionable (Harry et al., 1998).

A number of transformed cells have previously been used to model AD. Such lines include neuronal (SH-SY5Y), astrocytic (U-373) and monocytic (THP-1) cells. A number of studies have utilised these cells to investigate the effect of Aβ on co-cultures of either neuronal SH-SY5Y cells or astrocytic U373 as well as monocytic THP-1 (Klegeris and McGeer, 2001, Messmer and Reynolds, 2005).

Other studies have combined the use of primary cell cultures and transformed cells such as human microglia isolated from temporal lobe tissue and the monocytic THP-1 cell line in order to study the influence of cytokines on SH-SY5Y neuroblastoma cells (Klegeris and McGeer, 2005).

Whilst these cells have provided important information about the effects of Aβ these cells are derived from neoplastic tissue and continue to divide in culturetheir similarity to *in vivo* phenotypes is questionable (Harry et al., 1998).

1.9.2   Primary cultures

Primary cultures are derived from dissociation of brain tissue. The plating efficiency and characteristics depend upon many factors including culture environment, type of tissue, and dissociation technique (Harry et al., 1998). One of the major disadvantages of primary culture is the accessibility of the tissue samples. Additionally, as the cells are fully differentiated and post-mitotic, it is not possible to expand them in culture. Additional risks include variability in the state of preservation of the source tissue and the risks of handling, in terms of communicable human neurological diseases, such as Kuru and Creutzfeld-Jakob disease.

The majority of AD research is based on primary cell culture, which is mainly murine in origin, although in some cases human tissue has been used. Cells derived from

45

tissue samples from AD patients are probably the best source of information about the disease. However, such samples are not easy to obtain. In the UK several brain tissue resources (banks) have been established e.g. by the Medical Research Council, the Alzheimer's Society, the Alzheimer's Research UK and Brains for Dementia Research (BDR). Nevertheless there is currently a severe shortage of live brain tissue available for dementia research.

1.10   Stem cell models of AD

Human stem cells possess almost unlimited self-renewal capacity as well as potential to differentiate into any cell type. As such they provide an ideal model for the development of postmitotic cells of CNS. The therapeutic potential of stem cells has been extensively studied. Stem cells represent also a very dynamic system that would be useful for the identification of new molecular targets and the development of novel drugs, which can be tested *in vitro* for safety or to predict or anticipate potential toxicity in humans (Wobus and Boheler, 2005).

Human embryonic stem cells (hESCs) and induced pluripotent stem cells (iPSC) derived from human patients with Alzheimer's Disease or Down Syndrome are currently used to create models for investigation of Alzheimer's Disease (Nikoletopoulou and Tavernarakis, 2012, Wang and Doering, 2012). hESCs have been shown to efficiently differentiate into functional neurons and glia in a similar way to *in vivo* development (Verkhratsky and Butt, 2013, Oberheim et al., 2006). However, the excitement and optimism surrounding hESCs has been steadily decreasing due to a number of ethical issues surrounding their use. However, recent developments in the development of iPS cells overcome any of the ethical issues faced by the use of hESC.

1.10.1 Induced pluripotent stem cells

An important limitation in Alzheimer's Disease research is the availability of live human, patient specific cells. However, the development of iPS cell technology makes it possible to study human CNS neuronal cells, that carry information from patients with specific mutations or disease (Wang and Doering, 2012).

In most cases iPS cells are produced from primary fibroblasts cultured from a skin biopsy. The transduction of the fibroblasts with retroviruses encoding Oct4, Sox2, Klf4 and cMyc converts the cells into a pluripotent state (Takahashi and Yamanaka, 2006). These reprogrammed cell lines appear to divide indefinitely and in theory can be differentiated into any cell type of the body. Thus iPS cells can be a source of patient specific neurons and glia and be used to created models of disease, platforms for drug screening as well as sources for potential cell therapies (Wang and Doering, 2012). As the progress in cell reprogramming is accelerating, different reprogramming approaches are being tested such as DNA integration-free delivery systems as well as different reprogramming factors (Okita et al., 2011).

1.10.1.1 Differentiation

Reliable protocols for differentiation of iPS cells into specific cell types are one of the challenges in the field of stem cells. In terms of modelling AD, the cells of interest include microglia, neurons and astrocytes. As glutamatergic and basal forebrain cholinergic neurons are believed to degenerate early in the disease these cells have been of great interest for scientists seeking to model AD.

iPS cells have been found to readily differentiate into MAP2-positive neurons and GFAP-positive astrocytes. However, the cultures also contain a high percentage of uncharacterized cells (Israel and Goldstein, 2011). Many groups have focused on

differentiating iPS cells into specific neuronal subtypes. Dopaminergic neurons have been derived from iPS cells by a combination of SHH, GSK-3β inhibitor and FGF8 treatments (Xi et al., 2012). In addition, recent studies on motor neurons have shown that functionally mature motor neurons can be differentiated from iPS cells by protocols involving RA and SHH (Karumbayaram et al., 2009). More recently iPS cells have also been directed into cortical fate by dual inhibition of SMAD signalling (Chambers et al., 2009) or RA-based multistep protocol (Shi et al., 2012).

1.10.1.2   Modelling neurodegenerative diseases

Disease-specific iPS cells have been successfully generated from a number of neurodevelopmental disorders including Rett syndrome, Fragile X syndrome, Down syndrome or Angelman syndrome (Wang and Doering, 2012). In addition, iPS cell lines have also been generated from inherited neurodegenerative disorders such as spinal muscle atrophy, amyotrophic lateral sclerosis, Huntington's disease, Parkinson's Disease as well as Alzheimer's disease (Wang and Doering, 2012).

Alzheimer's disease research has focused heavily upon familial AD (FAD) patients. Indeed, iPS cells have been produced from patients with PS1 and PS2 mutations (Yagi et al., 2011). These cells were differentiated into neurons, characterized and were found to produce higher levels of Aβ(1-42). Aβ(1-42) secretion was blocked by a γ-secretase inhibitor which also shows that FAD derived iPS cells can be used as an effective model of AD. Other studies have produced iPS cells from patients with duplication of the APP gene (Israel et al., 2012). Neurons derived from these cell lines demonstrated increased levels of phospho-Tau and active glycogen synthase kinase-3β (aGSK-3β). Treatment of the cells with β-secretase inhibitors reduced the phospho-Tau and aGSK-3β levels. Neurons differentiated from iPS cells with PS1 mutation demonstrated a partial loss of γ-secretase function which resulted in lower

levels of Aβ(1-40) and an increase in the ratio of Aβ(1-42)/Aβ(1-40) ratio (Koch et al., 2012).

iPS cells are a very promising platform for modelling neurodegenerative diseases. However, they also have some limitations. In cases of disease that is caused by known mutations, it is likely that iPS cells derived from these patients will recapitulate the phenotype of the disease. It has been shown that cortical neurons derived from iPS cells taken from Down syndrome patients, demonstrate abnormal processing of APP and secretion of Aβ(1-42) peptide, which forms extracellular and intracellular insoluble aggregates (Oberheim et al., 2009). However, in the case of late-onset disease, patient derived iPS cells may not show typical brain pathology, such as Lewy bodies in PD or amyloid plaques in AD (Dolmetsch and Geschwind, 2011, Ming et al., 2011). Further research in this area may answer important questions as to the environmental/epigenetic impact on progression of the disease in these patients.

1.10.1.3   Drug screening

iPS cells could provide a highly desirable platform for discovery and testing of novel drugs (Wichterle and Przedborski, 2010, Ming et al., 2011, Wang and Doering, 2012). However, to make this technology useful it is very important to validate the phenotypes of iPS cells, as well as the neurons and glia derived from them. Ensuring a uniform population of neurons and glia that will be essential for successful high-throughput drug screening studies (Wang and Doering, 2012).

1.10.1.4   Cell therapy

In addition to their modelling potential, iPS cells could also provide a source of autologous cells for replacement therapies in patients with neurodegenerative

diseases. Studies have already been undertaken in animal models and early results are very promising e.g. improvement of behavioral symptoms in rat models of Parkinson's Disease (Hargus et al., 2010). In addition, transplantation of glial cells for neuroprotection may be possible (Inoue, 2010). In the area of cell therapy there are also other challenges that have to be overcome before iPS cells can be successfully used. The use of oncogenic genes and retroviruses for cell reprogramming could increase the risk of cancer (Ming et al., 2011). However, as mentioned above other reprogramming strategies are under investigation. In addition, the purification of the specific cell type and improved differentiation protocols are also required. However, improved understanding of genetic mutations associated with the neurological disease and technologies to correct them is required before the cells could be used for replacement therapies (Wang and Doering, 2012).

1.10.1.5   Accessibility

A recent paper by Wray *et al.* (2012) presents a readily available resource of fibroblast cell lines with mutations linked to many different neurological disorders. New cell lines are being added to the fibroblast cell bank that has been created at the National Institute for Neurological Disorders and Stroke (NINDS) Repository at the Cornell Insitute for Medical Research. This initiative represents one of many that has been established in the past couple of years and demonstrates how quickly the field of iPS cells is progressing.

1.10.2 NT2/D1 line

One form of stem cell that has not been fully explored in the context of Alzheimer's Disease is the NT2/D1 line. This is a clonally derived embryonal carcinoma (EC) cell line, isolated from Tera-2 cells (Andrews et al., 1984), which after treatment with

retinoic acid can differentiate into several cell types, including neurons (Andrews, 1984).

Further studies have shown that NT2/D1 cells have the ability to differentiate into both neurons (NT2.N cells) and astrocytes (NT2.A) following treatment with retinoic acid and mitotic inhibitors. The presence of mature neurons was previously confirmed by the expression of markers such as Neurofilament (NF) and Microtubule-associated protein 2 (MAP2) (Bani-Yaghoub et al., 1999). NT2.N cells were shown previously to possess TTX-sensitive Na^+ channels (Rendt et al., 1989) and form both glutamatergic excitatory (71%) and GABAergic inhibitory (29%) functional synapses (Hartley et al., 1999). This cell line has been also shown to express APP, BACE and produce Aβ (Satoh and Kuroda, 2000, Wertkin et al., 1993). The presence of NT2A cells was confirmed by Cx43 and GFAP staining (Bani-Yaghoub et al., 1999). Further characterization of astrocytes derived from NT2/D1 cell line detected mRNA encoding glutamate transporters GLT-1/EAAT2 and GLAST/EAAT1 and the functionality of the transporters was confirmed (Sandhu et al., 2002).

A recent report from my laboratory (Hill et al., 2012) has shown that NT2 derived neurons and astrocytes interact in co-culture. Investigation of NT2.A cells has shown that these cells exhibit glial cell type morphology and appropriate functional properties. In particular NT2.A has been found to respond to neuronal activity and exogenous neurotransmitters by calcium elevations and also demonstrate spontaneous calcium oscillations. Additionally, NT2.A cells generated calcium waves, which spread via gap junctions to neighbouring astrocytes in a purinergic dependent manner (Hill et al., 2012).

The NT2/D1 cell line has previously been used to study AD, however most research has focused on pure neuronal cultures (Satoh and Kuroda, 2000, Turner et al., 1996,

Wertkin et al., 1993). As astrocytes have been shown to enhance neuronal survival as well as axonal growth and synaptogenesis, it is essential to include them in studies on neurological diseases. Additionally, increasing numbers of studies have highlighted the important role of astrocytes in the AD (Bushong et al., 2002, Colombo and Reisin, 2004). Thus research in this thesis was focused on co-cultures of neurons and astrocytes in order to better understand the interactions of the cell types in AD. The importance of NT2/D1 derived astrocytes in toxicity screening has previously been evaluated (Woehrling et al., 2010). In this study astrocytes appeared to support neurons through maintenance of ATP, GSH, mitochondrial membrane potential and control of ROS levels following toxic insult. As such it is essential to consider them in neurodegenerative research (Woehrling et al., 2010).

As the majority of neurons in the brain are postmitotic it can be considered that the proposed co-culture model is more relevant to human CNS structure and function than the more commonly used continuous cell lines such as the SH-SY5Y neuroblastoma model (Woehrling et al., 2010). Additionally NT2/D1 cell line is relatively cheap to maintain and differentiate in comparison to other stem cell lines available. The differentiation process is also reproducible and faster than in iPS cells. Generation of iPS cells require up to 85 days with further differentiation into functional neurons for up to 8 weeks and into GFAP-positive astrocytes up to 3 months. In comparison, NT2/D1 cells differentiate into co-cultures of functional neurons and astrocytes within 2 months. The easy access to the NT2/D1 cell line and the previously reported characterisation of the neurons and astrocytes derived from these stem cells, are an additional advantage. All these characteristics make the NT2/D1 stem cell line a good model to study neuronal and astrocytic interactions as well as neurological disease.

1.11 Aims and objectives of the study

The aim of this PhD is to create a heterogeneous cellular model of the human nervous system for investigating the effects of Aβ on neurons and astrocytes.

As one of the earliest changes in AD is related to changes in metabolism the NT2/D1 derived neurons and astrocytes will be characterized, in terms of their metabolic coupling. The main focus of this part of the study is the astrocyte neuron lactate shuttle (ANLS) that has been shown to be involved in memory formation. ANLS has not been previously studied *in vitro* on a human stem cell derived model. As such one of the aims of this thesis is to establish whether NT2.D1 derived neurons and astrocyte co-cultures are metabolically competent and demonstrate functional metabolic coupling. NT2.N/A and NT2.A cells will be investigated for the expression of the main components of the ANLS model as well as functional characteristics consistent with their neuron-astrocyte metabolic coupling. This study will establish whether, stem cell derived astrocytes provide metabolic support to their neuronal counterparts, thus providing a human model to study this process and its relationship to neurodegeneration.

The effects of chronic exposure of the NT2.N/A to Aβ(1-42) will be studied in order to determine its effects of cellular metabolism. Aβ(1-42). Preparations will be characterized in order to establish protocols to produce oligomers and also determine its aggregation over time in culture. Investigation of the effects of Aβ(1-42) will include changes in metabolic markers, gene expression, oxidative stress and functionality of astrocytes in terms of calcium responses. These experiments will be performed on a mixed NT2.N/A co-cultures as well as pure astrocytes (NT2.A) and primary cortical mixed neuronal and glial cultures, which will be used to compare this model to a widely accepted cell culture preparation.

Chapter 2: Amyloid-beta and Alzheimer's disease

2.1   Introduction

2.1.1   Amyloid-beta – discovery and structure

Aβ was first isolated from meningeal vessel walls and was partially sequenced in 1984 (Glenner and Wong, 1984). This discovery eventually led to the amyloid hypothesis proposed by John Hardy and David Allsop (1991). In their original study, Glenner and Wong used the chaotropic salt guanidine hydrochloride to solubilize Aβ and then enriched it chromatographically (Glenner and Wong, 1984). The monomeric amyloid subunit ran as a ~4kDa band on SDS-PAGE gel. In this study Aβ was sequenced to residue 24 (Glenner and Wong, 1984).

Many other labs have now independently isolated and sequenced amyloid from plaques from AD brains. Several papers have been published on the methods for isolation of amyloid plaques, which have been shown to be insoluble in many denaturants (Allsop et al., 1983). Masters *et al.* (1985), used a nonionic detergent extraction of brain, followed by a pepsin digestion, and sucrose density gradient fractionation to isolate the amyloid plaque core which was partially soluble in 10% sodium dodecyl sulphate (SDS) and 2-mercaptoethanol (BME) and fully soluble in 70% formic acid. The solubilized core was shown to run at ~4 kDa but also at ~8, 12, and 16 kDa, demonstrating for the first time the aggregation of the monomeric Aβ into SDS-stable oligomers (Masters et al., 1985). A subsequent study by Selkoe *et al.* (1986) estimated the protein content of a single plaque to be 60 – 130 pg. The first biochemical analyses of Aβ isolated from meningeal vessels and cerebral plaques showed that in both cases the amyloid subunit was a hydrophobic protein of about 4kDa. It was also shown to have a unique sequence and to be prone to aggregation into dimers, trimmers and tetramers, as well as higher oligomers and amyloid fibrils.

The complexity of Aβ aggregation is determined by the microenvironment in which it is produced. It has been shown that small amounts of Aβ can be produced in the ER and other organelles in the secretory pathway. However, the majority of Aβ is produced from APP that has been trafficked to the cell surface and is then internalized and processed by β- and γ-secretases in the acidic environment of endosomes (Haass et al., 2012).

As mentioned above, Aβ has been shown to self-associate and can form a range of different aggregated forms, from dimers to fibrils (Powers and Powers, 2008). The biochemical properties of Aβ however, vary depending on the residues of the hydrophobic carboxyl terminus. Aβ(1-40) is the major species of Aβ that is produced in the brain and is far less prone to aggregation than Aβ(1-42).

It was initially proposed that Aβ fibrils mediated Aβ toxicity. However, more recent data has demonstrated the toxicity of non-fibrillar, soluble oligomers of Aβ (Shankar and Walsh, 2009). Indeed, analysis of AD brains has shown that levels of oligomers correlate more strongly with the degree of cognitive impairment and synaptic loss than amyloid plaques (Lue et al., 1999, Wang et al., 1999).

2.1.1.1 Aβ fibrils

The molecular structure of Aβ fibrils has been extensively studied. Aβ fibrils have a cross-β structure where individual β strands are orientated perpendicular to the long axis of the fibril (Ahmed et al., 2010). The Aβ(1-42) unit within the fibril has a U-shaped structure with two ß-strands connected and Phe19 in contact with Leu34 (Ahmed et al., 2010).

Kinetic studies of Aβ suggest that its aggregation is characteristic of nucleation-

dependent polymerization. The process has been shown to start with a lag phase, followed by elongation into mature fibrils (Hellstrand et al., 2010a). Studies on synthetic Aβ(1-40) and Aβ(1-42) fibrils have demonstrated similar protofilament structure with approximately 2.5 peptide per cross-β repeat per protofilament (Schmidt et al., 2009).

The conversion of α-helices within normally soluble protein into β-sheet enriched aggregates appears to be common in several neurodegenerative diseases (Masters and Selkoe, 2012).

2.1.1.2 Aβ oligomers

Over the past decade studies on Aβ have moved from an initial focus on fibrils and plaques to the smaller, soluble oligomers which demonstrate toxic effects on membranes including synapses (Masters and Selkoe, 2012).

The presence of SDS-stable dimers and trimers in the soluble fractions from isolated plaques (Funato et al., 1999, Enya et al., 1999), suggests that these SDS-stable oligomers are the building blocks of insoluble amyloid plaques and could mediate neuronal dysfunction (Moechars et al., 1999, Mucke et al., 2000). Evidence supporting the toxicity of soluble, oligomeric Aβ comes from studies on transgenic PDAPP (Aβ precursor protein (APP) mini-gene driven by a platelet-derived (PD) growth factor promoter) mice where memory deficits were reversed by a single intraperitoneal injection of anti-Aβ antibody (Dodart et al., 2002b). As amyloid deposits were not affected, it was suggested that the antibody was acting only on soluble oligomers of Aβ and that the clearance of these toxic species reversed memory deficits (Dodart et al., 2002b).

Many different forms of Aβ aggregates have been described (Masters and Selkoe, 2012). However, many of these studies have focused on synthetic Aβ and have used non-physiological concentrations of single length peptide under *in vitro* conditions. The presence of similar Aβ species in the brain has not been confirmed (Masters and Selkoe, 2012). Studies have demonstrated that natural Aβ oligomers isolated from AD brain are more potent in cytotoxicity assays than synthetically produced Aβ (Lambert et al., 1998). Similarly, natural Aβ oligomers are more toxic than protofibrils (Walsh et al., 1997). Protofibrils require high nanomolar concentrations to induce toxic effects, suggesting that they contain aggregated forms that do not interact with neuronal membranes to the same extent as less aggregated oligomers.

Despite these findings many groups study Aβ aggregation using synthetic peptides at supraphysiological concentrations due to difficulties in isolating naturally occurring peptides (Castano et al., 1986, Kirschner et al., 1987). The methods used for studying the aggregation of Aβ monomers into oligomers vary in terms of temperature, salts as well as detergents and metal ions (Sahoo et al., 2009, Ahmed et al., 2010).

Another advantage of synthetic peptides is the possibility of introducing amino acids substitutions such as those found at Glu22 and Asp23 which mimic "Arctic" and "Iowa" FAD mutations (Fig. 1.2) and have been shown to increase the rate of aggregation (Peralvarez-Marin et al., 2009).

Recombinant Aβ (produced in bacteria) has been used to study Aβ aggregation (Picone et al., 2009, Walsh et al., 2009). This recombinant Aβ has been particularly useful in research on low n-oligomers such as dimers and tetramers (Streltsov et al., 2011). However, as recombinant peptides are derived from bacteria, these preparations can contain impurities, which can interact and co-purify with the Aβ. In

addition, this recombinant Aβ has been found to aggregate quicker and is also more toxic, which raises questions about its similarity to natural Aβ peptides (Finder et al., 2010).

Natural Aβ oligomers extracted from cortex of AD brains have been shown to inhibit long-term potentiation (LTP), enhance long-term depression (LTD) as well as reduce dendritic spine density (Shankar et al., 2008). Interestingly amyloid plaque cores from the same brains did not affect LTP unless they were solubilized which demonstrates that plaques have low toxicity although oligomers released from them remain toxic (Shankar et al., 2008). Other studies have shown that Aβ oligomers extracted from AD brains can induce hyperphosphorylation of tau. This leads to collapse of the microtubule skeleton and dystrophy (Jin et al., 2011).

In addition to studies on dimers and trimers, attention has also turned to the toxic effects of nonomers and dodecamers. These species has been found in the brains of Tg2576 mice starting at 6 months of age when the first changes in performance on the Morris-water maze begin to appear (Lesne et al., 2006). Additionally, when dodecamers were purified and injected into the ventricle of normal wild type rats, their spatial memory performance decreased (Lesne et al., 2006). However, the appearance of dodecamers does not correlate with changes in other types of memory or synaptic dysfunction as these changes are seen long before the appearance of dodecamers (Jacobsen et al., 2006).

In the brain, a range of different oligomers exists in equilibrium with fibrils and plaques. This has been supported by the finding that a halo of dystrophic neuritis surrounds plaques, which decrease with distance from the plaque. This halo has been shown to be immunoreactive for antibodies that are selective for small oligomers (Koffie et al., 2009).

In addition to natural brain derived Aβ oligomers, oligomers derived from APP transfected cells *in vitro* have also been investigated. SDS-stable low-n oligomers have been detected in medium from a variety of cell lines (Podlisny et al., 1995, Townsend et al., 2006), including the Chinese hamster ovarian (CHO) cell line expressing mutant human APP (V717F). These cells (renamed to 7PA2) secrete nanomolar levels of SDS- stable Aβ oligomers (Podlisny et al., 1995) that have been confirmed on SDS gels as dimers, trimers and tetramers (Walsh et al., 2002). Injection of the conditioned medium from these cells into the lateral ventricle of the wild type rat has been shown to inhibit hippocampal LTP (Walsh et al., 2002). Additionally, immunodepletion of the conditioned medium with anti-Aβ antibody blocked the effect of oligomers on LTP. Interestingly, pre-treatment of the conditioned medium with insulin degrading enzyme (IDE), which degrades monomeric Aβ but not oligomers had no effect on the toxic effect of Aβ on LTP (Walsh et al., 2002). In addition, cell derived oligomers of Aβ have also been found to decrease the number of spines when neurons were incubated with sub-nanomolar levels (Shankar et al., 2007).

2.1.2 Aβ interactions with other molecules

Aβ has been found to interact with a variety of molecules which include metal ions, cell membranes, lipoproteins and membrane-associated proteins. Aβ plaques show immunoreactivity with many different molecules. These could arise from different cells which are associated with plaque formation such as neurons (axons and denrites), reactive astrocytes and microglia (Masters and Selkoe, 2012). Additionally, a recent interactome study of APP demonstrated over 200 entities interacting with different parts of APP, a significant number of which have been shown to interact with Aβ domain (Perreau et al., 2010).

2.1.2.1 Metal ions

Metal ions are ubiquitously present in human tissues and as such they have been intensively studied for possible Aβ associations. The results of these studies are controversial. Some studies have detected increases in Cu, Zn or Fe ions in plaques (Rajendran et al., 2009). It has been shown that both APP and Aβ contain sequences with metal binding motifs (Faller, 2009, Duce et al., 2010) suggesting the potential to interact with metal ions. An interesting overlap between brain regions rich in glutamatergic terminals, free vesicular zinc and Aβ plaques have been shown in APP transgenic mice (Stoltenberg et al., 2007).

Many metal ions interact with Aβ including copper, zinc and iron. The K_d of Cu^{2+} for Aβ is around 10^{-10}M and that includes both soluble and fibrillar Aβ (Rozga et al., 2010). This suggests that any proteins with higher affinities will compete with Aβ. Such proteins include human serum albumin (Perrone et al., 2010) suggesting that in CSF or blood Aβ should be unmetallated (Masters and Selkoe, 2012). Aβ has been suggested to have more than one copper binding site (Jun et al., 2009). Additionally, depending on its stoichiometry, Cu^{2+} interaction with Aβ can lead to aggregation through oligomer forming or fibril-forming pathways (Olofsson et al., 2009, Tougu et al., 2009). The main copper binding region is located within Aβ first 16 residues and includes His6, His13 and His14 as well as Asp1 and Ala2 (Drew et al., 2009a, Drew et al., 2009b). Additionally Aβ-Cu^{2+} complex has been found to facilitate the oxidation of a biological species and the reduction of molecular oxygen, generating H_2O_2 (Jiang et al., 2010). Whilst Cu^{2+} has been found to induce Aβ aggregation, a reduction in intracellular Cu^{2+} causes inhibition of Aβ oligomer formation (Crouch et al., 2009a).

Zn^{2+} can also bind to Aβ at different regions and drive its aggregation (Miller et al.,

2010). It has been proposed that the aggregation of Aβ into oligomers can be induced by Zn^{2+} in the vicinity of excitatory glutamatergic synapses and can contribute to synaptic degeneration in AD (Deshpande et al., 2009). In addition, zinc and Aβ complexes have also been shown to be more resistant to degradation (Crouch et al., 2009b) leading to accumulation of Aβ fibrils.

Fe^{3+} and Aβ complexes have been shown to catalyze the reduction of oxygen and production of H_20_2 (Jiang et al., 2009). Additionally, Aβ has been found to have a very strong affinity for Fe^{3+} and Fe^{2+} which suggests it can compete for iron. This could interfere with iron homeostasis, especially as Aβ has 8-times higher affinity to Fe^{2+} than transferrin (Jiang et al., 2009).

2.1.2.2 Other Aβ interactions

As an amphiphilic peptide, once released from a membrane, Aβ can interact with a number of different molecules (Masters and Selkoe, 2012). These interactions can be caused by phase/interface effects, electrostatic interactions or hydrophobic interactions (Masters and Selkoe, 2012).

Most *in vitro* studies on the aggregation of Aβ are done at supraphysiological concentrations. Additionally, microenvironmental conditions in which Aβ aggregates in the brain are not taken into account (e.g. high metal ions concentrations at synapses). Another variable that is not often considered is the interface between the interstitial fluid phase and the surface of the plasma membrane, which is thought to be important in aggregation of Aβ. Many studies have shown interface clustering of Aβ (Chi et al., 2010) which also affects the speed of fibril formation (Hellstrand et al., 2010b). The nature of the phase/interface effect strongly influences Aβ folding (Kayed et al., 2009) and therefore has to be taken into account in studies on Aβ

aggregation (Masters and Selkoe, 2012).

Electrostatic interactions between negatively charged phospholipid head groups or sphingolipids and Aβ as well as their effect on aggregation have been extensively studied (Kayed et al., 2009, Sureshbabu et al., 2010). It has been shown that smaller Aβ oligomers show a tendency to bind charged molecules, while larger oligomers do not (Cizas et al., 2010). The electrostatic interaction with phosphatidylserine has been shown to mediate the toxicity of Aβ in neuronal cells as the cells can be rescued by treatment with Annexin V which has a very high affinity for phosphatidylseirine (Ciccotosto et al., 2011). Additionally, gangliosides also have the potential to affect the folding of Aβ (Ogawa et al., 2011).

Once Aβ is released from its transmembrane location, it can re-insert itself into the hydrophobic lipid bilayer. A number of studies have examined the re-insertion of Aβ in order to determine whether this leads to formation of a transmembrane pore or whether this re-insertion would cause a disruption in the integrity of the lipid bilayer (Masters and Selkoe, 2012). Whilst there have been a number of molecular dynamics studies as well as an *in vitro* artificial lipid membrane models there is a significant lack of *in vivo* studies (Lemkul and Bevan, 2009, Morita et al., 2010).

It has been previously documented that Aβ interacts with various lipoproteins (Apolipoprotein E, A, J) via electrostatic or hydrophobic reactions (Holtzman et al., 2012). In addition, direct evidence for *in vivo* interactions of ApoE and ApoA1 with Aβ have also been demonstrated (Paula-Lima et al., 2009).

There is also increasing evidence of Aβ interactions with membrane proteins. These include NMDA (N-Methyl-D-aspartate) or α7-nicotinic acetylocholine receptors as well as cellular prion protein (Hu et al., 2009, Lauren et al., 2009, Liu et al., 2009). Many these studies have shown that an antagonist or a downstream regulator of the

receptor can prevent the effects of Aβ oligomers (Shankar et al., 2007, Li et al., 2009). There is no direct evidence of a physical interaction of Aβ with the receptor, although, it has been suggested that the binding of Aβ to certain lipids could disturb the lipid bilayer and therefore affect membrane associated neuronal receptors (Masters and Selkoe, 2012).

2.1.3   Degradation of Aβ

All humans accumulate Aβ during ageing (Funato et al., 1999). The progression from normal ageing through mild cognitive disorder to AD is primarily caused by acceleration of Aβ accumulation (Saido and Leissring, 2012). Aβ production is normally balanced by its degradation by a range of different processes working together such as proteolytic degradation, cell-mediated clearance as well as passive and active transport. There is increasing evidence to suggest that proteolytic degradation is affected in AD and that sporadic forms of AD might develop as a result of defective clearance of Aβ (Tanzi et al., 2004). Experiments investigating the rates of Aβ production and clearance have shown that in sporadic AD there is a defect in clearance of Aβ in CSF (Mawuenyega et al., 2010).

Normally Aβ is degraded by a large number of proteases, each with different characteristics. These Aβ-degrading proteases (AβDPs) belong to different families such as metallo, serine, aspartyl, cysteine and threonine proteases (Saido and Leissring, 2012). AβDPs can be either classified by their enzymological type (metalloproteases, aspartyl proteases etc.) or by the species of Aβ they can hydrolyze (peptidases, oligopeptidases etc). The metalloproteinases that have been found to degrade Aβ include neprilysin, NEP-like peptidases, endothelin- and angiotensin-converting enzymes, matrix-metalloproteinases and insulin-degrading enzyme. Amongst serine proteases that can degrade Aβ plasmin, acylpeptide

hydrolase and myelin basic protein have been described. Cathepsin B (cysteine protease) as well as cathepsin D, BACE1 and BACE2 which are aspartyl proteases, have also been found to degrade Aβ (Saido and Leissring, 2012).

Whilst Aβ is produced by two proteases which are found in specific subcellular compartments of primarily neuronal cells, Aβ degradation involves a large number of proteases with different Aβ avidities, optimum pH and subcellular as well as cellular localizations (Saido and Leissring, 2012).

AβDPs has been found to be vulnerable to environmental insults and oxidative stress (Caccamo et al., 2005). As age is the principal risk factor for AD, and oxidative stress has been previously found to increase during ageing (Zhu et al., 2007), it is likely that defects in Aβ clearance have a role in AD pathogenesis (Saido and Leissring, 2012).

2.1.3.1 Zinc-metalloproteases – neprilysin

Neprilysin (NEP) is the most well characterized AβDP. It is a member of the M13 family of zinc-metalloproteases (Hersh and Rodgers, 2008). NEP is a type II membrane-associated peptidase with the active site facing the luminal or extracellular side of membrane (Roques et al., 1993, Turner et al., 2001). This position is ideal for degradation of extracytoplasmic peptides such as Aβ. NEP is found almost exclusively in neurons and after its synthesis in the soma, it is axonally transported to presynaptic terminals (Fukami et al., 2002). These presynaptic terminals and nearby intracellular locations are probably the sites of degradation of Aβ by NEP (Iwata et al., 2004).

It has been found that in NEP KO mice levels of both Aβ(1-40) and Aβ(1-42) are twofold higher than in controls (Iwata et al., 2001). As such the levels of Aβ

correlated with gene dosage of NEP and its activity. It has been suggested that intraparenchymal degradation of Aβ by NEP could be as high as ~50% of total clearance (Saito et al., 2003). NEP's therapeutic potential has also been investigated. It has been shown that when crossed with a transgenic mouse expressing eightfold higher levels of NEP, the J20 APP transgenic mouse demonstrated a ~90% reduction in steady-state Aβ with no plaque formation (Leissring et al., 2003). However, a more recent study failed to show reversal in learning and memory deficits when NEP was overexpressed (Meilandt et al., 2009). NEP has been shown to degrade Aβ oligomers in APP-Tg mice (Huang et al., 2006) as well as monomers (Saido and Leissring, 2012). Interestingly, *in vitro* studies have shown that NEP is capable of degrading synthetic Aβ oligomers (Kanemitsu et al., 2003) but not naturally secreted Aβ oligomers (Leissring et al., 2003).

2.1.3.2 Zinc-metalloproteases – insulin degrading enzyme

Another well-studied AβDP is insulin-degrading enzyme (IDE). IDE is another zinc-metalloproteinase that is mainly found in the cytosol (Authier et al., 1996) and mitochondria (Leissring et al., 2004). Due to its unusual structure (clam shell), IDE is only able to degrade monomers of Aβ due to its restricted peptidase activity (Saido and Leissring, 2012). Other studies have demonstrated its presence in peroxisomes (Kuo et al., 1994), endosomes (Hamel et al., 1991) and the endoplasmic reticulum (Carpenter et al., 2010). However, these localizations have been less well studied. In addition, IDE is also present in the extracellular space (Qiu et al., 1998, Vekrellis et al., 2000).

Studies on IDE have shown that it is a major AβDP that is secreted into the medium of cells *in vitro* (Qiu et al., 1998). In primary neuronal cultures, deletion of IDE was shown to cause a 90% decrease in the degradation rate of Aβ monomers (Farris et

al., 2003). *In vivo* studies also shown an increase in Aβ levels after IDE deletion, however, the increase was less significant than that found *in vitro* (Farris et al., 2003).

2.1.4   The importance of Aβ aggregation studies

As discussed above, Aβ aggregation is determined by its microenvironment and has been shown to self-associate into different aggregated forms, which differ in their toxicity. It is therefore essential to determine what form of Aβ is being used and how it will behave in the conditions used in the study. However, many published reports do not characterise the form of the peptide that they are using. In many cases the characterisation is only limited to the peptide at the initial stage of the study. As AD is a chronic disease that develops over decades, it is essential to study the effects Aβ following chronic application. As such it is necessary to assess and characterise the Aβ preparation and its fate over the experimental period, as changes in the aggregation state of Aβ may lead to changes in its toxicity.

2.1.5   Aims and objectives of the study

The aim of this chapter was to investigate the best conditions for preparation and aggregation of Aβ(1-42). Several protocols were used to investigate the production of oligomers. In addition, western blotting and ThT assays were used to assess the stability of these preparations over time.

2.2 Material and Methods

2.2.1 Amyloid – beta

2.2.1.1 Aggregation protocol

Aβ(1-42) and Aβ(1-40) peptides were prepared under conditions to promote its solubility and limit the aggregation process (Burdick et al., 1992). Several methods for oligomerization of Aβ(1-42) and Aβ(1-40) were investigated.

Aβ(1-42) treated with HFIP (Anaspec, USA) and Aβ(1-40) treated with HFIP (Anaspec, USA) were resuspended in 200mM HEPES, pH 8.5 to a concentration of 100μM. The aliquots were stored at -80°C and used at working concentrations of 0.2, 2 and 20μM.

Additional methods to make oligomers that were also investigated, including a method described by Dahlgren *et al.* (2002). Briefly Aβ(1-42) treated with HFIP (Anaspec, USA) was resuspended in DMSO to a concentration of 5mM. Later phenol red-free DMEM was added to the DMSO to bring the peptide to the final concentration of 100μM. The peptide was then incubated at 4°C for 24 h.

To obtain the monomeric form of Aβ(1-42), the 5 mM stock in DMSO was diluted directly into cell culture media.

2.2.1.2 Aβ(1-42) and Aβ(1-40) aggregation over time

Aggregation of Aβ(1-42) and Aβ(1-40) over time was investigated to determine the speed and stability of different protein preparations from section 2.2.1.1 that would be expected to form under tissue culture conditions.

Aβ(1-42) and Aβ(1-40) prepared in HEPES, Aβ(1-42) prepared in phenol-free media and Aβ(1-42) prepared in DMSO were diluted to working concentrations of 0.2, 2 and 20µM. 100µl of each concentration was added into a 96-well cell culture plate in triplicates. The plate was then incubated at $37^{o}C$ in a humidified atmosphere of 5% CO_2. Samples were collected at 24, 48, and 72 hours and analyzed using western blotting.

2.2.2   Western blotting

To assess the presence of specific aggregates of Aβ following the aggregation procedure described in section 2.2.1.1 and 2.2.1.2, polyacrylamide gel electrophoresis followed by western blotting was performed on the samples.

2.2.2.1 SDS PAGE

Protein gels were electrophoresed using the Mini Protean® 3 Cell (Biorad, UK). 12% gels were cast according to the manufacturer's guidelines (see Appendix 1). Samples were prepared in sample buffer (deionised H_2O, 25% glycerol, 62.5mM Tris-HCl pH 6.8, 2% SDS, 0.01% bromophenol blue and 5% β-mercaptoethanol added fresh) and loaded onto the gel, together with PAGE Ruler Plus Prestained Protein Ladder (Thermofisher, UK). Electrophoresis was carried out at 200V (fixed), 60mA (max) in for approximately 45 minutes until the bromophenol blue reached the bottom of the resolving gel. Plates were then carefully separated, and the gel placed in Coomassie Brilliant blue stain (0.1% Coomassie, 50% methanol, 7% acetic acid), for approximately 1 hour on a slowly rocking platform. Gels were then destained (50% methanol, 7% acetic acid) and photographed using G:BOX Chemi HR1.4 (Syngene) and GeneSys software (Syngene).

2.2.2.2 Discontinuous Native PAGE

Protein gels were electrophoresed using the Mini Protean® 3 Cell (Biorad, UK). 10% gels were cast according to the manufacturer's guidelines (see Appendix 1). Samples were prepared in sample buffer (deionised H_2O, 40% glycerol, 62.5mM Tris-HCl pH 6.8, 0.01% bromophenol blue) and loaded onto the gel, together with NativeMark Unstained Protein Standard (Life Technologies, UK). Electrophoresis was carried out at 200V (fixed), 60mA (max) for approximately 45 minutes until the bromophenol blue reached the bottom of the resolving gel. Plates were then carefully separated, and the gel placed in Coomassie Brilliant blue stain (0.1% Coomassie, 50% methanol, 7% acetic acid), for approximately 1 hour on a slowly rocking platform. Gels were then destained (50% methanol, 7% acetic acid) and photographed using G:BOX Chemi HR1.4 (Syngene) and GeneSys software (Syngene).

2.2.2.3 Western blot transfer.

Proteins for western blot transfer were first separated by SDS PAGE (section 2.2.2.1) or native PAGE (section 2.2.2.2). Gels were then equilibrated in transfer buffer (25mM Tris, 192mM glycine, 10% methanol) before being transferred to pre-wetted (in transfer buffer) nitrocellulose membrane (Millipore, UK) trimmed to the exact dimensions of the gel. The gel and nitrocellulose were then sandwiched between four pieces of Whatman filter paper and two pieces of sponge, pre-soaked in transfer buffer. Transfers were performed using the mini trans-blot electrophoretic transfer cell (Biorad, UK) at 30V, 90mA overnight on ice.

2.2.2.4 Western blot analysis.

Nitrocellulose membranes (section 2.2.2.3) were blocked in TBS (8g NaCl, 0.2g KCl, 3g Tris-base in 1 litre H_2O) 5% powdered milk for 2 hours at room temperature, then rinsed in TBS 0.01% Tween (Sigma-Aldrich, UK). They were then placed in TBS 0.01 Tween, 3% powdered milk containing appropriate primary antibody and incubated overnight at 4°C on a shaking platform. Mouse anti-β-amyloid (1-42) (1:1000-1:3000) antibodies (6E10 Covance, UK), were used as primary antibody to detect the Aβ(1-42) as well as Aβ(1-40). This antibody detects amyloid oligomers up to 24mers as well as trace high molecular weight species (Chromy et al., 2003). The following day membranes were washed 6X for 5 minutes in 100ml TBS 0.01% Tween, to remove unbound antibody, and then placed in TBS 0.01% Tween 3% powdered milk, containing appropriate secondary antibody for 1 hour at room temperature, with agitation. To detect the anti-β-amyloid (1-42) antibody, the secondary antibody, anti-mouse IgG HRP (Cell Signaling Technology, USA) was used. After extensive washes in TBS 0.01% Tween, and then TBS alone, membranes were placed in chemiluminescent substrate (GE Healthcare, UK) for 5 minutes. Membranes were then immediately sandwiched between acetates and exposed to photographic film (Thermofisher, UK) in a developing cassette. To visualize the bound antibody, exposed films were developed using developer (Sigma-Aldrich, UK), and following extensive washes, fixed using fixer (Sigma-Aldrich, UK) in a darkroom.

2.2.3 ThT assay

Thioflavin T (ThT) is a benzothiazole dye which is has been used as an amyloid stain for senile plaques. ThT binds rapidly and specifically to β-sheets and upon binding the dye undergoes 120nm red shift in its excitation spectrum and can be selectively excited at 450nm, with the fluorescent signal at 482nm (LeVine, 1993).

In this study ThT was added to the Aβ(1-42) and Aβ(1-40) reaction mix during the aggregation process and fluorescence was monitored at specific time points.

ThT (Sigma-Aldrich, UK) was dissolved in 50mM glycine-NaOH buffer, pH 8.5 to the concentration of 5mM. On the day of the experiment the 5mM ThT was diluted to 1.25µM with 50mM glycine-NaOH buffer, pH 8.5. Aβ(1-42) and Aβ(1-40) were prepared as described in section 2.2.1.1 at concentrations 20, 2 and 0.2µM. 20µl of each Aβ preparation at each concentration was added to black 96-well plate (Nunc). Then 80µl of 1.25µM ThT was then added to each well (to the final concentration of 1µM in the total assay volume) and the plate was incubated at 37˚C. The fluorescence was then read at time point 0, 6, 24, 48, 72 and 96h using SpectraMAX GeminiXS microplate luminometer (Molecular Devices, UK) and SoftMaxPro software (excitation: 450nm, emission: 485nm). All readings were corrected for background and results were expressed as the mean of three samples ± standard error of the mean (SEM). Comparison between different time points and treatments was performed using two-way analysis of variance (ANOVA) followed by Bonferroni post-test using GraphPad Prism Software. Differences were considered significant for p values <0.05.

2.3   Results

Aggregation of Aβ can be affected by different environmental conditions such as pH, concentration or salts. In this study four different protocols were used to aggregate Aβ(1-42) and Aβ(1-40) in order to determine which method produces low-n oligomers. An additional aim was to monitor the stability of the Aβ preparations over time. Methods that were used to assess Aβ(1-42) and Aβ(1-40) aggregation and stability included western blotting and Tht fluorescence assay.

Freshly prepared samples of Aβ(1-42) and Aβ(1-40) at a concentration of 20μM were run on a SDS-PAGE gel and analysed using western blotting in order to assess the composition of each preparation (Fig. 2.1). Aβ(1-42) prepared in 100mM HEPES at pH 8.5 (Fig. 2.1, lane 1) demonstrated a large proportion of monomers at around ~4kDa and high n-oligomers at the top of the gel (~130-250 kDa). Aβ(1-40) (Fig. 2.1, lane 2) which was also prepared in 100 mM HEPES showed large amounts of monomers but few oligomers or large aggregates. Aβ(1-42) that was dissolved in culture medium and aggregated overnight at 4°C demonstrated a large proportion of monomers (~4kDa) as well as a mixture of oligomeric species representing monomers, dimers, trimers and tetramers as well as a small amount of larger aggregates at the top of the gel (Fig. 2.1, lane 3). Aβ(1-42) that was dissolved in DMSO (Fig. 2.1, lane 4) showed a distinct monomeric band as well as a number of faint oligomeric bands including dimer, trimers and tetramers.

Amyloid prepared using the four different protocols was used to prepare Aβ solutions that were incubated in culture media for up to 72h at 37°C to mimic the conditions of cell culture. Samples were taken at 24, 48 and 72 hours and then run on a SDS-PAGE and native gel and analysed using western blotting.

72
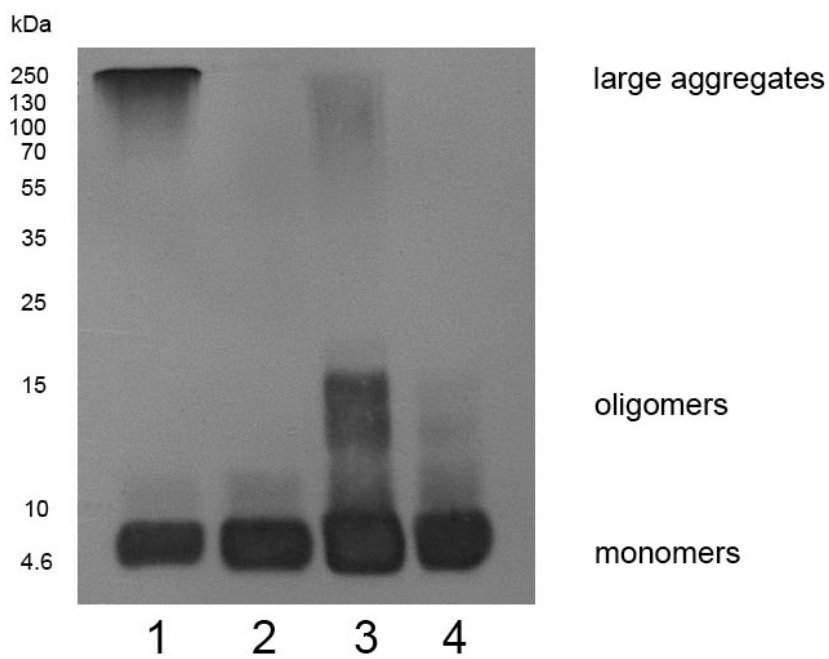
Figure 2.1   Representative western blot analysis of four fresh preparations of Aβ(1-42) and Aβ(1-40). Aβ preparations were separated using denaturing non-reducing conditions. 1) Aβ(1-42) in HEPES, 2) Aβ(1-40) in HEPES, 3) Aβ(1-42) in F12 media and aggregated overnight at 4°C, 4) Aβ(1-42) in DMSO.
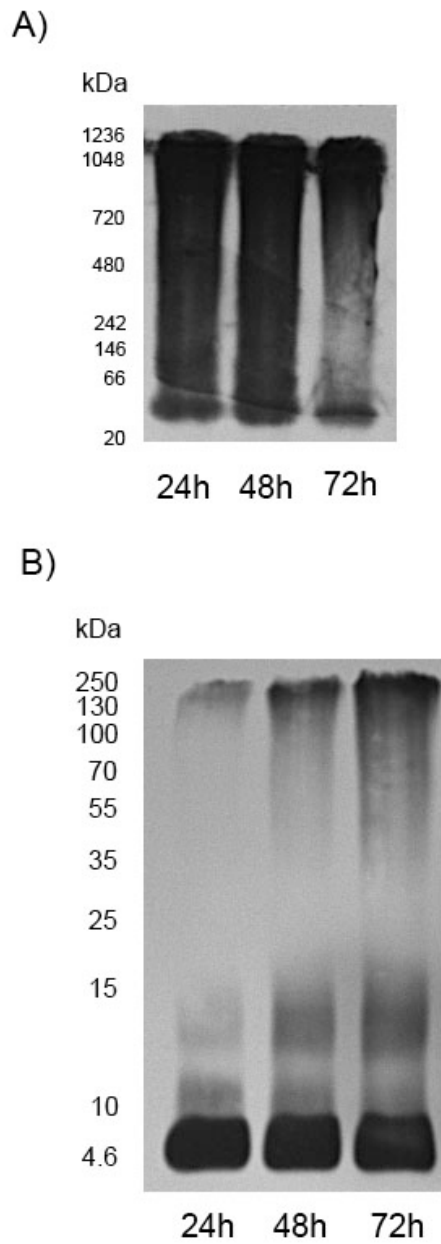
Figure 2.2 Representative western blot analysis of Aβ(1-42) dissolved in F12 media and aggregated overnight at 4°C. The preparation was then aged for up to 72h and separated using (A) native, non-reducing conditions, (B) denaturing, non-reducing conditions.

Aβ(1-42) prepared in culture medium and aggregated overnight at 4°C produced a range of different sized aggregates at 24h, ranging from ~40kDa to 1236kDa (Fig. 2.2A). At 48h the pattern of aggregation was similar to that seen at 24h. However, at 72h there was a steady increase in aggregation towards higher n-oligomers, with more intense staining above 720kDa and much less staining between 66kDa and 720kDa. On the SDS-PAGE gel there was a similar steady increase in aggregation with more low-n oligomers (trimers and tetramers) at around 15kDa band as well as larger aggregates above the 35kDa band (Fig. 2.2B).

The analysis of Aβ(1-42) prepared in HEPES and run on a native gel demonstrated lower amounts of small oligomers towards the bottom of the gel but with larger aggregates above 480kDa (Fig. 2.3A). Again there was a time dependent steady increase in the size of aggregation pattern with little staining below 480kDa ladder at 72h. When analysed on an SDS-PAGE gel over the incubation period there was a steady increase in the amount of low-n oligomers (trimers and tetramers) at around 15kDa with minor increases in the larger aggregates observed (Fig. 2.3B).

Aβ(1-42) that was dissolved in DMSO prior to incubation demonstrated a rapid aggregation pattern, with no staining below 480kDa ladder at 24h and at 72h staining was only limited to a band at the top of the native gel (1048 and 1236 kDa) (Fig. 2.6A). Samples run on an SDS-PAGE gel showed a steady increase in oligomers and large aggregates over the incubation period (Fig. 2.4B).

Analysis of the aggregation pattern of Aβ(1-40) prepared in HEPES at pH 8.5 by SDS-PAGE gel followed by western blotting analysis demonstrated a complete absence of oligomers (Fig. 2.5B). At all 3 time points the only band that was present was at ~4 kDa.
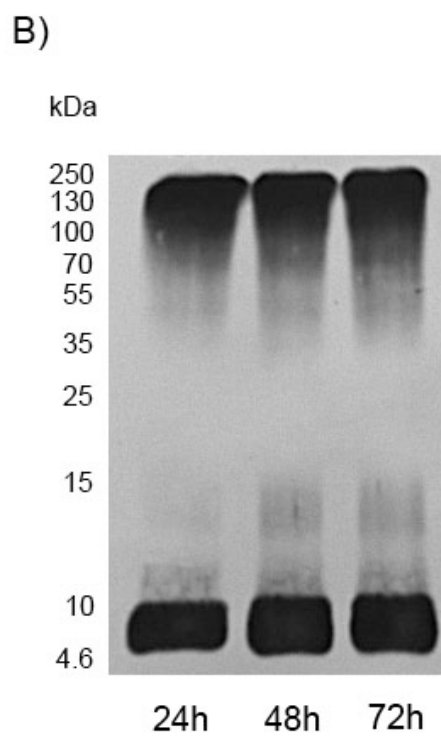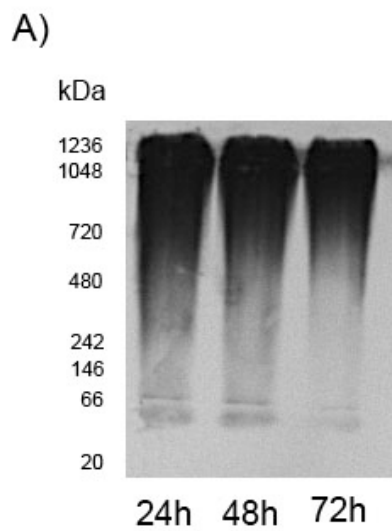
Figure 2.3 Representative western blot analysis of Aβ(1-42) dissolved in HEPES. The preparation was then aged for up to 72h and separated using (A) native, non-reducing conditions, (B) denaturing, non-reducing conditions.
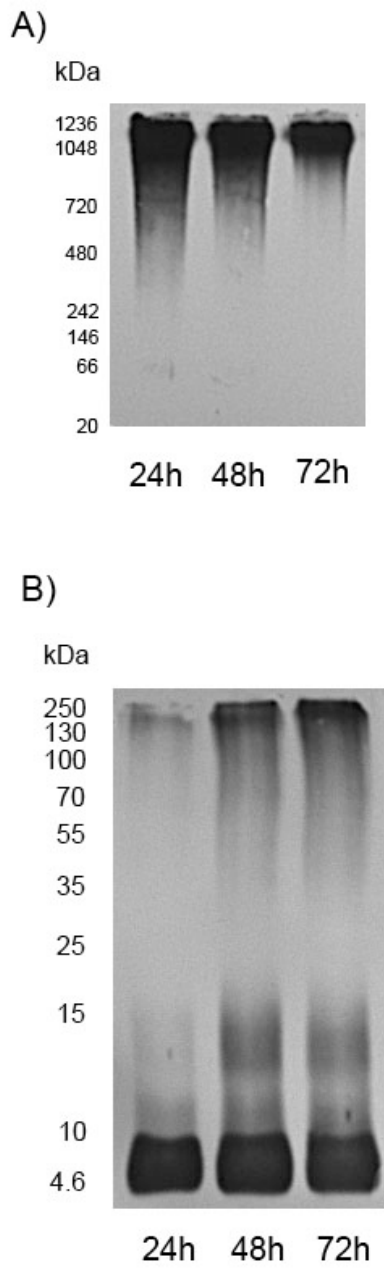
Figure 2.4 Representative western blot analysis of Aβ(1-42) dissolved in DMSO. The preparation was then aged for up to 72h and separated using (A) native, non-reducing conditions, (B) denaturing, non-reducing conditions.
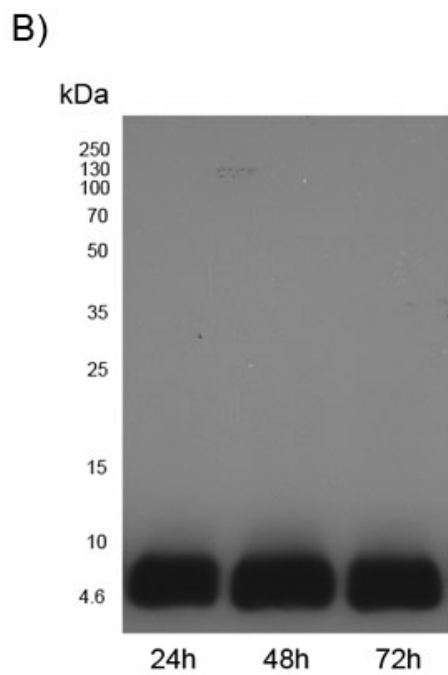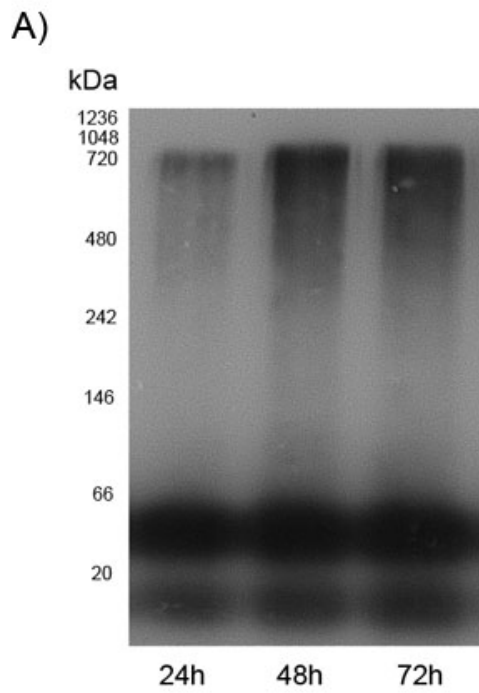
Figure 2.5   Representative western blot analysis of Aβ(1-40) dissolved in HEPES. The preparation was then aged for up to 72h and separated using (A) native, non-reducing conditions, (B) denaturing, non-reducing conditions.

Under native conditions Aβ(1-40) showed a different aggregation pattern over time, with more smaller aggregates at around 66kDa and an increase in larger aggregates present at the top of the gel. Additionally, the smallest species found on the native gel were below 20kDa ladder (Fig. 2.5A).

In order to further characterise 'aged' Aβ samples, the different preparations of Aβ were analysed using the ThT assay. ThT fluorescence increases upon binding to β-sheet structures and is therefore is a good indicator of Aβ aggregation. In this experiment the different Aβ preparations were incubated with ThT for up to 96h. The fluorescence of each sample was measured at 6, 24, 48, 72 and 96 hours (Fig. 2.6-2.8). At a concentration of 20µM the Aβ(1-42) prepared in DMSO aggregated rapidly, with the highest fluorescence at 72h and a slight decrease in fluorescence at 96h (Fig. 2.6). Aβ(1-42) prepared in media and pre-aggregated at 4°C showed a similar pattern. The highest fluorescence was recorded at 48h with a subsequent decrease in fluorescence at 72 and 96h. Aβ(1-42) prepared in HEPES showed a slight increase in fluorescence but overall remained stable over time. Aβ(1-40) showed no increase in fluorescence which was in line with previous western blotting analysis.

At a concentration of 2µM the Aβ(1-42) prepared in DMSO and in media showed very similar pattern with a steady increase in aggregation over time (Fig. 2.7). In contrast, Aβ(1-42) and Aβ(1-40) prepared in HEPES showed little aggregation and was stable over all 6 time points.

At a concentration of 0.2µM concentration none of the preparations demonstrated any increase in fluorescence over time (Fig. 2.8). However, there was a difference in the fluorescence displayed by each individual sample.
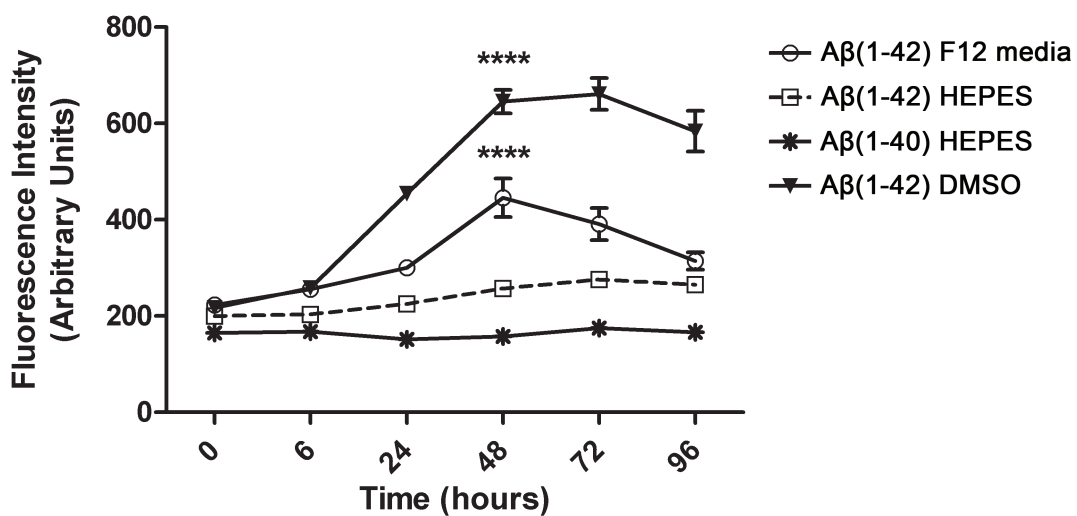
Figure 2.6   Aggregation of 20µM Aβ(1-42) and Aβ(1-40) preparations using ThT fluorescence. Each point is an average of 3 replicates ± SEM. *p*<0.0001 (****). For complete ANOVA see Appendix 2.
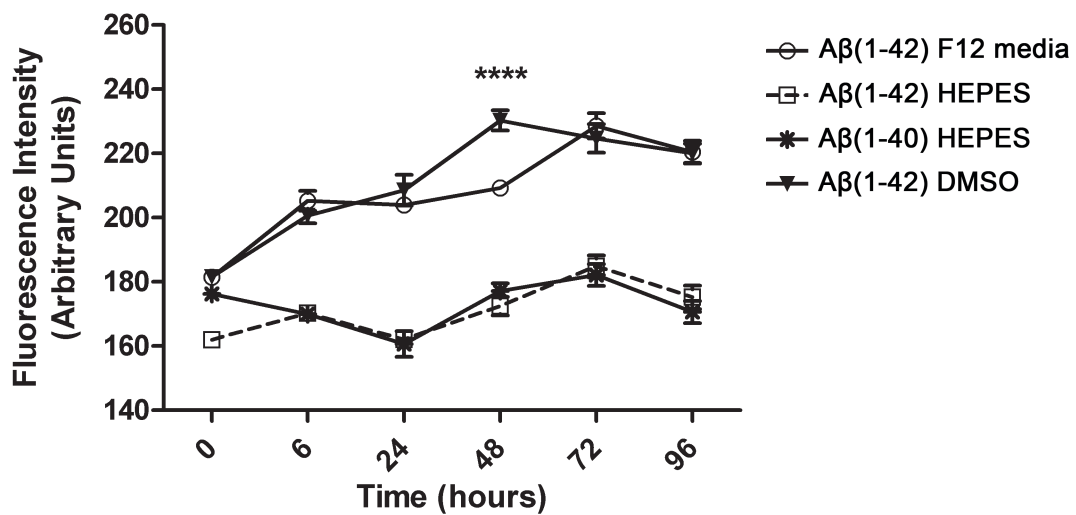
Figure 2.7   Aggregation of 2µM Aβ(1-42) and Aβ(1-40) preparations using ThT fluorescence. Each point is an average of 3 replicates ± SEM. $p<0.0001$ (****). For complete ANOVA see Appendix 3.
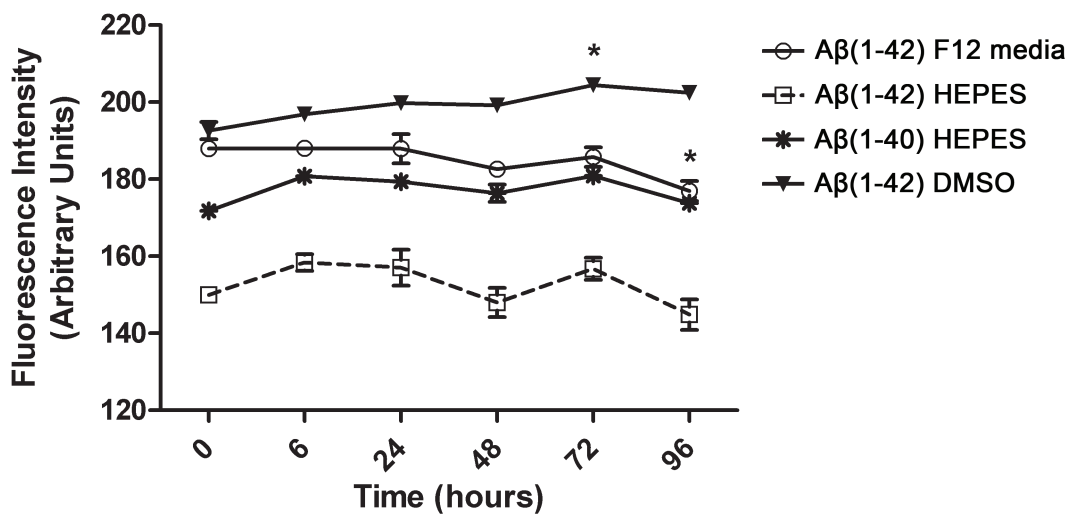
Figure 2.8 Aggregation of 0.2µM Aβ(1-42) and Aβ(1-40) preparations using ThT fluorescence. Each point is an average of 3 replicates ± SEM. $p < 0.05$ (*). For complete ANOVA see Appendix 4.

Aβ(1-42) dissolved in DMSO showed the highest fluorescence, followed by Aβ(1-42) prepared in media and Aβ(1-40) prepared in HEPES. Surprisingly Aβ(1-42) that was prepared in HEPES showed the lowest level of fluorescence of all four preparations.

2.4 Discussion

Numerous studies have demonstrated that Aβ(1-42) can aggregate and form oligomers which are toxic to CNS. Indeed, a number of studies have also shown that the formation of oligomers is a general phenomenon which applies to multiple proteinopathies (Conway et al., 2000, Kirkitadze et al., 2002). Although Aβ(1-42) oligomers are specifically associated with AD, an understanding of the aggregation process and its impact on pathology may inform other proteinopathies.

Aβ(1-40) and Aβ(1-42) are both produced naturally and are present in the brains and CSF of all humans during their life (Haass et al., 1992, Seubert et al., 1992). As such the presence of Aβ alone is not the cause of neurodegeneration. Indeed, a number of studies have shown that Aβ aggregation is essential for its toxicity.

Studies have shown that Aβ oligomers are toxic to cells at much lower concentrations that fibrils (Lambert et al., 1998) and are also able to rapidly block long-term potentiation. In addition, the concentration of oligomers has been shown to be up to a 70-fold higher in AD brain compared to controls (Gong et al., 2003).

The experimental handling of Aβ(1-42) is problematic due to its amphipathic sequence as well as its propensity to self-aggregate. These characteristics also make it very challenging to characterize its structure and function. As the toxicity of Aβ relies so heavily on its aggregation and form, it is essential to study and characterize different protocols for its preparation. In this study 4 different protocols were used in order to determine optimum conditions for oligomer production.

2.4.1 Hexafluoroisopropanol treatment (HFIP)

A critical factor for consistent preparation of oligomeric Aβ(1-42) is the ability to obtain exclusively monomeric peptide at the start of the process. Failure to eliminate fibril-nucleating seeds in previous studies has been shown to result in rapid fibril formation (Koo et al., 1999).

In order to minimize variability between different batches of synthetic Aβ and to remove any secondary or tertiary structure which could speed up Aβ aggregation, the peptide was dissolved in HFIP, a chemical which has been previously used for solubilisation of amylin (Nilsson et al., 2001) and prion peptides (Wille et al., 2000). This treatment has been found to dissolve higher aggregates, eliminating the 'nucleating seeds' and removing any secondary or tertiary structures (Dahlgren et al., 2002). Using Aβ(1-42) and Aβ(1-40) treated with HFIP different protocols for aggregation were investigated in terms of oligomer production and speed of aggregation.

2.4.2 Aβ(1-42) in HEPES

Aggregation of HFIP-treated Aβ(1-42) dissolved in 100mM HEPES led to formation of a range of species, including monomers/dimers, low oligomers (trimers/tetramers) as well as high oligomers and possibly protofibrils which accumulated at the top of the gels. Previous studies have shown that Aβ(1-42) in PBS or HEPES forms a broad range of structures including oligomers, protofibrils and fibrils regardless of HFIP pre-treatment (Chromy et al., 2003). When Aβ(1-42) is dissolved in HEPES at high monomer concentration (100 µM), it aggregates to a mixture of soluble oligomers of Aβ (i.e. amyloid-beta derived diffusible ligands, ADDLs) as well as

protofibrils. However, at lower concentrations only ADDLs are formed (Chromy et al., 2003).

Aβ(1-42) dissolved in 100mM HEPES has previously been used (Dineley et al., 2001) and has been found to activate α7 nicotinic acetylcholine receptors with higher concentrations being less effective at the receptor activation. Incubation with the α7 nicotinic acetylcholine receptor antagonist methyllycaconatine and the agonist 4-OH-GTS-21 blocked the Aβ induced activation of the receptor (Dineley et al., 2002). In addition, Aβ(1-42) has been found to activate the mitogen-activated protein kinase (MAPK) cascade via α7 nicotinic acetylcholine receptor and can upregulate expression of α7nAChR as well as downregulating the expression of extracellular signal-regulated kinase (ERK2) MAPK. As MAPK is known to play an important role in hippocampus synaptic plasticity and learning it has been suggested that the effect of Aβ(1-42) on this cascade provides a molecular basis for the disruptions of memory formation in AD (Dineley et al., 2001).

2.4.3 Aβ(1-42) in F12 media

Aggregation of Aβ(1-42) in fresh culture medium at 4°C overnight (Dahlgren et al., 2002) is widely used as a preparation method of Aβ. This method has been found to produce a mixture of monomers/dimers, trimers and tetramers as well as some large aggregates. However, the previous study only investigated aggregation over 24 hours. In the present study Aβ(1-42) prepared according Dahlgren *et al.* (2002) demonstrated a similar mixture of monomers and oligomers (trimers, tetramers) on a SDS-PAGE gel. However, the study by Dahlgren *et al.* (2002) did not run the Aβ(1-42) preparation on a native gel, therefore comparison of the results obtained in this thesis with the original paper is not possible.

Other studies on synthetic Aβ(1-42) prepared in F12 media has shown that the ADDLs (amyloid-beta derived diffusible ligands) formed were SDS-stable and consisted of trimers, tetramers, pentamers and other species up to 24mer sizes. AFM (atomic force microscopy) and gel electrophoresis showed that these ADDLs were stable structures that did not rapidly aggregate into protofibrils. When diluted solutions were incubated at 37°C for up to 24h, the smaller oligomers (trimer, tetramers) aggregated into larger 12-24mer species (Chromy et al., 2003). Both SDS-PAGE and native gels analysed using western blotting from this thesis showed a slow time-dependent aggregation of the Aβ(1-42) in F12 media. The results obtained in this thesis are therefore in agreement with the previous studies.

2.4.4 Aβ (1-42) in DMSO

Aβ(1-42) pre-treated with HFIP, dissolved in DMSO and used immediately has often been used in *in vitro* studies as a method to produce monomers (Kim et al., 2003, Cizas et al., 2010). Western blot analysis of the freshly prepared Aβ in DMSO only revealed monomeric/dimeric bands at ~4kDa. However, once the Aβ was added to culture media and incubated over time, the monomers aggregated rapidly. This very rapid aggregation is especially well presented on a native gel. The SDS-PAGE gel showed formation of SDS-stable oligomers (trimers/tetramers) which are normally toxic to the cells. It is therefore surprising that previous studies that have used Aβ dissolved in DMSO as a monomeric preparation, did not report any toxicity (Kim et al., 2003).

2.4.5 Aβ (1-40) in HEPES

SDS-stable oligomers were not detected in the HEPES preparations of Aβ(1-40) and this is consistent with previous studies (Chromy et al., 2003). In addition, under

native conditions Aβ(1-40) formed much smaller aggregates than Aβ(1-42). This supports the view that Aβ(1-40) is less prone to aggregation than Aβ(1-42).

2.4.6 Thioflavin T (ThT) fluorescence analysis

Previous kinetic aggregation studies have shown that the Aβ aggregation pattern demonstrates a sigmoidal appearance which is characteristic for nucleation-dependent polymerization. The process normally starts with a lag phase and is followed by an elongation and plateau phase once equilibrium is achieved (Hellstrand et al., 2010a). In this thesis the Aβ(1-42) aggregation was studied by ThT fluorescence in addition to electrophoresis and western blotting.

The study of Aβ(1-42) and Aβ(1-40) aggregation by ThT fluorescence showed a high level of reproducibility between replicates of the same solution. Aggregation of Aβ was dependent on both the concentration of the peptide, as well as the preparation protocol used. At 20μM the Aβ (1-42) dissolved in DMSO aggregated rapidly. This was also demonstrated by Aβ(1-42) prepared by the method described by Dahlgren *et al.* (2002). The Aβ(1-42) prepared in HEPES aggregated at a slower rate than the other methods tested. Aβ(1-40) demonstrated little aggregation according to ThT fluorescence which was in agreement with the results obtained by western blotting. At 2μM there was a similar pattern and in the presence of DMSO Aβ(1-42) aggregating rapidly. Surprisingly very similar results were obtained from Aβ(1-42) prepared in F12 medium. Again Aβ(1-42) in HEPES showed lower levels of aggregation over time. At the lowest concentration (0.2μM) the aggregation pattern was similar to other concentrations when measured by ThT fluorescence, with Aβ(1-42) in DMSO showing the highest fluorescence and Aβ(1-42) in HEPES the lowest. However, at this concentration the fluorescence was very low. It has been previously reported that Aβ(1-42) has a critical concentration below which fibrils cannot be

detected (Hellstrand et al., 2010a). Below a concentration of 0.2μM the fluorescence has been found to be below the background level (Hellstrand et al., 2010a) and as such the ThT assay is not recommended for the study of Aβ(1-42) aggregation at concentrations lower than 0.2μM. Previous studies have also shown that the critical concentration for Aβ(1-40) is higher, at 0.7-1.0μM (O'Nuallain et al., 2005) which may be due to different peptide length and ionic strength.

2.4.7 Conclusion

Gel electrophoresis and western blotting using antibodies against Aβ(1-42) have provided evidence that Aβ(1-42) prepared in F12 and HEPES form oligomers with little protofibril/fibril formation. Additionally Aβ(1-42) dissolved in HEPES produced more 24mer and higher species, whilst Aβ(1-42) freshly prepared in DMSO and diluted in medium rapidly aggregates. Electrophoresis in denaturing gels revealed a spectrum of SDS-stable oligomers including monomers, dimers, trimers and tetramers. Monomers appear to be a major species in both Aβ preparations. However, previous studies have shown that when two-dimensional native-SDS analysis was applied, the ADDL preparation contained only small amount of monomers (Chromy et al., 2003). This suggests that some of the oligomers can dissociate into monomers in the presence of SDS.

In all preparations tested, both native and SDS electrophoresis showed that size and Aβ aggregation depends on the incubation period as well as the environment. The western blot analysis also revealed a time-dependent increase in both oligomers as well as higher aggregates.

The ThT fluorescence assay was in agreement with the western blotting data. Aβ(1-42) dissolved in DMSO aggregated very quickly. According to western blot analysis,

both Aβ(1-42) aggregated in F12 medium and prepared in HEPES showed a similar aggregation pattern and oligomer formation. However, Aβ(1-42) pre-aggregated in F12 showed a more rapid aggregation pattern using the ThT fluorescence assay than Aβ(1-42) prepared in HEPES. These results suggested that Aβ(1-42) prepared in F12 aggregated much faster and could lead to the production of larger, less toxic forms over time. As experiments using cell cultures were planned to last up to 96h it was necessary to use Aβ(1-42) that produced more stable oligomers. Based on the results from western blotting and ThT assay, Aβ(1-42) in HEPES was therefore chosen for NT2.N/A, NT2.A and primary culture treatments.

Chapter 3: Astrocyte-neuron metabolic coupling

3.1   Introduction

Hypometabolism of the brain in AD has been widely accepted as one of the earliest signs of the disease. Changes in brain metabolism appear decades before any symptoms or pathological lesions. As astrocytes are essential for neuronal survival and are responsible for supply of metabolites to neurons from the blood stream, it is essential to investigate the astrocyte-neuron metabolic coupling in terms of AD onset and progression.

The astrocyte-neuron lactate shuttle (ANLS) was first described in 1994 by Pellerin and Magistretti and has since been extensively studied (Pellerin and Magistretti, 2012). In principle, the hypothesis states that glutamate release from neurons triggers a metabolic cascade which results in the production of lactate in astrocytes (Fig. 3.1). Lactate is then released for neurons to take up and use as an energy source during high activity associated with synaptic transmission (Pellerin and Magistretti, 2012).

In neurons, the release of glutamate leads to the activation of AMPA receptors and generation of excitatory postsynaptic potential by Na^+ entry. Depolarization leads to further Na^+ entry that activates the Na^+/K^+ ATPase, thus increasing the neurons' energy demand. Neuronal ATP is derived from oxidative phosphorylation and causes reduced nicotinamide adenine dinucleotide (NADH) levels in mitochondria to drop (Kasischke et al., 2004). Subsequent increases in the activity of the TCA cycle leads to an increase in NADH levels that support ATP production. This increase in TCA cycle activity leads to a drop in cytoplasmic pyruvate levels, which further enhances uptake of glucose and lactate (Pellerin and Magistretti, 2012).

91

In astrocytes, glutamate is taken up via the glutamate transporters GLAST and GLT-1. Glutamate is cotransported with Na^+ ultimately leading to a buildup of intracellular sodium levels and activation of Na^+/K^+ ATPase. This pump requires ATP which is provided by membrane-bound glycolytic enzymes (such as phosphoglycerate kinase; PGK) which in turn enhance aerobic glycolysis. An increase in aerobic glycolysis initially causes a large increase in cytosolic NADH (Pellerin and Magistretti, 2012). However, in order to maintain the glycolytic rate the cofactor nicotinamide adenine dinucleotide (NAD^+) has to be regenerated. Normally this takes place in mitochondria via the malate/aspartate shuttle which oxidizes NADH to NAD^+. However, astrocytes appear to lack key components of that shuttle and instead use the conversion of pyruvate to lactate by lactate dehydrogenase (LDH) to regenerate NAD^+ (Pellerin, 2008). Lactate is then released via monocarboxylate transporters (MCT1 and 4) and taken up by neurons via MCT2.

During prolonged stimulation, extracellular glucose levels may be too low to sustain a constant supply of energy. Hence, neurons rely upon astrocytes to meet their energetic needs. Indeed, astrocytes are the only cells in the brain that can store glycogen and it has been shown that during sustained stimulation astrocytes can produce lactate from glycogen to support the high energy demands of neurons (Pellerin and Magistretti, 2012).

3.1.1 Astrocytes and neuronal support

In the brain, neurons and astrocytes form a complex and symbiotic network. Astrocytes have long been thought to be responsible for supply of energy substrates to neurons from the blood stream (Andriezen, 1893).
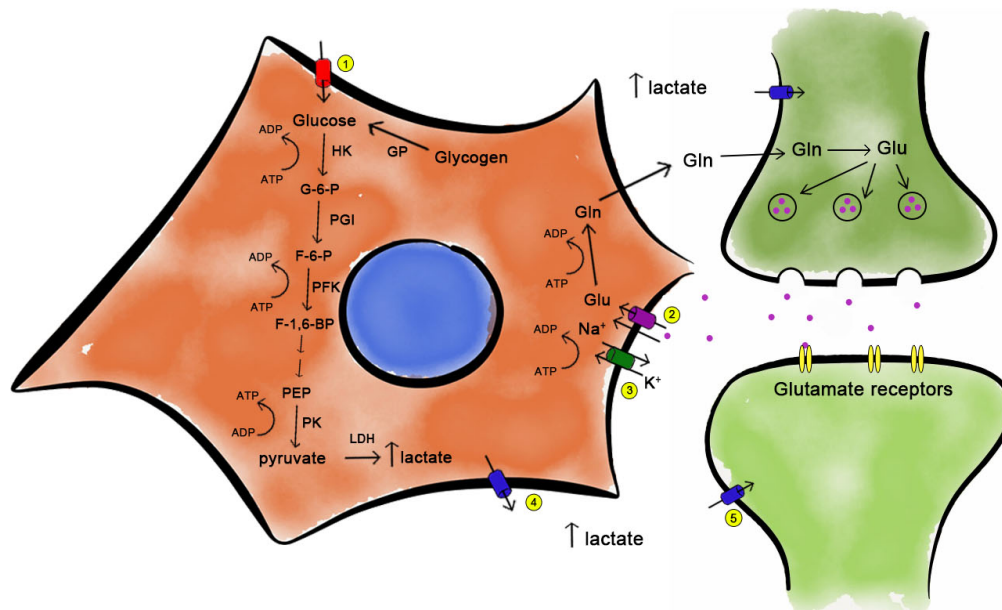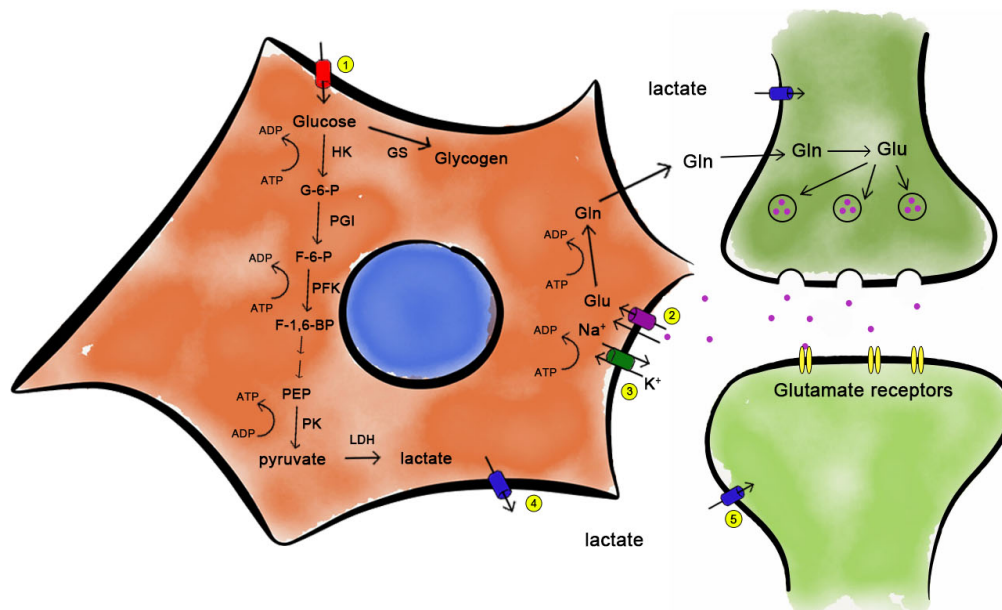
Figure 3.1 Schematic diagram of the ANLS at A) high brain activity and B) low brain activity. Release of glutamate from presynaptic terminal, triggers its uptake into astrocytes via glutamate transporters. Na$^+$, which is cotransported with glutamate, is then removed from astrocytes via Na$^+$/K$^+$ ATPase. This process is energy dependent and triggers glucose uptake or glycogen breakdown and glucose subsequent metabolism into lactate. Lactate is then released from astrocytes into the synaptic cleft via MCT1/4 and taken up by neuron via MCT2. Lactate acts as energy source in neurons during high-energy requirements associated with synaptic transmission. During low activity some of the glucose taken up by astrocytes is used to synthesize glycogen. 1) **GLUT1** (glucose transporter); 2) **GLAST/GLT-1** (glutamate transporter); 3) **Na+/K+ ATPase**; 4) **MCT1/4** (lactates transporter); 5) **MCT2** (lactate transporter).

Indeed, these cells have a very specialized morphology, which allows them to sense and respond to changes in their environment (Allaman et al., 2011). Astrocytes extend multiple processes that ensheath synapses or form so called 'end feet' that surround blood vessels. These structures possess specific glucose transporters GLUT1 that allow astrocytes to take up glucose from blood stream and then either provide it to the extracellular space or store it as glycogen (Magistretti and Allaman, 2007). Astrocytes have been shown to be critical in maintaining moderate levels of glucose in brain extracellular spaces (i.e. 0.5-1.5mM) (Abi-Saab et al., 2002).

Astrocytes also play an important role in many homeostatic processes, such as oxidative stress defence, glycogen storage, tissue repair, synapse remodeling and many more (Stevens, 2008, Belanger and Magistretti, 2009). They form a syncytium via gap junctions (Giaume et al., 2010) for extracellular homeostasis which includes Ca^{2+}, K^+, glutamate and glucose buffering (Tabernero et al., 2006). Additionally, astrocytic coupling contributes to the energetic support of neurons. Astrocytes also express glutamate transporters as well as glutamine synthase which make them an essential component in glutamate recycling during synaptic activity (Benarroch, 2005).

3.1.2 Characteristics of metabolism in neurons and astrocytes

Astrocytes and neurons exhibit different characteristics in terms of their energy metabolism. Results from enzymatic studies and transcriptomic studies all suggest the prevalence of glycolysis and the glycogen pathway in astrocytes and utilization of lactate in neurons (Hyden and Lange, 1962, Lovatt et al., 2007). In particular, expression of different lactate dehydrogenase (LDH) and monocarboxylate transporter (MCT) isoforms in neurons and astrocytes favour this view (Bittar et al., 1996, Pellerin et al., 2005). At the same time astrocytes do exhibit oxidative potential

that is comparable to neurons (Pellerin and Magistretti, 2012). Lovatt *et al.* (2007) showed that astrocytes express high levels of mRNA encoding TCA cycle enzymes, even though the same study provided evidence supporting ANLS.

Neurons also exhibit glycolytic activity (Bittner et al., 2010). However, glycolysis in neurons is reduced to a minimum due to continuous degradation of the 6-phosphofructo- 2 – kinase/fructose 2,6-biphosphatase, isoform 3 (PFKFB 3) which is an enzyme that activates phosphofructokinase (a rate-limiting enzyme involved in glycolysis) (Herrero-Mendez et al., 2009). In neurons, glucose is mainly metabolized through the pentose phosphate pathway that produces reducing equivalents which are then used in the removal of ROS (Pellerin and Magistretti, 2012). It has been shown that upregulation of PFKFB3 in neurons by either inhibition of Cdh1 (involved in proteasomal degradation of PFKFB3) or simply by overexpression of PFKFB3 increases the rate of glycolysis. However, this study also showed that the flow of glucose through pentose phosphate pathway was decreased, which led to increases in oxidative stress and apoptosis in neurons (Herrero-Mendez et al., 2009). In astrocytes, glycolysis is favoured as these cells demonstrate low expression levels for essential components of the malate-aspartate shuttle in mitochondria (Xu et al., 2007). The importance of glucose utilization in astrocytes and oxidative phosphorylation in neurons has been demonstrated by experiments using fluorescent deoxyglucose analogs. These studies have shown greater fluorescence signals in glial cells than neurons (Barros et al., 2009b). An interesting approach has also been used by Kasischke *et al.* (2004). The group used two-photon fluorescence imaging of reduced nicotinamide adenine dinucleotide (NADH) to define metabolic profiles of neurons and astrocytes. This method demonstrated a separate activation of oxidative phosphorylation in neurons and glycolysis in astrocytes (Kasischke et al., 2004).

Neurons and astrocytes also differ in glucose utilization following synaptic activity. While there is an increase in glucose uptake in astrocytes, no increase or even a decrease has been showed in neurons (Loaiza et al., 2003, Chuquet et al., 2010).

Glucose uptake is facilitated by a sodium-independent transport system which can be inhibited by cytochalasin B (Hara et al., 1989) and stimulated by thyroid hormone (Roeder et al., 1985), potassium ions (Brookes and Yarowsky, 1985), glutamate (Pellerin and Magistretti, 1994), endothelin-1 (Tabernero et al., 1996), arachidonic acid (Yu et al., 1993) or phorbol esters (Mudd et al., 1990).

Astroglial cells express hexokinase I which is the primary isoform found in the brain. Following phosphorylation by hexokinase I, glucose-6-phosphate becomes an intermediate form which forms the basis of a number of processes, namely: glycolysis, the pentose phosphate pathway and glycogen metabolism. In astroglial cells, the activity of the pentose phosphate pathway is relatively low but can be increased during oxidative stress (Ben-Yoseph et al., 1994).

3.1.3 Glycogen

Glycogen is a multibranched polysaccharide that acts as the principal storage form of glucose in mammalian systems and can be found in most tissues of the body including the brain (Brown and Ransom, 2007). The main deposits of glycogen can be found in liver and skeletal muscle. When blood glucose levels are normal, excess glucose may be stored as glycogen for when glucose intake is reduced. During periods of starvation glycogen in the liver is metabolized to release glucose (Brown and Ransom, 2007).

The function of glycogen depends on its location. The most widely accepted principle is that liver glycogen is used to supply glucose to the whole body, whilst skeletal muscle glycogen is for use by that tissue. However, recent studies have also shown that during intense exercise systemic blood glucose can drop but lactate levels increase almost tenfold. Under these conditions net lactate transfer switches from an efflux from the brain to a net uptake into the brain (Secher and Quistorff, 2005) which suggests a possible additional role for muscle glycogen (Brown and Ransom, 2007).

Glycogen levels in the brain are lower (6-12µmol) (Cruz and Dienel, 2002) than in liver (100-500µmol) (Brown and Ransom, 2007) and skeletal muscle (300-350µmol) (Chryssanthopoulos et al., 2004) which suggests that brain glycogen is not useful as a source of blood glucose and it seems most probable that it is intended for local use only (Brown, 2004).

3.1.3.1 Location of glycogen in the brain

In the adult brain glycogen is only present in astrocytes (Cataldo and Broadwell, 1986). It can also be stored in embryonic neural tissue (Brown and Ransom, 2007), however, this storage decreases as the neurons mature. The nature of glycogen stored in these cells is unknown, but it has been suggested that at the stage of embryonic development neuronal cells have higher metabolic demands and a less secure glucose supply (Brown and Ransom, 2007).

As glycogen is mainly stored in astrocytes, the enzymes that are involved in its metabolism such as glycogen phosphorylase or glycogen synthase are also found in these cells (Pellegri et al., 1996, Pfeiffer-Guglielmi et al., 2003).

Neurons do not usually store glycogen with the exception of some cells in the brainstem and peripheral nervous system (Sotelo and Palay, 1968). Surprisingly neurons do express glycogen synthase, however, glycogen storage is inhibited by two different mechanisms in these cells. First, is a proteasome-dependent mechanism which involves the malin-laforin complex that degrades glycogen synthase (Vilchez et al., 2007). The second mechanism involves phosphorylation of glycogen synthase. If either of these two mechanisms is modified, this leads to synthesis of glycogen in neurons, which leads to apoptosis. An interesting example is Lafora disease which is characterized by accumulation of glycogen deposits in neurons and results in myoclonus epilepsy. This disease is caused by a mutation in malin-laforin complex which leads to loss of function (Pellerin and Magistretti, 2012).

Glycogen is not evenly distributed evenly throughout the brain. It appears glycogen levels are higher in areas with the greatest synaptic density (Phelps, 1972). However some studies have also found high levels of glycogen in white matter that lacks synapses (Cruz and Dienel, 2002). Overall most studies have found higher levels of glycogen in grey as opposed to white matter (Sagar et al., 1987).

3.1.3.2 Role of astrocytic glycogen

Glycogen levels in the brain are relatively low in comparison to liver and skeletal muscle. In the absence of glucose, glycogen would be consumed within a few minutes (Brown and Ransom, 2007). It is thought that in these cells glycogen serves as an energy source during hypoglycaemia (Brown et al., 2003, Choi and Gruetter, 2003) but also during periods of high brain activity (Brown et al., 2003). Following neuronal activation, the cells release many different astrocytic and vascular mediators, which not only activate astrocytes but also initiate a vascular response which leads to enhancement of cerebral blood flow, which delivers glucose and O_2

(Dienel and Hertz, 2001, Gordon et al., 2008). These intermediates include K^+, glutamate, ammonia, lactate, oxygen, but also NO, H_2O_2 and superoxide (Turner and Adamson, 2011).

However, as active brain tissue has the same metabolic demand as exercising muscle, the demand for energy is instant, and there are many factors, which can affect energy supply (Shulman et al., 2004). Firstly, the signals to increase blood flow are not quick enough to supply glucose and oxygen to the brain. This results in initial shortage of glucose which could limit brain function. As astrocytes are ideally positioned to share substrates with neurons, they use glycogen as an instant energy supply (Brown and Ransom, 2007).

Hexokinase is one of the slower glycolytic enzymes which suggests that the initial glucose phosphorylation can be rate limiting (Brown and Ransom, 2007). However, glycogen phosphorylase demonstrates high activity and can ensure a rapid metabolism of brain glycogen (Shulman et al., 2001). It has been shown that even under normal glucose conditions, stimulation of brain tissue results in rapid breakdown of glycogen (Brown et al., 2003).

Glycogen is metabolized to glucose-6-phosphate (G6P) which can then be converted to lactate and released for neuronal uptake (Dringen et al., 1993a). The expression of the enzyme glucose-6-phosphatase in the brain is controversial. Even though some publications suggest that astrocytes do not express glucose-6-phosphatase (Brown and Ransom, 2007), other studies have demonstrated the presence of glucose-6-phosphatase in astroglial cells (Forsyth et al., 1993) Irrespective of the results, these studies failed to show astrocytic release of glucose derived from glucose-6-phosphate (Wiesinger et al., 1997).

The breakdown of glycogen in astrocytes not only ensures an energy supply to neurons in form of lactate, but also increases levels of glucose-6-phosphate in astrocytes. This in turn reduces the activity of hexokinase I, thus decreasing the phosphorylation of glucose by astrocytes. As such, more glucose from blood may be available for neuronal uptake (DiNuzzo et al., 2010).

It has also been shown that glycogenolysis in astrocytes is important for the astrocyte-neuron lactate transfer during synaptic plasticity and learning (Suzuki et al., 2011). Indeed inhibition of glycogenolysis by 1,4-dideoxy-1,4-imino-d-arabinitol (DAB) leads to a loss of long-term memory (Walls et al., 2008). Additionally, experimental block of lactate transport prevents glycogen from supporting neurons (Brown et al., 2003).

3.1.3.3 Glycogen synthesis

Glucose enters the brain via glucose transporter 1 (GLUT1) on luminal and abluminal sides of endothelial cells (Brown and Ransom, 2007). As endothelial cells have a relatively low metabolic rate, the glucose is not phosphorylated and can pass through them freely (Brown and Ransom, 2007). Astrocytic end feet that are in close proximity to endothelial cells are well positioned to take up glucose when it enters the brain. Astrocytes express GLUT1 (Vannucci et al., 1997) and neurons express GLUT3 (Brown and Ransom, 2007). As both neurons and astrocytes have a high metabolic rate, they phosphorylate glucose immediately, thus trapping it inside the cell (Brown and Ransom, 2007). Glucose-6-phosphate is then converted by phosphoglucomutase into glucose-1-phosphate (G-1-P) which then binds to uridine triphosphate (UTP) forming UDP glucose, which is the source of glycosyl units that are used to build the glycogen molecule. This reaction is catalyzed by UDP glucose pyrophosphorylase (UDPGPP). Glycosyl residues bind to glycogenin which forms a

skeleton of glycogen in the reaction facilitated by glycogen initiator synthase. Subsequently the glycogen is extended by glycogen synthase, which then adds the UDP glucose to the glycogen molecule forming α-1,4-glycosidic bonds. This releases UDP which is then converted to UTP by nucleoside diphosphate kinase. On every 8-10th glucosyl residue an enzyme amylo-(α-1,4-α-1,6)-transglycosylase forms a branch by creating an α-1,6-glycosidic bond. This makes the formation of glycogen more efficient but also allows simultaneous breakdown (Brown and Ransom, 2007).

3.1.3.4 Gluconeogenesis in astrocytes

Glucosyl residues, which are the subunits for building glycogen can be derived from substrates other than just glucose. These include lactate, pyruvate and amino acids such as alanine, serine, threonine, aspartate and glutamate (Wiesinger et al., 1997).

A wide variety of enzymes are required for gluconeogenesis to proceed. These include pyruvate carboxylase (PC), phosphoenolpyruvate carboxykinase (PEPCK), fructose-1,6-biphosphatase (F1,6Pase) as well as the enzymes of the glycolytic pathway. At least the presence of PC and F1,6Pase has been recorded in astrocytes (Wiesinger et al., 1997). It has also been shown that astrocytes from mouse brain are capable of incorporating glycosyl residues derived from labelled [^{14}C] lactate (Dringen et al., 1993b) or alanine, aspartate or glutamate (Schmoll et al., 1995) into glycogen.

3.1.3.5 Glycogen breakdown

The breakdown of glycogen is independent of glycogen synthesis. It involves glycogen phosphorylase which cleaves α-1,4-glycosidic bond realeasing glucose-1-phospate. This reaction proceeds until only four glycosyl units are left before a branch. Then another enzyme, oligo-(α-1,4-α-1,4)-glucantransferase removes the

last three glucosyl units and attaches them to a different end of the glycogen molecule. These units are then released by the action of glycogen phosphorylase. The last remaining glucosyl unit before the branch is removed by amylo-α-(1,6)-glucosidase which releases units as glucose (Brown and Ransom, 2007).

3.1.3.6 Glycogen metabolism regulation

The control of the glycogen metabolism is essential for brain function. The regulation of glycogen breakdown and synthesis involves phosphorylation of the two key enzymes, glycogen synthase and glycogen phosphorylase. Glycogen synthase exists in two forms; the phosphorylated form (GSb) which is inactive and a dephosphorylated active form (GSa). Dephosphorylation of GS is controlled by a family of phosphatases. Protein phosphatase 1 (PP1) is expressed at high levels in astrocytes and it binds glycogen through protein targeting to glycogen (PTG) which allows it to dephosphorylate glycogen synthase (Brown and Ransom, 2007).

Glycogen phosphorylase also exists in two forms – phosphorylated active form (GPa) and dephosphorylated inactive form (GPb). Phosphorylation of glycogen phosphorylase is facilitated by phosphorylase kinase (Brown and Ransom, 2007).

There are a number of neurotransmitters and modulators which promote glycogenolysis in astrocytes (Magistretti et al., 1981, Magistretti et al., 1986) These include noradrenaline (NA), vasoactive intestinal peptide (VIP) and adenosine. In addition, IGF I, IGF II and insulin increase glycogen levels in the brain by acting on insulin receptors. Activation of receptor tyrosine kinase phosphorylates protein PP1 which in turn activates glycogen synthase (Dent et al., 1990). NA and VIP act by elevating levels of cyclic AMP (Sorg and Magistretti, 1992). Additionally, an increase in Ca^{2+} can induce glycogen breakdown. Increased Ca^{2+} and cyclic AMP levels also

act on phosphorylase kinases which activate glycogen phosphorylase (Wiesinger et al., 1997).

3.1.4 Lactate

Production of lactate is not only important in supporting neurons but also astrocytes. As mentioned above astrocytes show low expression of components of mitochondrial aspartate/glutamate carrier which reduces their ability to regenerate NAD^+ through malate/aspartate shuttle (Pellerin and Magistretti, 2012). Instead, NADH is converted to NAD^+ during conversion of pyruvate to lactate by lactate dehydrogenase (Pellerin and Magistretti, 2012).

Monocarboxylate transporters play a key role in influx and efflux of lactate (Aubert et al., 2005). There are three known transporters, MCT1, MCT2 and MCT4 and one sodium-dependent transporter named sMCT1 (Martin et al., 2006). These different transporters are cell specific. MCT1 is mainly expressed in endothelial cells in blood vessels and on astrocytes and oligodendrocytes (Gerhart et al., 1997). MCT2 is specific for neurons and it is mainly found on axons and dendrites (Pierre et al., 2002). Dendritic spines appear especially enriched in this transporter (Bergersen et al., 2001). MCT4 is only expressed on astrocytes with most transporters concentrated on processes that are in close proximity to synapses (Pellerin et al., 2005). MCTs are also expressed in the neonatal blood brain barrier but the expression of these transporters decreases with time (Pellerin et al., 1998).

The transporters differ in their affinity for lactate. MCT2 is a high-affinity transporter with a Km of 0.7mmol/L, whilst MCT1 and MCT4 are both low-affinity transporters with a Km of 3.5 and 34mmol/L respectively (Pellerin and Magistretti, 2012). This low affinity for lactate leads to extrusion and very rarely uptake of lactate at normal

extracellular levels of ~2.5mM (Turner and Adamson, 2011). However, at higher levels of lactate (5 to 8mM) astrocytes may increase their uptake from the extracellular space (Turner and Adamson, 2011).

LDH isoforms also display cell type specificity and are expressed by different cell types. The isoform LDH-5 that is encoded by the LDHA gene is found in astrocytes whilst the LDH-1 isoform which has 4 subunits encoded by LDHB gene is expressed in neurons (Bittar et al., 1996, O'Brien et al., 2007). Neuronal LDH-1 tends to facilitate lactate to pyruvate conversion, while LDH-5 in astrocytes conversion of pyruvate to lactate (O'Brien et al., 2007).

This differential localization of MCTs as well as the cell specific expression of different isoforms of LDH favours the concept that lactate is produced and released from astrocytes and taken up by neurons (Pellerin and Magistretti, 2012).

Expression of neuronal MCT2 can be increased by different stimuli such as noradrenaline (NA), insulin, insulin-like growth factor-1 (IGF-1) and brain-derived neurotrophic factor (BDNF) (Chenal and Pellerin, 2007, Chenal et al., 2008, Robinet and Pellerin, 2010). *In vitro* studies have also shown that the translocation of MCT2 to the plasma membrane can be affected by exposing cortical neurons to glutamate and glycine (Pierre et al., 2009). As changes to expression and location of MCT2 appear to occur very quickly, they probably represent a process by which neurons adapt to their energetic needs (Pellerin and Magistretti, 2012). Studies on synaptic plasticity have shown that GluR2, which is known to be involved in synaptic plasticity at glutaminergic synapses (Isaac et al., 2007), interacts with MCT2 (Pierre et al., 2009). It has also been found that MCT2 affects the distribution and expression of GluR2 which supports the idea that energy supply is tightly linked to synaptic plasticity (Maekawa et al., 2009). Disruption of MCT4 expression can induce loss of

long-term memory. This effect is rescued by administration of lactate but not glucose. However, when the neuronal lactate transporter MCT2 was blocked the loss of long-term memory could not be rescued by administration of lactate (Suzuki et al., 2011).

Lactate has been found to be preferred by neurons over glucose as an oxidative energy substrate (Bouzier-Sore et al., 2003b, Bouzier-Sore et al., 2006, Ivanov et al., 2011). This preference appears to be inefficient as one molecule of lactate can only yield 17 ATPs during TCA cycle whilst glucose yields 31 molecules of ATP. However, lactate cannot substitute glucose completely and fulfill all neuronal requirements such as flux through glycolysis or pentose phosphate shunt (Dienel, 2010). Nevertheless, lactate has been shown to be important in many different mechanisms such as control of respiration (Erlichman et al., 2008), neurovascular coupling (Gordon et al., 2008), recovery from hypoxia (Schurr et al., 1997) and neuroprotection (Berthet et al., 2009).

3.1.5 Glutamate

More than 85% of the neurons within the cortex are glutamatergic. As such glutamate represents a major neurotransmitter within this region (Magistretti, 2009). At the postsynaptic sites glutamate can interact with three types of receptors. The A-amino-3-hydroxy-5-methylisoxazole-4-propionic acid (AMPA) receptor changes sodium permeability upon glutamate binding. In comparison the N-methyl-D-aspartate (NMDA) receptor affects both calcium and sodium permeability which invokes excitatory postsynaptic potential. The third type of receptors is the metabotropic glutamate receptor which modifies changes in calcium signaling through GTP-mediated processes (Magistretti, 2009). The action of glutamate is terminated by the uptake of glutamate by astrocytes (Danbolt, 2001). As glutamate is highly toxic and its accumulation can lead to excitotoxicity (Sattler and Tymianski, 2001), it is

essential that the astrocytes remove it from the extracellular space. Glutamate uptake is carried out by glutamate transporters GLT-1 and GLAST which use the extracellular sodium gradient as the driving force. The stoichiometry is that for one molecule of glutamate, astrocytes take up 3 ions of sodium (Magistretti, 2009).

Glutamate also stimulates glucose utilization. Indeed studies have shown that this effect is not receptor mediated as various glutamate receptor agonists and antagonists have no effect (Pellerin and Magistretti, 1994). However, glucose utilization was enhanced after treatment by D-aspartate but not D-glutamate strongly suggesting that the effect is mediated by glutamate transport (Magistretti, 2009). This finding is supported by experiments, which have shown that inhibition of glutamate transporters by threohydroxyaspartate abolishes glucose utilization in astrocytes (Pellerin and Magistretti, 1994).

Uptake of glutamate increases sodium levels inside the cell to such a level that Na^+/K^+ ATPase is activated (Pellerin and Magistretti, 1997, Chatton et al., 2000). More specifically glutamate transporter activation mobilizes α2 subunit of Na^+/K^+ ATPase, which co-localizes and interacts with glutamate transporters (Cholet et al., 2002, Rose et al., 2009). In addition, a specific Na^+/K^+ ATPase inhibitor ouabain completely inhibits glutamate stimulated glucose uptake.

The activation of the Na^+/K^+ ATPase enhances ATP utilization, which in turn stimulates glucose uptake and aerobic glycolysis (conversion of glucose into lactate in the presence of oxygen) (Pellerin and Magistretti, 1994, Pellerin and Magistretti, 1997).

There are several pathways by which astrocytes utilize glutamate after its uptake. Glutamate can be used as a metabolic intermediate in the TCA cycle. During this process astrocytes convert it into α-ketoglutarate in a process mediated by either

glutamate dehydrogenase or aspartate amino transferase. In both cases α-ketoglutarate can then enter TCA cycle (Magistretti, 2009).

Another pathway for glutamate in astrocytes is conversion into glutamine in process facilitated by glutamine synthase, which is almost exclusively localized in astrocytes. Additionally, astrocytes can use α-ketoglutarate and amino groups from leucine to form glutamate which is then converted into glutamine (Magistretti, 2009). Glutamine is then released by astrocytes and taken up by neurons where the enzyme glutaminase hydrolyzes it back to glutamate thus maintaining the glutamate pool in neurons.

Glutamate is also a substrate that can be utilised in the glutathione (GSH) synthesis pathway and therefore an important component of the antioxidant system. Metabolism of GSH involves two ATP-requiring steps. The first step is catalyzed by glutamate-cysteine ligase (GLC) which uses glutamate and cysteine to form γ-glutamylcysteine (γGluCys). This dipeptide is then combined with glycine by the action of glutathione synthetase (GSS) (Fernandez-Fernandez et al., 2012).

As presented in this chapter metabolic coupling between neurons and astrocytes involves many complex mechanisms. To date this hypothesis has only been tested in models derived from animals. As such relevant human models are required to study the complex cross-talk that occurs between these metabolically distinct cell types

3.1.6 Aims and objectives of the study

The aim of this chapter was to investigate the metabolic properties of NT2.N/A and NT2.A cultures and establish whether they demonstrate signs of metabolic coupling that could be perturbed in AD. The expression of the main components of the ANLS

was investigated as well as the ability to store glycogen by NT2.A cultures. The responses of the astrocytic network to known neuromodulators such as glutamate, potassium and dbcAMP were tested, in terms of glucose uptake and glycogen turnover. Finally, in order to establish whether NT2-derived astrocytes provide metabolic support to their neuronal counterparts, the modulation of glycogen was investigated during electrical stimulation

3.2   Materials and Methods

3.2.1   Cell culture

3.2.1.1 NT-2/D1 cells

Human teratocarcinoma NT2/D1 cells used in this study were kindly donated by Professor Andrews (University of Sheffield, UK).   The cells were cultured in Dulbecco's Modified Eagle Medium (DMEM) Glutamax high glucose, with pyruvate (Life Technologies, UK) containing 10% heat inactivated foetal bovine serum (Life Technologies, UK), 100 units/ml penicillin and 100 µg/ml streptomycin. NT2/D1 cells were differentiated according to the method described by Woehrling *et al.* (2007). Briefly, following treatment with 10µM retinoic acid for 4 weeks, NT2 cells were replated after scraping into fresh 75cm flasks at a lower density (1:3) in RA free medium. After 2 days neuronal clusters were detached from undifferentiated cells by sharp striking of the flasks against the palm of the hand. Cells were then plated into CellBIND 12-well plates (Corning, USA). After 2 days cells were treated with mitotic inhibitors to suppress the proliferation of non-neural cell types. To generate an NT2.N monoculture cells were treated with 1 µM cytosine arabinoside (ARAC), 10 µM fluorodeoxyuridine (FDU) and 10 µM uridine (U) for 1 week followed by 10 µM fluorodeoxyuridine (FDU) and 10 µM uridine (U) for a further 2 weeks. To produce NT2.N/A co-cultures, cells were treated with 0.1 µM cytosine arabinoside (ARAC) 3 µM fluorodeoxyuridine (FDU) and 5 µM uridine (U) for 10 days followed by 3 µM fluorodeoxyuridine (FDU) and 5 µM uridine (U) for a further 18 days. After this period cells were fed twice a week in normal DMEM without mitotic inhibitors and used within 1 month.

Cultures of NT2 astrocytes were isolated from co-cultures according to the method developed by Woehrling *et al.* (2010). NT2.N/A cells were washed 3 X using PBS

and then dissociated using Accutase (PAA laboratories, UK). Large NT2.N aggregates settled quickly leaving a single cell suspension containing astrocytes that were replated into a CellBIND 12 well plate (Corning, USA). After incubation for 4h any remaining NT2.N cells were washed off the more adherent NT2.A cells using media. All cells were maintained by incubation at 37°C in a humidified atmosphere of 5% CO_2.

3.2.1.2 Cell treatment

During experiments cells were maintained in Krebs-Ringer's-HEPES buffer (115mM NaCl, 5mM KCl, 1mM $MgCl_2$, 24mM $NaHCO_3$, 2.5mM $CaCl_2 \bullet 2H_20$, 25mM HEPES supplemented with 5mM glucose) unless otherwise stated. For the experiments cells were treated with 10µM 1,4-dideoxy-1,4-imino-d-arabinitol (DAB; Sigma-Aldrich, UK), 1mM dbcAMP (Tocris, USA), 100µM isoproterenol (Tocris, USA), 1mM or 0.5mM L-glutamic acid (Sigma-Aldrich, UK), 60mM or 15mM potassium chloride (Sigma-Aldrich, UK), 100µM ouabain (Tocris, USA) and 100µM DL-*threo*-β-benzyloxyaspartic acid (TBOA; Tocris, USA)

3.2.2   Immunohistochemistry
3.2.2.1 GFAP / β-tubulin-III staining

The cells cultured on coverslips were washed with PBS and fixed for 10 minutes with 4% paraformaldehyde. Following fixation coverslips were washed twice with PBS and permeabilized with 0.2% Triton/PBS. Cells were then incubated in 2% BSA/0.2%Triton/PBS for 1 hour to block non-specific binding of antibody. Subsequently, cells were incubated with different primary antibodies for 1 hour at RT. The following primary antibodies were used: mouse anti-GFAP (clone GA5 Millipore, 1:500) and rabbit anti-β-tubulin-III (Abcam, UK, 1:500).   Following incubation,

coverslips were washed three times in 2% BSA/0.2%Triton/PBS and then incubated with donkey anti-mouse Rhodamine (1:200, Jackson Immunoresearch, Europe) and goat anti-rabbit FITC (1:200; Jackson Immunoresearch, Europe).

After washing the nuclei were visualized by Hoechst 33342 staining (Life Technologies, UK) for 15 minutes and mounted with ProLong® Gold Antifade Reagent (Life Technologies, UK). The cells were examined using the Zeiss LSM510 confocal laser-scanning microscope and Zeiss Axiovert 200M fluorescent microscope.

3.2.2.2 Glycogen staining

Cytologic localization of glycogen was determined using the periodic acid-Schiff method (Rosenberg and Dichter, 1985). Briefly, the cells cultured on coverslips were washed with ice-cold PBS and fixed for 5 minutes at room temperature in methanol. After fixation coverslips were washed three times with 70% (vol/vol) ethanol. Next the cells were incubated for 30 minutes at room temperature with 1% (wt/vol) periodic acid dissolved in 70% ethanol. After incubation cells were washed three times with 70% ethanol and stained for 60 minutes at room temperature with 0.5% (wt/vol) basic fuchsin (Sigma-Aldrich, UK) dissolved in acid ethanol (ethanol/water/concentrated HCl, 80:19:1). Cells were then washed three times with 70% ethanol and the coverslips were counterstained for GFAP/Oct-4 as described in section 3.2.2.1 or directly examined using the Zeiss LSM510 confocal laser-scanning microscope and Zeiss Axiovert 200M fluorescent microscope.

3.2.3 Gene expression analysis

3.2.3.1 RNA extraction

RNA was isolated from undifferentiated NT2/D1 cells as well as treated/untreated NT2.N/A co-cultures. RNA was extracted from samples using Trizol® Reagent (Life Technologies, UK), chloroform and isopropanol (Fisher, UK). DNA was then precipitated by 75% ethanol and diluted in RNA-free water.

RNA was subsequently purified using RNeasy Mini Kit (QIAGEN, UK) in accordance with the manufacturer's instructions, and subsequently quantified using the Nanodrop 1000 (Thermofisher, UK).

3.2.3.2 Real-time RT-PCR

1 µg of total RNA was reverse transcribed by reverse transcriptase (Primer Design, UK) and oligo dT_{15} primers (Primer Design, UK). Real-Time PCR: cDNAs were amplified in a standard 40-cycle SYBR® green real-time PCR reaction using prevalidated primers for GLUT1, GLUT3, MCT2, MCT4, MCT1, GLT-1, GLAST and GLUL according to the manufacturer's instructions. The house keeping genes UBC, B2M, EIF4A2 and C14orf133 (supplied by PrimerDesign Ltd, UK) were assayed under the same conditions as above. The expression of UBC was found to be unchanged under the conditions imposed and was therefore used in the normalisation of qRT-CR data. Cycling conditions were as follows: 10min at 95°C, 15s at 95°C and 1min at 60°C for 40 cycles, 30s at 95°C, 30s at 55°C and 30s at 95°C. Fold changes >2 fold were considered significant.

3.2.4 Fluorescent glucose analogue 6-NBDG uptake

Uptake of the glucose analogue 6-NBDG in NT2.N/A and NT2.A cultures under various conditions was investigated using methods previously described (Loaiza et al., 2003). Briefly, before the measurement, culture medium was removed and cells were washed with Krebs'–Ringer HEPES (KRH) buffer supplemented with 5mM glucose. Then glucose in the medium was reduced to 0.5mM and cells were incubated for 5 min. Subsequently, the buffer in each well was changed to KRH buffer with 0.5mM glucose, 300µM 6-NBDG and treatments: 1mM glutamate (Sigma-Aldrich, UK), 20µM cytochalasin B (Sigma-Aldrich, UK), 1mM glutamate and 20µM cytochalasin B, 1mM glutamate and 100µM ouabain (Tocris, USA). Cultures were excited at 488 nm and imaged at 505–550 nm emission at 60min, 180min and 360min. The plate was read using SpectraMAX GeminiXS microplate luminometer (Molecular Devices, UK) and SoftMaxPro software.

3.2.5 Determination of glycogen levels

The method used to determine levels of glycogen in biological samples was previously described by Nahorski and Rogers (1972). It is an enzymatic reaction and is based on the breakdown of the glycogen into glucose by the enzyme amyloglucosidase. Subsequently, glucose undergoes phosphorylation by hexokinase in the presence of ATP. The third step involves oxidation of glucose 6-phosphate to gluconate-6-phosphate by glucose-6-phosphate dehydrogenase (G6P-DH). Fluorescence of the NADPH formed in the final reaction is then read on a fluorometer (excitation: 340 nm; emission: 450 nm). This method allows measurement of glycogen as well as glucose and glucose-6-phosphate in cell lysate according to the enzymes added.

$$\text{glycogen} + H_2O \xrightarrow{\text{Amyloglucosidase}} \text{glucose}$$

$$\text{glucose} + \text{ATP} \xrightarrow{\text{Hexokinase}} \text{glucose-6-phosphate} + \text{ADP}$$

$$\text{glucose-6-phosphate} + \text{NADP}^+ \xrightarrow{\text{G6P-DH}} \text{gluconate-6-phosphate} + \text{NADPH} + H^+$$
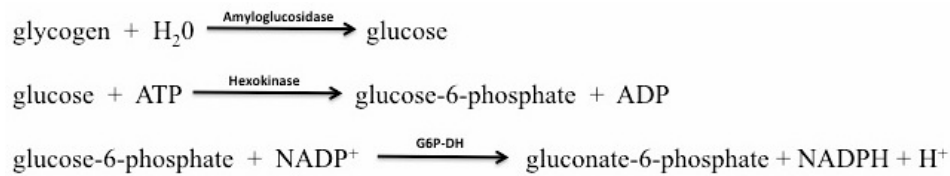
3.2.5.1 Sample preparation

NT2.N/A cultures were prepared as described in section 3.2.1.1. Cultures plated on 12-well plates were then exposed to a range of reagents described in section 3.2.1.2. Next plates were incubated for 60min and 180min in DAB and hypoglycaemic conditions, 180min during dbcAMP and isoproterenol treatment and 60min during potassium and glutamate treatments. Following the treatment cells were washed three times with ice-cold PBS and then scraped in 300µl of 30mM ice-cold HCl. Subsequently, samples were sonicated for 15 seconds and used for the glycogen assay (section 3.2.5.2) and protein determination (section 3.2.5.3).

3.2.5.2 Protocol

The assay was adapted to a 96-well plate (Sigma-Aldrich, UK). Two 10µl aliquots of cell lysate were sampled. To the first aliquot 30µl of acetate buffer (0.1M, pH 4.65) was added. To the second 30µl of 0.1mg/ml of amyloglucosidase (Sigma-Aldrich, UK) in acetate buffer was added. Both samples were incubated for 30min at room temperature. After incubation 200µl of Tris-HCl buffer (0.1M, pH 8.1) containing MgCl$_2$ (3.3 mM), ATP (0.33mM), NADP (38µM), hexokinase (4µg/ml) and glucose 6-phosphate dehydrogenase (2µg/ml) were added to both aliquots and incubated for 30min at room temperature. The third aliquot was used to determine the protein concentration (section 3.2.5.3)

Standards were prepared using a solution of glucose (1mg/ml; Sigma-Aldrich, UK) and 1:2 serially diluted using acetate buffer. Standards were treated as the first aliquot i.e. without amyloglucosidase treatment.

The plate was then read using SpectraMAX GeminiXS microplate luminometer (Molecular Devices, UK) and SoftMaxPro software. The first aliquot gives the sum of glucose and glucose 6-phosphate, and the second the sum of glycogen, glucose and glucose 6-phosphate. In this thesis one mole of glycogen corresponds to one mole of glycosyl units originating from glycogen.

3.2.5.3 Determination of protein levels

The protein concentration of the sample was determined using the BCA assay reagent kit (Thermofisher, UK) in accordance with the manufacturer's instructions. Briefly 25μl of sample, BSA standard (ranging from 25-2000 μg/ml) or 30mM HCl which acted as a BSA-free control were added to a 96-well microplate with the 200 μl of the working reagent (50:1, Reagent A:B). Reaction was then incubated at 37 °C for 30 min and then read at 590nm using a Thermo Multiscan EX 96-well plate reader (Thermofisher, UK).

3.2.6   Determination of lactate levels

A Lactate Assay Kit was used to measure lactate levels (Abcam, UK). The method is based on the oxidation of lactate by lactate oxidase into pyruvate and hydrogen peroxide. The product then interacts with the lactate probe to produce both colour and fluorescence.

3.2.6.1 Sample preparation

NT2.N/A cultures were prepared as described in section 3.2.1.1. Cultures plated on 12-well plates were then exposed to a range of reagents described in section 3.2.1.2. Next, plates were incubated for 60min and 180min in DAB and hypoglycaemic conditions, 180min during dbcAMP and isoproterenol treatment and 60min during potassium and glutamate treatments. Following the treatment cell culture media was collected and used for the lactate assay (section 3.2.6.2).

3.2.6.2 Protocol

Lactate levels were measured in accordance with the manufacturer's instructions. Briefly, the assay was set up in a 96-well microplate. 50µl of media samples were used per well and mixed with 50 µl reaction mix containing 46 µl Lactate Assay Buffer, 2 µl Probe and 2 µl Enzyme Mix. 50µl reaction mix was also added to lactate standards that were prepared at 0, 0.2, 0.4, 0.6, 0.8 and 1.0 nmol/well. The reaction was incubated at room temperature for 30 minutes, protected from light and then read at 570nm using a Thermo Multiscan EX 96-well plate reader (Thermofisher, UK). All readings were corrected for background and lactate concentration was expressed in mM.

3.2.7   Stimulation protocol

Synaptic stimulation was achieved with a computer controlled constant current isolated stimulator (STG1002, Multichannel Systems, Germany) and bipolar electrodes, which were placed within the petri dish. Stimulation was composed of bursts of ten 800µA current pulses delivered at 20Hz every 10s for 30 minutes. Cells were maintained in Krebs-Ringer's-HEPES buffer supplemented with 5mM glucose.

For the inhibition of glutamate uptake cells were pre-treated with 100μM TBOA for 15min and then maintained in Krebs-Ringer's-HEPES buffer, 5mM glucose and 100μM TBOA during stimulation

3.2.8 Statistics

Results were expressed as the mean of three samples ± standard error of the mean (SEM). Comparisons between treatments were performed using analysis of variance (ANOVA) followed by Dunnet's or Tukeys post-test or Students T-test using GraphPad Prism Software. Differences were considered significant for p values <0.05.

3.3   Results

3.3.1   Characterization of NT2.N/A cultures and components of ANLS

As the astrocyte-neuron lactate shuttle (ANLS) has been shown to be involved in memory formation, it is important that models used to investigate Alzheimer's disease and dementia reflect the co-operation of these two cell types. To demonstrate the presence of the ANLS in NT2.D1 derived neurons and astrocyte co-cultures it was essential to establish whether these cells are metabolically competent and demonstrate functional metabolic coupling. NT2.N/A and NT2.A cells were investigated for the expression of the main components of the ANLS, as well as responses of the astrocytic network to known neuromodulators such as glutamate, potassium and dbcAMP as well as inhibitors such as ouabain, catachalasin B and TBOA. In addition, to establish whether NT2-derived astrocytes provide metabolic support to their active neurons, the turnover of glycogen and production of lactate were monitored during electrical stimulation.

NT2/D1 derived neurons and astrocytes were identified microscopically by their characteristic morphology. Following treatment with retinoic acid and replating, the cultures begin to display distinct neuronal and astrocytic morphology. Neurons extend axons and dendrites, and astrocytes with projections appear in close proximity to aggregations of neuronal perikarya and neurites throughout the culture. Under the microscope astrocytes were identified by their flat phase dark appearance, whilst neurons were typically phase bright and often seen on top of the astrocytic monolayer. These cells were further identified using immunohistochemistry for the specific markers GFAP and β-tubulin (Fig. 3.2). To identify glycogen in NT2/D1 derived cultures the periodic acid–Schiff method was used to determine the localization of glycogen in cultures (Nahorski and Rogers, 1972). Glycogen was found to co-localize with GFAP positive cells (Fig. 3.3). No glycogen was found in β-

118

tubulin positive cells or undifferentiated Oct-4 positive NT2 cells (data not shown).

Using realtime PCR, cultures were also characterised for the expression of genes involved in the astrocyte-neuron lactate shuttle following differentiation. Genes included glucose transporters (GLUT1 and GLUT3), monocarboxylate transporters (MCT1, MCT2 and MCT4), glutamate transporters (GLT-1 and GLAST) and glutamine syntethase (GLUL). A comparison of NT2/D1 stem cells with differentiated co-cultures showed a significant upregulation of glutamate transporters (GLAST and GLT-1) and a downregulation of GLUT1, MCT1 and GLUT3, whilst other genes remained unchanged (MCT4/2 and GLUL) (Fig. 3.4A). However, Ct values for all genes tested were relatively low (<30) suggesting a high to moderate expression of these genes (Fig. 3.4B).
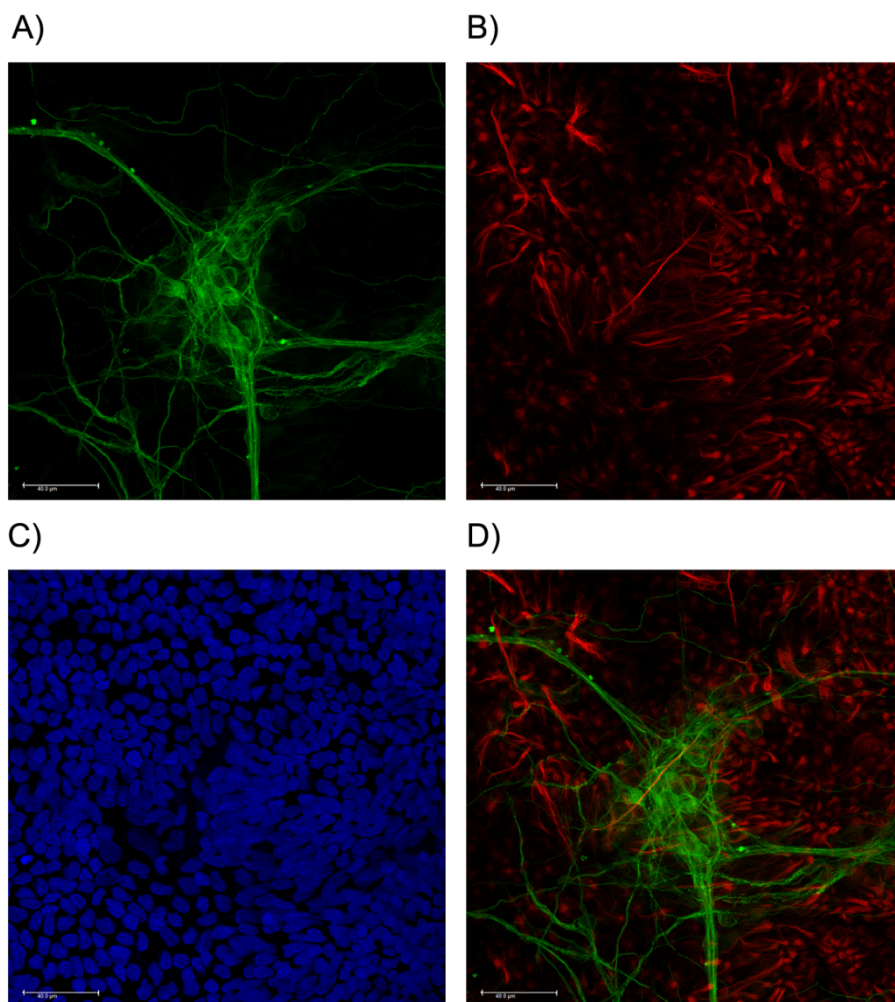
Figure 3.2   Immunofluorescent images of NT2/D1 derived neurons and astrocytes. Images showing: (A) β-tubulin positive neurons (green), (B) GFAP (red) positive astrocytes, (C) nuclei stained with Hoechst 33342, and (D) an overlay of GFAP positive astrocytes and β-tubulin positive neurons (D). Scale bar 40μM**.**
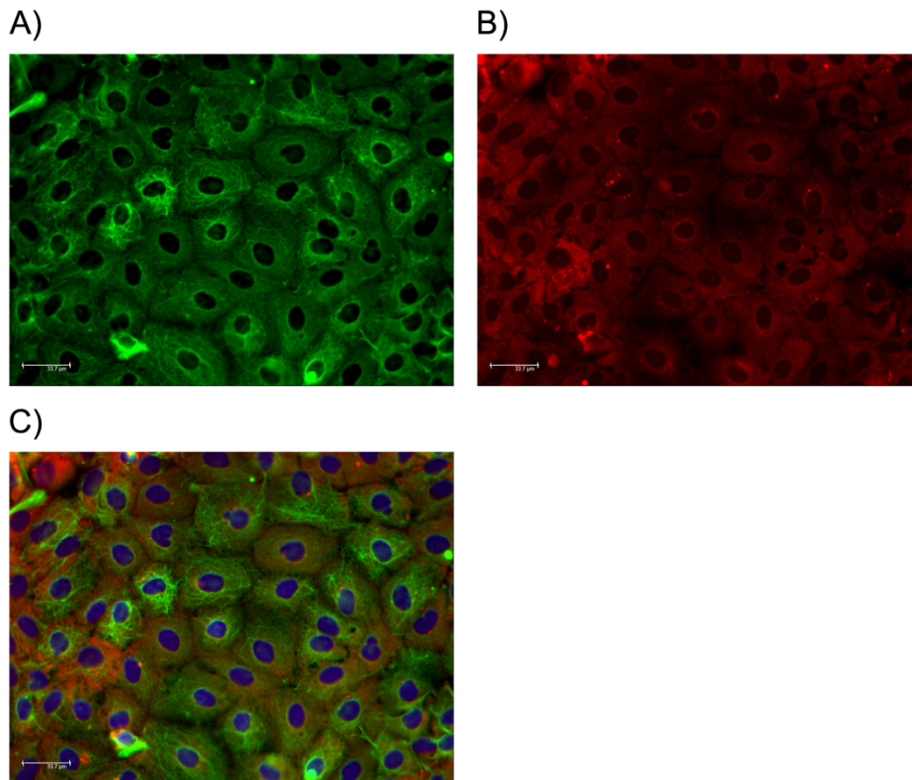
Figure 3.3   Immunofluorescent images of NT2/D1 derived astrocytes. Images showing: (A) GFAP (green) positive astrocytes and staining for (B) glycogen (red) using the periodic acid Schiff assay. (C) Representative image of co-localisation of glycogen and GFAP (yellow) with nuclei Hoechst 33342 staining (Blue). Scale bar 33.7µM.

A)
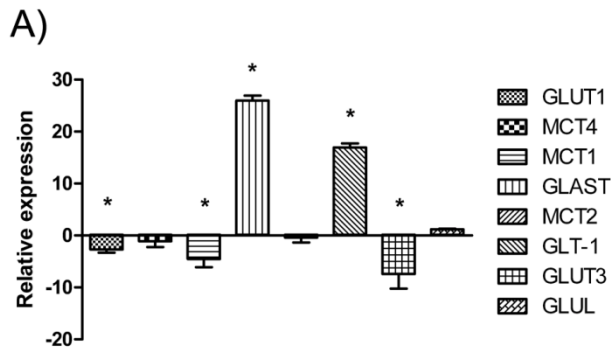
B)

Gene	Ct value ± SEM
GLUT1	19.96 ± 0.54
MCT4	19.97 ± 0.52
MCT1	16.25 ± 0.58
GLAST	16.15 ± 0.28
MCT2	22.35 ± 0.54
GLT-1	17.12 ± 0.42
GLUT3	16.25 ± 0.63
GLUL	14.51 ± 0.27
UBC	14.69 ± 0.26

Figure 3.4   mRNA expression in NT2/D1 derived neurons and astrocytes in comparison to undifferentiated NT2/D1 stem cells. mRNA expression of Glut1, Glut3, MCT2, MCT4, MCT1, GLT-1, GLAST and GLUL as well the house keeping gene UBC. Results are expressed as A) the average fold change ± SEM (n=3) and considered significant above 2-fold change B) Ct values ± SEM (n=3).

3.3.2 Glutamate stimulates uptake of fluorescent glucose analogue 6-NBDG in NT2.N/A cultures

Utilization of glucose in NT2.N/A and NT2.A cultures was monitored using a fluorescent glucose analog 6-NBDG. In control cultures dye accumulated 1.68 fold ± 0.165 over 360min. Following the treatment of the co-cultures with glutamate for 180min (Fig. 3.5A) 6-NBDG uptake increased 2.09 fold ± 0.144 ($p<0.01$) and 3.06 fold ± 0.197 ($p<0.001$) after 360min. The uptake of 6-NBDG induced by glutamate was completely blocked by ouabain, a Na^+/K^+ ATPase inhibitor, at all 3 time points with most significant difference at 360min (glutamate: 3.06 fold ± 0.197; glutamate/ouabain: 1.31 fold ± 0.07, $p<0.001$). Similarly treatment with cytochalasin B, a potent inhibitor of GLUT1 and GLUT4 mediated glucose uptake, blocked the uptake of 6-NBDG at all time points (Fig. 3.5A). At 360 minutes uptake of glucose in cultures with glutamate was increased 3.06 fold ± 0.197 whilst treatment with glutamate and cytochalasin B only increased 1.83 fold ± 0.13, $p<0.01$. Similar results were also obtained in pure astrocyte cultures, with glutamate significantly increasing 6-NBDG uptake and ouabain and cytochalasin B inhibiting uptake (Fig. 3.5B).

3.3.3 Hypoglycaemia and neuromodulators stimulate turnover of glycogen and production of lactate

Lactate release and glycogen levels were measured under hypoglycaemic conditions. In order to block glycogen breakdown, cells were also treated with 1,4-dideoxy-1,4-imino-d-arabinitol (DAB), a selective inhibitor of glycogen phosphorylase. Under hypoglycaemic conditions (Fig. 3.6A), cultures released significant amounts of lactate (60min: 0.25 ± 0.03, $p<0.01$; 180min: 0.42 ± 0.05mM, $p<0.01$) in comparison to undetectable levels at time 0 min. In addition, glycogen levels were decreased to 90.62 ± 2.33% at 60min, $p<0.05$ and 74.23 ± 4.48% at 180min, $p<0.01$ (Fig. 3.6B)

compared with the control at 0min. DAB treatment reduced the release of lactate in comparison to cell without DAB treatment but the decrease was only significant at 180min (0.24 ± 0.02, p<0.05). Breakdown of glycogen was completely blocked by DAB treatment (60min: 102.57 ± 1.28%, p<0.05; 180min: 103.27 ± 0.025%, p<0.01) in comparison to cells without DAB treatment.

Treatments with known modulators of glycogen phosphorylase, dbcAMP and the β_1 and β_2 adrenergic agonist isoproterenol induced a significant decrease in glycogen levels in comparison to non-treated control (dbcAMP: 70.72 ± 2.92%, p<0.001; isoproterenol: 77.43 ± 1.54%, p<0.001) (Fig. 3.7B). In comparison, lactate levels following exposure to dbcAMP did not show any significant increase (control: 0.77 ± 0.05mM; dbcAMP: 0.83 ± 0.06mM) whilst isoproterenol treatment resulted in a significant decrease in lactate levels to 0.42 ± 0.03mM, p<0.01 in comparison to control at 0.77 ± 0.05mM (Fig. 3.7A).

3.3.4 Glutamate and potassium stimulate glycogen breakdown and lactate production in NT2.N/A co-cultures

In order to investigate activation of the Na^+/K^+ ATPase by glutamate, cultures were exposed to glutamate in the presence and absence of ouabain (Fig. 3.8). The treatment of the cultures with glutamate increased the lactate levels (1mM glutamate: 0.26 ± 0.01mM p<0.05) but the increase was only significant at the higher concentration of glutamate (Fig. 3.8A). Incubation with both 1mM glutamate and ouabain blocked the release of lactate (1mM glutamate: 0.26 ± 0.01mM; 1mM glutamate + ouabain: 0.18 ± 0.02mM, p<0.01) and reduced the values to control levels (control: 0.21 ± 0.01mM).
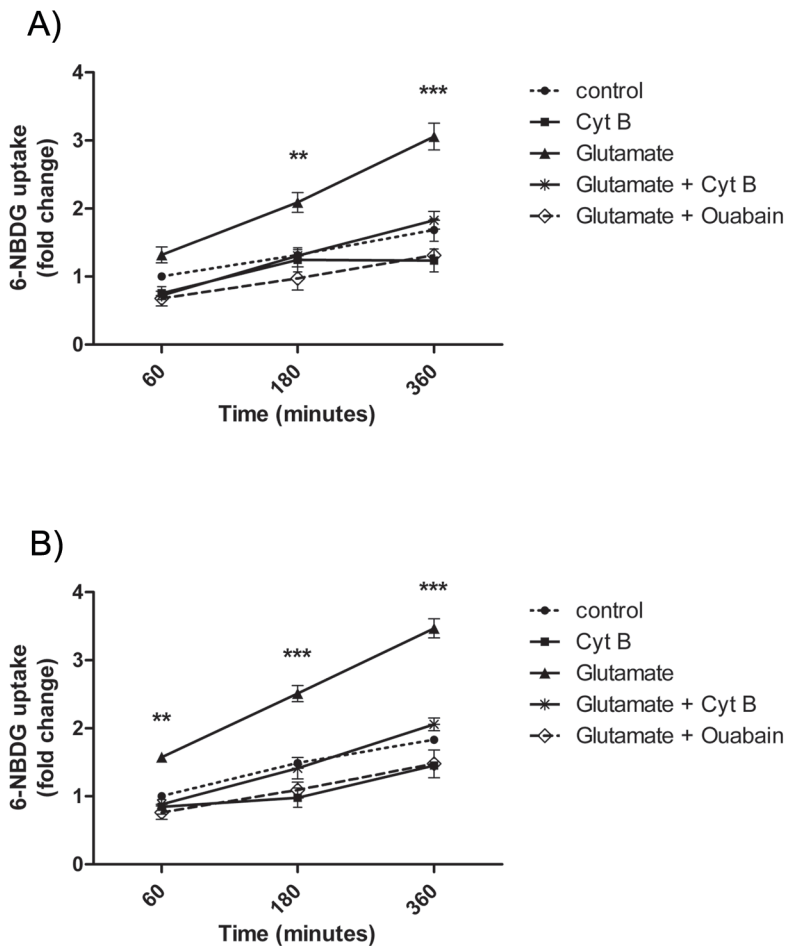
Figure 3.5 Glutamate stimulates uptake of fluorescent glucose analogue 6-NBDG. A) NT2/D1 derived neuron and astrocyte co-cultures and B) pure astrocytes. The uptake of 300µM 6NBDG was measured using a fluorescent plate reader measured at 60, 180 and 360 minutes. The uptake was measured in the presence of glutamate with and without oubain or cytochalasin B. Results are expressed as the mean fold change ± SEM (n=3). $p < 0.05$ (*), $p < 0.01$ (**), $p < 0.001$ (***).
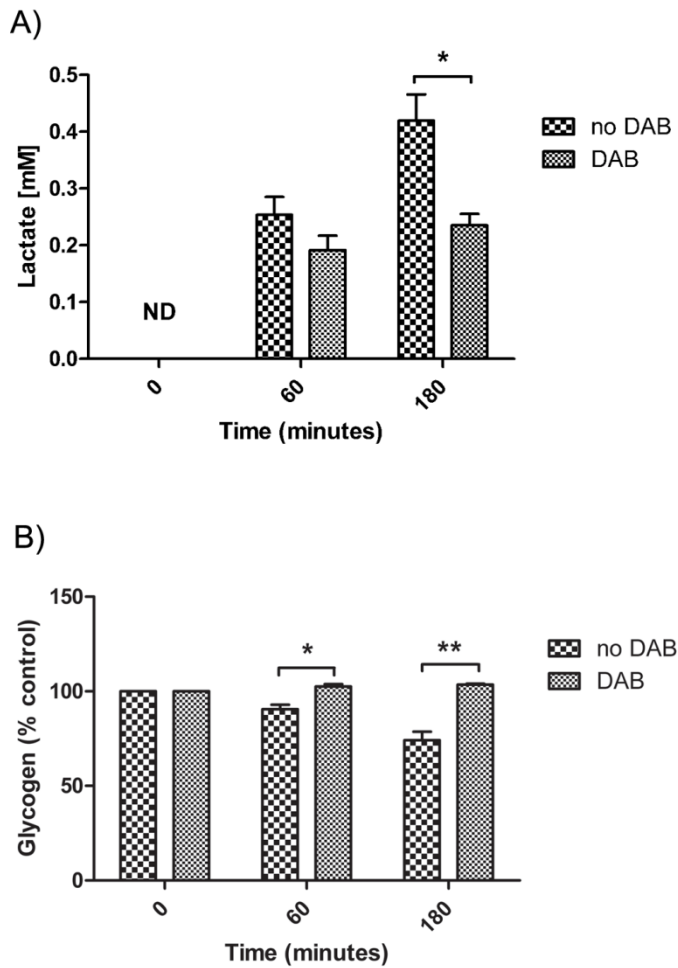
Figure 3.6 Effects of hypoglycaemia on lactate and glycogen levels. Neuron and astrocyte co-cultures were starved of glucose for 60 and 180 min in the presence/absence of DAB and assayed for A) production of lactate and B) glycogen turnover. Results are expressed as A) the mean ± SEM (n=3) and B) the mean percentage of control at time 0 ± SEM (n=3). $p<0.05$ (*), $p<0.01$ (**), $p<0.001$ (***). ND = not detected.
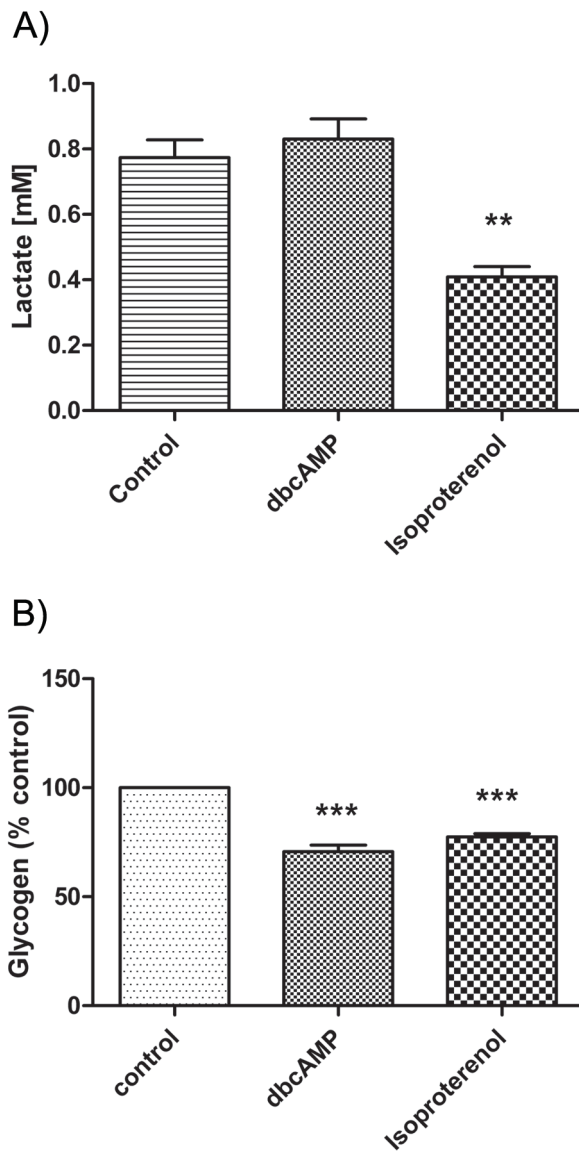
Figure 3.7   Effects of neuromodulators on lactate and glycogen levels. Neuron and astrocyte co-cultures were treated with dbcAMP and the β_1 and β_2 adrenergic agonist isoproterenol for 180min and assayed for A) production of lactate and B) glycogen breakdown. Results are expressed as A) the mean ± SEM (n=3) and B) the mean percentage of non-treated control ± SEM (n=3). $p<0.05$ (*), $p<0.01$ (**), $p<0.001$ (***).

Treatment with 0.5mM glutamate with or without ouabain demonstrated similar results (p<0.01). In addition, treatment with glutamate caused a significant breakdown of glycogen (1mM glutamate: 76.75 ± 2.36, *p*<0.01; 0.5mM glutamate: 81.73 ± 1.82%, *p*<0.05). This effect was completely blocked by ouabain (0.5mM glutamate + ouabain: 99.4 ± 3.04%, p<0.01; 1mM glutamate + ouabain: 99.12 ± 4.74%, p<0.05) (Fig. 3.8B).

To determine whether the effect seen in NT2/D1 neuron and astrocytes cultures was mediated by glutamate transporters and not glutamate receptors (Pellerin and Magistretti, 1994), cells were exposed to glutamate in the presence of DL-*threo*-β-benzyloxyaspartic acid (TBOA), a potent glutamate transport inhibitor (Fig. 3.9). In Fig. 3.9A it is clear that TBOA treatment blocks the release of lactate (1mM glutamate: 0.4 ± 0.01mM; 1mM glutamate and TBOA: 0.23 ± 0.01mM, p<0.001), reducing the levels to those of the control (control: 0.29 ± 0.02mM). Glycogen breakdown in response to glutamate was also attenuated (1mM glutamate: 76.75 ± 2.36%; 1mM glutamate and TBOA: 96.16 ± 2.83%, p<0.01) (Fig. 3.9B). Similar inhibition was also seen with lower concentrations of glutamate (p<0.001).

Potassium has also been shown to directly activate Na^+/K^+ ATPase (Bittner et al., 2011). The levels of lactate following treatment with ouabain only were actually decreased, suggesting a block of a basal Na^+/K^+ ATPase activity (control: 0.66 ± 0.01mM; ouabain: 0.5 ± 0.01mM, p<0.05) (Fig. 3.10A). Treatment with potassium at both 15 and 60mM triggered a significant increase in lactate (60mM potassium: 0.77 ± 0.05mM, p<0.001; 15mM potassium: 0.86 ± 0.02mM, p<0.01). This effect was completely inhibited in the presence of ouabain (60mM potassium + ouabain: 0.52 ± 0.01mM, p<0.001; 15mM potassium + ouabain: 0.57 ± 0.04mM, p<0.001) (Fig. 3.10A).
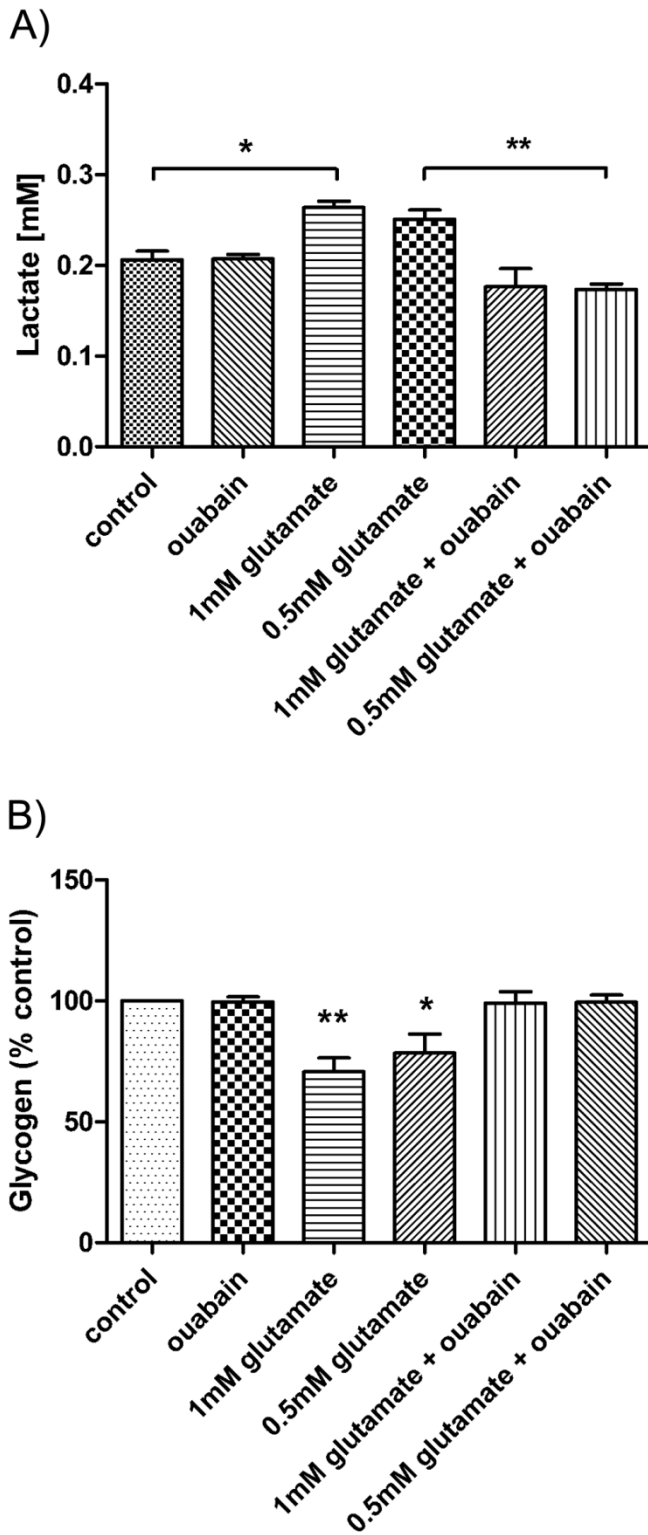
Figure 3.8 Effects of glutamate on neuron and astrocytes co-cultures. Co-cultures were treated with glutamate for 60min in the presence/absence of ouabain and assayed for A) production of lactate and B) glycogen turnover. Results are expressed as A) the mean ± SEM (n=3) and B) the mean percentage of non-treated control ± SEM (n=3). $p<0.05$ (*), $p<0.01$ (**), $p<0.001$ (***).
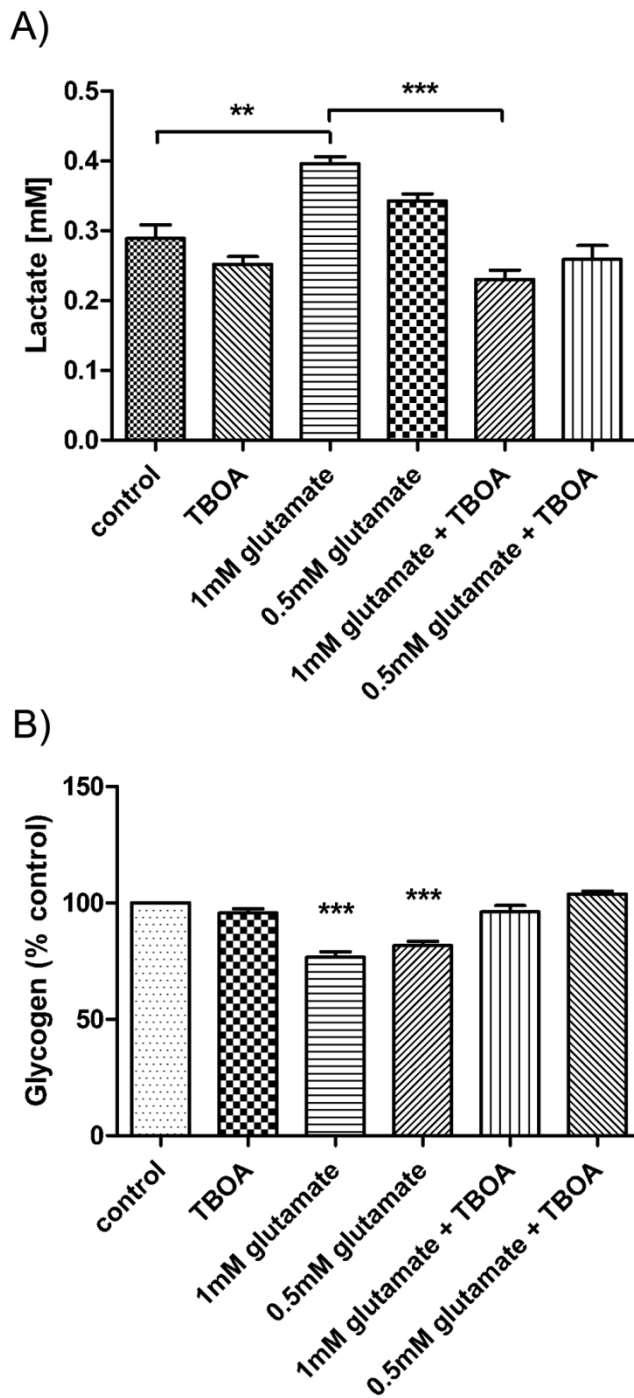
Figure 3.9 Effects of glutamate on neuron and astrocytes co-cultures. Co-cultures were treated with glutamate for 60min in the presence/absence of TBOA and assayed for A) production of lactate and B) glycogen breakdown. Results are expressed as A) the mean ± SEM (n=3) and B) the mean percentage of non-treated control ± SEM (n=3). $p<0.05$ (*), $p<0.01$ (**), $p<0.001$ (***).

In addition, glycogen levels were significantly reduced following treatment with potassium (60mM potassium: 83.25 ± 0.62%, $p<0.001$, 15mM potassium: 86.28 ± 0.54%, $p<0.01$). This effect was completely blocked with oubain (60mM potassium + ouabain: 100.6 ± 2.12%, $p<0.001$; 15mM potassium + ouabain: 98.29 ± 0.74%, $p<0.05$) (Fig. 3.10B).

3.3.5 NT2.N/A network activity induces glycogen turnover and lactate production

In order to investigate whether neuronal activity triggers the breakdown of glycogen and release of lactate in NT2.N/A cultures, the cells were stimulated electrically for 30 minutes in the presence and absence of TBOA (Fig. 3.11). Following electrical stimulation, the levels of lactate in the media were significantly increased (0.67 ± 0.04mM $p<0.01$) in comparison with control (0.36 ± 0.03mM) (Fig. 3.12A). In addition, glycogen levels inside the cells were significantly decreased (77.977 ± 3.62%, $p<0.01$) (Fig. 3.12C). These effects were completely blocked following treatment with TBOA (Fig. 3.12B and 3.12C). After pre-treatment of cells with TBOA for 15min and electrical stimulation in the presence of TBOA, lactate levels were slightly reduced (control: 0.69 ± 0.04mM; stimulation/TBOA: 0.53 ± 0.05mM) although the decrease was not significant. Glycogen breakdown was also blocked (stimulation: 77.98 ± 3.62%; stimulation/TBOA: 109.31 ± 2.9%, $p<0.001$) and the levels remained similar to the control.
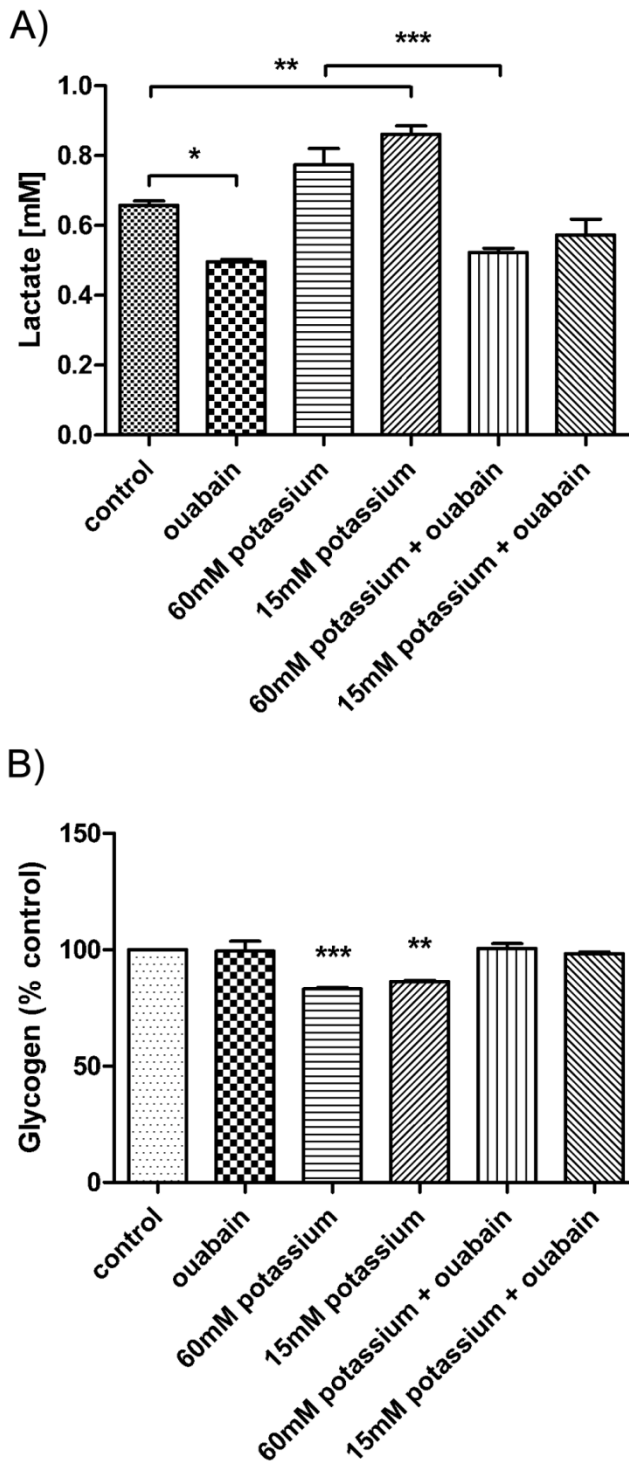
Figure 3.10 Effects of potassium on neuron and astrocyte co-cultures. Co-cultures were treated with potassium for 60min in the presence/absence of ouabain and assayed for A) production of lactate and B) glycogen breakdown. Results are expressed as A) the mean ± SEM (n=3) and B) the mean percentage of non-treated control ± SEM (n=3). $p<0.05$ (*), $p<0.01$ (**), $p<0.001$ (***).
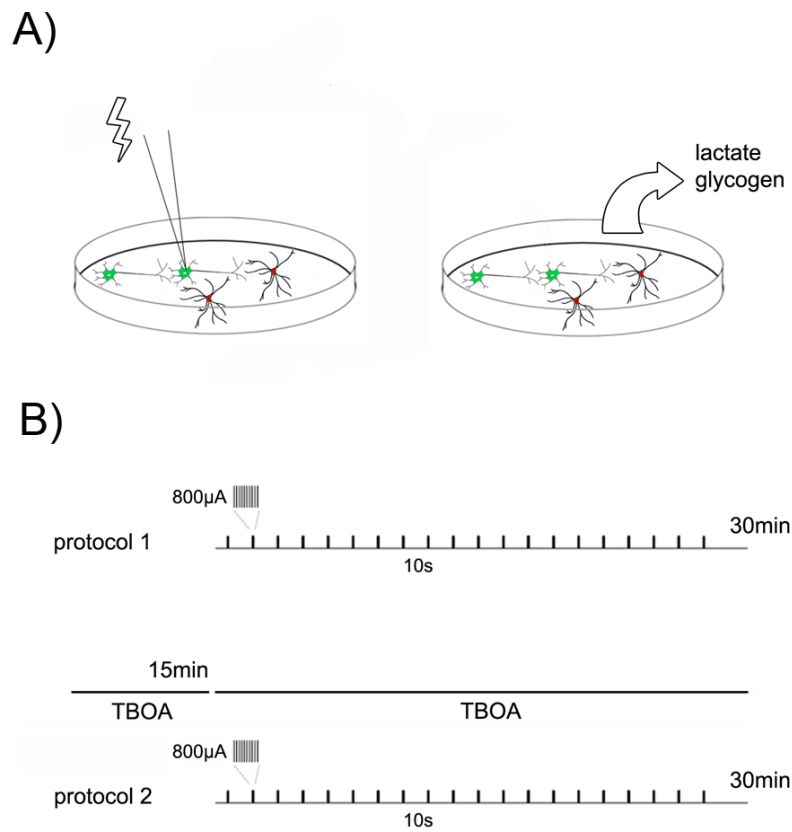
Figure 3.11 Schematic diagram of the experimental protocol for electrical stimulation.
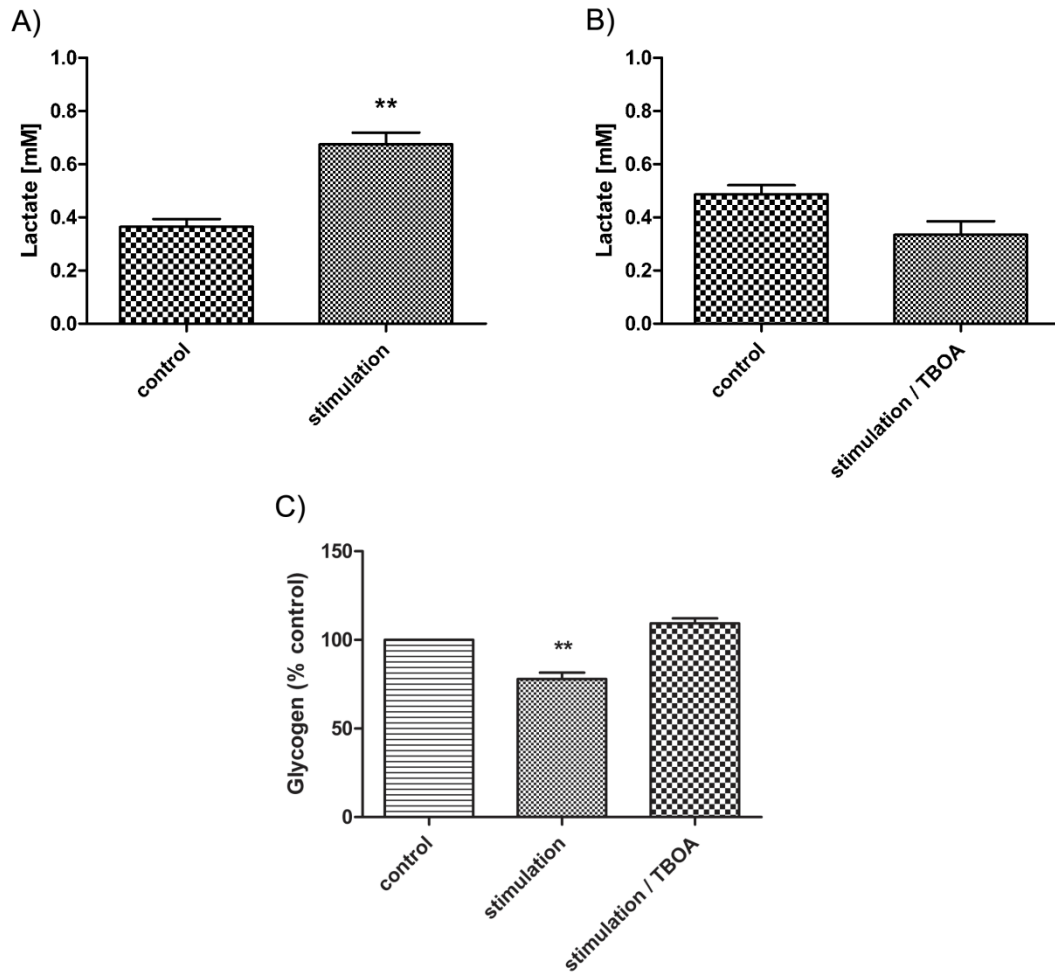
Figure 3.12   Effects of induced network activity on glycogen turnover and lactate production in neuron and astrocyte co-cultures. Production of lactate (A,B) and breakdown of glycogen (C) were measured in response to high frequency electrical activity in the presence and absence of TBOA. Results are expressed as A) the mean ± SEM (n=3) and B) the mean percentage of non-treated control ± SEM (n=3). $p<0.05$ (*), $p<0.01$ (**), $p<0.001$ (***).

3.4   Discussion

	glucose uptake	glycogen breakdown	lactate production
glutamate	↑	↓	↑
potassium		↓	↑
hypoglycaemia		↓	↑
dbcAMP		↓	=
isoproterenol		↓	↓
electrical stimulation		↓	↑
ouabain	✕	✕	✕
DAB		✕	✕
TBOA		✕	✕
cytochalasin B	✕		

Figure 3.13   Summary table of chapter 3 results. ↑ = increase; ↓ = decrease;
✕ = block; = no change

The astrocyte-neuron lactate shuttle (ANLS) was first proposed by Pellerin and
Magistretti (1994) and has since been extensively studied. Experiments supporting
ANLS have been carried out using brain slices, cultured primary neurons and
astrocytes as well as isolated nerves and sympathetic ganglia from rat, mouse and
chick (Pellerin, 2003). To the author's knowledge, these experiments have never
been carried out on human stem cell derived cultures. Human studies have been
limited to brain imaging techniques such as nuclear magnetic resonance
spectroscopy (NMR), Positron Emission Tomography (PET) or functional Magnetic
Resonance Imaging (fMRI) (Bouzier-Sore et al., 2003a, Bonvento et al., 2005).

135

Work in our laboratory has previously demonstrated that neuronal networks derived from NT2 cells signal to astrocytes, and that astrocytic networks communicate via gap junction mediated and gliotransmitter signalling (Hill et al., 2012). The results of this study show for the first time that human stem cell derived astrocytes synthesize glycogen and respond to classical neuromodulators that can induce glycogenesis and glycogenolysis in these cells as well as induce glucose uptake and lactate production.

In the NT2.N/A co-cultures, neurons and astrocytes display distinct differences in glycogen localization. The periodic acid-Schiff stain was co-localized with GFAP positive cells, while cells that stained for β-tubulin demonstrated no glycogen staining. The presence of glycogen as well as markers associated with its metabolism would suggest that these cells are well differentiated and resemble mature astrocytes (Brunet et al., 2010).

The importance of glucose utilization in astrocytes has been supported by experiments using radiolabelled and fluorescent deoxyglucose analogues (Pellerin and Magistretti, 1994, Barros et al., 2009a). Experiments presented here using 6-NBDG, show that NT2.N/A cultures respond to glutamate by increasing glucose uptake, an effect that was blocked by both cytochalasin B and ouabain in a manner previously shown in mouse cerebral cortical astrocytes (Pellerin and Magistretti, 1994) as well as rat neuronal and astrocytic cells (Hara et al., 1989, Roeder et al., 1985). However it should be noted that cytochalasin B, in addition to blocking glucose transport, also inhibits rate of actin polymerization and interaction of actin filaments (MacLean-Fletcher and Pollard, 1980). This can further lead to inhibition of transport of proteins and nucleotides (Plagemann and Estensen, 1972) as well as inhibition of cytokinesis (Carter, 1967) and a reduction in cell motility (Hosaka et al., 1980). The cells treated with cytochalasin B should therefore be assessed for any

toxicity caused by the compound.

The activation of the Na^+/K^+ ATPase enhances ATP utilization, which in turn stimulates glucose uptake and aerobic glycolysis which results in increased lactate production (Pellerin and Magistretti, 1994). Lactate production in astrocytes occurs not only as a part of the glycolytic part of glucose degradation but also during breakdown of glycogen (Dringen et al., 1993a) which is stimulated during brain activation and hypoglycaemia (Swanson et al., 1992, Swanson, 1992b, Cruz and Dienel, 2002).

In this study, hypoglycaemic conditions induced glycogenolysis in NT2.N/A cells as well as increased the production and release of lactate. This response was completely blocked by a known inhibitor of glycogen phosphorylase, 1,4-dideoxy-1,4-imino-d-arabinitol (DAB) (Walls et al., 2008). These results together with glycogen staining suggest that NT2.A cells possess the machinery required for glycogen synthesis and glycogen breakdown.

ANLS experiments have previously shown that glutamate stimulates glucose utilization and that this effect is not receptor mediated, as various glutamate receptor agonists and antagonists have no effect on hexose sugar usage (Pellerin and Magistretti, 1994).

NT2.N/A cells also demonstrate an increase in lactate production following treatment with both glutamate and potassium. This lactate increase was accompanied by a decrease in glycogen levels, suggesting that NT2 astrocytes respond to glutamate and potassium not only by increasing glucose uptake but also by degrading glycogen as demonstrated *in vivo* and in primary cultures (Hof et al., 1988, Swanson, 1992b, Swanson et al., 1992, Cruz and Dienel, 2002)

137
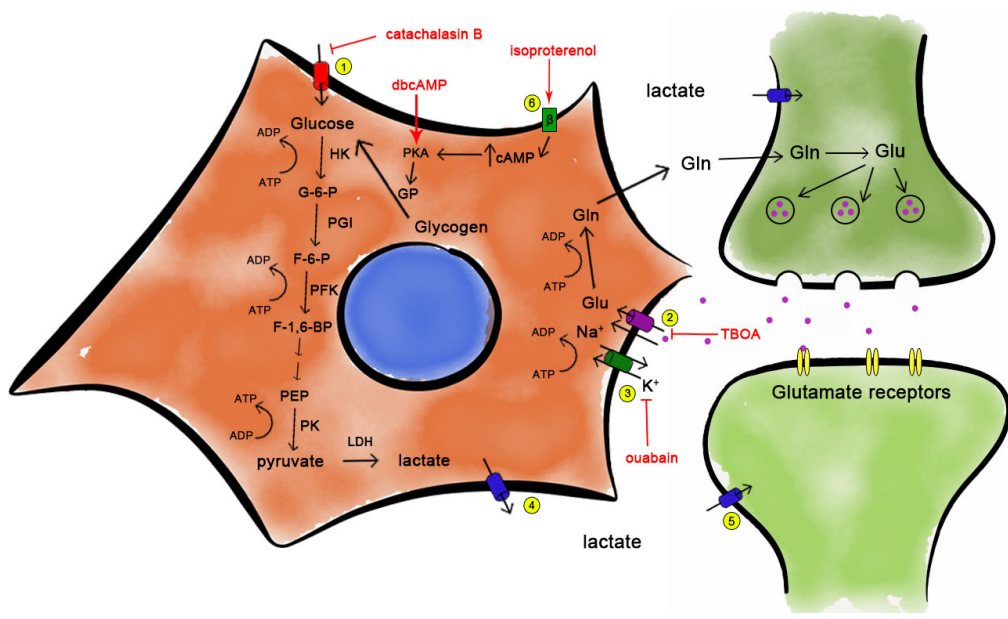
Figure 3.14   Schematic diagram of regulatory factors of ANLS, glycolysis and glycogenolysis. Neuromodulators and inhibitors that were used to investigate ANLS in NT2.N/A cocultures are highlighted.

Previous studies have shown that glutamate transport activates the Na^+/K^+ ATPase (Pellerin and Magistretti, 1997, Chatton et al., 2000), specifically mobilizing the α2 subunit of Na^+/K^+ ATPase, which co-localizes and interacts with glutamate transporters (Cholet et al., 2002, Rose et al., 2009, Gegelashvili et al., 2007). Additional evidence in support of the glutamate induced Na^+/K^+ ATPase activation comes from studies, which have used ouabain, a specific Na^+/K^+ ATPase inhibitor. The use of ouabain completely inhibited the glutamate stimulated glucose uptake (Pellerin and Magistretti, 1997).

In NT2.N/A cells, the glutamate and potassium-induced lactate production and glycogen breakdown were both inhibited by ouabain and glutamate-induced lactate production was also blocked using TBOA. These results provide further evidence for the existence of a functional astrocyte-neuron lactate shuttle and activity of NA^+/K^+ ATPase triggered by glutamate uptake in NT2.N/A cultures.

Experiments involving treatments of the co-cultures with dbcAMP and $β_1$ and $β_2$ adrenergic agonist isoproterenol demonstrated a decrease in glycogen load in the cells. dbcAMP, one of cAMP derivatives, activates glycogen phosphorylase through activation of protein kinase A leading to glycogen breakdown (Boer and Sperling, 2004). NA acts in a similar way, by elevating levels of cyclic AMP which in turn activates protein kinase A (Sorg and Magistretti, 1992). Interestingly, although isoproterenol increased glycogen turnover in these cultures there was a decrease the level of lactate in the media. At the same time dbcAMP also decreased glycogen levels but failed to increase lactate levels in the media samples. This is a suprising result as both substances act through activation of protein kinase A. However, both dbcAMP and isoproterenol have been shown to stimulate glycolysis and it is possible that pyruvate produced has been utilised in TCA cycle instead of lactate production (Auffermann et al., 1992, Suemori, 1975). Additionally, it has previously been shown

139

that NA enhances the expression of MCT2 in cortical neurons (Chenal and Pellerin, 2007). As such, it can be hypothesized that the lactate produced by the increase in glycogen metabolism may have been taken up by neurons due to increased MCT2 expression. Future studies will determine the dynamics of this change in expression in pure neuronal cultures.

The effect of neuronal activity on the lactate shuttle and glycogen utilization was investigated using electrical stimulation. After 30 minutes, glycogen levels significantly decreased whilst lactate levels increased. This suggests that lactate is released in response to neuronal activity. It has previously been shown in rat optic nerve preparations, that when cultured in glucose deprived aCSF, astrocytic glycogen was used as the primary source of lactate. Indeed, glycogen depletion in these cultures led to a failure in compound action potential (CAP) generation (Wender et al., 2000). In this study, stimulation-induced glycogen breakdown was blocked by administration of TBOA, an inhibitor of the glutamate transporter. These results indicate that activity-induced neuronal glutamate release and subsequent astrocyte uptake, were capable of inducing glycogen breakdown and lactate production.

Glycolysis and glycogenolysis are important processes in normal functioning of the brain but also in a number of disease processes such as ischaemia (Lowry et al., 1964) hypoglycaemia (Gruetter, 2003) and Alzheimer's (Allaman et al., 2010). This study demonstrates for the first time the metabolic coupling of neurons and astrocytes in a human derived stem cell model. This has important implications in the study of memory formation, plasticity, and neurodegeneration *in vitro*. This model may facilitate the future study of the active role and emerging understanding of the contribution of astrocytes in brain function as well as in neurodegenerative conditions, such as Alzheimer's disease. It is especially important as changes in

brain metabolism are one of the first signs of Alzheimer's Disease and appear decades before any other symptoms (Reiman et al., 2004, Mosconi et al., 2008b, Mosconi et al., 2009b). As such understanding of Aβ-associated metabolic changes in a human model of the disease may provide important insight into the disease process.

Chapter 4: Metabolism in Alzheimer's Disease

4.1   Introduction

Changes in brain metabolism during ageing and Alzheimer's Disease have been extensively studied for the past 30 years (Cunnane et al., 2011). It is now widely accepted that AD is accompanied by brain hypometabolism that varies between different regions of the brain. A decline in glucose utilization in the brain as well as mitochondrial function appear decades before any symptoms or histopathological changes occur, making it a useful biomarker of AD (Mosconi et al., 2008a, Mosconi et al., 2009a, Mosconi et al., 2009b, Reiman et al., 2004). Some of the evidence from kinetic FDG-PET studies suggests that hypometabolism is accompanied by a reduction in the rate of glucose transport (25%) and phosphorylation (23%-36%) (Mosconi et al., 2007).

Disturbances in brain metabolism could have long term adverse effects on the performance and survival of brain cells. Hypometabolism could also lead to decreased production of acetyl-coenzyme A (CoA) and ATP as well as acetylcholine which depends on availability of acetyl-coenzyme A and insulin (Cunnane et al., 2011). As impairment of cholinergic neurotransmission is one of the hallmarks of AD (Sims et al., 1983, Sims et al., 1981), hypometabolism would offer an interesting explanation. A reduction in ATP could also lead to damage in the ER and Golgi/trans-Golgi network resulting production of misfolded proteins. Energy deprivation could further lead to the induction of BACE1 (Velliquette et al., 2005, O'Connor et al., 2008), which would lead to an increase in Aβ(1-42) levels linking hypometabolism to the amyloid cascade.

Of particular interest in this process is the depletion of key metabolic intermediates such as nicotinamide adenine dinucleotide (NAD^+), which is essential for oxidative

phosphorylation-derived ATP. Depletion of NAD^+ could be caused by oxidative stress as well as the action of enzymes that require it as a substrate such as poly (ADP-ribose) polymerase (PARP) (Braidy et al., 2008, Alano et al., 2010). Another contributing factor of the energy deficit could be a decrease in activities of important glycolytic enzymes such as hexokinase or phosphofructokinase (Liguri et al., 1990, Sims et al., 1987) as well as enzymes of TCA cycle and oxidative phosphorylation such as pyruvate dehydrogenase (Yao et al., 2009), α-ketoglutarate dehydrogenase (Gibson et al., 1998) and cytochrome c oxidase (Yao et al., 2009).

4.1.1   Hypometabolism in AD

The cerebral metabolic rate of glucose (CMRg) in a healthy adult brain is 6-7mg/100g/min (Owen et al., 1967). The most widely used technique to study brain metabolism is Positron Emission Tomography (PET) using a tracer called [18F]-fluorodeoxyglucose (FDG). This tracer is able to mimic both glucose transport as well as phosphorylation (Phelps et al., 1979). FDG can be phosphorylated by hexokinase however it cannot be further metabolized (Cunnane et al., 2011). As PET has relatively poor spatial resolution, it is often combined with magnetic resonance imaging (MRI) or computed tomography (CT). This allows investigation of regional CMRg in specific areas of the brain (Cunnane et al., 2011).

FDG-PET studies of patients with AD have shown a progressive reduction in CMRg, which correlates with severity of the symptoms and cognitive performance (Mosconi, 2005). In addition, multiple studies have shown that in comparison with healthy age-matched controls, individuals with AD display a reduction in regional CMRg levels in parieto-temporal and posterior cingulate cortices (PCCs) as well as frontal areas in advanced disease (Friedland et al., 1983, Minoshima et al., 1997, Foster et al., 1984). Abnormalities in CMRg in medial temporal lobes (MTL: the hippocampus,

transentorhinal and entorhinal cortices, and parahippocampal gyrus) have been recently reported in studies that have used more sensitive PET equipment with higher spatial resolution (Mosconi et al., 2008a, Mosconi et al., 2007, Mosconi et al., 2006a, de Leon et al., 2001, Nestor et al., 2003).

One obvious explanation for a decrease in glucose utilization could be neuronal loss, which is one of the hallmarks of AD. However, many studies have shown a reduction in CMRg before the onset of the disease, in individuals at risk of developing AD such as APOE4 carriers, individuals carrying autosomal dominant mutations that are responsible for familial AD (FAD) or patients with mild cognitive impairment (MCI) (Mosconi et al., 2008b).

4.1.1.1 Familial AD (FAD)

Studies involving patients with FAD are very limited. Kennedy *et al.* (Kennedy et al., 1995) showed that presymptomatic FAD individuals have lower CMRg levels than age controls but higher than symptomatic FAD patients, suggesting a progression in CMRg impairment with the progression of the disease (Kennedy et al., 1995). However, as individuals in this study showed a substantial volume loss of the brain, it was not clear whether the decrease in CMRg was significant. A further study by Mosconi *et al.* (2006b) examined individuals with the PS1 mutation from families with FAD (on average 13 years before estimated disease onset). CMRg levels and volumes in several brain regions including hippocampus, entorhinal cortices (EC), posterior cingulate cortices (PCC), parietal and temporal cortices and the whole brain were measured in patients with FAD and controls. A significant decrease in CMRg was seen in all the regions whilst volume reductions were only found in the parietal cortex. CMRg was reduced by 12% in hippocampus and 20% in EC. Based on these results the authors concluded that FAD presymptomatic patients show widespread

CMRg reduction in the brain regions which typically show hypometabolism in symptomatic AD patients (Mosconi et al., 2006b).

4.1.1.2 APOE4 carriers

FDG-PET studies on individuals carrying APOE4 allele showed CMRg reduction in the same regions affected in AD which included posterior cingulate, parietal, temporal and prefrontal regions (Small et al., 1995, Reiman et al., 1996, Small et al., 2000, Reiman et al., 2001, Reiman et al., 2004, Reiman et al., 1998). However, the hypometabolism was not as severe as that seen in AD. In middle-aged APOE4 carriers hypometabolism was gradual and associated with cognitive performance (Small et al., 1995, Reiman et al., 2001). Studies on presymptomatic carriers of APOE4 allele aged 50-63 showed a greater reduction in CMRg (25%) than in healthy controls over time period of 2 years (Reiman et al., 2001).

4.1.1.3 Mild Cognitive Impairment (MCI)

MCI is widely accepted as an intermediate state between healthy ageing and AD (Mosconi et al., 2008b). Indeed, MCI individuals are also at higher risk of developing AD (Petersen et al., 2001, Gauthier et al., 2006). It is defined as a state where individuals are able to perform normal activities of a daily life but suffer memory loss, which isolates them or other difficulties which exceed those of normal ageing (Mosconi et al., 2008b).

MCI patients show mild global and regional hypometabolism in the same brain regions as AD patients (Mosconi et al., 2008a, Minoshima et al., 1997, De Santi et al., 2001, Nestor et al., 2003, Mosconi et al., 2006a, Drzezga et al., 2003, Drzezga et al., 2005), although the regional CMRg levels are more variable and are associated

more with cognitive abnormalities of individual subjects (Anchisi et al., 2005, Haxby et al., 1990). CMRg decreases in the hippocampus are found among most MCI patients while hypometabolism in cortices is more diverse (de Leon et al., 2001, Mosconi et al., 2008a, De Santi et al., 2001, Mosconi et al., 2006a). Longitudinal FDG-PET studies showed that CMRg reduction is more pronounced in patients with MCI that eventually develop AD than in those that do not. The accuracy of the prediction varies from 75% to 100% (Minoshima et al., 1997, Herholz et al., 1999, Arnaiz et al., 2001, Chetelat et al., 2003, Drzezga et al., 2005, Anchisi et al., 2005)

4.1.1.4 Ageing

FDG-PET studies in normal ageing showed a mild CMRg reduction, which mainly involved frontal regions (de Leon et al., 2001, Mosconi et al., 2008a, Herholz et al., 2002). Only a few studies have monitored progression from normal ageing to MCI and MCI to dementia (Mosconi et al., 2008a, Jagust et al., 2006). One such study has shown that a reduction in CMRg in EC can predict progression to MCI within 3 years with sensitivity of 83% and specificity 85% (de Leon et al., 2001). Reduction in CMRg in EC, hippocampus and lateral temporal cortex has been found during the progression to MCI and the reduction was found to be significant even after correction for volume loss (de Leon et al., 2001). Further studies have addressed the question as to whether these reductions were related to development of AD. In a study by Mosconi *et al.* (2008a) elderly patients were followed for between 6-14 years. Over this time course, 11 of these patients developed dementia, 6 of whom were diagnosed with AD and 19 developed MCI. The reduction in CMRg in the hippocampus was the only regional predictor of future cognitive decline (predicting a decline from normal to AD with 81% accuracy, from normal to dementia with 77% and from normal to MCI with 71% accuracy). Overall these studies provided direct evidence of a progression in hypometabolism which originates in MTL during normal

ageing and then progresses to PCC at the MCI stage and spreads to parieto-temporal cortices in AD (Mosconi et al., 2008a).

4.1.2 Mitochondrial changes

The main risk factor for AD is age and it is important to investigate common pathological mechanisms shared by normal ageing and in disease. As hypometabolism is the earliest change seen in AD, it indicates that changes in energy metabolism are not just a consequence of neuronal loss but they contribute to the development and progression of the disease (Yap et al., 2009).

The energy required for cell functioning in the majority of eukaryotic cells is generated by mitochondria during oxidative phosphorylation. Mitochondria play many important roles such as energy production, calcium homeostasis, apoptosis and cellular signalling through generation of oxidants such as hydrogen peroxide (H_2O_2) (Cadenas, 2004). Mitochondrial dysfunction has been implicated in normal ageing as well as many diseases (Storz, 2006). It has been well documented that gradual decline in the energetics of mitochondria i.e. production of ATP as well as an increase in production of oxidants and oxidative stress are characteristic of ageing and age related neurodegeneration (Mattson and Magnus, 2006, Navarro and Boveris, 2007, Boveris and Navarro, 2008, Rebrin et al., 2003, Butterfield et al., 1999, Calabrese et al., 2006).

In addition, a pro-oxidizing shift in glutathione status has been associated with ageing in humans and rodents (Rebrin et al., 2003, Jones et al., 2002). Longitudinal studies on humans aged 19-85 have demonstrated a chronic increase in oxidative stress throughout adulthood (Jones et al., 2002). Indeed, studies have shown a decrease in GSH levels and an increase in GSSG levels in AD patients (Calabrese et al., 2006),

which was also reflected by increased glutathionylation of proteins in AD brains (Newman et al., 2007).

It has been suggested that an age related decline in energy metabolism and the redox status of the cell should be viewed as interdependent (Yap et al., 2009). This is reflected in the 'so called' mitochondria energy – redox axis. The energy component includes the entry of glycolytic substrates into the TCA cycle and generation of reducing equivalents (NADH, $FADH_2$). The redox component includes mitochondrial redox indicators such as glutathione (GSH/GSSG), thioredoxin (Trx(-SH)/Trx-SS), glutaredoxin (Grx) and peroxiredoxins (Prx) and therefore mechanisms dependent on flux of NADPH. NADPH is generated by a reduction of $NADP^+$ by NADH in mitochondria as well as during pentose phosphate pathway when $NADP^+$ is reduced to NADPH. A decrease in energy production in the mitochondria would impact redox balance in the cell and vice versa. In addition, altered redox status in the cell could lead to post-translational modifications of proteins involved in metabolism (Yap et al., 2009).

4.1.2.1 Oxidative Phosphorylation

During oxidative phosphorylation NADH produced in TCA cycle is oxidized by the mitochondrial electron transport chain (ETC). It has been estimated that the terminal electron acceptor, cytochrome oxidase, uses up 95% of oxygen consumed by mammalian cells (Yap et al., 2009). As electrons flow through complexes of ETC, protons are transported across the inner mitochondrial membrane generating energy. The protons then flow back through ATP synthase (complex V), which uses the energy to generate ATP from ADP (Nicholls, 2002, Navarro and Boveris, 2007).

The effects of ageing on respiration are more pronounced in tissues composed of

post-mitotic cells such as brain, heart and skeletal muscles. Most tissues have a constant requirement for ATP, however muscles and neurons have very high and variable demand for ATP (Nicholls, 2002). It has been shown that activities of complexes I, III and IV decrease with age in mitochondria isolated from brain tissue (Navarro and Boveris, 2007). Decrease in activities of these complexes is further associated with morphological changes in mitochondria. This ultimately leads to neurons being unable to produce ATP during increased energy demand (Navarro and Boveris, 2004)

4.1.2.2 TCA cycle

The tricarboxylic acid cycle (TCA) in its most simple form involves a series of reactions in which the products of glycolysis are oxidized to generate reducing equivalents, NADH and $FADH_2$ (Nelson and Cox, 2005). NADH donates electrons for complex I during oxidative phosphorylation and is also important in the generation of NADPH, by reduction of $NADP^+$ by either $NADP^+$ dehydrogenase or $NADP^+$ transhydrogenase. NADPH is the only electron source for regeneration of glutathione and thioredoxin (Rydstrom, 2006).

The activities of several enzymes essential for the TCA cycle and NADH production have been shown to be decreased in ageing and AD. Activities of aconitase, α-ketoglutarate dehydrogenase (αKGDH) and pyruvate dehydrogenase have all been shown to decrease in ageing (Zhou et al., 2009). In addition, a decline in activities of α-ketoglutarate dehydrogenase (αKGDH) and pyruvate dehydrogenase (PDH) have been associated with AD (Gibson et al., 2000). It has been previously shown that aconitase and αKGDH are susceptible to H_2O_2 levels. In the presence of H_2O_2 the E_2 subunit of αKGDH has been shown to be glutathionylated which leads to decreased activity (Nulton-Persson et al., 2003, Applegate et al., 2008). A reduction in αKGDH

149

activity is associated with a decrease in the production of NADH during oxidative stress due to inability to utilize glutamate in TCA cycle (Tretter and Adam-Vizi, 2000). Any changes in the activity of TCA enzymes could lead to a decrease in NADH levels which results in decreased oxidative phosphorylation as well as a reduction in the NADPH pool (Yap et al., 2009).

Succinyl-CoA: 3-oxoacid Co-A transferase (SCOT) a mitochondrial matrix enzyme important for ketolysis is also reduced during ageing. Ketone bodies are the only alternative source of energy for the brain during hypoglycaemia. As such, a decrease in SCOT activity during ageing further increases brain sensitivity to energy deficits (Yap et al., 2009).

An overall decline in the activities of enzymes involved in acetyl-CoA production (PDH and SCOT) as well as TCA cycle enzymes such as αKGDH can lead to a decrease in ATP production as well as affecting the redox balance within the cell (Yap et al., 2009).

4.1.3   ROS and antioxidants

Reactive oxygen species (ROS) are generated constantly during oxidative phosphorylation (Dringen et al., 2000). They include inorganic molecules such as superoxide radical anion, H_2O_2 and hydroxyl radicals but also organic molecules such as alkoxyl and peroxyl radicals. ROS can cause damage to the cell such as DNA strand breaks, lipid peroxidation and protein modification. To avoid such damage cells have developed mechanisms to prevent generation of ROS or to limit the effect of its damage (Dringen et al., 1993a). These include thiol/disulfide redox buffers and the H_2O_2 removal system.

The thiol/disulfide exchange involves glutathione, thioredoxin and related enzymes and is important in maintaining redox status of the cell as well as the NADPH pool (Yap et al., 2009).

Glutathione (GSH) is synthesized in the cytosol by the consecutive action of two enzymes, γ-glutamylcysteine (γGluCys) and glutathione synthetase. The former enzyme uses glutamate and cysteine as substrates and produces the dipeptide γGluCys, the latter enzyme combines γGluCys with glycine to produce GSH (Dringen et al., 2000). GSH is present at high levels (~5-10mM) in most cell compartments and it has been found to quickly equilibrate between the mitochondria and cytosol although the exact mechanism of its transport is not well known (Hurd et al., 2005). GSH plays an important role in the removal of H_2O_2 generated during oxidative phosphorylation. GSH is oxidized to GSSG via a direct reaction of thiol group with H_2O_2. GSSG is then reduced back to GSH by action of glutathione reductase, an enzyme which requires NADPH (Han et al., 2006, Dalle-Donne et al., 2008). Under normal conditions GSSG levels are very low, at about 1/100th of the total GSH pool (Schafer and Buettner, 2001) (Fig. 4.1).

One of the consequences of altered GSH/GSSG redox status is the formation of protein mixed disulfides (glutathionylation). However, cells possess enzymes which are able to reduce protein disulfides or glutathionylated proteins such as glutaredoxin (Grx2) (Dalle-Donne et al., 2008).

4.1.3.1 ROS formation

As mentioned in section 4.1.2.1 and 4.1.2.2, several enzymes involved in TCA cycle and oxidative phosphorylation have been found to have decreased activities in AD brain. These include αKGDH and PDH (Gibson et al., 2000). As these enzymes are

involved in reduction of molecular oxygen, their decreased activity would increase

production of ROS, specifically superoxide (Zhu et al., 2005).
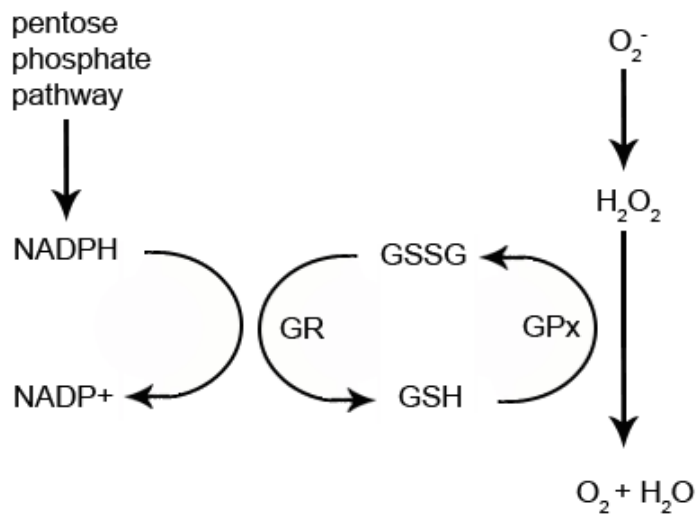
Figure 4.1 Schematic diagram showing removal of H_2O_2 by GPx and recycling of GSH from GSSG by GR.

Superoxide is normally converted to H_2O_2 via the action of Superoxide Dismutase 1 (SOD1) or 2 (SOD2). Indeed, levels of SOD1 have been found to be elevated in AD brains (Serra et al., 2001, Ozcankaya and Delibas, 2002), which together with increased O_2^- levels lead to an increase in concentration of H_2O_2 (Braidy et al., 2008).

Oxidants produced in mitochondria as a consequence of oxidative phosphorylation (O_2^- and H_2O_2) have been found to play an important role in signalling pathways (Han et al., 2009). Many metabolic pathways are regulated by H_2O_2 through either activation/inhibition of redox-sensitive proteins such as glycogen synthase kinase (GSK), protein kinase B (Akt) and c-Jun N-terminal kinase (JNK), or through post-translational modifications of proteins such as aconitase or PDH. O_2^- and H_2O_2 can both coordinate responses between cytoplasm and mitochondria. However, during ageing and AD ROS production is significantly increased. The increased production of O_2^- and H_2O_2 has been shown to dysregulate signalling cascades and cause damage to lipids, proteins and DNA (Yap et al., 2009).

O_2^- is a precursor for H_2O_2 and is converted by Mn-SOD (SOD-2) in the mitochondrial matrix or Cu/Zn-SOD (SOD-1) in the cytoplasm (Fernandez-Fernandez et al., 2012). However, O_2^- generated at complex III is released both into the matrix and intermembrane space (IMS) where it can modify proteins residing there (Han et al., 2003b, Han et al., 2001, Han et al., 2003a, Inarrea et al., 2005).

Levels of H_2O_2 generated in the mitochondria increase with age and changes in mitochondria bioenergetics (i.e. NADPH production) may contribute to that increase. Glutathionylation of proteins which is a sign of increased ROS production, results in an increase in the production of O_2^- as seen in complex I of liver mitochondria (Taylor et al., 2003). Additionally, glutathionylation increases with age and in AD (Dalle-Donne et al., 2008) and has been associated with further increases in the generation

of O_2^- and H_2O_2 (Yap et al., 2009).

H_2O_2 diffusion to the cytoplasm may act as a signal for many processes, which are regulated through the activation of cytosolic kinases (Cadenas, 2004). Many phosphatases and cytosolic kinases such as members of the insulin pathway, glycogen synthase kinase (GSK3β), Akt and JNK as well as members of MAP kinase family have been found to localize to mitochondria (Horbinski and Chu, 2005). One of the examples is translocation of JNK to mitochondria in response to increased H_2O_2. JNK can further regulate metabolism (Zhou et al., 2008, Nemoto et al., 2000) by phosphorylation of proteins in the mitochondrial matrix, as well as membranes such as pyruvate dehydrogenase E_1 subunit (Schroeter et al., 2003). Phosphorylation of PDH leads to a decrease in ATP levels (Zhou et al., 2008) and a decrease in PDH activity which is an early event in AD and has been associated with cognitive decline (Zhou et al., 2008).

In AD, the increase in ROS has also been suggested to be caused by insertion of Aβ(1-42) into neuronal and glial membrane (Butterfield, 1997, Varadarajan et al., 2000). Additionally, the reduction of metal ions such as Fe^{2+} in the presence of H_2O_2 can result in the production of highly reactive $HO^\bullet$ which in turn could cause significant damage to the cell (Huang et al., 1999). Normally accumulation of metals such as Fe^{2+} is prevented by ferritin and transferrin which bind to them with high affinity (Miranda et al., 2000). However, these mechanisms are limited in the brain leading to accumulation of Fe^{2+}, thus increasing the risk of metal-induced damage (Miranda et al., 2000). Dysfunction of metal homeostasis has been implicated in AD (Liu et al., 2006) and elevated levels of Fe^{2+} have been found in hippocampal neurons of AD patients (Smith et al., 1997).

In summary, changes in GSH redox status lead to glutathionylation of proteins such

as complex I and the oxidation of proteins. This further increases levels of O_2^- and H_2O_2, ultimately leading to dysregulation of signaling cascades such as JNK (Navarro and Boveris, 2007).

4.1.4   NAD$^+$/NADH and NADP$^+$/NADPH

NAD$^+$, reduced nicotinamide adenine dinucleotide (NADH), nicotinamide adenine dinucleotide phosphate (NADP$^+$) and reduced nicotinamide adenine dinucleotide phosphate (NADPH) have long been known to play important roles in energy metabolism, reductive biosynthesis and antioxidant activity (Belenky et al., 2007, Berger et al., 2004, Pollak et al., 2007). NAD$^+$ and NADH are mainly used by enzymes to catalyze oxidation, while NADP$^+$ and NADPH to catalyze reduction (Pollak et al., 2007). In recent years numerous studies have shown that pyridine nucleotides have numerous functions (Belenky et al., 2007, Berger et al., 2004, Pollak et al., 2007). They appear to have a role in ageing via NAD$^+$ -dependent histone deacetylase i.e. sirtuins (Blander and Guarente, 2004), oxidative cell death via poly (ADP-ribose) polymerase-1 (PARP) (Virag and Szabo, 2002, Ying, 2006), mobilization of intracellular calcium stores via cyclic ADP-ribose and nicotinic acid adenine dinucleotide phosphate (NAADP) (Lee, 2001) and generation of ROS via NADPH oxidase (Bedard and Krause, 2007).

NADPH is formed in mitochondria via three pathways involving NADP$^+$ isocitrate dehydrogenase, malic enzymes and nicotinamide nucleotide transhydrogenase (NNT) (Ying, 2008). NNT catalyzes the reaction in mitochondria, which includes reduction of NADP$^+$ from NADH. This provides an important link between bioenergetics and defence against reactive oxygen species (Yap et al., 2009). Additionally NNT activity depends on membrane potential of the mitochondria (Yap et al., 2009).

155

NADPH is required for regeneration of GSH in mitochondria and therefore is a limiting factor of this system (Rydstrom, 2006, Zhang et al., 2007a). In addition, decreases in mitochondrial membrane potential caused by a loss of electron flow through ETC as well as decreased availability of NADH might affect the conversion of $NADP^+$ to NADPH.

4.1.4.1 NAD^+ and PARP-1

Low levels of reactive oxygen species are a part of normal metabolism in the cell (Ogino and Wang, 2007) and normally they do not exert any harmful effects due to the action of antioxidants. However, an increase in oxidative stress such as that seen in AD (Mhatre et al., 2004, Moreira et al., 2005, Zhu et al., 2004) and an imbalance between production of ROS and antioxidant mechanisms may lead to cell damage. An increase in DNA damage induced by oxidative stress is a major factor associated with ageing and AD (Nunomura et al., 1999, Braidy et al., 2008). Therefore, it is important for the cell to have efficient repair mechanisms (Braidy et al., 2008). NAD^+ has been shown to have an important role in DNA repair as well as gene signalling pathways (Erdelyi et al., 2005, Malanga and Althaus, 2005).

NAD^+ was previously identified as a parent compound in the pyridine family (NADH, $NADP^+$ and NADPH), which is involved in several metabolic reactions. NAD^+ is also an electron transporter in oxidative phosphorylation and ATP production, and is involved in glutathione and thioredoxin antioxidant systems via NADPH (Braidy et al., 2008). Recent studies have also shown evidence that NAD^+ is important in DNA repair and gene silencing (Rafaeloff-Phail et al., 2004).

NAD^+ acts as a substrate for the enzyme poly (ADP-ribose) polymerase (PARP). PARP-1 is a DNA binding enzyme, which is activated by breaks in DNA caused by

ROS and is critical in the base excision repair (BER) process (Bouchard et al., 2003). PARP cleaves NAD^+ into adenosine 5'- diphosphoribose (ADPR) and nicotinamide and then attaches polymers of ADP-ribose to histones and other nuclear proteins (de Murcia et al., 1997).

In addition to its role in PARP activation, NAD^+ also acts as a substrate for the sirtuin family of enzymes (silent information regulators of gene function) (Sauve et al., 2006). These enzymes has been implicated in cell survival under conditions of stress and toxicity as well as longevity (Yang and Sauve, 2006).

During oxidative stress and increased ROS production, rapid NAD^+ depletion caused by PARP activation can induce a cellular energy 'crisis' by reducing ATP synthesis, ultimately leading to cell death (Pacher and Szabo, 2007, Pillai et al., 2005, Alano et al., 2004, Wang et al., 2003). Excessive activation of PARP can also lead to a decreased SIRT1 deacetylase activity through NAD^+ depletion. This in turn leads to accumulation of acetylated p53 and cell death (Furukawa et al., 2007). It has been shown that PARP-1 activation leads to translocation of the mitochondrial permeability transition pore (MPTP) (Alano et al., 2004) and apoptosis-inducing factor (AIF) (Yu et al., 2002). Multiple protein kinases have been shown to contribute to PARP-1 mediated cell death including JNK1, which appears to activate PARP-1 by a direct phosphorylation (Zhang et al., 2007b) and therefore is implicated in mitochondrial impairment and cell death induced by PARP-1.

These studies have been supported by the positive effect of pyruvate supplementation after PARP-1 activation. During hypoglycaemia induced by PARP-1 activation, the cells are unable to use glucose even when it is restored to normal levels. This happens due to absence of NAD^+ required for glycolysis. However, the cells are able to metabolise pyruvate in the absence of NAD^+ and therefore pyruvate

supplementation has been found to reduce energy metabolism impairments and cell death as well as improving neuronal survival both *in vitro* as well as in brain slices and animal models (Suh et al., 2005, Ying et al., 2002).

Depletion of NAD^+ associated with PARP activity has been implicated in AD (Love et al., 1999) and Aβ-induced neuronal death (Fonfria et al., 2005). An increase in the concentration of poly(ADP-ribose) polymers concentration in the temporal and frontal lobes of AD individuals has been shown (Love et al., 1999) suggesting overexpression or increased activity of PARP. It has also been shown that oxidative damage to DNA has negative effects on metabolism of carbohydrates, which may be caused by NAD^+ depletion induced by PARP (Braidy et al., 2008).

PARP-1 has been found to interact with cell cycle regulators such as p53 (Braidy et al., 2008). p53 induced by oxidative stress has been shown to regulate expression of several genes that can induce cell cycle arrest in G1 or prevent DNA replication before damage repair or induce apoptotic death (Malanga et al., 1998). Increased expression of PARP-1 and p53 have been found in neurons of AD patients as well as in cultured neurons treated with Aβ(1-42) (de la Monte et al., 1998, Culmsee et al., 2001). PARP-1 appears to activate DNA dependent protein kinase which then phosphorylate p53.

The combination of sirtuins and caloric restriction has been found to play an important role in cell survival during oxidative stress (Sauve et al., 2006). SIRT1 acts primarily by deacetylating lysine residues in targeted proteins in the presence of NAD^+ and therefore releases nicotinamide, acetyl ADP ribose (AADPR) and deacetylated substrates (Sauve et al., 2006). Caloric restriction appears to increase the NAD^+ pool and therefore activates SIRT1 (Sauve et al., 2006). An increase in NAD^+ levels may be associated with an increased life span as well as the

transcriptional silencing of telomeres and ribosomal DNA. Such silencing is seen as a way of measuring SIRT1 activity (Anderson et al., 2002).

NAD^+ depletion also affects gene expression (Bedalov and Simon, 2004). Indeed, increased SIRT1 has been shown to regulate gene expression by targeting transcription factors such as p53 (Luo et al., 2001), forkhead-box (FOXO) transcription family (Brunet et al., 2004) and NF-κB (Yeung et al., 2004). Depletion of NAD^+ due to PARP activity would impair SIRT1 and therefore promote p53, FOXO and Bax activities, which can trigger apoptosis (Pillai et al., 2005). However, enhanced NAD^+ levels could induce protective factors (Pallas et al., 2008).

Another factor that could affect NAD^+ levels is NADH dehydrogenase which is a part of complex I within mitochondria. NADH dehydrogenase oxidizes NADH to NAD^+ and has been found to have reduced activity in AD brains (Lin and Guarente, 2003). This suggests that regulation of NAD^+/NADH ratio is further impaired in AD (Braidy et al., 2008, Lin and Guarente, 2003).

As NAD^+ has an essential role in the production of energy, DNA repair and other cell functions, depletion of NAD^+ caused by oxidative stress in AD, can be an important step in development and progression of the disease (Braidy et al., 2008). In addition, NAD^+ deficit may provide an important target for treatments in AD (Belenky et al., 2007).

4.1.5   Supplementation

Studies on the use of metabolites to overcome the energy deficit have shown that mitochondrial energy substrates such as pyruvate, can have a neuroprotective role against oxidative stress (Wang et al., 2007) as well as Aβ toxicity (Alvarez et al.,

2003). Treatment of neurons under oxidative stress with pyruvate decreased mitochondrial membrane depolarization, production of O_2^- and prevented caspase 3 release following Aβ treatment (Alvarez et al., 2003, Wang et al., 2007). Pyruvate directly affects mitochondria through the regulation of $NADP^+$ redox status (Alvarez et al., 2003). Another promising approach is supplementation of glucose with ketone bodies (Henderson, 2008). These are normally produced from fat stores when glucose levels decrease. Although glucose is the primary source of energy in the brain, cells can metabolize ketones during prolonged fasting (Greene et al., 2003). Ketone bodies include acetoacetate and β-hydroxybutyrate and are derived from fatty acids in the liver. They are then transported into the brain through the blood-brain barrier via monocarboxylic transporters (MCTs) (Pellerin et al., 1998). Ketones can meet up to ~60% of brain energy requirements (Cahill, 2006). The metabolism of ketones in the brain involves conversion of β-hydroxybutyrate to acetoacetate, acetoacetate to acetoacetyl CoA, and acetoacetyl CoA to CoA (Cunnane et al., 2011). Interestingly ABAD has been found to be blocked by Aβ, facilitate the utilization of ketone bodies both *in vitro* and *in vivo* (Du Yan et al., 2000). Unfortunately, ketone bodies cannot completely substitute for glucose as it is essential for lactate production (Cunnane et al., 2011).

However, as mentioned above, the activity of the SCOT enzyme is decreased in AD which suggests ketolysis is also affected, leading to further reduction in energy production in AD (Yap et al., 2009).

4.1.6 Glucose transport

Glucose transport is facilitated by glucose transporters (GLUTs), of which several isoforms has been described. GLUT1 is localized on the membrane of blood-brain barrier endothelial cells, whilst GLUT3 is localized on neurons and GLUT2 is

expressed in astrocytes (Dwyer et al., 2002). Additionally, two more, insulin sensitive transporters were have been found to be expressed in neurons – GLUT4 and GLUTx1 (Watson and Craft, 2004).

Decreased levels of GLUT1 and GLUT3 have been found in AD brains in several regions including the frontal, parietal, occipital and temporal cortical areas as well as the caudate nucleus and hippocampus. This suggests that glucose transport may be in part responsible for the hypoglycaemia seen in AD patients (Liu et al., 2008).

Insulin sensitive transporters GLUTx1 and GLUT4 are expressed mainly in the hippocampus and hypothalamus. A significant overlapping distribution of insulin-sensitive glucose transporters, insulin receptors and insulin have been found in specific regions of the brain which support memory (Apelt et al., 1999). Additionally, changes in insulin levels modulate GLUT4 expression in the brain (Vannucci et al., 1998) suggesting a possible role of insulin in hypoglycaemia and AD (see section 4.1.8).

4.1.7 Glutamate

L-glutamate is the most common neurotransmitter in the mammalian CNS. Upon presynaptic depolarization, glutamate is released from vesicles into the synapse, increasing the glutamate concentration almost 1000-fold (Walton and Dodd, 2007). Glutamate then binds to postsynaptic receptors, triggering an influx of cations and cellular depolarization. Glutamate is then quickly removed from the synaptic cleft by high-affinity transporters on astrocytes (Walton and Dodd, 2007). This prevents over-stimulation and excitotoxicity. In the astrocytes, glutamate is converted into glutamine by glutamine synthase. Glutamine is then released from astrocytes and taken up by neurons, which convert it back to glutamate by phosphate-activated glutaminase.

Glutamate is further packed into vesicles (Walton and Dodd, 2007).

Any changes in glutamate neurotransmission and recycling can have severe consequences. Prolonged increases in glutamate levels leads to sustained neuronal depolarization, which in turn results in Na^+ and Ca^{2+} influx and further release of glutamate. Ca^{2+} can lead to delayed necrosis and to lesser extent apoptosis (Walton and Dodd, 2007). Continuous release of glutamate and the spreading of the process is called excitotoxicity, a process that has been previously found to be associated with Alzheimer's Disease (Hynd et al., 2004).

NMDA receptors can be activated by L-glutamate and glycine and are thought to be involved in synaptic plasticity and long-term potentiation (LTP). It has been previously shown that the density of NMDA receptors decreases with age (Segovia et al., 2001) and that a decrease in NMDA function can contribute to neurodegeneration (Olney et al., 1998). However, an FDA approved drug for treatment of moderate to severe AD, memantine, is a low affinity, non-competitive NMDA receptor antagonist. It competes with Mg^{2+} for binding to ion channel of the NMDA receptor and reduces NMDA activation. It has been suggested that memantine may reduce the pathophysiological activation of NMDA receptors but still allow physiological activation. Previous studies have shown that activation of NMDA leads to dissociation of PP-2A from NMDA complex and therefore leads to hyperphosphorylation of tau (Chan and Sucher, 2001). Treatment of organotypic hippocampal cultures with memantine restores tau phosphorylation to physiological levels (Li et al., 2004).

Additionally, studies have shown a decrease in GluR1 and GluR2 subunits of AMPA receptors in AD (Armstrong and Ikonomovic, 1996), as well as co-localization of APP with GluR2/3 (Thorns et al., 1997). Aβ-treated rat hippocampal neurons have shown increased Ca^{2+} levels and this effect was partially blocked by non-NMDA receptor

antagonists (Brorson et al., 1999), suggesting AMPA receptors play a role in Aβ induced neurodegeneration.

Numerous studies have also shown a direct interaction of Aβ with NMDA receptors. Aβ has been found to bind to NMDA receptors triggering neuronal damage through NMDA induced Ca^{2+} influx (De Felice et al., 2007). Aβ exposure led to an increase in intracellular Ca^{2+} and mitochondrial Ca^{2+} overload, oxidative stress, depolarization of mitochondrial membrane and cell death in rat cortical and hippocampal neurons through NMDA and AMPA receptor mechanisms (Alberdi et al., 2010). Neurons from transgenic mouse models of AD have also been found to express lower levels of NMDA. Despite the decrease in NMDA receptors they have been shown to be over reactive in AD (Ferreira et al., 2010). The loss or inactivation of NMDA receptors during AD progression has been suggested to be neuroprotective (Walton and Dodd, 2007).

In addition to glutamate receptors, glutamate transporters have also been found to be affected in AD (Walton and Dodd, 2007). Glutamate transporters are essential for the maintenance of glutamate levels in mammalian brain. High-affinity uptake is the only way to remove glutamate from the synaptic cleft and halt activation of its receptors (Logan and Snyder, 1972). Glutamate transport has been found to be significantly reduced in temporal, frontal, parietal and hippocampal cortices of AD brains (Masliah et al., 1996a). This decrease was associated with an increase in markers of neuronal death and decrease in the neuronal marker synaptophysin (Masliah et al., 1996a). Additionally, free radicals have been shown to inhibit glutamate uptake. ROS can act on transporters directly or through oxidative by-products such as 4-hydroxynonenal (HNE) (Volterra et al., 1994). Peroxidation of lipids in the membrane has been shown to lead to HNE formation and inactivation of GLT-1 (EAAT2) (Lauderback et al., 2001).

Glutamine synthase (GS) is an enzyme that uses ATP to convert glutamate and ammonium to glutamine. In the brain this reaction takes place in astrocytes and is essential for glutamate homeostasis (Walton and Dodd, 2007).

Previous studies have shown that GS activity declines with age. This decrease in activity is significantly increased in patients with AD (Smith et al., 1991). GS is very sensitive to oxidation and increased ROS can lead to conformational change that alters its activity (Butterfield et al., 1997). As mRNA changes have not been found this suggest that changes occur at protein level (Le Prince et al., 1995). Furthermore, a decrease in GS activity may lead to accumulation of glutamate inside the cell and therefore a reversal of glutamate transport which would contribute to excitotoxicity (Nicholls and Attwell, 1990). GS is normally found in astrocytes in all cortical layers. Astrocytic processes that surround capillaries demonstrate intense staining for GS. However, in AD GS is significantly reduced in vascular end-feet (Robinson, 2001). A decrease in GS activity could be due to a lack of substrate. As the activity of the transporters has been shown to be reduced in AD, this may also affect the level of glutamate that is taken up by astrocytes (Walton and Dodd, 2007). Another important enzyme in glutamate-glutamine cycle is phosphate-activated glutaminase (PAG), which in neurons converts glutamine into glutamate (Walton and Dodd, 2007). Immunocytochemical staining of AD brains demonstrated a decrease in levels of PAG (Akiyama et al., 1989).

Even small disturbances in glutamate homeostasis can have adverse effects. Increased levels of glutamate can lead to increased energy requirements (chapter 3), ROS production, receptor overstimulation and reduction of excitatory signals (Danbolt, 2001). These effects can lead to excitotoxicity and neuronal cell death. AD individuals demonstrate a decreased ability to take up and store glutamate. In addition, glutamate transporters have been found to be more sensitive to oxidative

stress in AD patients (Begni et al., 2004).

4.1.8   Insulin

Normal healthy individuals demonstrate a tightly controlled relationship between glucose metabolism and insulin. Disruption in this relationship can lead to diseases such as diabetes mellitus, which is characterized by hyperinsulinaemia and insulin resistance. Numerous studies have demonstrated cognitive impairments in individuals with type 2 diabetes (T2D) (Ryan and Geckle, 2000). In addition, T2D increases risk of developing vascular dementia and may increase the risk of developing AD (Messier, 2003). As such attention has been focussed on the possible effects of insulin on neurodegeneration in AD (Watson and Craft, 2004).

Insulin is a hormone, which is almost exclusively synthesized and secreted by pancreatic β cells. Its main role is in regulation of glucose metabolism in peripheral tissue (Correia et al., 2012). A large number of studies have shown that insulin is transported from the periphery into the brain via blood-brain barrier (BBB) by a saturable transport mechanism (Banks, 2004, Woods et al., 2003). However, whilst some evidence supports local synthesis of insulin (Schechter et al., 1994) it is widely accepted that little or no insulin is produced in the brain (Woods et al., 2003).

Insulin has an important effect on brain function such as cognition, memory and synaptic plasticity as well as processes such as homeostasis or neuronal survival (Zhao and Alkon, 2001). Insulin acts through the insulin receptor (IR) with the highest insulin binding in specific brain regions, which include olfactory bulb, cerebral cortex, hippocampus, hypothalamus, amygdala and septum (Unger et al., 1991). Insulin binding to its receptor activates two major signalling pathways: the mitogen-activated protein kinase (MAPK) and the phosphoinositide 3-kinase (PI3-K)/Akt (Cardoso et al.,

165

2009). It has also been shown that insulin promotes expression of NMDA receptors (Skeberdis et al., 2001), which are important in long-term potentiation (LTP). It has been proposed that neurodegeneration seen in AD could be caused, at least in part, by disruption in insulin signalling (de la Monte and Wands, 2005). This hypothesis has been supported by evidence showing reduced insulin levels and insulin receptor expression in brains of AD patients (Frolich et al., 1998). In addition, progression through AD Braak stages was associated with a decrease in expression of IGF-1, IGF-2 and their receptors (Rivera et al., 2005). It has also been shown that individuals with AD have increased fasting plasma insulin levels and decreased cerebrospinal fluid (CSF) insulin levels (Watson and Craft, 2004) although other studies failed to show increase in fasting plasma insulin levels (Umegaki et al., 2002). In support of these findings it has been shown that administration of glucose and insulin has a beneficial effect on memory in AD patients (Manning et al., 1993).

4.1.8.1 Insulin and Aβ

The effect of insulin on Aβ is somewhat controversial. The hormone has been found to modulate Aβ processing in CNS (Watson and Craft, 2004). One particular study has shown that subjects over 70 years old had increased levels of Aβ (1-42) in CSF after administration of insulin and the greatest increase of Aβ was associated with reduced memory (Watson and Craft, 2004). It has been suggested that the effect of insulin could include modulation of Aβ release and clearance (Gasparini et al., 2001).

It has previously been shown that insulin increases Aβ levels by enhancing trafficking from ER and trans-Golgi network to the plasma membrane (Gasparini et al., 2001). Additionally, insulin can also competitively inhibit insulin-degrading enzyme (IDE),

which is a major enzyme that can degrade Aβ (Qiu and Folstein, 2006). As type 2 diabetes (T2D) is associated with increased levels of insulin in the CSF (Watson et al., 2003), this could explain higher incidence of AD in individuals diagnosed with T2D (Correia et al., 2012). Interestingly, increased activity of IDE in IDE/APP double transgenic mice resulted in decreased levels of Aβ in the brain (Leissring et al., 2003).

However, insulin signalling has been shown to have beneficial effects on APP and its processing by acting on IR and GSK3 activity suppression. This leads to an increase in the secretion of sAPPα (Solano et al., 2000). Other reports have also shown that inhibition of GSK3β expression or activity prevents Aβ induced neurodegeneration (Takashima et al., 1993, Alvarez et al., 1999). Additionally, GSK3α modulates APP processing thus increasing secretion of Aβ (Phiel et al., 2003).

4.1.8.2 Insulin in AD

A decrease in the concentration of insulin in the CSF of individuals with AD has been suggested to result from the so called "insulin-resistant brain state". This includes downregulation of blood-brain barrier (BBB) function and IR activity and consequently a decrease in insulin transport. Insulin resistance in the brain results in decreased activity of IDE and could lead to a decrease in the degradation of Aβ (Correia et al., 2012).

The presence of both insulin resistance and insulin deficiency has been proposed to be responsible for neurodegeneration in AD (Kroner, 2009). Under normal conditions insulin binding to the receptor activates PI3-K/Akt signaling pathway. PI3-Akt in turn phosphorylates and therefore inhibits glycogen synthase kinase-3β (GSK-3β). GSK-3β inhibition results in a reduction of tau phosphorylation, which promotes its binding

167

to microtubules (Hong and Lee, 1997). Insulin resistance in the brain could lead to decreased activation of PI3-K/Akt signaling pathway and therefore an increase in levels of phosphorylated tau (Schubert et al., 2004). It has been shown that insulin resistance potentiates Aβ deposition and hyperphosphorylation of tau leading to neuronal dysfunction and death and ultimately cognitive decline (Jolivalt et al., 2008).

4.1.8.3 Insulin and glucose administration and memory

It has previously been shown that acute hyperglycaemia can facilitate memory whereas chronic hyperglycemia (such as associated with T2D) may disrupt memory. Studies in rodents have demonstrated beneficial effects of glucose on memory (Lee et al., 1988, Hughes, 2003) but the effect was most beneficial when glucose was administered prior or just after training (Lee et al., 1988, Messier, 1997) as opposed to extended periods of time. This suggests that glucose is important in consolidation rather than retrieval of information. The positive effect of glucose on memory has been suggested to be caused by changes in cholinergic activity in hippocampus (Stone et al., 1988, Okaichi and Okaichi, 2000).

Studies on healthy humans have shown that glucose changes can affect memory. Severe hypoglycaemia can impair higher cortical functions leading to disruptions of memory (Sommerfield et al., 2003). On the other hand acute hyperglycaemia can facilitate memory and other cognitive functions (Craft et al., 1992, Sunram-Lea et al., 2002).

Clinical studies have also shown that treatment with insulin while maintaining euglycaemic conditions facilitates memory in patients with AD as well as healthy control (Craft et al., 1996, Craft et al., 2003).

4.1.9 (β-site APP cleaving enzyme-1) BACE

Previous studies have shown that synaptic activity and brain metabolism have an effect on BACE enzyme expression, which is essential in the production of Aβ (Struble et al., 2010). Based on this evidence, Struble *et al.* (2010) suggested a hypothesis for the metabolic cause of the AD.

BACE1 protein levels and activity are increased in sporadic AD (Fukumoto et al., 2002). In addition, BACE expression is also up-regulated as a result of decreased metabolism (Yan et al., 2007). Some *in vivo* studies have used unilateral naris closure to block stimuli from reaching olfactory receptors and therefore suppress synaptic and metabolic activity in the olfactory bulb. This results in a decline in the activity of mitochondrial enzymes such as cytochrome *c* oxidase and succinic dehydrogenase, as well as upregulation of BACE and an increase in production of c-terminal fragments of AβPP and the Aβ (Yan et al., 2007). Additionally, in mice where BACE has been knocked out, unilateral closure also results in a decrease in activity of mitochondrial enzymes but without an increase in BACE and Aβ, suggesting that metabolic deficits are the initial response to a decline in synaptic activity (Yan et al., 2007).

Evidence for the role of BACE and Aβ in normal functioning of the brain is limited. It has been hypothesized that Aβ modulates neuroplasticity by a concentration-dependent mechanism (Puzzo et al., 2008). In addition, BACE also has been found to modulate synaptic plasticity and synaptogenesis by regulating axonal growth (Zhang et al., 2009).

Brain metabolic activity and mitochondrial function begin to decline at around 30 years of age (De Santi et al., 1995, Petit-Taboue et al., 1998). This decline may

result in increases in BACE expression and further lead to increases in Aβ production (Struble et al., 2010). As a result Aβ accumulation could further affect mitochondrial function and energy metabolism (Uemura and Greenlee, 2001, Atamna and Frey, 2007) and therefore cause increases in ROS production and a decrease in synaptic activity. This may result in a vicious cycle where initial suppression of metabolic activity would lead to increases in Aβ production that further affects metabolism (Struble et al., 2010). This hypothesis could also account for the manifestation of familial AD. As metabolic activity starts to decline at 30 years of age, up-regulation of BACE and an increase in Aβ in individuals carrying mutations may occur. This would accelerate the onset of the disease, which may not be observed earlier, when high metabolism in the brain suppresses BACE activity (Struble et al., 2010).

4.1.10 Aims and objectives of the study

Within view of the large body of evidence suggesting impaired metabolism in AD, it is important to study metabolic changes in a relevant human model. To date most of the studies on hypometabolism in AD have used transgenic animals or imaging studies of human brain. The aim of this chapter therefore, was to investigate the effects of Aβ on metabolism in terms of changes in glucose, glycogen, glutamate and lactate metabolism as well as oxidative stress and calcium signalling using a human stem cell derived culture of neurons and astrocytes.

4.2 Materials and Methods

4.2.1 Cells

4.2.1.1 Primary cultures

Mixed cortical neuronal and glial cultures were prepared from Wistar rat pups 2-3 days post-partum. The pups were killed by cervical dislocation. The cortex was dissected and placed in ice-cold Gey's salt solution (Sigma-Aldrich, UK) containing 20µg/ml gentamycin (Life Technologies, UK). The tissue was then minced using a scalpel and placed in Ca^{2+}-free and Mg^{2+}-free Hanks' buffered saline solution (Life Technologies, UK), containing 0.1 % trypsin (Life Technologies, UK) for 30 min at 37°C. The trypsin was inactivated by adding Neurobasal medium (Life Technologies, UK) containing B27 (Life Technologies, UK), 100 units/ml penicillin and 100 µg/ml streptomycin and 10% horse serum (Life Technologies, UK). Cells were then centrifuged at 1200rpm (258 x g) for 5 min and then medium was replaced with 5ml of fresh Neurobasal medium. Cells were dissociated by trituration with a glass Pasteur pipette with a flame-rounded tip and passed through 70µm filter (BD Biosciences, UK). Cells were then counted using a haemocytometer and plated onto poly-D-lysine coated 12 well plates at a final concentration of 5 x 10^5 cells/ml. Cells were maintained at 37°C and 5% CO_2 and fed twice a week and were used after 5 days.

Plates for primary cultures were coated with poly-D-lysine (Sigma-Aldrich, UK) at concentration of 50µg/ml. Briefly, poly-D-lysine was resuspended in sterile H_2O and filtered through 0.22µm filter, the wells were coated with 2ml of the solution and incubated at 37°C overnight. The poly-D-lysine was aspirated and plates were rinsed with sterile H_2O and dried.

4.2.2   Immunohistochemistry: GFAP / β-tubulin-III staining

Primary cultures were stained according to protocol described in section 3.2.2.1.

4.2.3.   Treatment of NT2.N/A, NT2.A and primary cultures with Aβ(1-42)

NT2/D1 derived co-cultures and pure astrocytes were prepared as described in section 3.2.1.1 and primary cultures were prepared according to the protocol outlined in section 4.2.1.1. Cultures plated on 12-well plates were treated with 20, 2 and 0.2µM of oligomeric Aβ(1-42) prepared in HEPES (as described in section 2.2.1.1) Subsequently plates were incubated for 6, 24, 48, 72 and 96 hours. Following the treatment various assays were performed.

4.2.4   Viability assay

The viability of the cultures following treatment with Aß(1-42) was determined using the Cell-titre Blue^{TM} assay (Promega, UK). Following experimental treatment, medium was removed from the wells of the 12-well cell-culture plate. Subsequently the plate was washed with 500µl phenol red-free DMEM media, supplemented with 10% heat inactivated FBS (NT2.N/A, NT2.A) or 10% horse serum (primary cultures), 100 units/ml penicillin and 100 µg/ml streptomycin and 2mM L-glutamine. 1ml of Cell-titre Blue^{TM} reagent was mixed with 10mls of the DMEM medium. 500µl of this solution was added to each well of the plate. The plate was incubated for 3 hours at 37°C. Following incubation medium was transferred to a 96-well plate and the absorbance was measured at 590nm using a Thermo Multiscan EX 96-well plate reader (Thermofisher, UK).

4.2.5   Gene expression

Changes in gene expression following exposure to Aβ were investigated using qRTPCR. Changes in genes associated with AD were monitored using the Human Alzheimer's Disease RT² Profiler™ PCR Array (Qiagen, UK).

The Human Alzheimer's Disease RT² Profiler™ PCR Array (Qiagen, UK), investigated changes in gene expression following treatment of NT2.N/A co-cultures with 2μM Aβ for 48h. This array profiles the expression of 84 genes that are important in the onset, development, and progression of Alzheimer's disease such as genes contributing to Aβ generation, clearance, and degradation or genes involved in Aβ signal transduction leading to neuronal toxicity and inflammation.

In order to determine changes in genes associated with ANLS, oxidative stress and cell death following treatment of NT2.N/A co-cultures with 0.2, 2 and 20μM Aβ for 48, 72 and 96h primers were obtained from PrimerDesign, UK. This method has been described in section 3.2.3.2. Primers for GLUT1, GLUT3, MCT2, MCT4, MCT1, GLT-1, GLAST, GLUL, GPX1, SOD2, CASP3, INSR and HIF1A were used.

4.2.5.1 RNA extraction

RNA was isolated from NT2.N/A cultures following treatment with Aβ(1-42) and untreated controls according to protocol described in section 3.2.3.1

4.2.5.2 Real-time RT-PCR (Human Alzheimer's Disease RT² Profiler™ PCR Array)

First-strand cDNA synthesis. 1μg of total RNA was reverse transcribed using the RT^2 First strand kit (Qiagen, UK) according to the manufacturer's instructions. cDNA was diluted to 100μl by adding DEPC treated RNase-free water and placed on ice. The PCR was carried out using a Stratagene MX3000P Real-time PCR machine. For one 96-well plate of the Alzheimer's Disease PCR Array (Qiagen, UK), a 2450μl PCR master mix (Qiagen, UK) containing RT^2 PCR master mix and 98μl of diluted cDNA was prepared, and an aliquot of 25 μl was added to each well. For quality control the RT² Profiler™ PCR Arrays include built-in positive control elements for the proper normalization of the data, for the detection of genomic DNA contamination, for the quality of the RNA samples, and for general PCR. The cycling conditions for the PCR reaction were: 10 min at 95 °C, 15 s at 95 °C, 1 min at 60 °C for 40 cycles were used. Three replicates were run for each differentiated sample and controls. Genes measured in this assay are listed in Appendix 8.

4.2.5.3 Data normalization and analysis (Human Alzheimer's Disease RT² Profiler™ PCR Array)

Five endogenous control genes; Beta-2-Microglobulin (B2M), hypoxanthine phosphoribosyltransferase (HPRT1), ribosomal protein L13a (RPL13A), glyceraldehyde-3-phosphate dehydrogenase (GAPDH), and β- actin (ACTB) — present on the PCR Array were used for normalization. Each replicate cycle threshold (CT) was normalized to the average CT of 5 endogenous controls on a per plate basis. The comparative CT method was used to calculate the relative quantification of gene expression. The following formula was used to calculate the relative amount of the transcripts in the chemical treated samples (treat) and the

vehicle-treated samples (control), both of which were normalized to the endogenous controls. $\Delta\Delta CT = \Delta CT$ (treat) – ΔCT (control) for biological RNA samples or $\Delta\Delta CT = \Delta CT$ (Human Brain Reference RNA, HBRR) – ΔCT (Universal Human Reference RNA, UHRR) for reference RNA samples. ΔCT is the difference in CT between the target gene and endogenous controls by subtracting the average CT of controls from each replicate. The fold change for each treated sample (relative to the control sample (or UHRR) = $2^{-\Delta\Delta CT}$.

4.2.5.4 Sensitivity detection and identification of differentially expressed genes (Human Alzheimer's Disease RT² Profiler™ PCR Array)

PCR Array quantification was based on the CT number. A gene was considered not detectable when CT >32. CT was defined as 35 for the ΔCT calculation when the signal was under detectable limits. A list of differentially expressed genes was identified using a 2-tailed t-test. The criteria were a p value less than 0.05 and a mean difference equal to or greater than 2-fold. The statistical calculation was based on ΔCT values.

4.2.6   Determination of glucose levels

Glucose levels were measured using Glucose (HK) Assay Kit (Sigma-Aldrich, UK). The assay is based on enzymatic reaction where glucose undergoes phosphorylation by hexokinase in the presence of ATP. The next step involves oxidation of glucose 6-phosphate to gluconate-6-phosphate by glucose-6-phosphate dehydrogenase. During the oxidation an equimolar amount of NAD^+ is reduced to NADH. The increase in absorbance is then read on a spectrophotometer at 340nm.

$$\text{glucose} + \text{ATP} \xrightarrow{\text{Hexokinase}} \text{glucose-6-phosphate} + \text{ADP}$$

$$\text{glucose-6-phosphate} + \text{NAD} \xrightarrow{\text{G6P-DH}} \text{gluconate-6-phosphate} + \text{NADH}$$
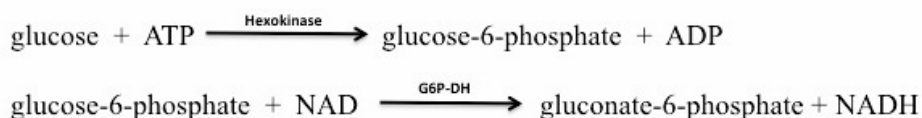
4.2.6.1 Sample preparation

NT2.N/A and NT2.A were prepared as described in section 3.2.1.1 and primary cultures as described in section 4.2.1.1. Cultures plated on 12-well plates were then exposed to a range of concentrations of Aβ(1-42). Aβ(1-42) was prepared using protocol from section 2.2.1.1 and then diluted to 20, 2 and 0.2µM in DMEM Glutamax high glucose, with pyruvate (Life Technologies, UK) containing 10% inactivated foetal bovine serum (Life Technologies, UK), 100 units/ml penicillin and 100 µg/ml streptomycin (for NT2.N/A and NT2.A cultures) or Neurobasal with B27 (Life Technologies, UK) with 10% horse serum (Life Technologies, UK) and 100 units/ml penicillin and 100 µg/ml streptomycin (for primary cultures). Next plates were incubated for 6, 24, 48, 72 and 96 hours. Following the treatment cell culture medium was collected and used for the glucose assay.

4.2.6.2 Protocol

The assay was adapted to a 96-well microplate. Briefly, 200 µl Glucose (HK) Assay Reagent was added to 40 µl of sample in each well. Standards were prepared using a solution of glucose (1 mg/ml) and 1:2 serially diluted using dH$_2$O giving concentrations of 500, 250, 125, 62.5, 31.25, 15.625, 7.813 and 3.906 µg/ml. The reaction was incubated for 15 minutes at room temperature and absorbance was measured at 340nm using a Thermo Multiscan EX 96-well plate reader (Thermofisher, UK). All readings were corrected for background and glucose concentration was expressed in µg/ml.

4.2.7 Determination of glycogen levels

Glycogen levels were measured according to method described in section 3.2.5.

4.2.7.1 Sample preparation

Samples were prepared as described in section 4.2.6.1

4.2.7.2 Determination of protein levels

Protein levels were measured according to protocol described in section 3.2.5.3.

4.2.8 Determination of glucose and glucose-6-phosphate levels

Glucose and glucose-6-phosphate levels inside the cells were measured using method described in section 3.2.5.

4.2.8.1 Sample preparation

Samples were prepared as described in section 4.2.6.1

4.2.8.2 Determination of protein levels

Protein levels were measured according to protocol described in section 3.2.5.3.

4.2.9 Determination of lactate levels

Lactate levels were measured according to method described in section 3.2.6.

4.2.9.1 Sample preparation

Samples were prepared as described in section 4.2.6.1

4.2.10 Determination of pyruvate levels

A Pyruvate Assay Kit was used to measure pyruvate levels (Abcam, UK). The method is based on the oxidation of pyruvate by pyruvate oxidase. The product then interacts with pyruvate probe to produce colour (λ= 570 nm) and fluorescence (at Ex/Em = 535/587 nm).

4.2.10.1 Sample preparation

Samples were prepared as described in section 4.2.6.1

4.2.10.2 Protocol

Pyruvate levels were measured in accordance with the manufacturer's instructions. Briefly, the assay was set up in a 96-well microplate. 50µl of media samples were used per well and mixed with 50µl reaction mix containing 46µl Pyruvate Assay Buffer, 2µl Pyruvate Probe and 2µl Enzyme Mix. 50µl reaction mix was also added to pyruvate standards that were prepared at 0, 2, 4, 6, 8 and 10 nmol/well. The reaction was incubated at room temperature for 30 minutes, protected from light and then read at 570nm using a Thermo Multiscan EX 96-well plate reader (Thermofisher, UK). All readings were corrected for background and pyruvate concentration was expressed in µM.

4.2.11 Determination of glutamate levels

Glutamate levels were measured using Amplex® Red Glutamic Acid/Glutamate Oxidase Assay kit (Life Technologies, UK). It provides a sensitive method for a continuous detection of glutamic acid. In the assay L-glutamic acid undergoes oxidation by glutamate oxidase to produce α-ketoglutarate, NH_3 and H_2O_2. L-glutamic acid can be regenerated using L-alanine and L-glutamate-pyruvate transaminase by transamination of α-ketoglutarate. This creates multiple cycles of the initial reaction, thus increasing H_2O_2 levels. In a reaction catalysed by horseradish peroxidase, H_2O_2 reacts with 10-acetyl-3,7-dihydroxyphenoxazine in a 1:1 stoichiometry. This reaction generates resorufin which is highly fluorescent.

4.2.11.1 Sample preparation

Samples were prepared as described in section 4.2.6.1

4.2.11.2 Protocol

Glutamate levels were measured in media samples according to manufacturer's instructions. Briefly 50 µl of media samples were used for each reaction. L-glutamic acid standards were prepared in 1x reaction buffer at concentrations ranging from 0 to 20 µM. 1x reaction buffer was used as a negative control and 10 µM H_2O_2 as positive control. Next 50 µl of working solutions of 100 µM Amplex® Red reagent containing 0.25 U/ml HRP, 0.08 U/ml L-glutamate oxidase, 0.5 U/ml L-glutamate-pyruvate transaminase, and 200 µM L-alanine was added to each well. The reaction was incubated for 30 minutes at 37°C protected from light. Then the fluorescence was read using SpectraMAX GeminiXS microplate luminometer (Molecular Devices, UK) and SoftMaxPro software (excitation: 540nm, emission: 590nm). All readings

were corrected for background and glutamate concentrations are expressed in µM or as a percentage of glutamate in normal full media.

4.2.12 Determination of glutamine levels

Glutamine levels were measured using Glutamine determination Kit (Sigma-Aldrich, UK). The method is based on two step reaction. First involves enzymatic deamination of L-glutamine by glutaminase that produces L-glutamate. In the second reaction L-glutamate undergoes dehydrogenation by L-glutamate dehydrogenase to produce α-ketoglutarate. This step is accompanied by reduction of NAD^+ to NADH that results in an increase in absorbance at 340nm. In the samples containing both L-glutamine and L-glutamate, the endogenous L-glutamate must also be measured.

$$L\text{-glutamine} + H_2O \xrightarrow[H^+]{\text{Glutaminase}} L\text{-glutamate} + NH_4^+$$

$$L\text{-glutamate} + NAD^+ + H_2O \xrightarrow{\text{L-GLDH}} \alpha\text{-Ketoglutarate} + NH_4^+ + NADH$$
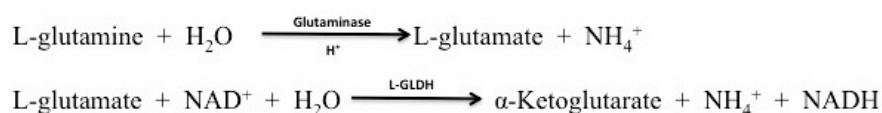
4.2.12.1 Sample preparation

Samples were prepared as described in section 4.2.6.1

4.2.12.2 Protocol

The assay was adapted to a 96-well microplate. To measure L-glutamine levels in samples containing both L-glutamate and L-glutamine two 25µl media aliquots were examined. To the first aliquot 20µl of Acetate buffer, 10µl of glutaminase and 45µl of H_2O were added. To the second aliquot 20µl of Acetate buffer and 55µl of H_2O were added. Standards were prepared as follows. 20µl of Acetate buffer and 10µl of glutaminase were added to varying amounts of 2mM glutamine standards and H_2O to

give standards at concentrations of 1.0, 0.9, 0.8, 0.7, 0.6, 0.5, 0.4, 0.3, 0.2 and 0.1 mmoles/L. All samples were later incubated for 1 hour at 37°C. After incubation 100µl of Tris-EDTA-Hydrazine buffer, 10µl of NAD$^+$ solution, 1µl of ADP solution and 39µl H$_2$O were added to each sample. Absorbance was read using a Thermo Multiscan EX 96-well plate reader (Thermofisher, UK) at 340nm to obtain background reading. Then 2µl of L-glutamic dehydrogenase was added the each well and samples were incubated at room temperature for 40 minutes. After incubation absorbance was read at 340nm. The readings were corrected for background and L-glutamine levels were measured by subtracting endogenous L-glutamate concentration from total L-glutamate concentration (derived from both L-glutamine and L-glutamate). The results were expressed as mmoles/L.

4.2.13 Determination of total glutathione levels

The method to investigate levels of total glutathione (GSH+GSSG) was first described by Owens and Belcher (1965). The sensitivity of the assay was then improved by Tietze (1969) and it was later adapted to a microplate method (Clarke et al., 1996). This assay is based on enzymatic reaction involving oxidation of GSH by 5,5'-dithiobis(2-nitrobenzoic) (DTNB), to produce chromophore TNB which results in increases in absorbance at 410nm. The sensitivity is increased by recycling GSH by glutathione reductase (GSR) and NADPH.

4.2.13.1 Sample preparation

Samples were prepared as described in section 4.2.6.1. Following the treatment cells were washed three times with PBS and then scraped in 1ml of PBS. Samples were then centrifuged at 6600g for 2.5 minutes. Next the supernatant was removed and the pellet was resuspended in 3.3µl of 100% sulphosalicylic acid (SSA) to precipitate

protein. Samples were centrifuged at 13000g for 90 seconds. Next 96.6 µl of stock buffer (125mM sodium phosphate, 6.3mM disodium EDTA, pH 7.5) was added to the samples and they were centrifuged at 13000g for 90 seconds. Supernatant was then used in the total glutathione assay and the pellet for protein determination.

4.2.13.2 Protocol

The assay was designed in a 96-well microplate. Standards were prepared by diluting 100mM GSH in H_20 and SSA to generate 0, 20, 40, 60 and 80 µM samples. 150 µl of a 0.35mM NADPH in stock buffer and 50 µl of a 6mM DTNB in stock buffer was added to each well. Next 25 µl of samples (from section 4.2.13.1) or standards were added to each well and incubated at 30°C for 5 minutes. The absorbance was then read using a Thermo Multiscan EX 96-well plate reader (Thermofisher, UK) at 410nm to obtain background readings. Subsequently 25 µl of GSR (4U/ml) was added to each sample and absorbance was read immediately. The absorbance readings were taken over a period of 10 minutes. The glutathione levels were calculated using standard curve and were corrected for background and expressed as nmoles per mg of protein.

4.2.13.3 Determination of protein levels

The pellet from section 4.2.13.1 was used to determine protein levels. The protein content was determined using the DC protein assay reagent kit (Bio-Rad, UK), according to the manufacturer's instructions. Briefly, 127µl working reagent A' was added to the protein pellet. The pellet was then vortexed until solubilised. 127µl of working reagent A' was also added to 100µl of BSA standards (125-2000µg/ml) or water which acted as a BSA-free control and vortexed. Then 100µl of water was

added to the solubilised pellet to correct for volume difference between samples and standard curve. The samples and standard solutions were then transferred to a test-tube and 1ml of reagent B was added. Tubes were then vortexed and incubated at room temperature for 15min. The solution was transferred to a 96-well plate and the absorbance was measured at 750nm using Multiskan Go microplate spectrophotometer (Thermo Scientific, UK)

4.2.14 Determination of NAD$^+$/NADH ratio

A NAD$^+$/NADH Quantification Kit was used to measure NAD$^+$ and NADH levels (Abcam, UK). This method allows detection of the intracellular nucleotides: NADH, NAD$^+$ as well as their ratio. The method includes NAD cycling enzyme as the cycling reaction increases the detection and specificity of the assay.

4.2.14.1 Sample preparation

NT2.N/A were prepared as described in section 3.2.1.1. Cultures plated on 12-well plates were then exposed to 2µM Aβ(1-42) (section 2.2.1.1) and then diluted in DMEM Glutamax high glucose, with pyruvate (Life Technologies, UK) containing 10% inactivated foetal bovine serum (Life Technologies, UK), 100 units/ml penicillin and 100 µg/ml streptomycin. Next plates were incubated for 6, 24, 48, 72 and 96 hours.

Following the treatment cells were washed with cold PBS and scraped. Cells were then centrifuged at 2000rpm (400g) for 5 min and PBS was removed. 400 µl of NADH/NAD$^+$ Extraction Buffer was added to the pellet. NADH and NAD$^+$ were extracted by two freeze and thaw cycles (20min on dry-ice and 10min at room temperature). Following the extraction, the lystate was vortexed for 10 sec and

centrifuged at 12000rpm (13,800g) for 5 min. The supernatant containing extracted NADH and NAD$^+$ was transferred to a new tube and used in the assay.

4.2.14.2 Protocol

NAD$^+$ and NADH levels were measured in accordance with the manufacturer's instructions. Briefly, to detect NADt (NADH and NAD$^+$) 50 µl of the extract was transferred into 96-well plate in duplicates. To detect NADH, NAD$^+$ is firstly decomposed. This was done by aliquoting 200 µl of the extract into microcentrifuge tubes and heating at 60°C for 30min on a heating block. Samples were then cooled on ice and 50 µl of the NADH samples were transferred into 96-well plate in duplicates. Samples were then mixed with 100 µl of the NAD Cycling Mix that was prepared by adding 2 µl of NAD cycling enzymes mix to 100 µl NAD cycling buffer. The cycling mix was also added to NADH standards that were prepared at 0, 20, 40, 60, 80 and 100 pmol/well. Plate was then incubated at room temperature for 5 min to convert NAD$^+$ to NADH. 10 µl of NADH developer was added to each well and the plate was incubated at room temperature for 1 to 4 hours. The plate was then read at 450nm using a Thermo Multiscan EX 96-well plate reader (Thermofisher, UK). All readings were corrected for background and protein content. NAD$^+$ levels were calculated by subtracting NADH readings from NADt. Results were expressed as NAD$^+$/NADH ratio.

4.2.14.3 Determination of protein levels

The protein concentration of sample was determined using the Bradford assay reagent kit from BioRad in accordance with the manufacturer's instructions. Briefly 800µl of diluted sample, BSA standard (ranging from 2-12 µg/ml) or NAD/NADH Extraction Buffer which acted as a BSA-free control were added to a microcentrifuge

tube with the 200µl of dye reagent concentrate. Each sample was vortex and incubated at room temperature for 5 min. The samples and standards were then transferred into a 96-well plate and read at 590nm using a Thermo Multiscan EX 96-well plate reader (Thermofisher, UK).

4.2.15 Determination of ATP levels

The CellTiter-Glo® Luminescent Cell Viability Assay was used to measure ATP levels in cell lysate (Promega, UK). This method relies on mono-oxygenation of luciferin which is catalyzed by luciferase in the presence of Mg^{2+}, ATP and oxygen.

4.2.15.1 Sample preparation

NT2.N/A were prepared as described in section 3.2.1.1. Cultures plated on 12-well plates were then exposed to 2µM Aβ(1-42) which was prepared using protocol from section 2.2.1.1 and then diluted in DMEM Glutamax high glucose, with pyruvate (Life Technologies, UK) containing 10% inactivated foetal bovine serum (Life Technologies, UK), 100 units/ml penicillin and 100 µg/ml streptomycin. Next plates were incubated for 6, 24, 48, 72 and 96 hours.

4.2.15.2 Protocol

ATP levels were measured in accordance with the manufacturer's instructions (see Appendix 7). Briefly, following the treatment cells were scraped in 400µl of cell media and transferred into a microcentrifuge tube. 400µl of CellTiter-Glo® Reagent was added to the cells as well as ATP standards (ranging from 10 – 1000 nM) and the tubes were mixed for 2 minutes on a shaker to induce cell lysis. Then the tubes were left on a bench for 10min to equilibrate. The luminescence was recorded using

SpectraMAX GeminiXS microplate luminometer (Molecular Devices, UK) and SoftMaxPro software.

4.2.15.3 Determination of protein levels

Protein levels were measured according to protocol described in section 3.2.5.3.

4.2.16 Enzyme-linked Immunoabsorbant Assay (ELISA)

4.2.16.1 Sample preparation

For all ELISAs samples were prepared as described in section 4.2.6.1

4.2.16.1 IL-6 ELISA (Bender MedSystems)

An ELISA to detect IL-6 was used in accordance with the manufacturer's instructions. A Maxi-sorp immune-plate (NUNC) was coated by transferring 100µl of coating antibody (2.5µg/ml) to each well. The plate was sealed with an adhesive film and stored at 4˚C overnight. The next day each well was washed 3 times with 0.05% Tween 20 in PBS. The plate was then blocked using 250µl assay buffer (0.5% BSA, 0.05% Tween 20 in PBS) and incubated for 2 hours at room temperature. After blocking the wells were washed twice as previously described. 100µl of standards prepared in assay buffer (100, 50, 25, 12.5, 6.25, 3.125, 1.56 pg/ml) were then added in duplicates to the plate. 50µl of samples were added per well together with 50µl of assay buffer. Biotin-conjugate anti-human IL-6 monoclonal antibody was diluted 1:1000 in assay buffer and 50µl was added to each well. Plate was then covered with adhesive film and incubated at room temperature for two hours. The plate was then washed four times as described previously. 100µl Streptavidin-HRP diluted 1:5000 in assay buffer was then added to each well. The plate was then sealed and incubated

at room temperature for 1 hour. Following incubation the plate was washed four times as described above. 100µl of tetramethylbenzidine (TMB) solution was then added to each well. The plate was then incubated at room temperature, protected from light, until a suitable colour had developed. The reaction was stopped with 50µl of 0.5M H_2SO_4 per well. The absorbance was then read using a Thermo Multiscan EX 96-well plate reader (Thermofisher, UK) at 450nm. The results were corrected for background.

4.2.16.2 IL-1β ELISA (eBioscience)

An ELISA to detect IL-1β was used in accordance with the manufacturer's instructions. A Maxi-sorp immune-plate (NUNC) was coated by transferring 100µl of anti-human IL1-β capture antibody (1:250 dilution in Coating buffer) to each well. The plate was sealed with an adhesive film and stored at 4°C overnight. The next day each well was washed 5 times with 0.05% Tween 20 in PBS. The plate was then blocked using 200µl 1X Assay Diluent and incubated for 1 hours at room temperature. After blocking the wells were washed five times as previously described. 100µl of human IL-1β standard protein prepared in 1X Assay Diluent (500, 250, 125, 62.5, 31.25, 15.625, 7.813, 3.906 pg/ml) and samples were added in duplicated to the plate. Plate was then covered with adhesive film and incubated at room temperature for two hours. The plate was then washed five times as described previously. 100µl of Biotin-conjugate anti-human IL-1β diluted 1:250 in 1X Assay Diluent was then added to each well and plated was sealed and incubated for 1 hour at room temperature. The plate was then washed five times as described above. Next 100µl of Avidin-HRP diluted 1:250 in 1X Assay Diluent was added to each well and plate was covered with adhesive film and incubated for 30 minutes at room temperature. The plate was then washed seven times as described previously, allowing the wells to soak in Wash buffer for 1-2 minutes. 100µl of 1X TMB solution

was added to each well and the plate was incubated at room temperature for 15 minutes. The reaction was stopped with 50µl of 0.5M H_2SO_4 per well. The absorbance was then read using a Thermo Multiscan EX 96-well plate reader (Thermofisher, UK) at 450nm. The results were corrected for background.

4.2.16.3 TNF-α ELISA (R&D Systems)

An ELISA to detect TNF-α was used in accordance with the manufacturer's instructions. A Maxi-sorp immune-plate (NUNC) was coated by transferring 100µl of mouse anti-human TNF-α coating antibody (4µg/ml) to each well. The plate was sealed with an adhesive film and incubated overnight at room temperature. The next day each well was washed 3 times with 0.05% Tween 20 in PBS. The plate was then blocked using 300µl Reagent Diluent (1% BSA in PBS) and incubated for 1 hour at room temperature. After blocking the wells were washed three times as previously described. 100µl of TNF-α protein standards prepared in Reagent Diluent (1000, 500, 250, 125, 62.5, 31.25 and 15.625 pg/ml) and samples were then added in duplicates to the wells. The plate was covered with adhesive film and incubated at room temperature for 2 hours. Following incubation each well was washed three times as described previously. Biotinylated goat anti-human TNF-α antibody was diluted in Reagent Diluent to concentration of 350 ng/ml and 100 µl was added to each well. The plate was sealed and incubated for 2 hour at room temperature. Each well was then washed three times as described above. Next 100µl of Streptavidin-HRP (1:200 dilution in Reagent Diluent) was added to each well and plate was covered with adhesive film and incubated for 20 minutes at room temperature, protected from light. The plate was then washed three times as described previously. 100µl of TMB solution was added to each well and the plate was incubated at room temperature for 20 minutes, protected from light. The reaction was stopped with 50µl of 0.5M H_2SO_4

per well. The absorbance was then read using a Thermo Multiscan EX 96-well plate reader (Thermofisher, UK) at 450nm. The results were corrected for background.

4.2.16.4 β-NGF ELISA (R&D Systems)

An ELISA to detect β-NGF was used in accordance with the manufacturer's instructions. A Maxi-sorp immune-plate (NUNC) was coated by transferring 100µl of mouse anti-human β-NGF coating antibody (2µg/ml) to each well. The plate was sealed with an adhesive film and incubated overnight at room temperature. The next day each well was washed 3 times with 0.05% Tween 20 in PBS. The plate was then blocked using 300µl Reagent Diluent (1% BSA in PBS) and incubated for 1 hour at room temperature. After blocking the wells were washed three times as previously described. 100µl of β-NGF protein standards prepared in Reagent Diluent (2000, 1000, 500, 250, 125, 61.25 and 31.25 pg/ml) and samples were then added in duplicates to the wells. The plate was covered with adhesive film and incubated at room temperature for 2 hours. Following incubation each well was washed three times as described previously. Biotinylated goat anti-human β-NGF antibody was diluted in Reagent Diluent to concentration of 50 ng/ml and 100 µl was added to each well. The plate was sealed and incubated for 2 hour at room temperature. Each well was then washed three times as described above. Next 100µl of Streptavidin-HRP (1:200 dilution in Reagent Diluent) was added to each well and plate was covered with adhesive film and incubated for 20 minutes at room temperature, protected from light. The plate was then washed three times as described previously. 100µl of TMB solution was added to each well and the plate was incubated at room temperature for 20 minutes, protected from light. The reaction was stopped with 50µl of 0.5M H_2SO_4 per well. The absorbance was then read using a Thermo Multiscan EX 96-well plate reader (Thermofisher, UK) at 450nm. The results were corrected for background.

4.2.16.5 BDNF ELISA (R&D Systems)

An ELISA to detect BDNF was used in accordance with the manufacturer's instructions. A Maxi-sorp immune-plate (NUNC) was coated by transferring 100µl of mouse anti-human BDNF coating antibody (2µg/ml) to each well. The plate was sealed with an adhesive film and incubated overnight at room temperature. The next day each well was washed 3 times with 0.05% Tween 20 in PBS. The plate was then blocked using 300µl Reagent Diluent (1% BSA in PBS) and incubated for 1 hour at room temperature. After blocking the wells were washed three times as previously described. 100µl of BDNF protein standards prepared in Reagent Diluent (1500, 750, 375, 187.5, 93.75, 46.875 and 23.437 pg/ml) and samples were then added in duplicates to the wells. The plate was covered with adhesive film and incubated at room temperature for 2 hours. Following incubation each well was washed three times as described previously. Biotinylated mouse anti-human BDNF antibody was diluted in Reagent Diluent to concentration of 25 ng/ml and 100 µl was added to each well. The plate was sealed and incubated for 2 hour at room temperature. Each well was then washed three times as described above. Next 100µl of Streptavidin-HRP (1:200 dilution in Reagent Diluent) was added to each well and plate was covered with adhesive film and incubated for 20 minutes at room temperature, protected from light. The plate was then washed three times as described previously. 100µl of TMB solution was added to each well and the plate was incubated at room temperature for 20 minutes, protected from light. The reaction was stopped with 50µl of 0.5M H_2SO_4 per well. The absorbance was then read using a Thermo Multiscan EX 96-well plate reader (Thermofisher, UK) at 450nm. The results were corrected for background.

4.2.17 Calcium

NT2.N/A cultures following treatment with 2μM Aβ for 48h as well as controls were loaded with Fluo-4 (Life Technologies, UK). The staining was carried out by incubating for 60min at 37°C with 5μM of Fluo-4 and 0.01% pluronic acid. The recording chamber was mounted on a motorized moveable bridge (Luigs and Neumann, Germany) and fluorescence dye was excited using an Optoscan monochromator system (Cairn, UK) at excitation wavelength 488nm and emission wavelength 516nm, fitted to a Nikon FN1 upright microscope; filter cubes were obtained from Chroma (Chroma VT, USA). Images of areas of 444μm x 341μm were routinely acquired every 5s for 15 min with a x20 objective lens (NA=0.8) using an ORCA ER CCD camera (Hamamatsu) and analysed using Simple PCI software (Compix Hamamatsu, Digital Pixel, UK). Statistical analysis was performed using GraphPad Prism Software.

4.2.18 Statistics

Results were expressed as the mean of three samples ± standard error of the mean (SEM). Comparisons between treatments were performed using analysis of variance (ANOVA) followed by Dunnett's or Tukeys post-test or Students T-test using GraphPad Prism Software. Differences were considered significant for p values <0.05.

4.3   Results

The study presented in chapter 3 provided evidence for functional metabolic coupling of NT2 derived neurons and astrocytes that is consistent with the ANLS model. Based on these results, NT2.N/A and NT2.A cultures were used to investigate changes in metabolism caused by treatment with Aβ(1-42). The methods used covered a range of biochemical assays that measured extracellular or intracellular levels of metabolites such as glucose, glycogen or lactate as well as ATP or reducing agents such as NADH. In addition, cells were investigated for signs of oxidative stress and calcium changes. The results obtained from NT2 derived cultures were compared to commonly used *in vitro* model, namely rat primary cortical cultures.

4.3.1   Preparation of primary cultures

The primary mixed glial and neuronal cultures were prepared from cortices of Wistar rat pups. Initially the cultures were maintained in two different types of media: Neurobasal and DMEM F12. Five days after plating the cultures were stained for β-Tubulin and GFAP and analysed to establish which media combination resulted in cultures with highest confluence and cell growth similar to NT2.N/A cultures. As seen in Fig. 4.2A and 4.2B the cultures grown in F12 media were sparse in comparison to cultures maintained in Neurobasal media. Both cultures displayed typical neuronal and astrocytic morphology, with neurons extending axons and dendrites together with astrocytes. Cultures grown in neurobasal media in Fig. 4.2C and 4.2D produced a large number of astrocytes and networks of neurons with fine processes (Fig. 4.2B). As these cultures were considered to be most similar to NT2 networks in terms of the ratio of neurons to astrocytes these culture conditions were chosen to produce cultures for treatment with Aβ. An example of such culture is shown in Fig. 4.3.

4.3.2 Viability studies

NT2.N/A co-cultures, NT2.A cultures and mixed rat glial and neuronal cultures were treated with different concentrations of Aβ(1-42) (20, 2, 0.2μM) for 6, 24, 48, 72 and 96h. Following the treatment, viability of the cells was measured using Cell-titre Blue^{TM} assay (Promega, UK).

In the co-cultures the only significant change was seen at the highest concentration of Aβ(1-42) (Fig. 4.4A). 20μM Aβ caused an increase in viability at 6h (111.84 ± 4.17%, $p<0.05$) and a decrease in viability at 48h (88.69 ± 4.29%, $p<0.05$). In the pure astrocytic cultures there was a significant increase in the viability of the cells treated with 0.2μM Aβ for 72h (106.07 ± 2.11%, $p<0.05$) (Fig. 4.4B). Similarly the primary cultures did not show any significant cell death over time (Fig. 4.4C). After 24h treatment with 20μM and 0.2μM the cultures showed an increase in viability (20μM: 106.88 ± 1.67, $p<0.05$; 0.2μM: 107.91 ± 1.25%, $p<0.05$). The same increase in viability was seen after 72h treatment with the highest concentration of Aβ (105.46 ± 0.99%, $p<0.05$).

4.3.3 Glucose studies

Glucose uptake from the medium was measured using Glucose (HK) Assay Kit (Sigma-Aldrich, UK). NT2.N/A, NT2.A and primary cultures all showed a significant decrease in glucose uptake following treatment with 2μM and 0.2μM Aβ at all time points. Glucose levels in the medium from co-cultures were significantly increased ($p<0.001$) at all time points (Fig. 4.5A). Similar increases in glucose levels were seen in primary cultures ($p<0.001$) at all time points except for 2μM Aβ treatment at 6h ($p<0.01$) (Fig. 4.5C). Astrocytic cultures also demonstrated a decrease in glucose uptake although to a lesser extent than neuronal and astrocytic cultures (Fig. 4.5B).

At 24h the glucose levels in the media were significantly increased following the treatment with Aβ (<u>control</u>: 1829.14 ± 52.73µg/ml; <u>2µM</u>: 2222.39 ± 16.89µg/ml, $p<0.001$; <u>0.2µM</u>: 2257.82 ± 44.35µg/ml, $p<0.001$). Decrease in glucose uptake became less significant over time in astrocytes. At 72h the increase in glucose is at $p<0.05$ for both concentrations and at 96h only 0.2µM Aβ treatment cause any substantial impact ($p<0.05$).

The glucose uptake over time differed between the cultures. In all cases the starting concentration of glucose in the medium was 4500µg/ml. The NT2.N/A cultures used up over 50% of the available glucose in the first 6h (<u>control</u>: 1814.84 ± 34.02 µg/ml) (Fig. 4.5A). Pure astrocytic cultures took up less glucose than co-cultures (<u>control</u>: 2064.3 ± 65.7 µg/ml) whilst uptake in primary cultures was even slower (<u>control</u>: 2955.77 ± 55.08 µg/ml) (Fig. 4.5B and 4.5C).

The primary cultures were also more sensitive to Aβ treatment and glucose uptake was blocked to a greater extent than in NT2.N/A or NT2.A cultures. After 96h primary cultures treated with 0.2µM Aβ used up 57.72 ± 1.98% of the glucose from the media (<u>control</u>: 98.64 ± 0.25%) while NT2.N/A used up 92.8 ± 0.28% (<u>control</u>: 96.05 ± 0.05%) and NT2.A 87.54 ± 0.34% (<u>control</u>: 89.1 ± 0.17%).

4.3.4   Glycogen studies

Following the treatment of the cultures with Aβ glycogen levels inside the cells were measured at 6, 24, 48, 72 and 96h. NT2.N/A co-cultures showed an initial decrease in glycogen levels at 6h (<u>0.2µM</u>: 96.05 ± 0.47%, $p<0.001$; <u>2µM</u>: 96.59 ± 0.15%, $p<0.001$) (Fig. 4.6A). Glycogen levels increased, to control levels at 24h, with significant ($p<0.001$) increases at 72hr to 129.3 ± 5.57% when treated with 2µM Aβ and 123.35 ± 3.94% with 0.2µM Aβ. At 96h the differences were less apparent with

only 0.2µM Aβ having a significant effect (113.24 ± 4.32%, $p<0.05$) (Fig. 4.6A). Primary cultures demonstrated a similar pattern, with glycogen levels increasing at 48h. However, the increase in glycogen was much more significant and at 96h levels of glycogen reached 277.06 ± 16.47% ($p<0.001$) after treatment with 2µM Aβ and 258.75 ± 19.97% ($p<0.001$) when treated with 0.2µM Aβ (Fig. 4.6C). Additionally, from 48h there was a decrease in glycogen levels in cells treated with 20µM Aβ which was significant at 48h ($p<0.001$) and 72h ($p<0.001$).

Pure astrocytes also demonstrated an increase in glycogen levels from 6h (2µM: 129.99 ± 7.13, $p<0.01$) (Fig. 4.6B). Increases were observed at all time points, but were only significant at 24 and 96h.
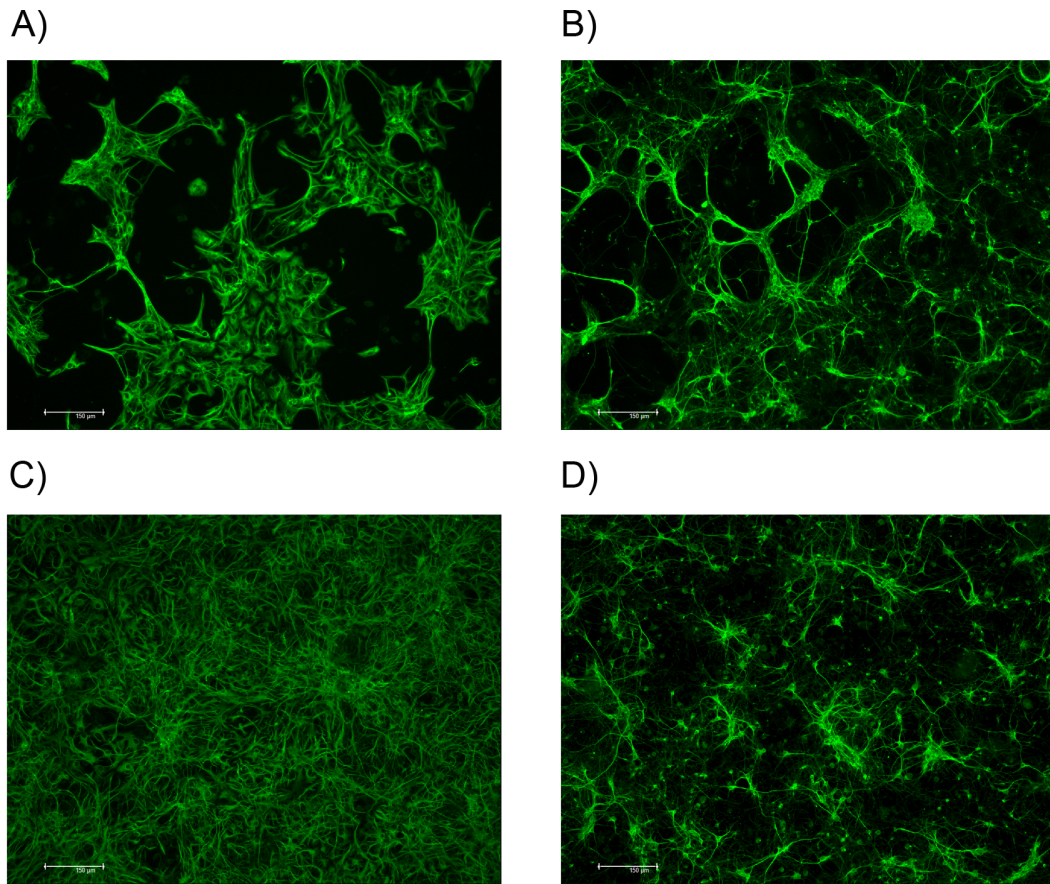
Figure 4.2   Immunofluorescent images of primary cortical mixed neuronal and glial cultures. Images showing (A) GFAP positive astrocytes and (B) β-tubulin positive neurons grown in F12 medium and (C) GFAP positive astrocytes and (D) β-Tubulin positive neurons grown in Neurobasal medium. Scale bar 150μM.
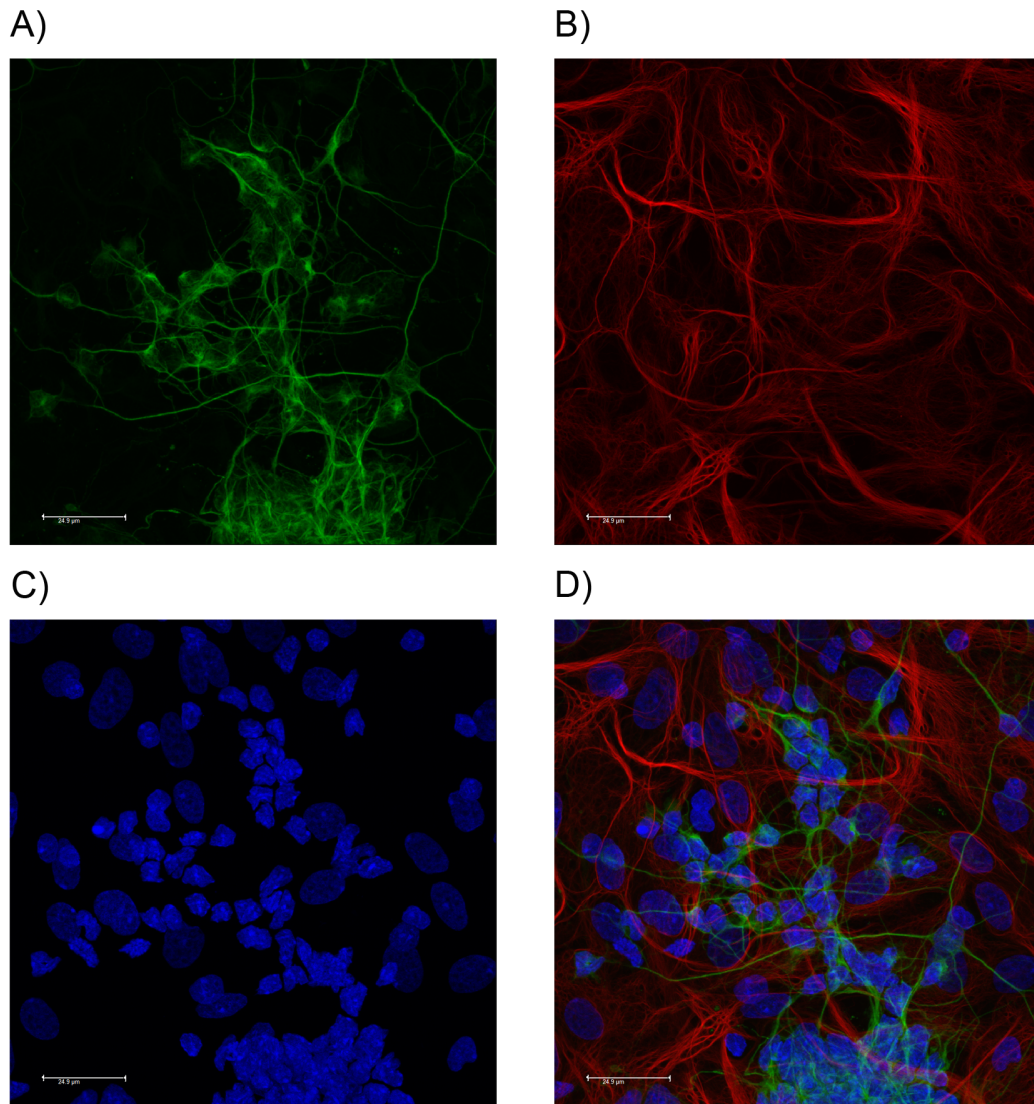
Figure 4.3 Immunofluorescent images of primary cortical mixed neuronal and glial cultures. Images showing (A) β-tubulin positive neurons (green), (B) GFAP (red) positive astrocytes, (C) nuclei stained with Hoechst and (D) an overlay. Scale bar 24.9μM.
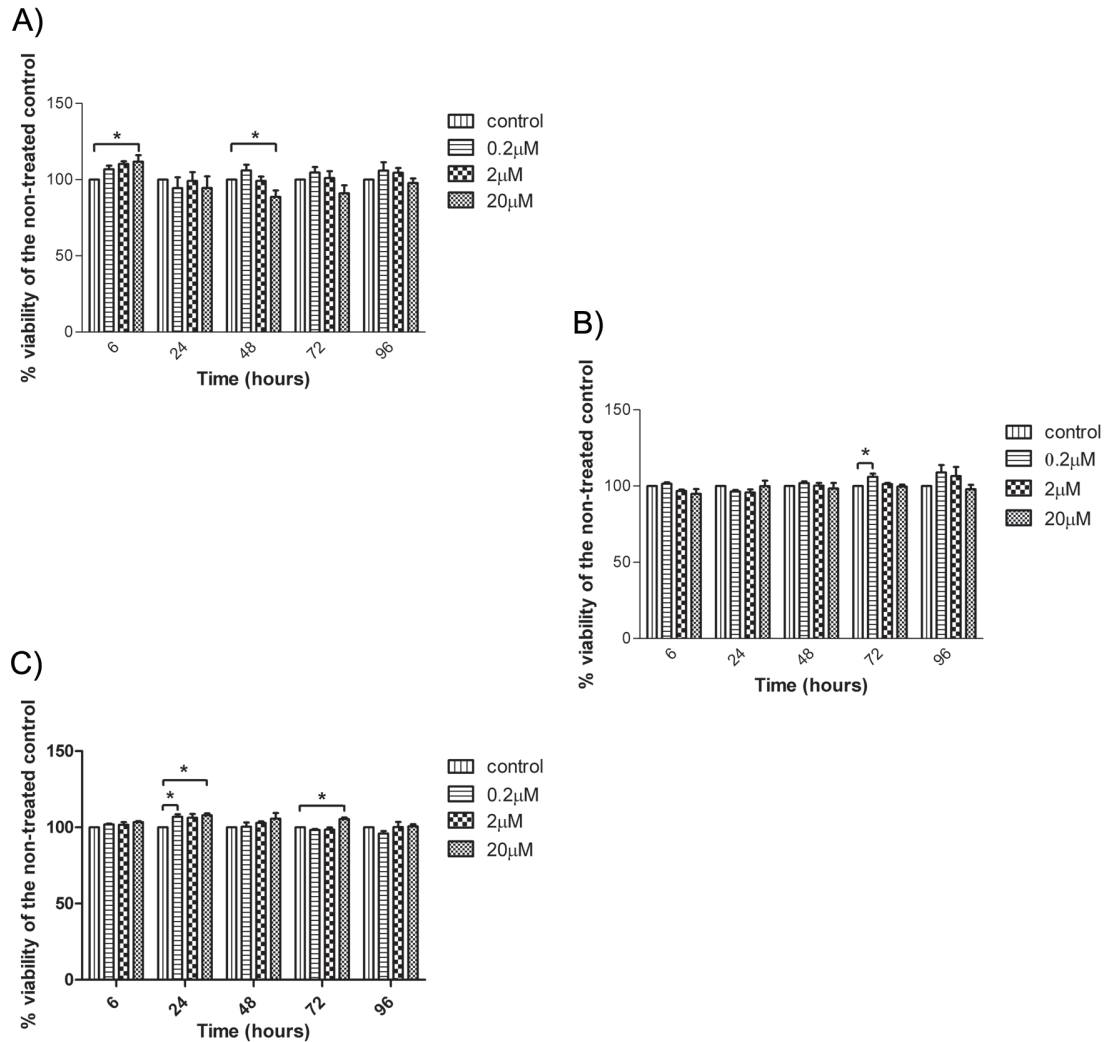
Figure 4.4 Viability results following treatment with 20μM, 2μM, 0.2μM Aβ measured by CellTitre Blue[TM] assay. (A) NT2.N/A, (B) NT2.A and (C) primary cultures. Viability was measured after 6, 24, 48, 72 and 96h. Results are expressed as percentage of non-treated control ± SEM, n=3. $p<0.05$ (*), $p<0.01$ (**), $p<0.001$ (***).

Figure 4.5 Glucose levels in the media following treatment with 20µM, 2µM, 0.2µM Aβ. (A) NT2.N/A, (B) NT2.A and (C) primary cultures. Glucose was measured after 6, 24, 48, 72 and 96h. Results are expressed as µg/ml ± SEM, n=3. $p<0.05$ (*), $p<0.01$ (**), $p<0.001$ (***).

4.3.5 Glucose and glucose-6-phosphate

Glucose and glucose-6-phosphate levels inside the cells were measured after the treatment with Aβ. As in previous experiments the effect was restricted to two lower concentrations of Aβ, 2µM and 0.2µM. The NT2.N/A co-cultures showed an accumulation of glucose and glucose-6-phosphate at all time points (Fig. 4.7A). The increase was most significant at 6h (control: 116.29 ± 5.61 nmol/mg protein; 0.2µM: 171.71 ± 9.06 nmol/mg protein, $p<0.01$) and 24h time point (control: 84.84 ± 3.93 nmol/mg protein; 0.2µM: 139.34 ± 14.07 nmol/mg protein, $p<0.01$). The accumulation of glucose and glucose-6-phosphate was more significant and reached higher levels in astrocytes than in co-cultures, with 6h (control: 110.01 ± 8.41 nmol/mg protein; 0.2µM: 213.76 ± 13.95 nmol/mg protein, $p<0.001$) and 24h time points (control: 142.8 ± 8.58 nmol/mg protein; 0.2µM: 211.36 ± 6.32 nmol/mg protein, $p<0.001$) showing the largest increase (Fig. 4.7B). Similarly primary cultures also showed a very significant ($p<0.001$) accumulation of glucose and glucose-6-phosphate at all time points (Fig. 4.7C).

In addition to the effect of Aβ, there was a significant difference in the levels glucose and glucose-6-phosphate between control of NT2–derived cultures (N/A and A) and primary cultures. In controls primary cultures, levels of glucose and glucose-6-phosphate decreased with time, reaching very low levels at 96h time point (0.44 ± 0.29 nmol/mg protein), while in NT2-derived control cultures levels of glucose and glucose-6-phosphate decreased more slowly.

Figure 4.6 Glycogen levels inside the cells following treatment with 20μM, 2μM, 0.2μM Aβ. (A) NT2.N/A, (B) NT2.A and (C) primary cultures. Glycogen was measured after 6, 24, 48, 72 and 96h. Results are expressed as percentage of non-treated control ± SEM, n=3. $p<0.05$ (*), $p<0.01$ (**), $p<0.001$ (***).
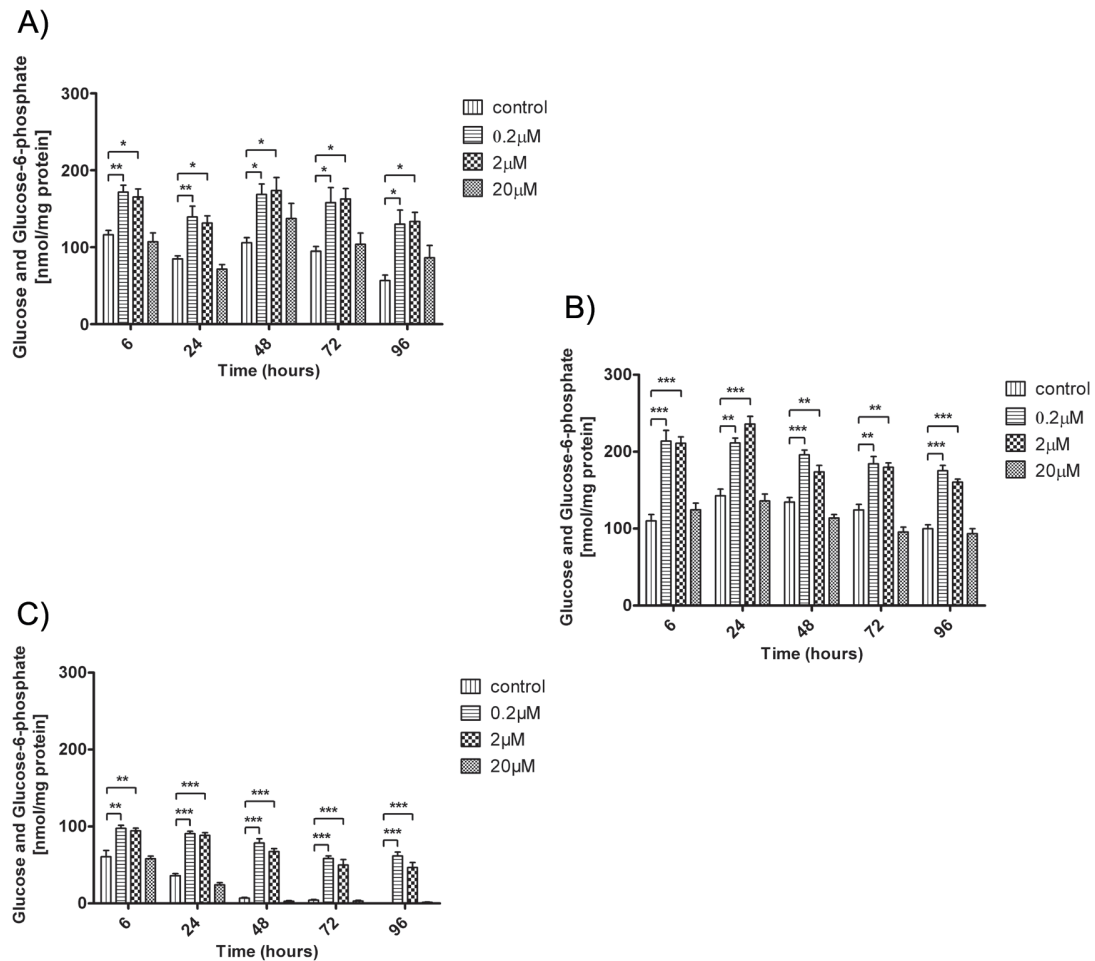
Figure 4.7 Glucose and Glucose-6-phosphate levels inside the cells following treatment with 20µM, 2µM, 0.2µM Aβ. (A) NT2.N/A, (B) NT2.A and (C) primary cultures. Glucose and Glucose-6-phosphate were measured after 6, 24, 48, 72 and 96h. Results are expressed as nmol/mg protein ± SEM, n=3. $p<0.05$ (*), $p<0.01$ (**), $p<0.001$ (***).

4.3.6 Lactate studies

Lactate levels in the cell conditioned media following treatment with Aβ were found to be significantly decreased in NT2.N/A co-cultures. At 6h there was no significant change in lactate levels.

However, after 24h the levels were decreased following treatment with both 0.2μM and 2μM Aβ treatments (control: 13.59 ± 0.26mM; 2μM: 10.63 ± 0.11mM, $p<0.01$; 0.2μM: 9.47 ± 0.6mM, $p<0.001$) (Fig. 4.8A). The decrease was also seen at 48h and 72h, however, at 96h levels of lactate were similar to control levels (control: 19.95 ± 0.18mM; 2μM: 19.89 ± 0.78mM; 0.2μM: 21.31 ± 0.33mM). Pure astrocytes did not demonstrate any change following the treatment with Aβ. Interestingly, levels of lactate in pure astrocyte cultures were much lower than in co-cultures (Fig. 4.8B). In primary cultures, the decrease in lactate was very significant and was seen from 6h (control: 5.23 ± 0.41mM; 2μM: 3.75 ± 0.10mM, $p<0.01$; 0.2μM: 3.81 ± 0.10mM, $p<0.01$) through to 96h (control: 19.41 ± 0.97mM; 2μM: 13.30 ± 0.87mM, $p<0.001$; 0.2μM: 10.16 ± 1.08mM, $p<0.001$) (Fig. 4.8C).

Lactate was found to accumulate over time in all cultures. In NT2.N/A cultures and primary cultures the lactate levels were much higher than in pure astrocytes. Additionally, in NT2.N/A co-cultures the accumulation was slower than in primary cultures. NT2.N/A reached 19.95 ± 0.18mM levels at 96h while primary cultures reached 20.59 ± 0.84mM levels at 48h after which time the levels remained stable.

4.3.7   Pyruvate studies

The levels of pyruvate level in the medium were measured following the treatment with Aβ. The initial pyruvate concentration in NT2.N/A and NT2.A medium supplied was 1mM while in primary cultures medium the concentration was 200µM.

All cultures demonstrated a significant reduction in pyruvate levels over time regardless of treatment. In NT2.N/A cultures treated with both 0.2µM and 2µM Aβ, the levels of pyruvate were higher than in control. The most significant increase was seen at 24h (control: 397.55 ± 7.7µM; 2µM: 446.48 ± 15.89µM, $p<0.05$; 0.2µM: 460.75 ± 8.34µM, $p<0.01$) and 48h (control: 326.78 ± 8.71µM; 2µM: 364.02 ± 7.6µM, $p<0.05$; 0.2µM: 379.62 ± 6.97µM, $p<0.01$) (Fig. 4.9A). However, at 96h the level of pyruvate dropped significantly in comparison to control. In pure astrocytes there was no change in the concentration of pyruvate after the treatment with Aβ (Fig. 4.9B). Primary cultures demonstrated a similar pattern to NT2.N/A co-cultures, with an increase in pyruvate concentration that became more significant after 6h (Fig. 4.9C). Conversely to NT2.N/A co-cultures there was no decrease at 96h in primary culture (control: 4.19 ± 0.44µM; 2µM: 19.62 ± 0.89µM, $p<0.001$; 0.2µM: 21.0 ± 0.91µM, $p<0.001$).

4.3.8   Glutamate studies

Treatment with Aβ was also found to have an effect on glutamate levels in the media. In NT2.N/A co-cultures there was a significant decrease in glutamate levels from 24h with the largest decrease at 72h and 96h (control: 22.31 ± 1.19µM; 2µM: 13.33 ± 0.41µM, $p<0.001$; 0.2µM: 13.05 ± 1.52µM, $p<0.001$) (Fig. 4.10A). This decrease became more significant with time, as the control and 20µM Aβ treated cells accumulated more glutamate in the media. In pure astrocytes, the decrease was also

present but to a lesser extent (Fig. 4.10B). Overall the levels of glutamate in the media samples were much lower in pure astrocytic cultures than co-cultures of neurons and astrocytes. Primary cells also showed a significant decrease in glutamate levels after treatment with 2µM and 0.2µM Aβ. The decrease was significant from 24h and most significant at 96h (control: 9.08 ± 0.34µM; 2µM: 5.51 ± 0.37µM, $p<0.001$; 0.2µM: 5.35 ± 0.43µM, $p<0.001$) (Fig. 4.10C).

Additionally when 0.5mM glutamate was added to the NT2.N/A co-cultures in the presence of 2µM Aβ, the uptake of glutamate was significantly decreased in comparison to controls at both 6h and 48h (Fig. 4.11).

A)

B)

C)
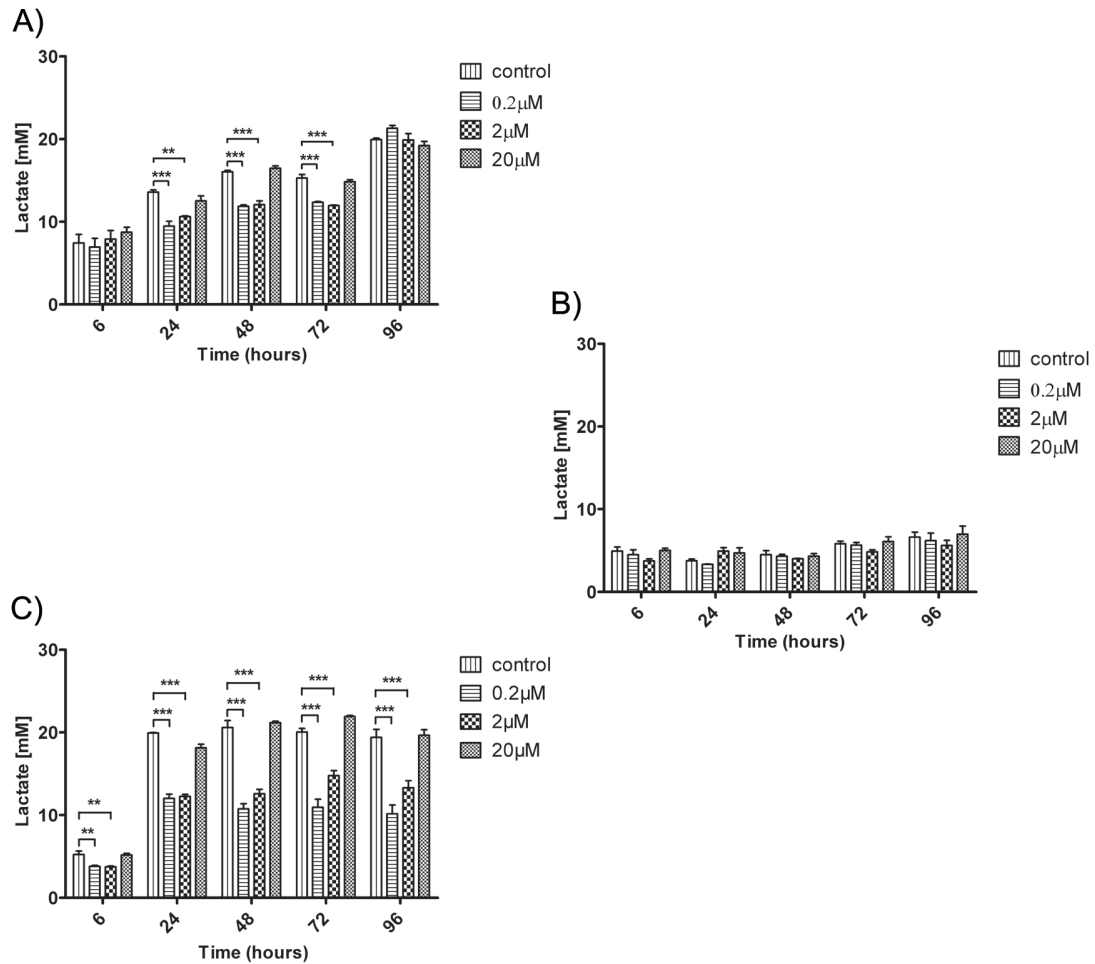
Figure 4.8 Lactate levels in the media following treatment with 20µM, 2µM, 0.2µM Aβ. (A) NT2.N/A, (B) NT2.A and (C) primary cultures. Lactate was measured after 6, 24, 48, 72 and 96h. Results are expressed as mM ± SEM, n=3. $p<0.05$ (*), $p<0.01$ (**), $p<0.001$ (***).
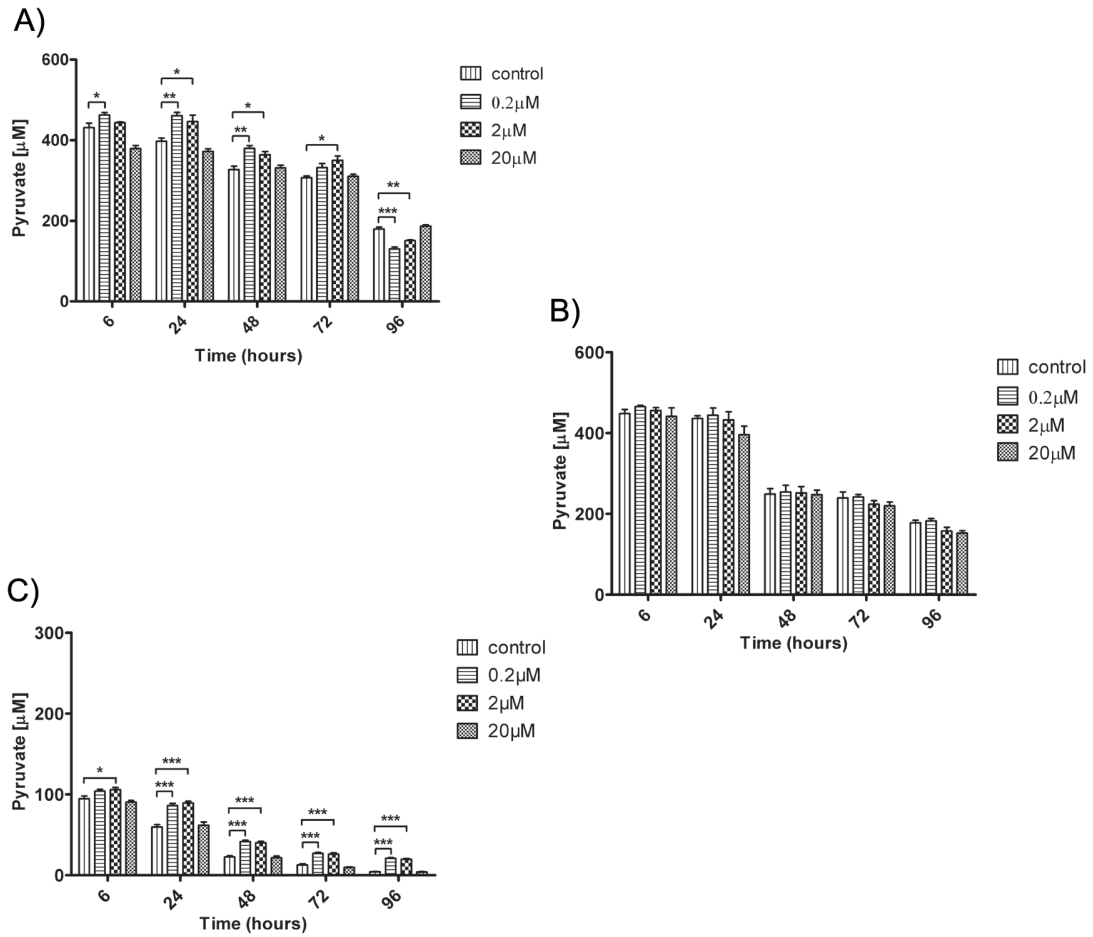
Figure 4.9 Pyruvate levels in the media following treatment with 20µM, 2µM, 0.2µM Aβ. (A) NT2.N/A, (B) NT2.A and (C) primary cultures. Pyruvate was measured after 6, 24, 48, 72 and 96h. Results are expressed as mM ± SEM, n=3. *p*<0.05 (*), *p*<0.01 (**), *p*<0.001 (***).
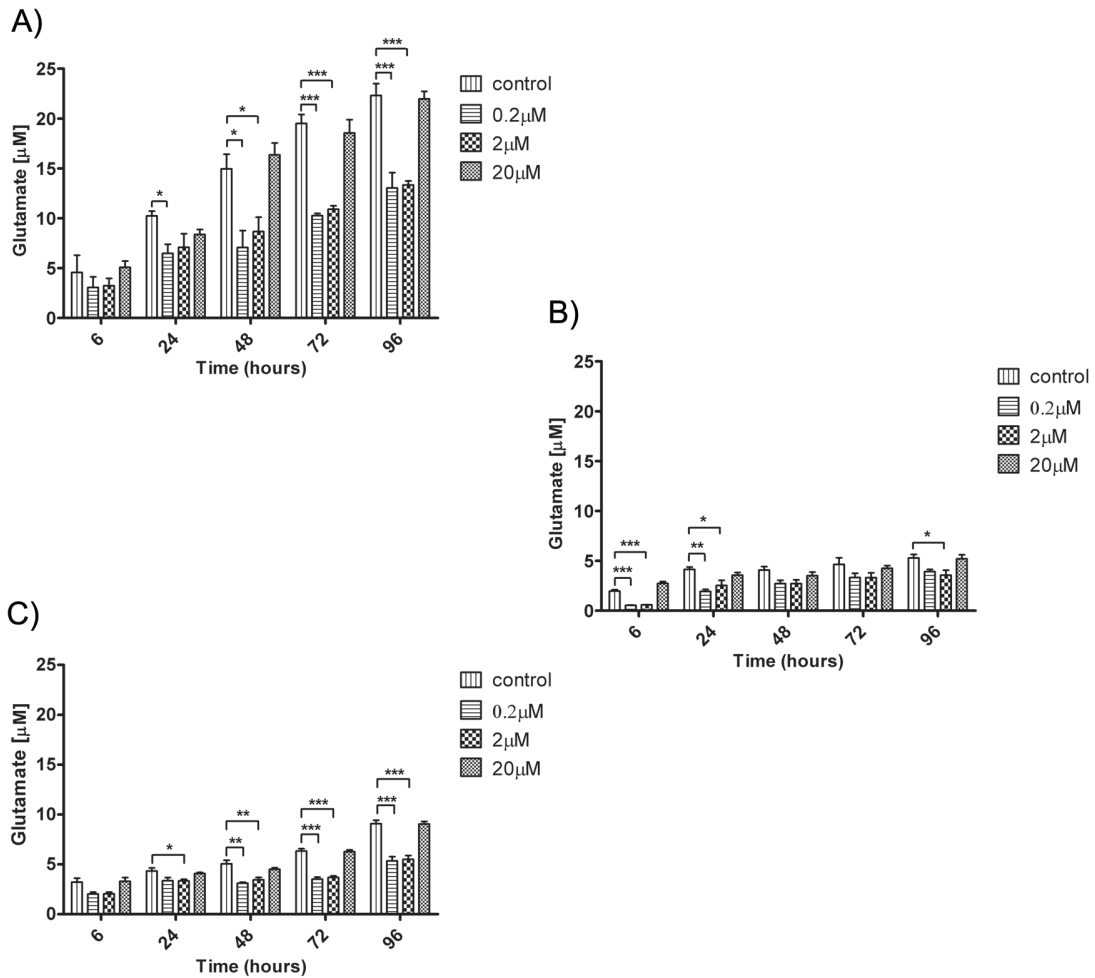
Figure 4.10   Glutamate levels in the media following treatment with 20µM, 2µM, 0.2µM Aβ. (A) NT2.N/A, (B) NT2.A and (C) primary cultures. Glutamate was measured after 6, 24, 48, 72 and 96h. Results are expressed as µM ± SEM, n=3. $p<0.05$ (*), $p<0.01$ (**), $p<0.001$ (***).
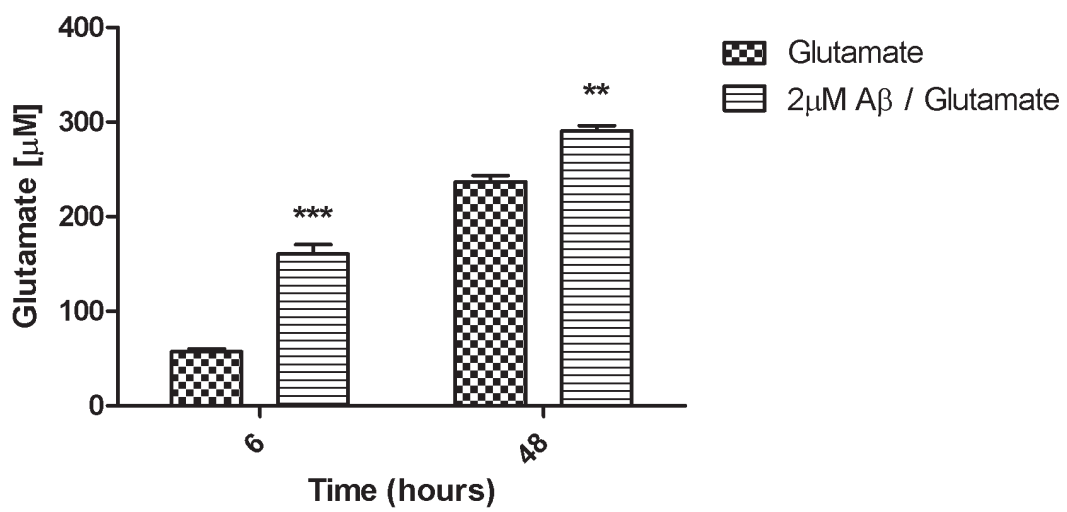
Figure 4.11   Glutamate levels in the media following treatment of NT2.N/A co-cultures with 2μM Aβ and 0.5mM glutamate. Glutamate was measured after 6 and 48h. Results are expressed as μM ± SEM, n=3. $p<0.05$ (*), $p<0.01$ (**), $p<0.001$ (***).

4.3.9 Glutamine studies

Glutamine levels in the media samples demonstrated a small increase, which was only significant in NT2.N/A co-cultures treated with both 0.2μM and 2μM Aβ for 72h (control: 28.51 ± 1.22mM; 0.2μM: 34.33 ± 0.56mM; 2μM: 33.42 ± 0.53mM p<0.05) (Fig. 4.12A). Pure astrocytic cultures did not show significant changes except for 72h treatment with 0.2μM Aβ (control: 27.95 ± 0.96mM; 0.2μM: 32.13 ± 0.76mM, p<0.05) (Fig. 4.12B). Primary cultures showed no increase in glutamine following the treatment with Aβ. However, the primary cultures accumulated more glutamine than NT2.N/A and NT2.A cultures, with higher levels seen already at 6h (NT2.N/A: 9.33 ± 1.76mM: NT2.A: 8.67 ± 1.76mM; primary cells: 20.56 ± 1.86mM).

4.3.10 GSH/GSSG ratio

NT2.N/A co-cultures treated with all concentrations of Aβ showed a significant decrease in GSH/GSSG ratio at 6 and 24h (Fig. 4.13A). The trend remained similar at 48h, 72h and 96h, however, the decrease was not significant. Pure astrocytes also showed a decrease in GSH/GSSG ratio from 6h time point (Fig. 4.13B). This decrease was significant up to 48h time point. After 72h the GSH/GSSG ratio increased to control levels (control: 18.44 ± 1.67; 20μM: 18.65 ± 1.8; 2μM: 23.1 ± 1.8; 0.2μM: 21.77 ± 1.22). At 96h there was a further increase in the ratio which was significant at all three concentrations ($p<0.05$).

4.3.11 NAD$^+$/NADH and ATP

NAD$^+$/NADH ratios and ATP levels were measured in NT2.N/A co-cultures following treatment with 2μM Aβ. The NAD$^+$/NADH ratio followed a bell shaped trend, with an increase in the ratio at 24h and then a steady decrease at 48, 72 and 96h (Fig.

4.14A). Both Aβ-treated and control cells follow this trend. There was an initial increase in NAD^+/NADH ratio following the treatment with Aβ was for 24h (control: 0.66 ± 0.06; 2μM: 0.91 ± 0.02, $p<0.05$). However, after this time point the ratio was much lower following the Aβ treatment and became more significant with time reaching its highest levels at 96h (control: 0.52 ± 0.03; 2μM: 0.18 ± 0.01, $p<0.001$). This decrease in ratio was due to a decrease in NAD^+ levels (see Appendix 5 and 6). At 96h NAD^+ levels in control were 819.6 ± 17.5 pmol/mg of protein, whilst after treatments with 2μM Aβ 347.5 ± 20.2 pmol/mg of protein. ATP levels following treatment with 2μM Aβ decreased from 6h, becoming significant at 24h (Fig. 4.14B). ATP levels reached their lowest levels at 72h and 96h (control: 8.34 ± 0.86nmol/mg protein; 2μM: 3.29 ± 0.20nmol/mg protein, $p<0.01$).

4.3.12 ELISA determinations

Five different types of ELISA were used to analyse samples from NT2.N/A and NT2.A cultures, including IL-6, IL-1β, TNF-α, β-NGF and BDNF. No changes were found following the treatment with Aβ(1-42) (data not shown). NT2.N/A cultures released low levels of IL-6 (48h: 6.07±1.23 pg/ml), however, IL-1β, TNF-α, β-NGF and BDNF were not detected by ELISAs.

4.3.13 Calcium imaging studies

As changes in calcium signalling have previously been shown in astrocytes following Aβ treatment (Abramov et al., 2003), calcium changes in stem cell derived astrocytes were determined following Aβ treatment. Calcium responses were recorded following exposure of NT2.N/A co-cultures to 2μM Aβ as well as in controls. The excitability of astrocytes which is defined by variations in intracellular calcium (Volterra and Meldolesi, 2005) was investigated by fluorescent calcium imaging.
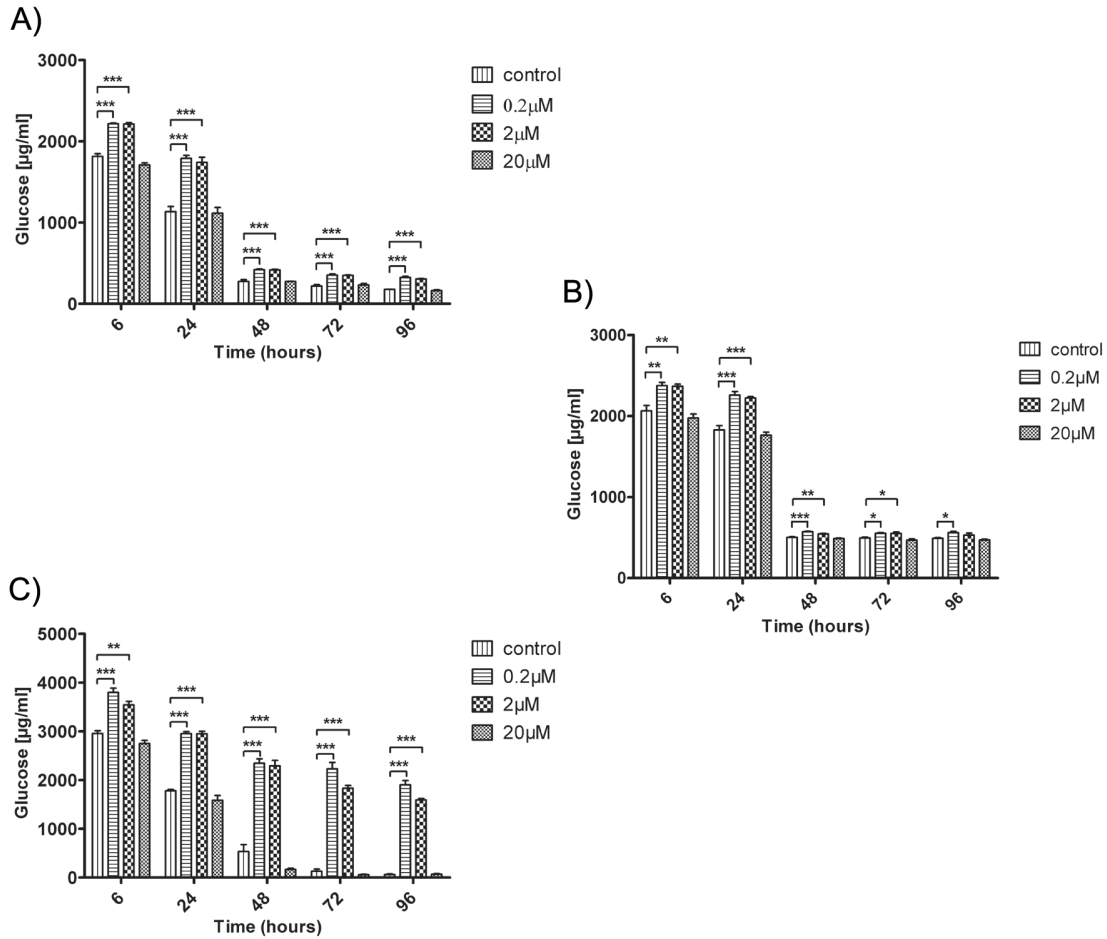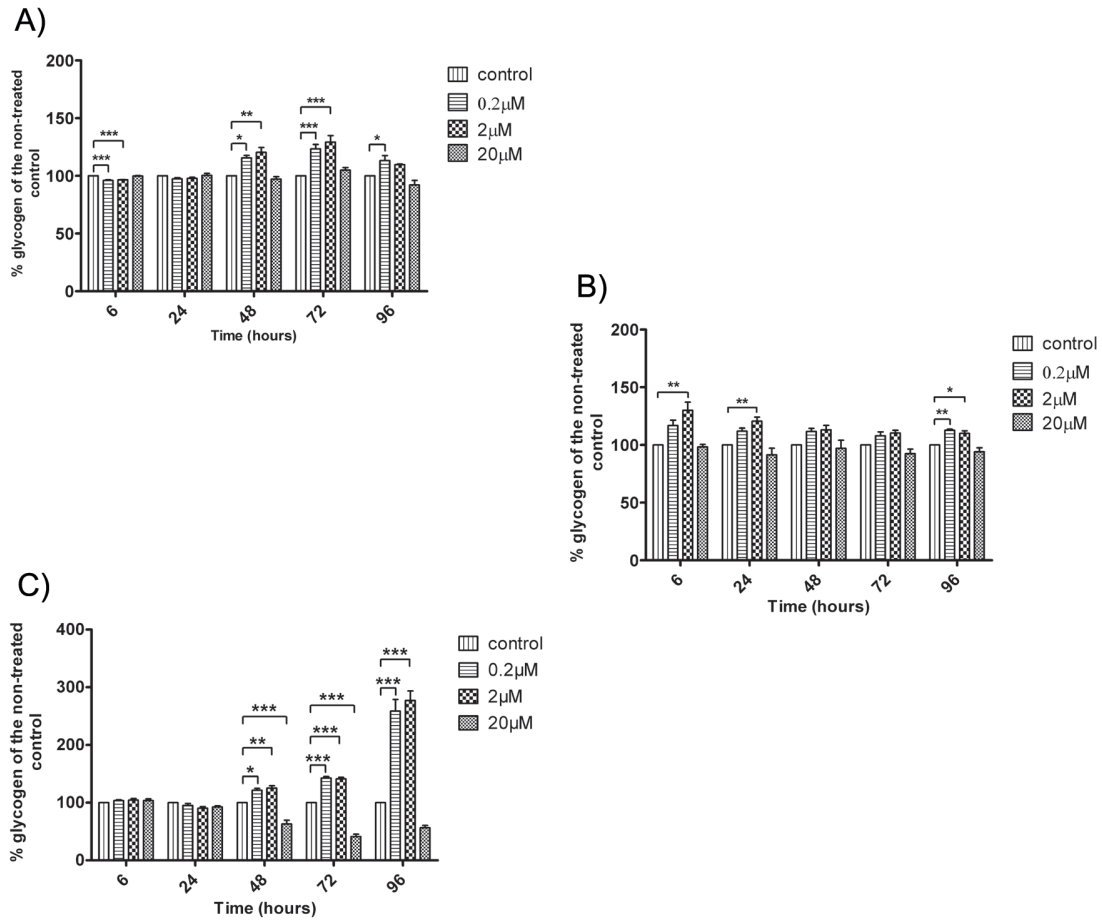
211
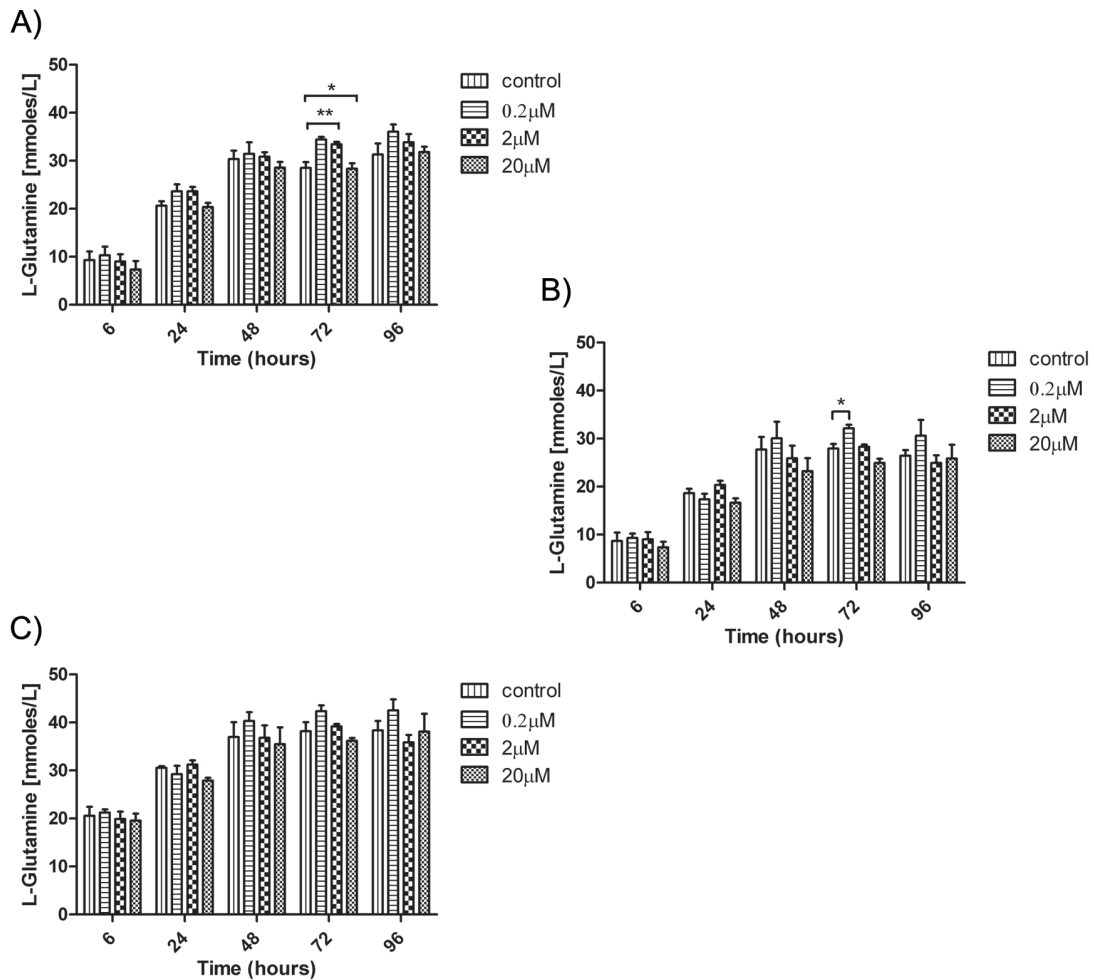
Figure 4.12 Glutamine levels in the media following treatment with 20µM, 2µM, 0.2µM Aβ. (A) NT2.N/A, (B) NT2.A and (C) primary cultures. Glutamate was measured after 6, 24, 48, 72 and 96h. Results are expressed as mmoles/L ± SEM, n=3. $p<0.05$ (*), $p<0.01$ (**), $p<0.001$ (***).
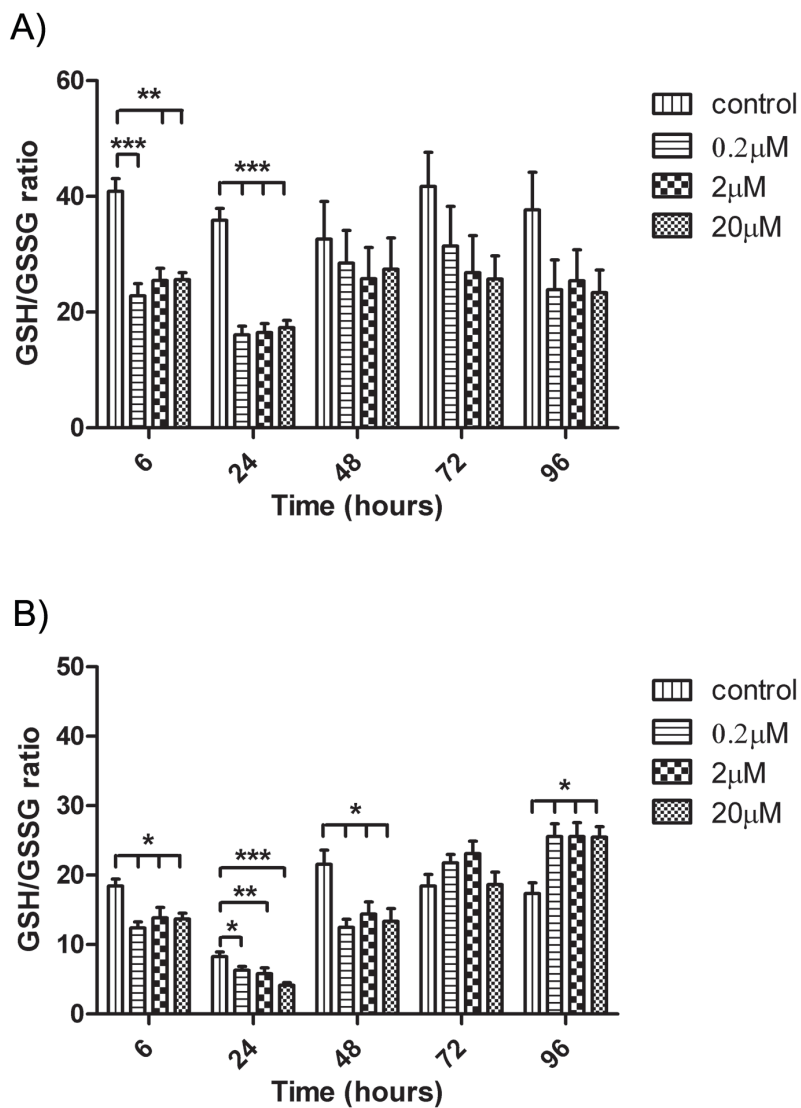
Figure 4.13 GSH/GSSG ratio inside the cells following treatment with 20μM, 2μM, 0.2μM Aβ. (A) NT2.N/A and (B) NT2.A. Glutamate was measured after 6, 24, 48, 72 and 96h. Results are expressed as ratio ± SEM, n=3. $p<0.05$ (*), $p<0.01$ (**), $p<0.001$ (***).
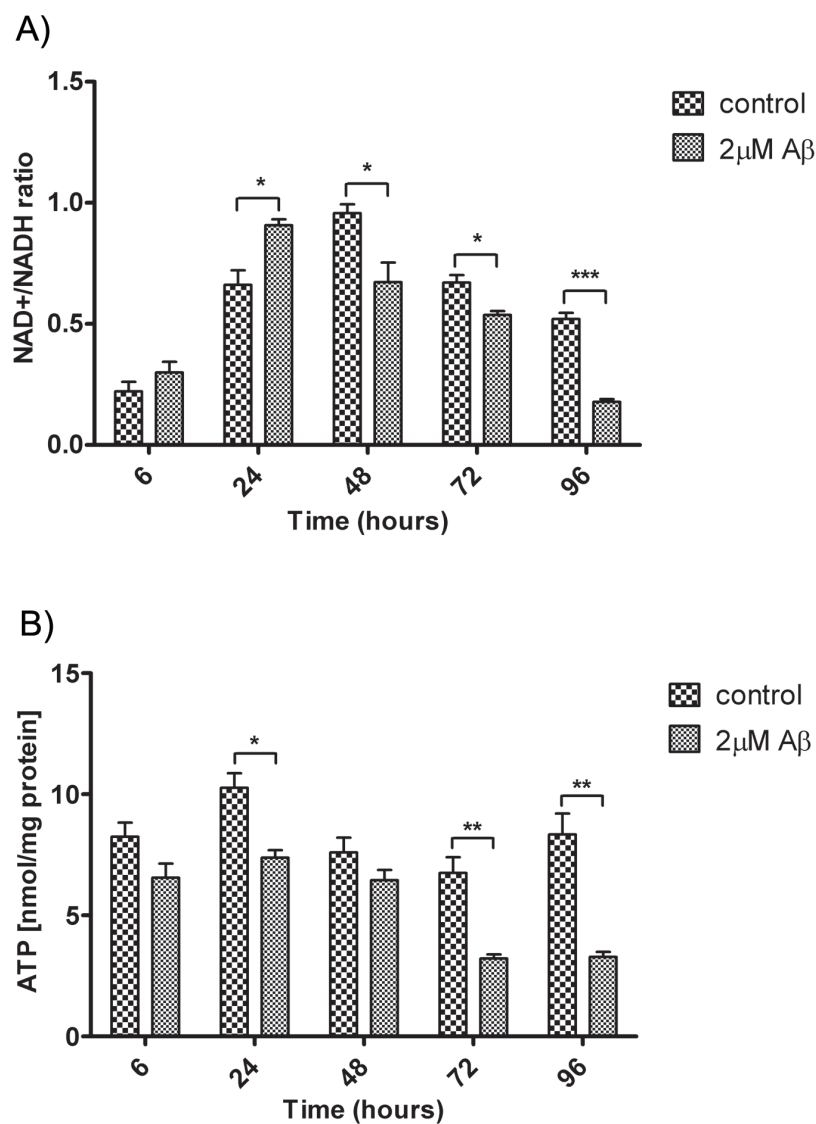
Figure 4.14   NAD+, NADH and ATP levels inside the cells following treatment of NT2.N/A with 2µM Aβ. (A) NAD+, NADH and (B) ATP were measured after 6, 24, 48, 72 and 96h. Results are expressed as ratio ± SEM (A) and nmol/mg protein ± SEM (B), n=3. $p<0.05$ (*), $p<0.01$ (**), $p<0.001$ (***).

Following loading of the cells with the cell permeable calcium indicator fluo-4, the activity was recorded over time.

Fig. 4.15 shows a control culture with spontaneously active cells (A) and a graphical representation of calcium oscillations in 3 representative astrocytes (B). In control cells only 32.29 ± 7.6% of cells demonstrated calcium oscillations (Fig. 4.16A) with low oscillation frequency (control: 0.22 ± 0.02 per min; Fig. 4.16B). Following treatment with Aβ there was a significant increase in the number of astrocytes displaying calcium oscillations (69.55 ± 3.09%; $p<0.05$; Fig. 4.16A). A representative culture treated with Aβ is presented in Fig. 4.15C and D. Additionally, the frequency of oscillation in the astrocytes was significantly increased (Aβ: 0.31 ± 0.03 per min; $p<0.05$; Fig. 4.16B)

4.3.14 Gene expression determinations

Changes in gene expression following the treatment with Aβ were investigated. The Human Alzheimer's Disease RT² Profiler™ PCR Array (SABiosciences) was used to determine changes in AD associated genes whilst additional qRT-PCR was performed to determine changes in genes associated with astrocyte-neuron lactate shuttle, oxidative stress and cell death.

Gene arrays were run using samples from control and NT2.N/A co-cultures treated with 2µM Aβ for 48h. The results showed significant up-regulation of the following genes: *A2M* (α$_2$-macroglobulin)*, APBB2* (β-amyloid precursor protein-binding family B member 2)*, BACE1* (β-site APP-cleaving enzyme 1)*, CASP4* (caspase-4)*, GAP43* (growth-associated calmodulin-binding phosphoprotein)*, GNG8* (guanine *nucleotide* binding protein (G protein), gamma 8)*, GSK3β* (glycogen synthase kinase-type 3, isozyme β)*, IDE* (insulin-degrading enzyme)*, LPL* (lipoprotein lipase)*, SNCA* (α-

synuclein) and downregulation of *BCHE* (butyrylcholinesterase) (Fig. 4.18). The highest fold change was seen in the upregulated genes: *GAP43* (10.13), *CASP4* (4.76) and *LPL* (3.54).

qRT-PCR experiments to determine changes in genes associated with the lactate shuttle, oxidative stress and cell death were carried out using RNA samples from NT2.N/A co-cultures treated with 20, 2, 0.2µM Aβ for 48, 72 and 96h as well as appropriate controls. The results demonstrated no significant changes in any of the genes analysed (see Appendix 9, 10 and 11).
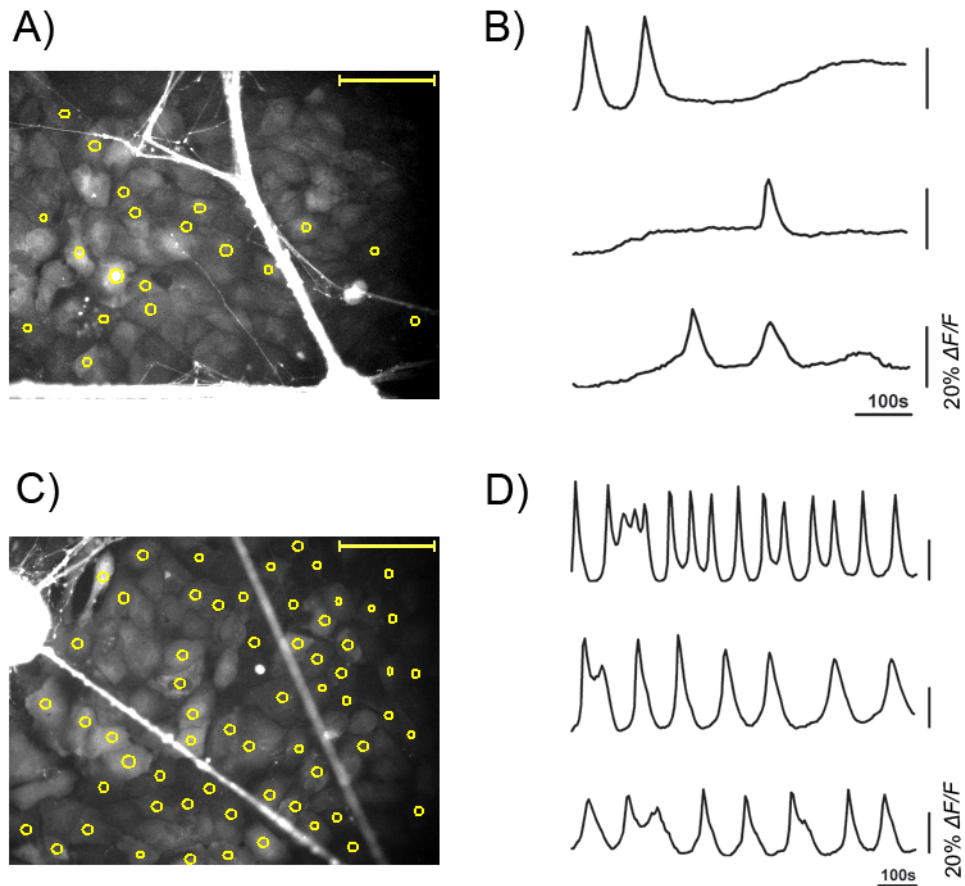
Figure 4.15 Calcium oscillations in NT2.N/A co-cultures. (A) Image of NT2.N/A control co-culture. Yellow circles indicate spontaneously active astrocytes. Scale bar 100µm. (B) Representative fluorescence time course from 3 different astrocytes from image (A). (C) Image of NT2.N/A co-culture treated with 2µM Aβ for 48h. Yellow circles indicate active astrocytes. Scale bar 100µm. (B) Representative fluorescence time course from 3 different astrocytes from image (A).
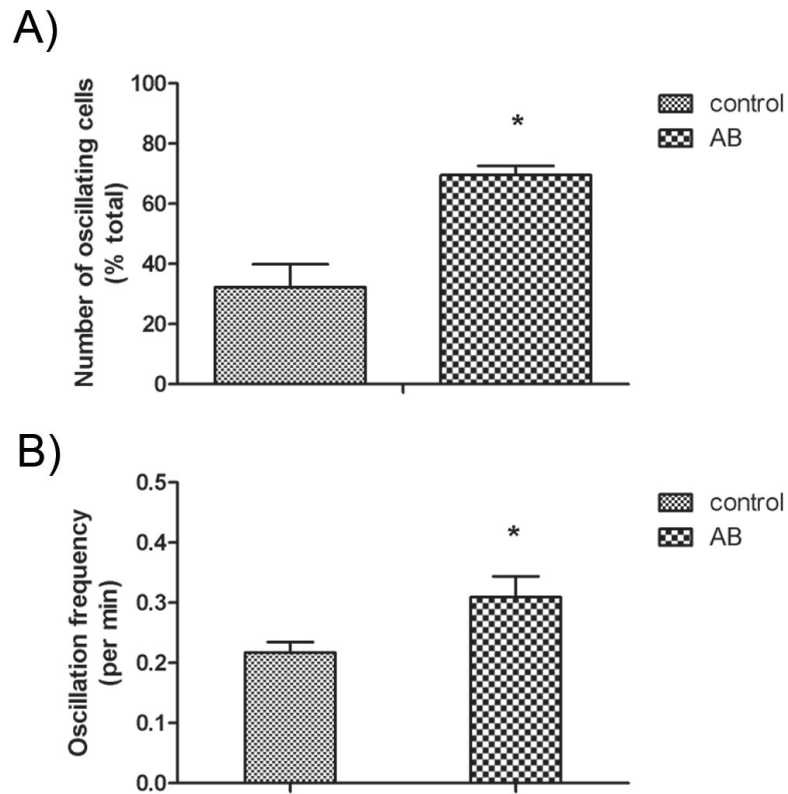
Figure 4.16　Quantified changes in calcium oscillations in response to 2μM Aβ. (A) Bar graph displaying the number of astrocytes responding with calcium elevations to 2μM Aβ and control. (B) Bar graph displaying frequency of calcium oscillations in response to 2μM Aβ and control. Results are expressed as percentage ± SEM (A) and oscillation per minute ± SEM (B), n=3. $p<0.05$ (*), $p<0.01$ (**), $p<0.001$ (***).

Symbol	Well	Fold Difference	t-test	Fold Up- or Down-regulation
		Test Sample / Control Sample	P value	Test Sample / Control Sample
A2M	A01	2.29	0.0319	2.29
APBB2	A08	3.50	0.0306	3.50
BACE1	B04	2.32	0.0318	2.32
BCHE	B06	0.30	0.0487	-3.29
CASP4	B09	4.76	0.0222	4.76
GAP43	C10	10.13	0.0433	10.13
GNG8	D11	2.27	0.0184	2.27
GSK3B	E03	3.41	0.0458	3.41
IDE	E05	3.23	0.0038	3.23
LPL	E09	3.54	0.0454	3.54
SNCA	G08	2.13	0.0165	2.13

Figure 4.17   Changes in the expression of genes associated with Alzheimer's Disease following treatment of NT2.N/A cultures with 2μM Aβ.The table shows the fold change in gene expression and p value from a t-test. The change in gene expression was considered significant at p<0.05 and fold change ≥ 2. For full list of genes and p values see Appendix 8.

4.4 Discussion

Multiple studies have demonstrated disturbances in glucose uptake and utilization in the brains of Alzheimer's disease patients. This chapter also demonstrates for the first time, similar disturbances in neurons and astrocyte cultures derived from human stem cells following exposure to Aβ.

	Change		
	NT2.N/A	**NT2.A**	**primary**
viability	no change	no change	no change
extracellular glucose	↑	↑	↑↑
intracellular glycogen	↑	↑	↑↑
intracellular glucose / glucose-6-phosphate	↑	↑	↑
extracellular lactate	↓	no change	↓↓
extracellular pyruvate	↑	no change	↑↑
extracellular glutamate	↓↓	↓	↓↓
extracellular glutamine	no change	no change	no change
intracellular GSH/GSSG ratio	↓	↓	✕
intracellular NAD⁺/NADH ratio	↓	✕	✕
intracellular ATP	↓	✕	✕
intracellular calcium	↑	✕	✕

Figure 4.18 Summary table of chapter 4 results. ↑ = moderate increase; ↑↑ = high increase; ↓ = moderate decrease; ↓↓ = high decrease; ✕ = no data available.

4.4.1 Comparison of NT2.N/A cocultures and primary cultures

The results shown in this thesis reveal distinct differences in the severity of response from rat primary co-cultures and human NT2 derived co-cultures. Primary cultures appear more vulnerable to perturbation by Aβ and the changes in the metabolism are also more enhanced. One possible explanation is the use of human Aβ(1-42), which could be more toxic to rat cultures than human cells. However, another, more plausible explanation could be differences in the cells present in both cultures. Astrocytes in particular have been shown to be distinctly different in terms of glial function and diversity in humans when compared with rodents (Verkhratsky and Butt, 2013).

It has been suggested that increases in the complexity of the mammalian brain and intellectual power, are accompanied by an increase in the number and complexity of glial cells (Oberheim et al., 2006). This difference is particularly apparent in human brains (Oberheim et al., 2009). Human astrocytes are larger and more complex than those found in rodent brains (Verkhratsky and Butt, 2013). The average diameter of a human protoplasmic astrocyte is 2.5% larger than an equivalent rat astrocyte (Verkhratsky and Butt, 2013). Similarly fibrous astrocytes in white matter are ~2.2 times larger in human brain than rodent brain (Verkhratsky and Butt, 2013). In addition, human protoplasmic astrocytes have ~ 10 times more processes than rodent astrocytes and as a result human protoplasmic astrocytes contact ~2 million synapses whereas rodent astrocytes only contact ~20,000 – 120,000 synapses (Oberheim et al., 2009, Bushong et al., 2002). Primate's brains also include astroglial subtypes that are not found in other vertebrates such as interlaminal astrocytes (Colombo and Reisin, 2004, Colombo et al., 1995). Additionally the possibility of primary cultures containing microglial cells cannot be ruled out. As microglial cells have both positive and negative effects in Alzheimer's disease (Hanisch and

Kettenmann, 2007, Wyss-Coray, 2006), it is possible that they contribute to the response seen following Aβ(1-42) treatment.

In the light of the different effects of Aβ(1-42) on rodent and human NT2 co-cultures it will be necessary to characterize both cell preparations in more detail before any conclusions can be drawn. However, these results strongly suggest that human stem cell derived neurons and astrocytes could be used to determine the interactions between human brain cells in disease.

4.4.2   No change in viability of the cultures

Following treatment with Aβ(1-42) none of the cultures showed any changes in viability. Occasional increase or decrease that has been shown to be statistically significant, is not necessarly biologically significant. Additionally the nature of the Cell-titre Blue^{TM} viability assay should be considered. This assay uses a dye, resazurin, which is actively reduced in mitochondria to give a fluorescent resorufin. This reaction uses diaphorase as enzymes and requires presence of NAD(P)H (Candeias et al., 1998). This assay can be therefore used to study mitochondrial metabolic activity. As Aβ(1-42) has been shown to affect metabolism and mitochondrial function, other methods should be used to investigate cell death such TUNEL assay to look at DNA fragmentation or caspase assay to look at apoptosis.

4.4.2   Decrease in glucose uptake and utilization

The studies described in this chapter have revealed increased levels of glucose in media samples from stem cell derived and primary cultures following treatment with Aβ. Increased levels of glucose suggest a decrease in uptake and/or utilization. These results support previous research including PET studies on patients with

Alzheimer's disease as well as *in vivo* and *in vitro* studies using animal models (described in detail in chapter 4.1). The mechanisms of glucose uptake inhibition and decrease in glucose utilization have been extensively investigated and several possible causes have been proposed. A study by Uemura and Greenlee (2001) has shown that SNARE complex-mediated docking and fusion of GLUT3 vesicles is inhibited by Aβ thus decreasing glucose uptake. Other studies have suggested that a decrease in glucose uptake could be due to a decrease in amount of glucose transporters in the brain. Studies on AD brains has shown that the amounts of GLUT1 and GLUT3, as measured by immunoblotting analysis, were significantly decreased in comparison to aged-matched controls (Simpson et al., 1994). However, the decrease has also been shown to be associated with translational or post-translational changes, as mRNA levels of GLUT1 have not been shown to be reduced in AD brains (Mooradian et al., 1997). Additionally, deficits in the upregulation of GLUT3 protein in response to energy requirements in old rat neurons when compared to young rats suggest that age-related changes in glucose transport occur during ageing (Patel and Brewer, 2003). In the data presented in this chapter gene expression analysis of samples collected from co-cultures of neurons and astrocytes did not show any significant changes in expression of either GLUT1 or GLUT3.

Conversely, not all published reports have demonstrated a decrease in glucose uptake. A recent study by Allaman *et al.* (2010) demonstrated an increase in glucose uptake and various downstream pathways such as glycolysis, TCA cycle and pentose phosphate shunt in response to Aβ. Discrepancies between the results from this chapter and previous reports could stem from the use of different cell types. In their study Allaman *et al.* (2010) used pure primary astrocytes and pure neuronal cultures from mice. Additionally, the protocol for preparation of Aβ differed from the one used here, as Allaman *et al.* (2010) solubilized Aβ in DMSO or sterile deionized

water. As shown in Chapter 1, DMSO causes a very rapid aggregation of Aβ which could explain differences in results obtained in this study and in paper by Allaman *et al.* (2010).

In this study, a decrease in glucose uptake upon treatment with 2µM and 0.2µM Aβ(1-42) could be explained by an accumulation of glucose and glucose-6-phosphate inside the cells. Previous studies by DiNuzzo *et al.* (2010) have shown that a rapid increase in intracellular glucose-6-phosphate leads to a 40% decrease in glucose flow through the hexokinase pathway in astrocytes. This could potentially leads to a decrease in glucose phosphorylation in astrocytes and might therefore increase the amount of free glucose that is available to neurons in the brain. Accumulation of glucose/glucose-6-phosphate inside the cells shown in this thesis suggests a block in glucose phosphorylation or pathways downstream glucose phosphorylation stage, including glycolysis, the pentose phosphate pathway or glycogenesis.

4.4.3   Increase in glycogen load in the cells

An increase in glycogen levels following the treatment with 2µM and 0.2µM Aβ(1-42) could be explained by accumulation of glucose-6-phosphate which instead of passing through glycolysis is directed through glycogen synthesis pathways.

The metabolism of glycogen is tightly regulated through kinases and phosphorylases. One specific phosphatase, protein phosphatase 1 (PP-1) plays an important role in the regulation of glycogen metabolism (section 3.1.3.6). Glycogen synthase is activated by PP-1 via dephosphorylation. At the same time PP-1 dephosphorylates glycogen phosphorylase, thus inactivating it. An interesting study by Knobloch *et al.* (2007) has shown that impairment of LTP by Aβ(1-42) involves PP-1 and that LTP

impairment can be fully reversed by PP1 inhibition *in vitro* and *in vivo*. Inhibition of PP1 has also been shown to stimulate secretion of sAPP through nonamyloidogenic processing. A similar effect has been obtained by treatment of cells with phorbol esters via protein kinase C-mediated phosphorylation (da Cruz e Silva et al., 1995). These studies therefore suggest a beneficial effect of protein kinases and a detrimental effect of protein phosphatases in AD. However, it has been shown that in AD brains levels of protein phosphatases such as PP1, PP2A or PP5 are decreased while protein kinase levels such as GSK3β or Cdk5 are increased (Chung, 2009). GSK3β has been also shown to be responsible for phosphorylation of tau protein and formation of tangles as well as has been implicated in Aβ(1-42) toxicity and interaction with PS1 (Lucas et al., 2001, Hooper et al., 2008). Interestingly, NT2.NA co-cultures treated with 2μM Aβ(1-42) demonstrate an increase in GSK3β expression, which is to be expected considering the involvement of GSK3β in AD. However, this kinase has the opposite effect to PP-1 as it phosphorylates glycogen synthase and therefore inactivates it. Under normal conditions GSK3β inhibits glycogen synthesis and glucose uptake, as well as altering the expression of genes regulated by insulin (Jope and Johnson, 2004). However, in this chapter, co-cultures, pure astrocytes and rat primary cultures demonstrated an increase in glycogen load. As phosphorylation of GSK3β influence its activity, an increase in the level of expression may not translate to changes in activity. Additionally, glycogen synthase (GS) must be pre-phosphorylated by casein kinase II (CKII) for GSK3 to phosphorylate GS efficiently and down-regulate its activity (Jope and Johnson, 2004). Many substrates of GSK3β have been shown to require pre-phosphorylation (priming) before phosphorylation by GSK3β. This means that the activity of such priming kinases may be a limiting factor in the activity of GSK3β (Hooper et al., 2008). It is possible that that the expression of GSK3β is increased, however, the kinase itself is inactive, or that casein kinase II that is involved in the phosphorylation

225

of glycogen synthase is inactive. Further experiments will aim to determine the phosphorylation state of GSK3β following treatment with Aβ in these cultures.

In addition to an increase in glycogen levels in the cultures, the results also showed a small decrease in NT2.N/A cocultures at 6h. This initial decrease in glycogen load in cocultures, even though statistically significant, may not reflect biological significance.

4.4.4   Changes in glutamate levels

In this chapter glutamate production as well as glutamate uptake was shown to be affected by treatments with Aβ(1-42). Glutamate levels in the media were much lower when cells were exposed to 2μM and 0.2μM Aβ(1-42). Similar results were also obtained from rat cortical cultures. Overall glutamate levels in pure astrocytic cultures were lower than in co-cultures. This is not unexpected as the majority of glutamate is produced by neurons whilst astrocytes take up the glutamate released by neurons and convert it to glutamine. However, it should be noted that astrocytes have been shown to produce and release glutamate as well as other gliotransmitters such as ATP (Parpura and Zorec, 2010).

Previous studies of AD brains have demonstrated a marked decrease in phosphate-activated glutaminase (Akiyama et al., 1989) an enzyme which converts glutamine to glutamate in neurons. As neurons are unable to synthesise glutamate through intermediary metabolism (Waagepetersen et al., 2005), glutaminase is the only enzyme which can ensure glutamate production in neurons. In addition, previous studies have shown a decrease in glutamine synthase (GS) in AD brain (Smith et al., 1991, Le Prince et al., 1995, Butterfield et al., 1997). This enzyme converts glutamate taken up by astrocytes into glutamine which is then released and taken up

by neurons. The reduction in both enzymes would lead to disturbances in glutamate production in the AD brain.

Stem cell derived co-cultures in this thesis also demonstrated a decrease in the uptake/production of glutamate. When treated with 2μM Aβ(1-42) in the presence of 0.5mM glutamate, cultures contained higher levels of glutamate in their media than cells not exposed to Aβ(1-42). These results are supported by previous studies which have shown that Aβ treatment inhibits glutamate uptake in hippocampal astrocytes (Harris et al., 1995, Harris et al., 1996, Parpura-Gill et al., 1997). However, the mechanisms causing the inhibition of glutamate transport are not well understood. It has been previously suggested that Aβ(1-42) could inhibit glutamate uptake through generation of oxygen-dependent free radicals (Harris et al., 1995, Harris et al., 1996). Other studies have shown that inhibition of glycolysis blocks glutamate uptake (Swanson, 1992a). Furthermore, the inhibition of glucose uptake by Aβ(25-35) have been found to affect glutamate transport (Parpura-Gill et al., 1997). The decrease in the uptake of glucose seen in NT2 co-cultures, pure astrocytes and rat primary cultures could be responsible for the decrease in glutamate uptake. However, gene expression analysis of the NT2 co-cultures treated with Aβ did not demonstrate any changes in the expression of glutamate transporters.

Numerous studies have linked excitotoxicity to the development of AD (Parihar and Brewer, 2007). In addition, an increase in NMDA receptor activation by Aβ, a downregulation of glutamate transporters in AD brain, inhibition of the glutamate uptake by Aβ and increase in hyperphosphorylation of tau following activation of NMDA receptors have been reported (Parihar and Brewer, 2007). The efficiency of memantine (NMDA receptor antagonist) used in the treatment of AD also supports the active role of glutamate and excitotoxicity in AD (Lipton, 2006).

In neurodegenerative diseases, uptake of glutamate can be disturbed due to a decline in energy metabolism (Parihar and Brewer, 2007). Studies on the use of creatine to improve energy metabolism have shown that neurons preloaded with creatine were protected from glutamate and Aβ(1-42) toxicity (Brewer and Wallimann, 2000). This group hypothesized that long-term energy deficiency can lead to a failure in the reduction of intracellular calcium and therefore over-activation of NMDA receptors.

Other studies have linked NMDA receptors activation to ROS production (Lafon-Cazal et al., 1993). Indeed Schulz *et al.* (2000) have shown that excitotoxicity leads to ROS production and depletion of glutathione. It has also been suggested that glutamate toxicity may lead to ETC complex defects and mitochondrial dysregulation and therefore an increase in the production of free radicals (Halliwell, 1992).

4.4.5   Changes in lactate production and pyruvate uptake

Following exposure to Aβ(1-42) lactate levels were significantly decreased in co-cultures (both stem cell derived and primary). Under physiological conditions the rate of glucose utilization is higher in astrocytes than neurons (Magistretti and Pellerin, 1996). Glucose taken up by astrocytes is metabolized into lactate, which is then released to be taken up by neurons and can sustain synaptic activity (Bittar et al., 1996). The results shown in this thesis strongly suggest that Aβ(1-42) leads to inhibition of the glycolytic pathway which results in the accumulation of glucose-6-phosphate, decreased uptake of glucose and therefore lactate production. Interestingly, this effect is not seen in pure astrocytes. According to the ANLS hypothesis, lactate is produced by astrocytes in response to glutamate release from neurons and subsequent uptake by astrocytes (Pellerin and Magistretti, 2012). The

absence of neurons and low glutamate levels may explain the very low lactate levels in the media and thus limit the effect of Aβ(1-42) on lactate production.

Pyruvate is another important energy source in the brain (Nicklas et al., 1971). The transport of lactate and pyruvate across the blood-brain barrier is limited and thus it cannot substitute for glucose to maintain brain function (Pardridge and Oldendorf, 1977). However, when produced inside the brain, pyruvate and lactate are useful energy sources for neurons (Ide et al., 1969). Media used to grow and maintain both stem cell derived co-cultures and primary cultures in the experiments presented here contained high levels of pyruvate. However, following treatment with low levels of Aβ(1-42) the uptake of pyruvate was decreased in NT2.N/A co-cultures and primary cultures, further limiting availability of substrates for TCA cycle.

4.4.6   Aβ(1-42) treatment affects the cellular NAD$^+$/NADH ratio in NT2.N/A co-cultures

NAD$^+$ is a coenzyme and a parent compound to NADH, NADP$^+$ and NADPH. It is involved in many crucial processes for cell survival as a cofactor for enzyme-catalyzed oxidation (Berger et al., 2004), a donor of electrons for ETC during oxidative phosphorylation (Araki et al., 2004) and as a contributor for ATP production. NAD$^+$ is mainly located in mitochondrial matrix and together with NADP$^+$ is important in signal transduction, DNA repair, glutathione metabolism and recycling and the thioredoxin system (Ziegler and Schulz, 2000).

As the treatment of the cells with Aβ leads to a decrease of substrates available for entry into the TCA cycle, it was necessary to investigate changes in NAD$^+$/NADH ratio. Co-cultures demonstrated an initial increase in NAD$^+$/NADH ratio in both control and Aβ treated cells and this was followed by a significant decrease, particularly in

Aβ treated cells. Increases in the NAD$^+$/NADH ratio seen in the control is possibly a result of increased glycolysis and subsequent production of lactate following feeding of the cells. During this process NAD$^+$ is reduced to NADH. However, in order to allow aerobic glycolysis to continue in astrocytes NADH must be oxidised back to NAD$^+$ via the production of lactate by lactate dehydrogenase As Aβ treatment partially blocks glucose uptake, this could lead to a decrease in the NAD$^+$/NADH ratio in comparison to control.

A decrease in the availability of substrates (glucose, pyruvate) and an increase in the requirement for NAD$^+$ can lead to NAD$^+$ depletion. This scenario is typical of both acute and chronic neurodegenerative diseases (Parihar and Brewer, 2007). The level of NAD$^+$ in mitochondria can be affected by different factors such as ROS and Ca^{2+} via permeability transition pore (PTP) opening (Di Lisa et al., 2001). PTP opening can result in release of NAD$^+$ to the cytoplasm where it is rapidly consumed by enzymes which are abundant in the cytoplasm e.g. glycohydrolases which hydrolyse NAD$^+$ into ADP-ribose and nicotinamide. Glycohydrolases could also catalyze formation of cADP-ribose which triggers release of Ca^{2+} from sarcoplasmic reticulum causing further opening of PTP and subsequent release of NAD$^+$ (Dodoni et al., 2004). However, these mechanisms as well as their association with AD and ageing are poorly understood (Parihar and Brewer, 2007).

Another enzyme which relies heavily upon accessibility of NAD$^+$ is PARP. PARP-1 activity has been found in neuronal and also non-neuronal cells in CNS. In addition, excessive PARP-1 activity has been shown to have detrimental effects in cells due to a reduction in NAD$^+$ (Ha, 2004). As described in section 4.1.4.1, PARP has been previously detected in frontal and temporal cortex of AD patients which suggests an increase in the consumption of NAD$^+$ (Love et al., 1999). PARP-associated depletion of NAD$^+$ has been found in conditions linked to increased ROS and DNA damage

(Schraufstatter et al., 1986). A decrease in NAD^+ stores, leads to a heavy demand on ATP stores for synthesis of new NAD^+ (Pieper et al., 1999). This can lead to an energy crisis in the cell which can cause further cell death via necrosis (Ha and Snyder, 1999).

NAD^+ is also required for Sir2 activity which has been found to increase life span in *C. elegans* and *S. cerevisiae* (Kaeberlein et al., 1999). In humans SIRT1 is involved in chromatin remodeling and regulation of transcription factors such as p53 (Luo et al., 2001). However, SIRT1 and the Sir2 family as well as PARP require NAD^+ for their nuclear activities. An increase in NAD^+ synthesis and activation of SIRT1 has been previously found to protect against axonal degeneration (Araki et al., 2004). As such a decrease in NAD^+ could lead to neurodegeneration.

NAD^+ is a precursor for NADH and it is converted into NADH mainly during the TCA cycle. This NADH is then required for the phosphorylation of ADP by ATP synthase during oxidative phosphorylation. As such there is a relationship between the rate of ATP production and the ratio of NADH to NAD^+ (redox ratio) whereby a decline in NAD^+ can limit ATP synthesis through the TCA cycle.

It has been shown that in 24 month old rats there is an age related decline in NAD(P)H (Parihar and Brewer, 2007). Additionally, exposure to glutamate causes an influx of Ca^{2+} which results in a much faster decline of NAD(P)H in old neurons in comparison to middle aged or embryonic neurons. This has been suggested to be a result of complex I activity attempting to meet the requirement for electrons which power proton gradient and ATP production (Parihar and Brewer, 2007). As such low NAD(P)H levels in aged neurons could explain the vulnerability of cells to metabolic stress (Brewer, 1998).

Another factor that could influence NADH to NAD$^+$ ratio is NADH dehydrogenase (part of complex I). In AD it has been shown that there are changes in expression of mitochondrial and nuclear genes encoding NADH dehydrogenase, specifically a down-regulation of mitochondrial genes in temporal cortex of AD (Manczak et al., 2004). Additionally, activity of NADH dehydrogenase was also shown to be impaired in homogenates of plaques (Mattson, 2000).

4.4.7   Effect of Aβ on ATP production

Experiments in this chapter have demonstrated changes in glycolysis as well as the availability of substrates for entry into the TCA cycle and the ratio of NAD+/NADH. As such it was important to establish whether there was a subsequent effect on production of ATP. NT2 derived co-cultures treated with Aβ demonstrated a decrease in ATP from 6h, which became most significant at 72 and 96h. This demonstrates a detrimental effect of Aβ on the metabolism of the cells and is in line with previous studies. Studies of AD brains have shown a reduction in the activities of enzymes involved in glycolysis such as hexokinase (Liguri et al., 1990) and phosphofructokinase (Sims et al., 1987) but also in mitochondrial components such as pyruvate dehydrogenase complex (PDHC), α-ketoglutarate dehydrogenase complex (KGDHC) and cytochrome oxidase c (COX). A reduction in the activity of key enzymes of the TCA cycle, KGDHC and PDHC, has long been associated with neurodegeneration and AD (Sorbi et al., 1983, Blass, 2000). The reduction in KGDHC could be responsible for a general decline in brain metabolism and its activity has been found to have a higher correlation with cognitive decline than amyloid plaques or neurofibrillary tangles (Gibson et al., 1999). Some studies of AD brains have also demonstrated that decreased activity of PDHC is not only found not only in damaged regions of the brain but also in those showing no neuropathological changes (Butterworth and Besnard, 1990). COX has also been shown to have

abnormal kinetics but its activity is also decreased in AD brain and peripheral tissue. Additionally, it has been shown that the localization of such decreases in COX levels correspond to pre-mortem decreases in glucose metabolism (Rapoport et al., 1991). Decreases in COX activity have also been linked to a decrease in neuronal firing, a decrease in Na+/K+-ATPase activity and therefore a decrease in utilization and demand for ATP (Wong-Riley, 1989).

The decrease in ATP levels following exposure to low concentrations of Aβ presented in this thesis is also supported by previous studies on mitochondria isolated from rat brains. These studies show a direct effect of micromolar levels of Aβ on mitochondrial respiration (Canevari et al., 1999), ATP synthesis (Moreira et al., 2003) as well as the activities of various enzymes associated with energy transfer (Shoffner, 1997, Casley et al., 2002). It has been suggested that Aβ can interact directly with mitochondrial membranes causing changes in mitochondrial function (Parihar and Brewer, 2007) but also the inhibition of COX activity that is seen in AD (Canevari et al., 1999). Indeed, other studies have also shown a concentration-dependent decrease in ATP/O ratio (moles of ATP produced per g-atom of oxygen consumed), ETC inhibition, increase in production of ROS and COX release in response to Aβ (Aleardi et al., 2005).

4.4.8   Antioxidant defence and ROS production

The brain is very susceptible to oxidative damage particularly due to its high metabolic rate, high levels of unsaturated lipid levels and a limited ability to regenerate (Andersen, 2004). In addition, oxidative stress and damage have been previously linked to AD (Perry et al., 1998, Butterfield, 2002).

For normal functioning of the brain it is essential to maintain the balance between generation of ROS and antioxidant defence mechanisms. Endogenous antioxidants, which protect from ROS damage include enzymatic systems and cellular molecules (Aliev et al., 2008). Three primary enzymes include SOD, catalyse and glutathione peroxidase (GPx), but there are also secondary enzymes involved such as glutathione reductase (GR), glucose-6-phosphate dehydrogenase, and cytosolic GST (Aliev et al., 2008). The function of these enzymes is to decrease peroxide levels or to maintain supply of intermediates such as glutathione (GSH) or NADPH (Vendemiale et al., 1999). GSH reacts directly with free radicals in a nonenzymatic reactions and is also an electron donor in the process of reduction of peroxides catalyzed by GPx. The product of this reaction is GSSG which is subsequently converted back into GSH by the action of glutathione GR which uses NADPH as a cofactor (Scott et al., 1963). In a healthy cell, GSSG levels rarely exceed 10% of total cellular GSH (Aliev et al., 2008). The ratio of GSH/GSSG has been therefore used as an indicator for oxidative stress *in vivo* (Asensi et al., 1999).

In the work presented here NT2.N/A and NT2.A cultures were investigated for changes in GSH and GSSG following treatment with Aβ. Pure astrocytic cultures demonstrated a decrease in total GSH levels and an increase in GSSG levels which translated into a decrease in GSH/GSSG ratio. After 48h the ratio increased suggesting a recovery from the initial insult. A similar decrease in the GSH/GSSG ratio was seen in co-cultures at 6 and 24h. After 24h there still appears to be a decrease in GSH/GSSG ratio, however, it is not significant at any of the later time points. Nevertheless, we can conclude that treatment with Aβ leads to a decrease in GSH and an increase in GSSG levels. This suggests increased oxidative stress and is in line with previous studies. It has been shown that GSH levels decrease in red blood cells during normal ageing as well as in AD (Liu et al., 2004) and that GSSG levels are increased in AD (Benzi and Moretti, 1995). A study by Abramov *et al.*

234

(2003) performed on rat mixed hippocampal neuronal and glial cultures as well as pure cortical astrocytes linked sporadic $[Ca^{2+}]_c$ signals caused by Aβ to GSH depletion. These sporadic fluctuations of $[Ca^{2+}]_c$ were only seen in astrocytes and led to a decrease in GSH in those cells. As astrocytes supply neighbouring neurons with precursors for GSH (Sagara et al., 1993), a reduction in GSH levels in astrocytes could cause a decrease in GSH levels in neurons. This could further impair neuronal viability as neurons become vulnerable to oxidative stress (Abramov et al., 2003).

A decrease in GSH has also been associated with downregulation of glutamate cysteine ligase (GCL), which is the first enzyme involved in *de novo* synthesis of GSH (Liu et al., 2004). This group have also demonstrated age-related decreases in the activity and mRNA content of glutathione synthase (GS), the second enzyme involved in the synthesis of glutathione (Liu et al., 2004). In addition they were also able to show that a decrease in GSH levels in red blood cells from male AD patients was linked to decrease in GCL and GS activity (Liu et al., 2004).

In this chapter, gene expression analysis did not show any significant changes in antioxidant enzymes, such as GPx or SOD following treatment of NT2.N/A cells with Aβ. Further analysis of the expression and activity of enzymes associated with GSH synthesis is required before conclusions can be drawn on the impact of Aβ on the oxidative status of the cultures.

Increases in GSSG levels following treatment with Aβ in this study suggest an increase in ROS production. Mitochondria are a major source of ROS, which at low levels are beneficial to the cell (Gericke, 2006) but can cause cell damage and lead to cell death at higher levels (Parihar and Brewer, 2007). It has been shown that during ageing, ROS levels increase as well as antioxidant activity which suggests upregulation of self-protective mechanisms (Pratico and Delanty, 2000). Evidence

from experiments on isolated mitochondria supports the hypothesis of oxidative stress in ageing (section 1.7). As ageing is the major risk factor in AD, it has been suggested that increases in ROS production associated with ageing is a major contributor to the development of the disease (Parihar and Brewer, 2007).

An increase in Aβ has been found to induce oxidative stress in AD transgenic mice (Matsuoka et al., 2001) and also leads to an increase in production of H_2O_2 in cultured cells (Behl et al., 1994). Together these studies demonstrate an association between oxidative stress and Aβ production, however it is not possible to determine which process occurs first in the development of the disease (Parihar and Brewer, 2007).

Results from post-mortem tissue of AD patients have shown markers for lipid peroxidation and protein nitration in the cortex and hippocampus (Butterfield and Lauderback, 2002). They have also demonstrated increases in the levels of protein carbonyls in AD compared to age matched controls (Smith et al., 2000). In addition, markers for oxidative damage of DNA (8-hydroxy-2'-deoxyguanosine) have been found in the CSF of AD patients. The accumulation of ROS could have a significant effect not only on nuclear DNA but also on mtDNA. mtDNA damage has been implicated in AD and could lead to mitochondrial dysfunction and a decline in ATP production (Parihar and Brewer, 2007). Additionally, free radicals may increase levels of oxidized proteins (section 4.1.3), which could lead to altered conformation and activity of enzymes involved in oxidative phosphorylation and the ETC such as cytochrome oxidase c (section 4.1.3). Oxidative stress can also lead to a reduction in the expression of metabolic enzymes by signalling pathways involving redox sensitive transcription factors, kinases and phosphatases (Thannickal and Fanburg, 2000). These changes associated with ROS production could lead to further mitochondrial dysfunction (Parihar and Brewer, 2007).

4.4.9 Calcium changes

Calcium release in cells has a very significant effect on cellular functioning, including mitochondrial energy metabolism. It can activate mitochondrial matrix dehydrogenases which produce more NADH and therefore donate electrons through ETC as well as affecting ATP production (McCormack et al., 1990). Calcium influxes can depolarize mitochondrial membrane potential (Vergun, 2007) but they also activate neurotransmitter release after action potential firing in neurons (Khvotchev et al., 2000). In addition, increases in calcium levels can affect enzymes such as protein kinases and phospholipases (Clapham, 2007), integrity of the cytoskeleton (Schlaepfer and Zimmerman, 1985) as well as play important role in excitotoxicity which is a major feature of neurodegenerative diseases (Parihar and Brewer, 2007).

Dysregulation of intracellular calcium signalling in AD has been intensively studied (Mattson, 2004). Increases in intracellular calcium has been found to cause accumulation of Aβ and hyperphosphorylation of tau and can lead to neuronal death (LaFerla, 2002). Presenillin 1 has also been linked to calcium homeostasis and it has been shown that mutations in PS1 can cause changes in inositol triphosphate-coupled intracellular calcium stores and calcium pathways (Yoo et al., 2000). Dysregulation of calcium homeostasis has been confirmed in both fibroblast and neurons from AD patients and transgenic mice with PS1 mutations (Huang et al., 2005).

The effects of Aβ on $[Ca^{2+}]_c$ signalling has been extensively studied. However, the results of these studies are controversial, as Aβ has been found to increase and decrease $[Ca^{2+}]_c$, modulate Ca^{2+} channel activity or alter the dynamic of $[Ca^{2+}]_c$ signals. In this thesis, Aβ increased calcium oscillations as well as the number of activated astrocytes. Abramov *et al.* (2003) demonstrated that in mixed neuronal and

astrocytic co-cultures Aβ had no effect on $[Ca^{2+}]_c$ in neurons but triggered complex and sporadic $[Ca^{2+}]_c$ fluctuations in astrocytes (Abramov et al., 2003). In addition, they demonstrated that the calcium changes were dependent on extracellular calcium and independent of the ER calcium stores. This suggests that Aβ causes Ca^{2+} influx selectively into astrocytes (Abramov et al., 2003). This supports the suggestion that Aβ can form pores in cell membranes that allow influx of Ca^{2+} (Lin et al., 2001). Additionally, the same study found that Aβ induces ROS generation in astrocytes and that this leads to GSH depletion in both neurons and astrocytes, in a calcium-dependent manner (Abramov et al., 2003).

ROS production was found to be dependent upon activation of NADPH oxidase which generates oxidative stress and depletion of GSH (Abramov et al., 2004). Astrocytes can withstand this insult and are resistant to cell death, whilst neurons have been found to die within 24h after exposure (Abramov et al., 2003). As GSH depletion was blocked by glutathione precursors and NADPH oxidase inhibitors, it was suggested that neuronal death is a result of oxidative stress (Abramov et al., 2004). In a recent study, neuronal death was shown to be mediated by overactivation of PARP-1 in response to oxidative stress, NAD+ depletion and loss of mitochondrial membrane potential Abeti *et al.* (Abeti et al., 2011).

Increases in calcium oscillations and the number of cells that were activated in this study as well as decrease in NAD^+/NADH and GSH/GSSG ratio are in agreement with studies done by Abramov *et al.* (2003,2004,2011). In addition, this study provides a link between Aβ and oxidative stress and changes observed in cellular metabolism.

4.4.10 Gene expression changes

Changes in gene expression following exposure to 2µM Aβ(1-42) were investigated using the Human Alzheimer's Disease RT² Profiler™ PCR Array (QIAGEN, UK). This array profiles the expression of 84 genes that are important in the onset, development, and progression of Alzheimer's disease such as genes contributing to Aβ generation, clearance, and degradation or genes involved in Aβ signal transduction leading to neuronal toxicity and inflammation.

Analysis showed significant upregulation and downregulation of several genes which have been previously shown to be associated with AD. However as the gene expression analysis was only performed on NT2.N/A co-cultures, it is impossible to determine whether the changes affected only one specific cell type or both. As such further investigation of pure cultures is required.

4.4.10.1   Upregulation of *A2M*

A2M is a gene that encodes α_2-macroglobulin (α_2M) which is a 718 kDa glycoprotein of a similar structure and function to a group of proteins called α-macroglobulins (Kovacs, 2000). It is found at high levels in the serum and cerebrospinal fluid (CSF) (Borth, 1992). It is also produced in the brain where it binds different extracellular ligands which are internalized by neurons and astrocytes (Kovacs, 2000). The most well characterised function of α_2M is its pan-protease inhibitory activity (Barrett and Starkey, 1973). α_2M binds to proteases and entraps them (Borth, 1992). The proteases are unable to dissociate from α_2M, however they are still active and able to cleave small substrates (Lauer et al., 2001).

In AD, α_2M has been found to be associated with amyloid plaques (Kovacs, 2000) as

239

well as binding to soluble Aβ (Hughes et al., 1998). Binding of α₂M to Aβ has been shown to inhibit Aβ fibril formation and neurotoxicity (Hughes et al., 1998) as well as promoting its degradation by proteases already bound to α₂M (Lauer et al., 2001). Additionally, α₂M/Aβ complexes can undergo LPR-mediated endocytosis and lysosomal degradation (Narita et al., 1997). However, large amounts of α₂M can be neurotoxic (Kovacs, 2000) and it has also been found to be a risk factor for late onset AD genes such as APOE. A DNA polymorphism in A2M gene has been associated with AD and increases in amyloid plaque formation in AD brains (Blacker et al., 1998). However, subsequent studies have not consistently confirmed this positive association (Wavrant-DeVrieze et al., 1999, Myllykangas et al., 1999). The connection of A2M polymorphism to late onset AD is still controversial.

Gene expression analysis following exposure of NT2.N/A cells to Aβ show that A2M is significantly upregulated. This is in line with previous studies that have shown an increase of α₂M in cortical and hippocampal senile plaques as well as intracellular staining of hippocampal neurons (Bauer et al., 1991).

4.4.10.2   Upregulation of *APBB2*

Gene expression analysis demonstrated an increase in expression of APBB2 gene. This gene codes for β-amyloid precursor protein-binding family B member 2 which is an adaptor protein that can bind the cytoplasmic domain of βAPP (Golanska et al., 2008). It is believed to be involved in the βAPP processing. Previous experiments have shown that overexpression of APBB2 increases γ-secretase processing of βAPP thus promoting Aβ production (Chang et al., 2003).

4.4.10.3   Upregulation of *BACE1*

Gene expression analysis of NT2.N/A cells exposed to Aβ demonstrated an upregulation of BACE1. This gene codes for the β-site APP-cleaving enzyme 1 (Sinha et al., 1999), a type 1 transmembrane aspartic protease. BACE1 is highly expressed in neurons (Sinha et al., 1999), and it is involved in APP processing and production of Aβ (described in detail in section 1.4.1). It has previously been shown that overexpression of BACE1 leads to an increase in Aβ production whilst BACE1 knockdown abolishes Aβ production (Vassar et al., 1999). BACE1 has been found to cleave APP with the Swedish familial mutation ~10-fold to 100-fold more efficiently than normal APP (Sinha et al., 1999, Vassar et al., 1999). Interestingly, it has been proposed that hypometabolism can affect BACE1 expression (section 4.1.9).

Recent studies have shown that BACE1 can also affect metabolism in the SH-SY5Y cell line. Stable overexpression of BACE1 has led to impairment of utilization of glucose and lactate as well as reduction in activities of hexokinase and pyruvate dehydrogenase (Prof. M. Ashford: personal communication).

Results discussed above suggest that hypometabolism seen in NT2.N/A, NT2.A and primary cultures treated with Aβ could lead to increases in expression of BACE1. This could lead to further increases in Aβ production as well as hypometabolism seen in the cells. However, this link requires further investigation.

4.4.10.4   Downregulation of *BCHE*

BCHE gene encodes butyrylcholinesterase (BChE) which together with acetylcholinesterase (AChE) is a part of cholinesterases (ChEs) family. AChE is a key component of the cholinergic brain synapses and its function is to terminate

nerve impulses by rapid hydrolysis of acetylocholine (ACh) (Ul-Haq et al., 2010). In the human brain, BChE plays a secondary role in hydrolysis of ACh as AChE is the more active enzyme (Greig et al., 2002). According to the cholinergic hypothesis, sporadic AD is caused by a deficiency in cholinergic function. Levels of ACh have been found to be very low in the hippocampi and cortexes of AD patients (Terry and Buccafusco, 2003). Additionally, many of the available treatments focus on improving ACh levels either by replacement of ACh precursors (choline or lecithin) or the use of AChE inhibitors (physostigmine). Other treatments include specific M1 muscarinic or nicotinic agonists, M2 muscarinic antagonists.

The function of BChE is not fully known but it appears to be involved in regulation of cell proliferation and differentiation during early neuronal development but also acts as a scavenger in the detoxification of certain chemicals, and is involved in lipoprotein (very-low-density lipoprotein; VLDL) metabolism (Ul-Haq et al., 2010). Some neurons also demonstrate BChE activity in the hydrolysis of ACh (Wright et al., 1993). Studies on AChE and BChE activity in the AD brain have shown that, with progression of the disease, the activity of AChE decreases while BChE levels increase (Perry et al., 1978, Arendt et al., 1992). This suggests that BChE might be compensating for decrease in AChE activity (Giacobini, 2003).

However, the gene expression analysis presented in this study showed a decrease in expression of BChE. Differences may stem from a relatively short exposure to Aβ in comparison to development and progression of disease in AD brains.

4.4.10.5 Upregulation of *CASP4*

CASP4 gene encodes human caspase-4 which is an inflammatory caspase. It is located in the ER and is activated by proteolytic cleavage when cells are exposed to

ER stress-inducing reagents (Hitomi et al., 2004). Activation of caspase-4 has been shown to trigger either apoptosis or an inflammatory response (Salminen et al., 2009) and may be associated with neuronal stress in AD (Katayama et al., 2004). It has also been shown that mutations in PS2 mutation can trigger cleavage and activation of caspase-4 and subsequently activation of caspases 3 and 9 (Yukioka et al., 2008). Additionally, some studies have shown that exposure of cells to Aβ activates both caspase-4 and 12 (Katayama et al., 2004). In AD, the amyloidogenic cleaving of APP has been associated with a negative feedback on caspase-4 activation. The release of AICD and its interacting partner, FE65 transcription factor, leads to its translocation to the nucleus where the AICD-FE65 complex can bind to the promoter region of caspase-4 thus blocking its action (Kajiwara et al., 2009). In the gene expression analysis CASP4 gene was significantly upregulated suggesting an initial ER stress-related response to Aβ treatment.

4.4.10.6   Upregulation of *GAP43*

GAP43 encodes a 43 kDa growth-associated calmodulin-binding phosphoprotein (GAP-43, neuromodulin, B50). GAP-43 is mainly found in neurons (Basi et al., 1987), and is particularly concentrated in growth cones (Nelson et al., 1989). GAP-43 has been shown to be involved in axonal growth and is often used as a marker of synaptogenesis (Benowitz and Routtenberg, 1997).

It is regulated by phosphorylation via protein kinase C (PKC) and there appears to be a correlation between GAP-43 phosphorylation state and enhancement of LTP (Gianotti et al., 1992) as well as behavioural learning (Young et al., 2002).

GAP-43 has been shown to be affected in AD, although the nature of these changes remains controversial. An early study has suggested a "trend" towards an increase in

GAP-43 levels in hippocampus of AD brains. The authors of this study suggested that it was a sign of neuritic sprouting (Masliah et al., 1991). More recent studies have shown a decrease in GAP-43 in the cortex and hippocampus (Bogdanovic et al., 2000). These results were in line with other studies that have shown aberrant localization and a decrease in GAP-43 levels in different areas of AD brains (de la Monte et al., 1995). Another study which tried to address controversy around GAP-43 analysed hippocampal samples within short post-mortem times (Rekart et al., 2004). The authors of this study demonstrated an increase in GAP-43 in AD patients and again suggested that it may represent a sign of axonal sprouting.

In the study presented here gene expression analysis showed a significant increase in GAP-43 expression following exposure to Aβ.

4.4.10.7 Upregulation of *GSK3B*

GSK3β gene encodes glycogen synthase kinase-type 3, isozyme β (GSK3β). GSK3 was initially described as a regulator of glycogen metabolism. It phosphorylates glycogen synthase and therefore inhibits its activity and glycogen synthesis (Embi et al., 1980). The effects of GSK3β on metabolism and glycogen turnover were discussed in details in sections 4.4.2 and 4.1.8.

GSK3β is localized in neuronal and astrocytic compartments, in rough endoplasmic reticulum, free ribosomes, mitochondria and within post-synaptic densities in dendritic spines (Perez-Costas et al., 2010). This kinase has been associated with NMDA-dependent long-term potentiation (LTP) and long-term depression (LTD). The signaling cascade involved in regulation of LTP and LTD includes PI3K/AKT/GSK3 mechanisms, which lead to phosphorylation of GSK3β and inhibition of its activity. This pathway has been shown to be critical for LTD or LTP formation (Hooper et al.,

2007). GSK3β also plays a role in NMDA receptor trafficking (Chen et al., 2007) and pre-synaptic functions in developing and mature nerve terminals (Smillie and Cousin, 2011).

GSK3β has been previously shown to play an important role in development of AD. and has been identified as a key kinase which is able to phosphorylate tau both *in vitro* and *in vivo* (Ishiguro et al., 1993, Terwel et al., 2008). GSK3β transgenic mice have been shown to display hyper-phosphorylation of tau and neurodegeneration (Lucas et al., 2001).

The upregulation of GSK3β following the treatment with Aβ is consistent with previous studies.

4.4.10.8 Upregulation of *IDE*

The IDE gene codes for insulin-degrading enzyme (IDE, insulysin), a 110kDa thiol zinc-metalloendopeptidase. It is located in cytosol, peroxisomes, endosomes and also on the cell membrane (Duckworth et al., 1998). IDE cleaves small proteins which share one characteristic, i.e. formation of β-pleated sheet-rich amyloid fibrils. These proteins include amyloid β-protein (Aβ), insulin, glucagon, amylin, atrial natriuretic factor, and calcitonin (Kurochkin, 2001). As IDE is a major enzyme that can degrade Aβ (Qiu and Folstein, 2006) in both neuronal and microglial cultures (Qiu et al., 1997, Vekrellis et al., 2000), it can thus eliminate its neurotoxic effects (Mukherjee et al., 2000). The link between insulin, IDE, AD and diabetes has been described in detail in section 4.1.8 The upregulation of IDE following exposure of NT2 co-cultures to Aβ suggests an activation of a protective mechanism in these cells.

4.4.10.9   Upregulation of *LPL*

The LPL gene encodes lipoprotein lipase, an enzyme which catalyzes the hydrolysis of triacylglycerol, but also mediates uptake of lipoproteins by acting as a bridging molecule between lipoproteins and sulphated glycosaminoglycans (GAGs) (Williams et al., 1992). It has previously been shown that LPL is highly expressed in the brain (Goldberg et al., 1989). In AD it has been shown that LPL accumulates in amyloid plaques (Rebeck et al., 1995). Additionally, SNPs in the LPL gene have been found to be associated with an increased risk of AD (Blain et al., 2006). A recent study by Nishitsuji *et al.* (2011) has shown that LPL forms a complex with Aβ, leading to an increase in uptake and lysosomal degradation of Aβ in astrocytes. The upregulation of LPL gene after exposure to Aβ in NT2 co-cultures suggests that multiple mechanisms of Aβ clearance may be active in these cells.

4.4.10.10   Upregulation of *SNCA*

The SNCA gene encodes α-synuclein, a 18-20 kDa peptide (Spillantini et al., 1995). Synucleins are highly expressed in the central nervous system as well as, skeletal muscles and spleen (Hong et al., 1998). In the brain, they are localized in the neocortex, hippocampus, and substantia nigra (Suh and Checler, 2002). α-Synuclein has been shown to be a key molecule involved in Parkinson's disease (PD) and dementia with Lewy bodies (DLB). Whilst very rare, inherited cases of PD appear to be associated with mutations in α-synuclein gene (Kruger et al., 1998). In AD α-synuclein is associated with amyloid plaques. Apart from amyloid β-peptides, the plaques are also composed of a component known as non-Abeta component (NAC) (Masliah et al., 1996b). NAC has been shown to be derived from a precursor protein, which was later determined to be α-synuclein (Ueda et al., 1993). The expression of α-synuclein in the brain appears to correlate with the severity of AD cases (Iwai et al.,

1996). It has also been shown that aged transgenic mice overexpressing APP have amyloid plaques, which were immunoreactive to α-synuclein (Yang et al., 2000). However, the specific role of α-synuclein in AD still remains to be determined. The upregulation of SNCA gene in NT2 cultures shows that Aβ treatment alone is sufficient to trigger an increase in the expression of α-synuclein and suggests an important role of this protein in AD.

4.5 Conclusion

Data presented in this chapter provides evidence for a detrimental effect of Aβ on cellular metabolism. Cultures treated with low concentrations of Aβ showed a clear hypometabolism, particularly with regards to changes in glucose, lactate, pyruvate and glycogen metabolism. Interference with metabolic pathways led to a deficit in ATP production as well as NAD^+/NADH ratio. This effect would have serious implications in the brain which has a high energy demand, especially in terms of memory formation and antioxidant mechanisms. An increase in calcium responses as well as a decrease in GSH/GSSG ratio, all point towards Aβ-induced metabolic and oxidative stress. In addition, gene expression analysis suggests an increase in factors involved in the clearance and degradation of Aβ.

Chapter 5: Conclusions and future experimental approaches

As numerous cell types interact during the progression of Alzheimer's disease, it is important that any *in vitro* model of the disease reflects this arrangement. The model described here has previously been used in our laboratory to model neurotoxicity and has demonstrated the importance of including astrocytes to realistically model toxic effects. During the course of this project this model was utilised in order to study the response of neurons and astrocytes to Aβ(1-42).

Previous studies in our laboratory have demonstrated that NT2.D1-derived neurons and astrocytes are functional and can generate action potentials (neurons) as well as spontaneous and induced calcium oscillations (astrocytes) (Hill et al., 2012). This human model of functional neurones and astrocytes therefore offers a unique opportunity to investigate functional changes in response to toxic Aβ(1-42). In addition, changes in biochemical endpoints such as metabolites, cellular viability and calcium responses can also be demonstrated. Such an advanced and relevant model has not thus far been applied to the study of the aetiology of Alzheimer's Disease.

This study has demonstrated for the first time metabolic coupling between neurons and astrocytes derived from human stem cells. The ANLS hypothesis proposes that during neuronal activity, glutamate released into the synaptic cleft is taken up by astrocytes and triggers glucose uptake, which is converted into lactate and released via monocarboxylate transporters for neuronal use. Using NT2 derived co-culture it was possible to successfully model this *in vitro.*

In this study, mixed cultures of NT2.N/A cells were utilised to investigate the metabolic properties of these cells and measured the response of the astrocytic network to well characterised neuromodulators. Using expression analysis and

metabolic approaches it was shown that NT2.N/A cells express the main tenets of the ANLS model and display functional characteristics consistent with their neuron-astrocyte metabolic coupling. This study shows that NT2.N/A cultures modulate their glucose uptake in response to glutamate, an effect that was blocked by cytochalasin B and ouabain. Additionally, the experiments presented that in response to increased neuronal activity and under hypoglycaemic conditions, co-cultures modulate glycogen turnover and increase lactate production. Similar results were also shown following treatment with glutamate, potassium, isoproterenol and dbcAMP. Together these results demonstrate that NT2 human stem cell derived co-culture model is metabolically competent and demonstrates a functional astrocyte neuron lactate shuttle (ANLS). This study therefore lays the foundation for further development of stem cell derived neurons and astrocytes to better understand the metabolic coupling between neurons and astrocytes and its relationship to plasticity and neurodegeneration.

Changes in metabolism of the brain during ageing and Alzheimer's Disease has been extensively studied. It is now widely accepted that AD is accompanied by brain hypometabolism that varies between different regions of the brain.

Analysis of the effects of Aβ(1-42) on co-cultures of neurons and astrocytes revealed a significant changes in the metabolism of cells that is analogous to that seen both in human studies and animal models. A major feature of this cellular response is a clear hypometabolism particularly with regards to glucose as well as changes in the metabolism of pyruvate, lactate and glycogen, which can act as alternate sources of fuel during hypoglycaemia. These changes lead to a reduction in ATP production which suggests a significant energy deficit in the cultures (Fig. 5.1A). This has serious implications in the brain which has a very high energy demand, particularly with regard to memory formation and protection from oxidative stress in neurons.
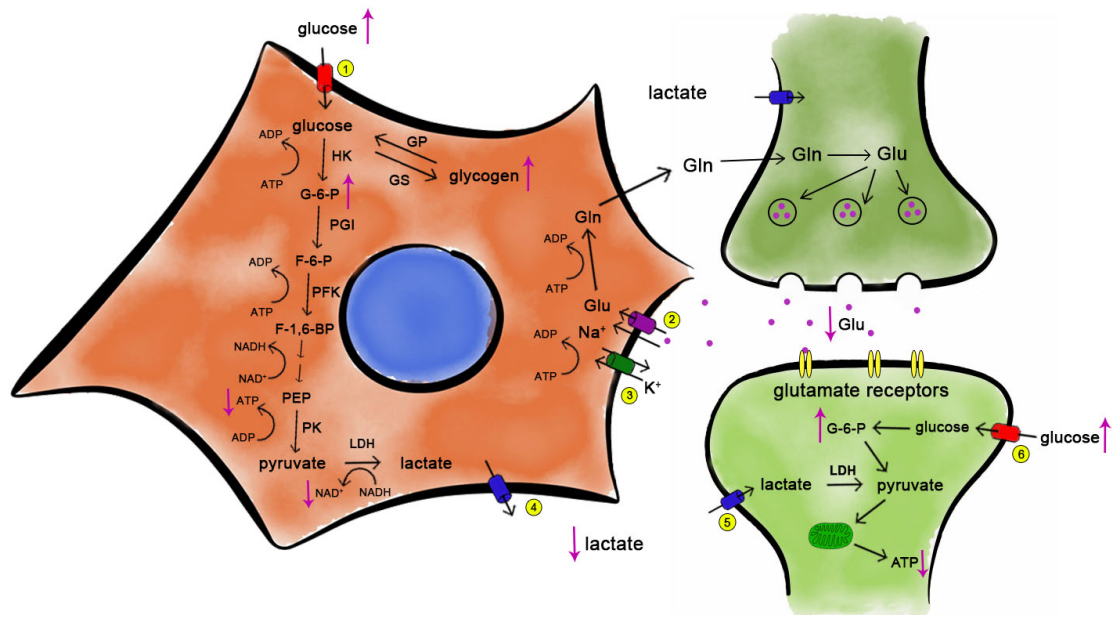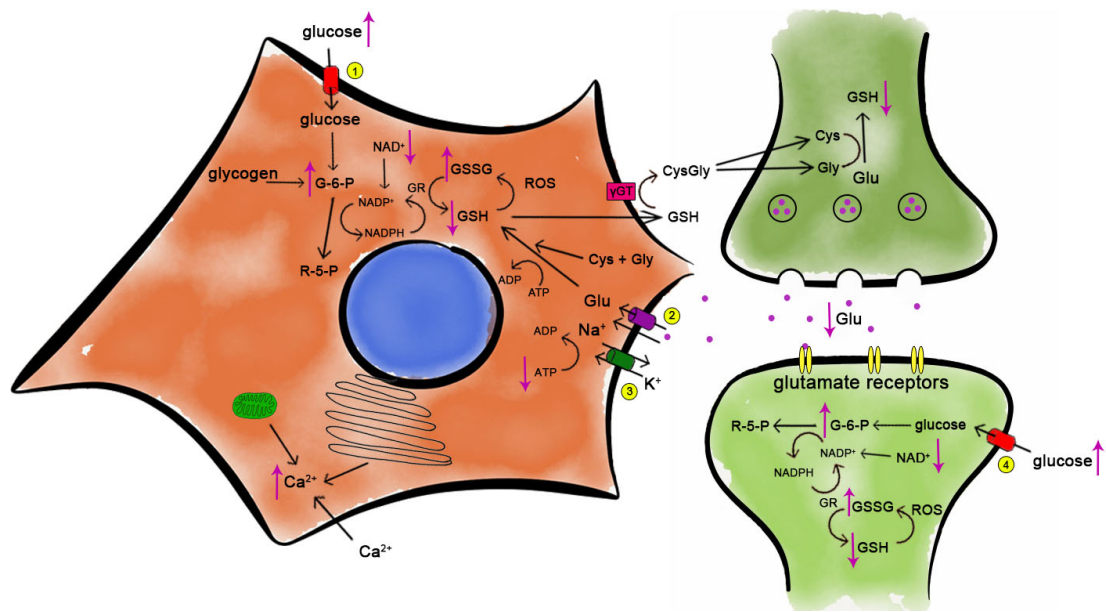
Figure 5.1 Summary conclusion figure showing Aβ(1-42) induced metabolic changes (A) and oxidative stress (B). Figure A) shows changes in ANLS, glycolysis in astrocytes and oxidative phosphorylation in neurons. Figure B) represents changes in the pentose phosphate shunt pathway in neurons and astrocytes as well as antioxidant defence (GSH/GSSG recycling pathway).

Indeed, Aβ(1-42) has also been shown to increase oxidative stress, trigger calcium responses and decrease NAD$^+$ availability (Fig. 5.1B). This would not only affect the antioxidant defence of the cells but also the ability to produce ATP and repair DNA via PARP. As the effect was less pronounced in pure astrocytic cultures this study suggests that the astrocytes are able to cope with the Aβ(1-42) insult, whilst in the presence of neurons which require protection, astrocytes are put under higher metabolic and antioxidant demands.

At present, models of AD fail to recapitulate all of the major features of the disease. This may also be reflected in the fact that many of the new therapies for the treatment of AD have failed to have a significant impact on the development of the disease. Human stem cell derived models of the brain are increasingly proving to provide useful tools in the study of human disease.

Overall, this project presents a unique departure from standard experimental models of the brain. It provides a realistic model of basic human neuronal and astrocytic interactions which can be used to simulate human neurodegeneration *in vitro*.

5.1 Future experimental approaches

The ability to control the aggregation state of Aβ(1-42) is a crucial step, as monomers, oligomers and fibrils have different toxicity profiles. In the study presented here Aβ(1-42) and Aβ(1-40) were monitored using two experimental techniques – western blotting and ThT assay. However, more studies should be performed to ensure a replicable process of Aβ(1-42) aggregation such as Atomic Force Microscope (AFM) which has been previously used (Dahlgren et al., 2002). An additional advantage for future studies on effects of Aβ(1-42) would be the use of natural peptide as opposed to a synthetic one This could be achieved by overexpression human APP or expressing human APP with Swedish mutation in a cell line e.g. SY5Y or NT2. As natural forms of Aβ(1-42) are more toxic than synthetically derived peptides this would ensure an appropriate modelling of the disease (Lambert et al., 1998).

To fully understand how Aβ(1-42) causes metabolic changes in NT2.N/A cultures, it is necessary to investigate changes in enzyme expression and activity e.g. hexokinase or pyruvate dehydrogenase. These enzymes have been found to decrease in AD (Gibson et al., 1998) and it is essential that it is confirmed whether a similar effect is seen in NT2.N/A cultures. Additionally, more advanced method could be used to investigate metabolic trafficking between neurons and astrocytes. One of such methods is *in vitro* ^{13}C-NMR spectroscopy. As it does not require isolation of metabolites due to incorporation of the label into specific carbon positions, it provides information about many different metabolites and metabolic pathways. The use of this method would allow investigation of the fate of the glucose and glutamate, not only in terms of ANLS but also glutamate-glutamine cycling. It would be advantageous to study metabolic changes following the treatment with Aβ(1-42) in real-time. This could be achieved by the use of specialized equipment such as

Seahorse Bioscience XF Extracellular Flux analyser. This system measures the oxygen consumption rate (a measure of mitochondrial respiration) as well as extracellular acidification rate (a measure of glycolysis) and fatty acid oxidation. Additionally it is able to measure mitochondrial stress (by determining basal respiration, ATP turnover, proton leak, and maximal respiration) and glycolysis stress (by determining glycolysis, glycolytic capacity, and glycolytic reserve).

It is probably important to mention that the experiments presented in this thesis should also be performed on pure neuronal and astrocytic cultures. Studying the cells in isolation as well as in co-culture would allow to determine how each cell type is affected by Aβ(1-42) treatments.

In addition, more focus should be directed to mitochondrial function. This could be done by determining mitochondrial membrane potential, using lipophylic cationic dye such as JC-1.

An interesting hypothesis linking hypometabolism and Aβ production has been previously described (Struble et al., 2010). It proposes a possible impact of hypometabolism on BACE1 expression. Creation of NT2.N/A cultures overexpressing APP or mutated APP would allow investigation into the effects of APP processing on metabolic endpoints in these cells. In addition, RNAi or shRNA could be used to silence particular genes in order determine their involvement in response to Aβ. As changes in glycogen metabolism have not been described *in vivo* it would be useful to determine, glycogen load in transgenic mice during the disease progression.

Further functional studies of neurons and astrocytes should also be carried out. The stimulation and recording of electrical activity from cultures following exposure to Aβ(1-42) using multi-electrode array (MEA) analysis would be of great value.

The results obtained in this thesis on NT2.D1 derived cultures of neurons and astrocytes provide a good foundation for future experiments on more patient-specific platforms such as iPS cells. The progress in reprogramming and differentiation of iPS cells makes them an ideal candidate for studies on metabolic coupling between neurons and astrocytes in Alzheimer's Disease. As iPS cells are derived from patient, they therefore express factors associated with AD at physiological levels that cannot be carried simulated overexpression studies or via the application of exogenous Aβ.

Patient specific models of AD could be generated from fibroblasts taken from patients with APP/presenillin mutations as well as controls (Wray et al., 2012). iPS cells could be differentiated into mixed cultures of neurons and astrocytes. Such cultures could then be monitored for changes in metabolism using ^{13}C-NMR or the Seahorse Bioscience XF Extracellular Flux analyser. Additionally changes in glycogen, NAD$^+$/NADH ratio and ATP could be investigated as well as antioxidant defences using GSH assay.

Alzheimer's disease is devastating neurodegenerative condition with no beneficial treatment available. This is in part, due to a lack of relevant human models of the brain. Stem cells such as the NT2/D1 cell line or iPSC provide advantegous alternatives to animal models. These cells allow investigation of more than one cell type in a co-culture as well as individually, thus creating a more comprehensive approach. The ability to investigate functional postmitotic neurons and astrocytes could significantly enhance our understanding of neurodegenerative diseases, which could translate into better treatments. In addition, the use of patient specific iPSC would allow a more tailored patient (genotypic) specific approach to new treatments.

List of references

ABETI, R., ABRAMOV, A. Y. & DUCHEN, M. R. 2011. Beta-amyloid activates PARP causing astrocytic metabolic failure and neuronal death. *Brain,* 134**,** 1658-72.

ABI-SAAB, W. M., MAGGS, D. G., JONES, T., JACOB, R., SRIHARI, V., THOMPSON, J., KERR, D., LEONE, P., KRYSTAL, J. H., SPENCER, D. D., DURING, M. J. & SHERWIN, R. S. 2002. Striking differences in glucose and lactate levels between brain extracellular fluid and plasma in conscious human subjects: effects of hyperglycemia and hypoglycemia. *J Cereb Blood Flow Metab,* 22**,** 271-9.

ABRAMOV, A. Y., CANEVARI, L. & DUCHEN, M. R. 2003. Changes in intracellular calcium and glutathione in astrocytes as the primary mechanism of amyloid neurotoxicity. *J Neurosci,* 23**,** 5088-95.

ABRAMOV, A. Y., CANEVARI, L. & DUCHEN, M. R. 2004. Beta-amyloid peptides induce mitochondrial dysfunction and oxidative stress in astrocytes and death of neurons through activation of NADPH oxidase. *J Neurosci,* 24**,** 565-75.

AHMED, M., DAVIS, J., AUCOIN, D., SATO, T., AHUJA, S., AIMOTO, S., ELLIOTT, J. I., VAN NOSTRAND, W. E. & SMITH, S. O. 2010. Structural conversion of neurotoxic amyloid-beta(1-42) oligomers to fibrils. *Nat Struct Mol Biol,* 17**,** 561-7.

AKIYAMA, H., MCGEER, P. L., ITAGAKI, S., MCGEER, E. G. & KANEKO, T. 1989. Loss of glutaminase-positive cortical neurons in Alzheimer's disease. *Neurochem Res,* 14**,** 353-8.

ALANO, C. C., GARNIER, P., YING, W., HIGASHI, Y., KAUPPINEN, T. M. & SWANSON, R. A. 2010. NAD+ depletion is necessary and sufficient for poly(ADP-ribose) polymerase-1-mediated neuronal death. *J Neurosci,* 30**,** 2967-78.

ALANO, C. C., YING, W. & SWANSON, R. A. 2004. Poly(ADP-ribose) polymerase-1-mediated cell death in astrocytes requires NAD+ depletion and mitochondrial permeability transition. *J Biol Chem,* 279**,** 18895-902.

ALBERDI, E., SANCHEZ-GOMEZ, M. V., CAVALIERE, F., PEREZ-SAMARTIN, A., ZUGAZA, J. L., TRULLAS, R., DOMERCQ, M. & MATUTE, C. 2010. Amyloid beta oligomers induce Ca2+ dysregulation and neuronal death through activation of ionotropic glutamate receptors. *Cell Calcium,* 47**,** 264-72.

ALEARDI, A. M., BENARD, G., AUGEREAU, O., MALGAT, M., TALBOT, J. C., MAZAT, J. P., LETELLIER, T., DACHARY-PRIGENT, J., SOLAINI, G. C. & ROSSIGNOL, R. 2005. Gradual alteration of mitochondrial structure and function by beta-amyloids: importance of membrane viscosity changes, energy deprivation, reactive oxygen species production, and cytochrome c release. *J Bioenerg Biomembr,* 37**,** 207-25.

ALIEV, G., OBRENOVICH, M. E., REDDY, V. P., SHENK, J. C., MOREIRA, P. I., NUNOMURA, A., ZHU, X., SMITH, M. A. & PERRY, G. 2008. Antioxidant therapy in Alzheimer's disease: theory and practice. *Mini Rev Med Chem,* 8**,** 1395-406.

ALLAMAN, I., BELANGER, M. & MAGISTRETTI, P. J. 2011. Astrocyte-neuron metabolic relationships: for better and for worse. *Trends Neurosci,* 34**,** 76-87.

ALLAMAN, I., GAVILLET, M., BELANGER, M., LAROCHE, T., VIERTL, D., LASHUEL, H. A. & MAGISTRETTI, P. J. 2010. Amyloid-beta aggregates cause alterations of astrocytic metabolic phenotype: impact on neuronal viability. *J Neurosci,* 30**,** 3326-38.

ALLINSON, T. M., PARKIN, E. T., TURNER, A. J. & HOOPER, N. M. 2003. ADAMs family members as amyloid precursor protein alpha-secretases. *J Neurosci Res,* 74**,** 342-52.

ALLSOP, D., LANDON, M. & KIDD, M. 1983. The isolation and amino acid composition of senile plaque core protein. *Brain Res,* 259**,** 348-52.

ALVAREZ, G., MUNOZ-MONTANO, J. R., SATRUSTEGUI, J., AVILA, J., BOGONEZ, E. & DIAZ-NIDO, J. 1999. Lithium protects cultured neurons against beta-amyloid-induced neurodegeneration. *FEBS Lett,* 453**,** 260-4.

ALVAREZ, G., RAMOS, M., RUIZ, F., SATRUSTEGUI, J. & BOGONEZ, E. 2003. Pyruvate protection against beta-amyloid-induced neuronal death: role of mitochondrial redox state. *J Neurosci Res,* 73**,** 260-9.

ANANDATHEERTHAVARADA, H. K., BISWAS, G., ROBIN, M. A. & AVADHANI, N. G. 2003. Mitochondrial targeting and a novel transmembrane arrest of Alzheimer's amyloid precursor protein impairs mitochondrial function in neuronal cells. *J Cell Biol,* 161**,** 41-54.

ANANDATHEERTHAVARADA, H. K. & DEVI, L. 2007. Amyloid precursor protein and mitochondrial dysfunction in Alzheimer's disease. *Neuroscientist,* 13**,** 626-38.

ANCHISI, D., BORRONI, B., FRANCESCHI, M., KERROUCHE, N., KALBE, E., BEUTHIEN-BEUMANN, B., CAPPA, S., LENZ, O., LUDECKE, S., MARCONE, A., MIELKE, R., ORTELLI, P., PADOVANI, A., PELATI, O., PUPI, A., SCARPINI, E., WEISENBACH, S., HERHOLZ, K., SALMON, E., HOLTHOFF, V., SORBI, S., FAZIO, F. & PERANI, D. 2005. Heterogeneity of brain glucose metabolism in mild cognitive impairment and clinical progression to Alzheimer disease. *Arch Neurol,* 62**,** 1728-33.

ANDERSEN, J. K. 2004. Oxidative stress in neurodegeneration: cause or consequence? *Nat Med,* 10 Suppl**,** S18-25.

ANDERSON, R. M., BITTERMAN, K. J., WOOD, J. G., MEDVEDIK, O., COHEN, H., LIN, S. S., MANCHESTER, J. K., GORDON, J. I. & SINCLAIR, D. A. 2002. Manipulation of a nuclear NAD+ salvage pathway delays aging without altering steady-state NAD+ levels. *J Biol Chem,* 277**,** 18881-90.

ANDREWS, P. W. 1984. Retinoic acid induces neuronal differentiation of a cloned human embryonal carcinoma cell line in vitro. *Dev Biol,* 103**,** 285-93.

ANDREWS, P. W., DAMJANOV, I., SIMON, D., BANTING, G. S., CARLIN, C., DRACOPOLI, N. C. & FOGH, J. 1984. Pluripotent embryonal carcinoma clones derived from the human teratocarcinoma cell line Tera-2. Differentiation in vivo and in vitro. *Lab Invest,* 50**,** 147-62.

ANDRIEZEN, W. L. 1893. On a system of fiber-like cells surrounding the blood vessels of the brain of man and mammals, and its physiological significance. *Int. Monatsschr. Anat. Physiol.,* 10**,** 532-540.

APELT, J., MEHLHORN, G. & SCHLIEBS, R. 1999. Insulin-sensitive GLUT4 glucose transporters are colocalized with GLUT3-expressing cells and demonstrate a chemically distinct neuron-specific localization in rat brain. *J Neurosci Res,* 57**,** 693-705.

APPLEGATE, M. A., HUMPHRIES, K. M. & SZWEDA, L. I. 2008. Reversible inhibition of alpha-ketoglutarate dehydrogenase by hydrogen peroxide: glutathionylation and protection of lipoic acid. *Biochemistry,* 47**,** 473-8.

ARAKI, T., SASAKI, Y. & MILBRANDT, J. 2004. Increased nuclear NAD biosynthesis and SIRT1 activation prevent axonal degeneration. *Science,* 305**,** 1010-3.

ARENDT, T., BRUCKNER, M. K., LANGE, M. & BIGL, V. 1992. Changes in acetylcholinesterase and butyrylcholinesterase in Alzheimer's disease resemble embryonic development--a study of molecular forms. *Neurochem Int,* 21**,** 381-96.

ARISPE, N., ROJAS, E. & POLLARD, H. B. 1993. Alzheimer disease amyloid beta protein forms calcium channels in bilayer membranes: blockade by tromethamine and aluminum. *Proc Natl Acad Sci U S A,* 90**,** 567-71.

ARMSTRONG, D. M. & IKONOMOVIC, M. D. 1996. AMPA-selective glutamate receptor subtype immunoreactivity in the hippocampal dentate gyrus of patients with Alzheimer disease. Evidence for hippocampal plasticity. *Mol Chem Neuropathol,* 28**,** 59-64.

ARNAIZ, E., JELIC, V., ALMKVIST, O., WAHLUND, L. O., WINBLAD, B., VALIND, S. & NORDBERG, A. 2001. Impaired cerebral glucose metabolism and cognitive functioning predict deterioration in mild cognitive impairment. *Neuroreport,* 12**,** 851-5.

ASENSI, M., SASTRE, J., PALLARDO, F. V., LLORET, A., LEHNER, M., GARCIA-DE-LA ASUNCION, J. & VINA, J. 1999. Ratio of reduced to oxidized glutathione as indicator of oxidative stress status and DNA damage. *Methods Enzymol,* 299**,** 267-76.

ATAMNA, H. & FREY, W. H., 2ND 2007. Mechanisms of mitochondrial dysfunction and energy deficiency in Alzheimer's disease. *Mitochondrion,* 7**,** 297-310.

AUBERT, A., COSTALAT, R., MAGISTRETTI, P. J. & PELLERIN, L. 2005. Brain lactate kinetics: Modeling evidence for neuronal lactate uptake upon activation. *Proc Natl Acad Sci U S A,* 102**,** 16448-53.

AUFFERMANN, W., BUSER, P., WU, S., PARMLEY, W. W. & WIKMAN-COFFELT, J. 1992. Activation of glycolysis with isoproterenol but not digoxin reverses chronic alcohol depression in hamster hearts. *Alcohol Clin Exp Res,* 16**,** 505-10.

AUTHIER, F., POSNER, B. I. & BERGERON, J. J. 1996. Insulin-degrading enzyme. *Clin Invest Med,* 19**,** 149-60.

BANI-YAGHOUB, M., FELKER, J. M. & NAUS, C. C. G. 1999. Human NT2/D1 cells differentiate into functional astrocytes. *NeuroReport,* 10**,** 3843-3846.

256

BANKS, W. A. 2004. The source of cerebral insulin. *European Journal of Pharmacology,* 490**,** 5-12.

BARRETT, A. J. & STARKEY, P. M. 1973. The interaction of alpha 2-macroglobulin with proteinases. Characteristics and specificity of the reaction, and a hypothesis concerning its molecular mechanism. *Biochem J,* 133**,** 709-24.

BARRIENTOS, A., CASADEMONT, J., CARDELLACH, F., ESTIVILL, X., URBANO-MARQUEZ, A. & NUNES, V. 1997. Reduced steady-state levels of mitochondrial RNA and increased mitochondrial DNA amount in human brain with aging. *Brain Res Mol Brain Res,* 52**,** 284-9.

BARROS, L. F., BITTNER, C. X., LOAIZA, A., RUMINOT, I., LARENAS, V., MOLDENHAUER, H., OYARZUN, C. & ALVAREZ, M. 2009a. Kinetic validation of 6-NBDG as a probe for the glucose transporter GLUT1 in astrocytes. *J Neurochem,* 109 Suppl 1**,** 94-100.

BARROS, L. F., COURJARET, R., JAKOBY, P., LOAIZA, A., LOHR, C. & DEITMER, J. W. 2009b. Preferential transport and metabolism of glucose in Bergmann glia over Purkinje cells: a multiphoton study of cerebellar slices. *Glia,* 57**,** 962-70.

BASI, G. S., JACOBSON, R. D., VIRAG, I., SCHILLING, J. & SKENE, J. H. 1987. Primary structure and transcriptional regulation of GAP-43, a protein associated with nerve growth. *Cell,* 49**,** 785-91.

BAUER, J., STRAUSS, S., SCHREITER-GASSER, U., GANTER, U., SCHLEGEL, P., WITT, I., YOLK, B. & BERGER, M. 1991. Interleukin-6 and alpha-2-macroglobulin indicate an acute-phase state in Alzheimer's disease cortices. *FEBS Lett,* 285**,** 111-4.

BEDALOV, A. & SIMON, J. A. 2004. NAD to the rescue. *Science,* 305**,** 954-5.

BEDARD, K. & KRAUSE, K. H. 2007. The NOX family of ROS-generating NADPH oxidases: physiology and pathophysiology. *Physiol Rev,* 87**,** 245-313.

BEGNI, B., BRIGHINA, L., SIRTORI, E., FUMAGALLI, L., ANDREONI, S., BERETTA, S., OSTER, T., MALAPLATE-ARMAND, C., ISELLA, V., APPOLLONIO, I. & FERRARESE, C. 2004. Oxidative stress impairs glutamate uptake in fibroblasts from patients with Alzheimer's disease. *Free Radic Biol Med,* 37**,** 892-901.

BEHL, C., DAVIS, J. B., LESLEY, R. & SCHUBERT, D. 1994. Hydrogen peroxide mediates amyloid beta protein toxicity. *Cell,* 77**,** 817-27.

BELANGER, M. & MAGISTRETTI, P. J. 2009. The role of astroglia in neuroprotection. *Dialogues Clin Neurosci,* 11**,** 281-95.

BELENKY, P., BOGAN, K. L. & BRENNER, C. 2007. NAD+ metabolism in health and disease. *Trends Biochem Sci,* 32**,** 12-9.

BEN-YOSEPH, O., BOXER, P. A. & ROSS, B. D. 1994. Oxidative stress in the central nervous system: monitoring the metabolic response using the pentose phosphate pathway. *Dev Neurosci,* 16**,** 328-36.

BENARROCH, E. E. 2005. Neuron-astrocyte interactions: partnership for normal function and disease in the central nervous system. *Mayo Clin Proc,* 80**,** 1326-38.

BENOWITZ, L. I. & ROUTTENBERG, A. 1997. GAP-43: an intrinsic determinant of neuronal development and plasticity. *Trends Neurosci,* 20**,** 84-91.

BENZI, G. & MORETTI, A. 1995. Age- and peroxidative stress-related modifications of the cerebral enzymatic activities linked to mitochondria and the glutathione system. *Free Radic Biol Med,* 19**,** 77-101.

BERGER, F., RAMIREZ-HERNANDEZ, M. H. & ZIEGLER, M. 2004. The new life of a centenarian: signalling functions of NAD(P). *Trends Biochem Sci,* 29**,** 111-8.

BERGERSEN, L., WAERHAUG, O., HELM, J., THOMAS, M., LAAKE, P., DAVIES, A. J., WILSON, M. C., HALESTRAP, A. P. & OTTERSEN, O. P. 2001. A novel postsynaptic density protein: the monocarboxylate transporter MCT2 is co-localized with delta-glutamate receptors in postsynaptic densities of parallel fiber-Purkinje cell synapses. *Exp Brain Res,* 136**,** 523-34.

BERTHET, C., LEI, H., THEVENET, J., GRUETTER, R., MAGISTRETTI, P. J. & HIRT, L. 2009. Neuroprotective role of lactate after cerebral ischemia. *J Cereb Blood Flow Metab,* 29**,** 1780-9.

BITTAR, P. G., CHARNAY, Y., PELLERIN, L., BOURAS, C. & MAGISTRETTI, P. J. 1996. Selective distribution of lactate dehydrogenase isoenzymes in neurons and astrocytes of human brain. *J Cereb Blood Flow Metab,* 16**,** 1079-89.

BITTNER, C. X., LOAIZA, A., RUMINOT, I., LARENAS, V., SOTELO-HITSCHFELD, T., GUTIERREZ, R., CORDOVA, A., VALDEBENITO, R., FROMMER, W. B. &

BARROS, L. F. 2010. High resolution measurement of the glycolytic rate. *Front Neuroenergetics,* 2.

BITTNER, C. X., VALDEBENITO, R., RUMINOT, I., LOAIZA, A., LARENAS, V., SOTELO-HITSCHFELD, T., MOLDENHAUER, H., SAN MARTIN, A., GUTIERREZ, R., ZAMBRANO, M. & BARROS, L. F. 2011. Fast and reversible stimulation of astrocytic glycolysis by K+ and a delayed and persistent effect of glutamate. *J Neurosci,* 31**,** 4709-13.

BLACKER, D., WILCOX, M. A., LAIRD, N. M., RODES, L., HORVATH, S. M., GO, R. C., PERRY, R., WATSON, B., JR., BASSETT, S. S., MCINNIS, M. G., ALBERT, M. S., HYMAN, B. T. & TANZI, R. E. 1998. Alpha-2 macroglobulin is genetically associated with Alzheimer disease. *Nat Genet,* 19**,** 357-60.

BLAIN, J. F., AUMONT, N., THEROUX, L., DEA, D. & POIRIER, J. 2006. A polymorphism in lipoprotein lipase affects the severity of Alzheimer's disease pathophysiology. *Eur J Neurosci,* 24**,** 1245-51.

BLANDER, G. & GUARENTE, L. 2004. The Sir2 family of protein deacetylases. *Annu Rev Biochem,* 73**,** 417-35.

BLASS, J. P. 2000. The mitochondrial spiral. An adequate cause of dementia in the Alzheimer's syndrome. *Ann N Y Acad Sci,* 924, 170-83.

BOER, P. & SPERLING, O. 2004. Modulation of glycogen phosphorylase activity affects 5-phosphoribosyl-1-pyrophosphate availability in rat hepatocyte cultures. *Nucleosides Nucleotides Nucleic Acids,* 23**,** 1235-9.

BOGDANOVIC, N., DAVIDSSON, P., VOLKMANN, I., WINBLAD, B. & BLENNOW, K. 2000. Growth-associated protein GAP-43 in the frontal cortex and in the hippocampus in Alzheimer's disease: an immunohistochemical and quantitative study. *J Neural Transm,* 107**,** 463-78.

BONVENTO, G., HERARD, A. S. & VOUTSINOS-PORCHE, B. 2005. The astrocyte--neuron lactate shuttle: a debated but still valuable hypothesis for brain imaging. *J Cereb Blood Flow Metab,* 25**,** 1394-9.

BORTH, W. 1992. Alpha 2-macroglobulin, a multifunctional binding protein with targeting characteristics. *FASEB J,* 6**,** 3345-53.

BOSETTI, F., BRIZZI, F., BAROGI, S., MANCUSO, M., SICILIANO, G., TENDI, E. A., MURRI, L., RAPOPORT, S. I. & SOLAINI, G. 2002. Cytochrome c oxidase and mitochondrial F1F0-ATPase (ATP synthase) activities in platelets and brain from patients with Alzheimer's disease. *Neurobiology of Aging,* 23**,** 371-376.

BOUCHARD, V. J., ROULEAU, M. & POIRIER, G. G. 2003. PARP-1, a determinant of cell survival in response to DNA damage. *Exp Hematol,* 31**,** 446-54.

BOUZIER-SORE, A. K., SERRES, S., CANIONI, P. & MERLE, M. 2003a. Lactate involvement in neuron–glia metabolic interaction: 13C-NMR spectroscopy contribution. *Biochimie,* 85**,** 841-848.

BOUZIER-SORE, A. K., VOISIN, P., BOUCHAUD, V., BEZANCON, E., FRANCONI, J. M. & PELLERIN, L. 2006. Competition between glucose and lactate as oxidative energy substrates in both neurons and astrocytes: a comparative NMR study. *Eur J Neurosci,* 24**,** 1687-94.

BOUZIER-SORE, A. K., VOISIN, P., CANIONI, P., MAGISTRETTI, P. J. & PELLERIN, L. 2003b. Lactate is a preferential oxidative energy substrate over glucose for neurons in culture. *J Cereb Blood Flow Metab,* 23**,** 1298-306.

BOVERIS, A. & NAVARRO, A. 2008. Brain mitochondrial dysfunction in aging. *IUBMB Life,* 60**,** 308-14.

BRAIDY, N., GUILLEMIN, G. & GRANT, R. 2008. Promotion of cellular NAD(+) anabolism: therapeutic potential for oxidative stress in ageing and Alzheimer's disease. *Neurotox Res,* 13**,** 173-84.

BRAIDY, N., GUILLEMIN, G. J., MANSOUR, H., CHAN-LING, T., POLJAK, A. & GRANT, R. 2011. Age related changes in NAD+ metabolism oxidative stress and Sirt1 activity in wistar rats. *PLoS One,* 6**,** e19194.

BREWER, G. J. 1998. Age-related toxicity to lactate, glutamate, and beta-amyloid in cultured adult neurons. *Neurobiol Aging,* 19**,** 561-8.

BREWER, G. J. & WALLIMANN, T. W. 2000. Protective effect of the energy precursor creatine against toxicity of glutamate and beta-amyloid in rat hippocampal neurons. *J Neurochem,* 74**,** 1968-78.

BROOKES, N. & YAROWSKY, P. J. 1985. Determinants of deoxyglucose uptake in cultured astrocytes: the role of the sodium pump. *J Neurochem,* 44**,** 473-9.

BRORSON, J. R., ZHANG, Z. & VANDENBERGHE, W. 1999. Ca(2+) permeation of AMPA receptors in cerebellar neurons expressing glu receptor 2. *J Neurosci,* 19**,** 9149-59.

BROWN, A. M. 2004. Brain glycogen re-awakened. *J Neurochem,* 89**,** 537-52.

BROWN, A. M. & RANSOM, B. R. 2007. Astrocyte glycogen and brain energy metabolism. *Glia,* 55**,** 1263-71.

BROWN, A. M., TEKKOK, S. B. & RANSOM, B. R. 2003. Glycogen regulation and functional role in mouse white matter. *J Physiol,* 549**,** 501-12.

BRUNET, A., SWEENEY, L. B., STURGILL, J. F., CHUA, K. F., GREER, P. L., LIN, Y., TRAN, H., ROSS, S. E., MOSTOSLAVSKY, R., COHEN, H. Y., HU, L. S., CHENG, H. L., JEDRYCHOWSKI, M. P., GYGI, S. P., SINCLAIR, D. A., ALT, F. W. & GREENBERG, M. E. 2004. Stress-dependent regulation of FOXO transcription factors by the SIRT1 deacetylase. *Science,* 303**,** 2011-5.

BRUNET, J. F., ALLAMAN, I., MAGISTRETTI, P. J. & PELLERIN, L. 2010. Glycogen metabolism as a marker of astrocyte differentiation. *J Cereb Blood Flow Metab,* 30**,** 51-5.

BURDICK, D., SOREGHAN, B., KWON, M., KOSMOSKI, J., KNAUER, M., HENSCHEN, A., YATES, J., COTMAN, C. & GLABE, C. 1992. Assembly and aggregation properties of synthetic Alzheimer's A4/beta amyloid peptide analogs. *J Biol Chem,* 267**,** 546-54.

BUSHONG, E. A., MARTONE, M. E., JONES, Y. Z. & ELLISMAN, M. H. 2002. Protoplasmic astrocytes in CA1 stratum radiatum occupy separate anatomical domains. *J Neurosci,* 22**,** 183-92.

BUTTERFIELD, D. A. 1997. beta-Amyloid-associated free radical oxidative stress and neurotoxicity: implications for Alzheimer's disease. *Chem Res Toxicol,* 10**,** 495-506.

BUTTERFIELD, D. A. 2002. Amyloid beta-peptide (1-42)-induced oxidative stress and neurotoxicity: implications for neurodegeneration in Alzheimer's disease brain. A review. *Free Radic Res,* 36**,** 1307-13.

BUTTERFIELD, D. A., HENSLEY, K., COLE, P., SUBRAMANIAM, R., AKSENOV, M., AKSENOVA, M., BUMMER, P. M., HALEY, B. E. & CARNEY, J. M. 1997. Oxidatively induced structural alteration of glutamine synthetase assessed by analysis of spin label incorporation kinetics: relevance to Alzheimer's disease. *J Neurochem,* 68**,** 2451-7.

BUTTERFIELD, D. A., HOWARD, B., YATIN, S., KOPPAL, T., DRAKE, J., HENSLEY, K., AKSENOV, M., AKSENOVA, M., SUBRAMANIAM, R., VARADARAJAN, S., HARRIS-WHITE, M. E., PEDIGO, N. W., JR. & CARNEY, J. M. 1999. Elevated oxidative stress in models of normal brain aging and Alzheimer's disease. *Life Sci,* 65**,** 1883-92.

BUTTERFIELD, D. A. & LAUDERBACK, C. M. 2002. Lipid peroxidation and protein oxidation in Alzheimer's disease brain: potential causes and consequences involving amyloid beta-peptide-associated free radical oxidative stress. *Free Radic Biol Med,* 32**,** 1050-60.

BUTTERWORTH, R. F. & BESNARD, A. M. 1990. Thiamine-dependent enzyme changes in temporal cortex of patients with Alzheimer's disease. *Metab Brain Dis,* 5**,** 179-84.

CACCAMO, A., ODDO, S., SUGARMAN, M. C., AKBARI, Y. & LAFERLA, F. M. 2005. Age- and region-dependent alterations in Abeta-degrading enzymes: implications for Abeta-induced disorders. *Neurobiol Aging,* 26**,** 645-54.

CADENAS, E. 2004. Mitochondrial free radical production and cell signaling. *Mol Aspects Med,* 25**,** 17-26.

CAHILL, G. F., JR. 2006. Fuel metabolism in starvation. *Annu Rev Nutr,* 26**,** 1-22.

CALABRESE, V., SULTANA, R., SCAPAGNINI, G., GUAGLIANO, E., SAPIENZA, M., BELLA, R., KANSKI, J., PENNISI, G., MANCUSO, C., STELLA, A. M. & BUTTERFIELD, D. A. 2006. Nitrosative stress, cellular stress response, and thiol homeostasis in patients with Alzheimer's disease. *Antioxid Redox Signal,* 8**,** 1975-86.

CANDEIAS, L. P., MACFARLANE, D. P. S., MCWHINNIE, S. L. W., MAIDWELL, N. L., ROESCHLAUB, C. A., SAMMES, P. G. & WHITTLESEY, R. 1998. The catalysed NADH reduction of resazurin to resorufin. *Journal of the Chemical Society, Perkin Transactions 2,* 0**,** 2333-2334.

CANEVARI, L., CLARK, J. B. & BATES, T. E. 1999. beta-Amyloid fragment 25-35 selectively decreases complex IV activity in isolated mitochondria. *FEBS Lett,* 457**,** 131-4.

CAPELL, A., MEYN, L., FLUHRER, R., TEPLOW, D. B., WALTER, J. & HAASS, C. 2002. Apical sorting of beta-secretase limits amyloid beta-peptide production. *J Biol Chem,* 277**,** 5637-43.

CAPELL, A., STEINER, H., WILLEM, M., KAISER, H., MEYER, C., WALTER, J., LAMMICH, S., MULTHAUP, G. & HAASS, C. 2000. Maturation and pro-peptide cleavage of beta-secretase. *J Biol Chem,* 275**,** 30849-54.

CARDOSO, S., CORREIA, S., SANTOS, R. X., CARVALHO, C., SANTOS, M. S., OLIVEIRA, C. R., PERRY, G., SMITH, M. A., ZHU, X. & MOREIRA, P. I. 2009. Insulin is a two-edged knife on the brain. *J Alzheimers Dis,* 18**,** 483-507.

CARDOSO, S. M., SANTANA, I., SWERDLOW, R. H. & OLIVEIRA, C. R. 2004. Mitochondria dysfunction of Alzheimer's disease cybrids enhances Abeta toxicity. *J Neurochem,* 89**,** 1417-26.

CARPENTER, J. E., JACKSON, W., DE SOUZA, G. A., HAARR, L. & GROSE, C. 2010. Insulin-degrading enzyme binds to the nonglycosylated precursor of varicella-zoster virus gE protein found in the endoplasmic reticulum. *J Virol,* 84**,** 847-55.

CARTER, S. B. 1967. Effects of cytochalasins on mammalian cells. *Nature,* 213**,** 261-4.

CASLEY, C. S., LAND, J. M., SHARPE, M. A., CLARK, J. B., DUCHEN, M. R. & CANEVARI, L. 2002. Beta-amyloid fragment 25-35 causes mitochondrial dysfunction in primary cortical neurons. *Neurobiol Dis,* 10**,** 258-67.

CASPERSEN, C., WANG, N., YAO, J., SOSUNOV, A., CHEN, X., LUSTBADER, J. W., XU, H. W., STERN, D., MCKHANN, G. & YAN, S. D. 2005. Mitochondrial Abeta: a potential focal point for neuronal metabolic dysfunction in Alzheimer's disease. *FASEB J,* 19**,** 2040-1.

CASTANO, E. M., GHISO, J., PRELLI, F., GOREVIC, P. D., MIGHELI, A. & FRANGIONE, B. 1986. In vitro formation of amyloid fibrils from two synthetic peptides of different lengths homologous to Alzheimer's disease beta-protein. *Biochem Biophys Res Commun,* 141**,** 782-9.

CASTELLANO, J. M., KIM, J., STEWART, F. R., JIANG, H., DEMATTOS, R. B., PATTERSON, B. W., FAGAN, A. M., MORRIS, J. C., MAWUENYEGA, K. G., CRUCHAGA, C., GOATE, A. M., BALES, K. R., PAUL, S. M., BATEMAN, R. J. & HOLTZMAN, D. M. 2011. Human apoE isoforms differentially regulate brain amyloid-? peptide clearance. *Science Translational Medicine,* 3.

CATALDO, A. M. & BROADWELL, R. D. 1986. Cytochemical identification of cerebral glycogen and glucose-6-phosphatase activity under normal and experimental conditions. II. Choroid plexus and ependymal epithelia, endothelia and pericytes. *J Neurocytol,* 15**,** 511-24.

CHAMBERS, S. M., FASANO, C. A., PAPAPETROU, E. P., TOMISHIMA, M., SADELAIN, M. & STUDER, L. 2009. Highly efficient neural conversion of human ES and iPS cells by dual inhibition of SMAD signaling. *Nat Biotechnol,* 27**,** 275-80.

CHAN, S. F. & SUCHER, N. J. 2001. An NMDA receptor signaling complex with protein phosphatase 2A. *J Neurosci,* 21**,** 7985-92.

CHANG, Y., TESCO, G., JEONG, W. J., LINDSLEY, L., ECKMAN, E. A., ECKMAN, C. B., TANZI, R. E. & GUENETTE, S. Y. 2003. Generation of the beta-amyloid peptide and the amyloid precursor protein C-terminal fragment gamma are potentiated by FE65L1. *J Biol Chem,* 278**,** 51100-7.

CHATTON, J. Y., MARQUET, P. & MAGISTRETTI, P. J. 2000. A quantitative analysis of L-glutamate-regulated Na+ dynamics in mouse cortical astrocytes: implications for cellular bioenergetics. *Eur J Neurosci,* 12**,** 3843-53.

CHEN, P., GU, Z., LIU, W. & YAN, Z. 2007. Glycogen synthase kinase 3 regulates N-methyl-D-aspartate receptor channel trafficking and function in cortical neurons. *Mol Pharmacol,* 72**,** 40-51.

CHENAL, J. & PELLERIN, L. 2007. Noradrenaline enhances the expression of the neuronal monocarboxylate transporter MCT2 by translational activation via stimulation of PI3K/Akt and the mTOR/S6K pathway. *J Neurochem,* 102**,** 389-97.

CHENAL, J., PIERRE, K. & PELLERIN, L. 2008. Insulin and IGF-1 enhance the expression of the neuronal monocarboxylate transporter MCT2 by translational activation via stimulation of the phosphoinositide 3-kinase-Akt-mammalian target of rapamycin pathway. *Eur J Neurosci,* 27**,** 53-65.

CHETELAT, G., DESGRANGES, B., DE LA SAYETTE, V., VIADER, F., EUSTACHE, F. & BARON, J. C. 2003. Mild cognitive impairment: Can FDG-PET predict who is to rapidly convert to Alzheimer's disease? *Neurology,* 60**,** 1374-7.

CHI, E. Y., FREY, S. L., WINANS, A., LAM, K. L., KJAER, K., MAJEWSKI, J. & LEE, K. Y. 2010. Amyloid-beta fibrillogenesis seeded by interface-induced peptide misfolding and self-assembly. *Biophys J,* 98**,** 2299-308.

CHOI, I. Y. & GRUETTER, R. 2003. In vivo 13C NMR assessment of brain glycogen concentration and turnover in the awake rat. *Neurochem Int,* 43**,** 317-22.

CHOLET, N., PELLERIN, L., MAGISTRETTI, P. J. & HAMEL, E. 2002. Similar perisynaptic glial localization for the Na+,K+-ATPase alpha 2 subunit and the glutamate transporters GLAST and GLT-1 in the rat somatosensory cortex. *Cereb Cortex,* 12**,** 515-25.

CHROMY, B. A., NOWAK, R. J., LAMBERT, M. P., VIOLA, K. L., CHANG, L., VELASCO, P. T., JONES, B. W., FERNANDEZ, S. J., LACOR, P. N., HOROWITZ, P., FINCH, C. E., KRAFFT, G. A. & KLEIN, W. L. 2003. Self-assembly of Abeta(1-42) into globular neurotoxins. *Biochemistry,* 42**,** 12749-60.

CHRYSSANTHOPOULOS, C., WILLIAMS, C., NOWITZ, A. & BOGDANIS, G. 2004. Skeletal muscle glycogen concentration and metabolic responses following a high glycaemic carbohydrate breakfast. *J Sports Sci,* 22**,** 1065-71.

CHUNG, S. H. 2009. Aberrant phosphorylation in the pathogenesis of Alzheimer's disease. *BMB Rep,* 42**,** 467-74.

CHUQUET, J., QUILICHINI, P., NIMCHINSKY, E. A. & BUZSAKI, G. 2010. Predominant enhancement of glucose uptake in astrocytes versus neurons during activation of the somatosensory cortex. *J Neurosci,* 30**,** 15298-303.

CICCOTOSTO, G. D., TEW, D. J., DREW, S. C., SMITH, D. G., JOHANSSEN, T., LAL, V., LAU, T. L., PEREZ, K., CURTAIN, C. C., WADE, J. D., SEPAROVIC, F., MASTERS, C. L., SMITH, J. P., BARNHAM, K. J. & CAPPAI, R. 2011. Stereospecific interactions are necessary for Alzheimer disease amyloid-beta toxicity. *Neurobiol Aging,* 32**,** 235-48.

CITRON, M., OLTERSDORF, T., HAASS, C., MCCONLOGUE, L., HUNG, A. Y., SEUBERT, P., VIGO-PELFREY, C., LIEBERBURG, I. & SELKOE, D. J. 1992. Mutation of the beta-amyloid precursor protein in familial Alzheimer's disease increases beta-protein production. *Nature,* 360**,** 672-4.

CIZAS, P., BUDVYTYTE, R., MORKUNIENE, R., MOLDOVAN, R., BROCCIO, M., LOSCHE, M., NIAURA, G., VALINCIUS, G. & BORUTAITE, V. 2010. Size-dependent neurotoxicity of beta-amyloid oligomers. *Arch Biochem Biophys,* 496**,** 84-92.

CLAPHAM, D. E. 2007. Calcium signaling. *Cell,* 131**,** 1047-58.

CLARKE, J. B., FORTES, M. A., GIOVANNI, A. & BREWSTER, D. W. 1996. Modification of an Enzymatic Glutathione Assay for the Microtiter Plate and the Determination of Glutathione in Rat Primary Cortical Cells. *Toxicology Mechanisms and Methods,* 6**,** 223-230.

COLE, S. L. & VASSAR, R. 2007. The Alzheimer's disease beta-secretase enzyme, BACE1. *Mol Neurodegener,* 2**,** 22.

COLOMBO, J. A. & REISIN, H. D. 2004. Interlaminar astroglia of the cerebral cortex: a marker of the primate brain. *Brain Res,* 1006**,** 126-31.

COLOMBO, J. A., YANEZ, A., PUISSANT, V. & LIPINA, S. 1995. Long, interlaminar astroglial cell processes in the cortex of adult monkeys. *J Neurosci Res,* 40**,** 551-6.

CONNERN, C. P. & HALESTRAP, A. P. 1994. Recruitment of mitochondrial cyclophilin to the mitochondrial inner membrane under conditions of oxidative stress that enhance the opening of a calcium-sensitive non-specific channel. *Biochem J,* 302 (Pt 2)**,** 321-4.

CONWAY, K. A., LEE, S. J., ROCHET, J. C., DING, T. T., WILLIAMSON, R. E. & LANSBURY, P. T., JR. 2000. Acceleration of oligomerization, not fibrillization, is a shared property of both alpha-synuclein mutations linked to early-onset Parkinson's disease: implications for pathogenesis and therapy. *Proc Natl Acad Sci U S A,* 97**,** 571-6.

CORDER, E. H., SAUNDERS, A. M., STRITTMATTER, W. J., SCHMECHEL, D. E., GASKELL, P. C., SMALL, G. W., ROSES, A. D., HAINES, J. L. & PERICAK-VANCE, M. A. 1993. Gene dose of apolipoprotein E type 4 allele and the risk of Alzheimer's disease in late onset families. *Science,* 261**,** 921-3.

CORREIA, S. C., SANTOS, R. X., CARVALHO, C., CARDOSO, S., CANDEIAS, E., SANTOS, M. S., OLIVEIRA, C. R. & MOREIRA, P. I. 2012. Insulin signaling, glucose metabolism and mitochondria: major players in Alzheimer's disease and diabetes interrelation. *Brain Res,* 1441**,** 64-78.

CRAFT, S., ASTHANA, S., COOK, D. G., BAKER, L. D., CHERRIER, M., PURGANAN, K., WAIT, C., PETROVA, A., LATENDRESSE, S., WATSON, G. S., NEWCOMER, J. W., SCHELLENBERG, G. D. & KROHN, A. J. 2003. Insulin dose-response effects on memory and plasma amyloid precursor protein in Alzheimer's disease: interactions with apolipoprotein E genotype. *Psychoneuroendocrinology,* 28**,** 809-22.

CRAFT, S., NEWCOMER, J., KANNE, S., DAGOGO-JACK, S., CRYER, P., SHELINE, Y., LUBY, J., DAGOGO-JACK, A. & ALDERSON, A. 1996. Memory improvement following induced hyperinsulinemia in Alzheimer's disease. *Neurobiol Aging,* 17**,** 123-30.

CRAFT, S., ZALLEN, G. & BAKER, L. D. 1992. Glucose and memory in mild senile dementia of the Alzheimer type. *J Clin Exp Neuropsychol,* 14**,** 253-67.

CROUCH, P. J., HUNG, L. W., ADLARD, P. A., CORTES, M., LAL, V., FILIZ, G., PEREZ, K. A., NURJONO, M., CARAGOUNIS, A., DU, T., LAUGHTON, K., VOLITAKIS, I., BUSH, A. I., LI, Q. X., MASTERS, C. L., CAPPAI, R., CHERNY, R. A., DONNELLY, P. S., WHITE, A. R. & BARNHAM, K. J. 2009a. Increasing Cu bioavailability inhibits Abeta oligomers and tau phosphorylation. *Proc Natl Acad Sci U S A,* 106**,** 381-6.

CROUCH, P. J., TEW, D. J., DU, T., NGUYEN, D. N., CARAGOUNIS, A., FILIZ, G., BLAKE, R. E., TROUNCE, I. A., SOON, C. P., LAUGHTON, K., PEREZ, K. A., LI, Q. X., CHERNY, R. A., MASTERS, C. L., BARNHAM, K. J. & WHITE, A. R. 2009b. Restored degradation of the Alzheimer's amyloid-beta peptide by targeting amyloid formation. *J Neurochem,* 108**,** 1198-207.

CRUZ, N. F. & DIENEL, G. A. 2002. High glycogen levels in brains of rats with minimal environmental stimuli: implications for metabolic contributions of working astrocytes. *J Cereb Blood Flow Metab,* 22**,** 1476-89.

CULMSEE, C., ZHU, X., YU, Q. S., CHAN, S. L., CAMANDOLA, S., GUO, Z., GREIG, N. H. & MATTSON, M. P. 2001. A synthetic inhibitor of p53 protects neurons against death induced by ischemic and excitotoxic insults, and amyloid beta-peptide. *J Neurochem,* 77**,** 220-8.

CUNNANE, S., NUGENT, S., ROY, M., COURCHESNE-LOYER, A., CROTEAU, E., TREMBLAY, S., CASTELLANO, A., PIFFERI, F., BOCTI, C., PAQUET, N., BEGDOURI, H., BENTOURKIA, M., TURCOTTE, E., ALLARD, M., BARBERGER-GATEAU, P., FULOP, T. & RAPOPORT, S. I. 2011. Brain fuel metabolism, aging, and Alzheimer's disease. *Nutrition,* 27**,** 3-20.

CURTI, D., ROGNONI, F., GASPARINI, L., CATTANEO, A., PAOLILLO, M., RACCHI, M., ZANI, L., BIANCHETTI, A., TRABUCCHI, M., BERGAMASCHI, S. & GOVONI, S. 1997. Oxidative metabolism in cultured fibroblasts derived from sporadic Alzheimer's disease (AD) patients. *Neuroscience Letters,* 236**,** 13-16.

DA CRUZ E SILVA, E. F., DA CRUZ E SILVA, O. A., ZAIA, C. T. & GREENGARD, P. 1995. Inhibition of protein phosphatase 1 stimulates secretion of Alzheimer amyloid precursor protein. *Mol Med,* 1**,** 535-41.

DAHLGREN, K. N., MANELLI, A. M., W. BLAINE STINE, J., BAKER, L. K., KRAFFT, G. A. & LADU, M. J. 2002. Oligomeric and Fibrillar Species of Amyloid-β Peptides Differentially Affect Neuronal Viability. *The Journal of Biological Chemistry,* 277**,** 32046-32053.

DALLE-DONNE, I., MILZANI, A., GAGLIANO, N., COLOMBO, R., GIUSTARINI, D. & ROSSI, R. 2008. Molecular mechanisms and potential clinical significance of S-glutathionylation. *Antioxid Redox Signal,* 10**,** 445-73.

DANBOLT, N. C. 2001. Glutamate uptake. *Prog Neurobiol,* 65**,** 1-105.

DE FELICE, F. G., VELASCO, P. T., LAMBERT, M. P., VIOLA, K., FERNANDEZ, S. J., FERREIRA, S. T. & KLEIN, W. L. 2007. Abeta oligomers induce neuronal oxidative stress through an N-methyl-D-aspartate receptor-dependent mechanism that is blocked by the Alzheimer drug memantine. *J Biol Chem,* 282**,** 11590-601.

DE LA MONTE, S. M., NG, S. C. & HSU, D. W. 1995. Aberrant GAP-43 gene expression in Alzheimer's disease. *Am J Pathol,* 147**,** 934-46.

DE LA MONTE, S. M., SOHN, Y. K., GANJU, N. & WANDS, J. R. 1998. P53- and CD95-associated apoptosis in neurodegenerative diseases. *Lab Invest,* 78**,** 401-11.

DE LA MONTE, S. M. & WANDS, J. R. 2005. Review of insulin and insulin-like growth factor expression, signaling, and malfunction in the central nervous system: relevance to Alzheimer's disease. *J Alzheimers Dis,* 7**,** 45-61.

DE LEON, M. J., CONVIT, A., WOLF, O. T., TARSHISH, C. Y., DESANTI, S., RUSINEK, H., TSUI, W., KANDIL, E., SCHERER, A. J., ROCHE, A., IMOSSI, A., THORN, E., BOBINSKI, M., CARAOS, C., LESBRE, P., SCHLYER, D., POIRIER, J., REISBERG, B. & FOWLER, J. 2001. Prediction of cognitive decline in normal elderly subjects with 2-[(18)F]fluoro-2-deoxy-D-glucose/poitron-emission tomography (FDG/PET). *Proc Natl Acad Sci U S A,* 98**,** 10966-71.

DE MURCIA, J. M., NIEDERGANG, C., TRUCCO, C., RICOUL, M., DUTRILLAUX, B., MARK, M., OLIVER, F. J., MASSON, M., DIERICH, A., LEMEUR, M., WALZTINGER, C., CHAMBON, P. & DE MURCIA, G. 1997. Requirement of poly(ADP-ribose) polymerase in recovery from DNA damage in mice and in cells. *Proc Natl Acad Sci U S A,* 94**,** 7303-7.

DE SANTI, S., DE LEON, M. J., CONVIT, A., TARSHISH, C., RUSINEK, H., TSUI, W. H., SINAIKO, E., WANG, G. J., BARTLET, E. & VOLKOW, N. 1995. Age-related changes in brain: II. Positron emission tomography of frontal and temporal lobe glucose metabolism in normal subjects. *Psychiatr Q,* 66**,** 357-70.

DE SANTI, S., DE LEON, M. J., RUSINEK, H., CONVIT, A., TARSHISH, C. Y., ROCHE, A., TSUI, W. H., KANDIL, E., BOPPANA, M., DAISLEY, K., WANG, G. J., SCHLYER, D. & FOWLER, J. 2001. Hippocampal formation glucose metabolism and volume losses in MCI and AD. *Neurobiol Aging,* 22**,** 529-39.

DE STROOPER, B., CRAESSAERTS, K., DEWACHTER, I., MOECHARS, D., GREENBERG, B., VAN LEUVEN, F. & VAN DEN BERGHE, H. 1995. Basolateral secretion of amyloid precursor protein in Madin-Darby canine kidney cells is disturbed by alterations of intracellular pH and by introducing a mutation associated with familial Alzheimer's disease. *J Biol Chem,* 270**,** 4058-65.

DENT, P., LAVOINNE, A., NAKIELNY, S., CAUDWELL, F. B., WATT, P. & COHEN, P. 1990. The molecular mechanism by which insulin stimulates glycogen synthesis in mammalian skeletal muscle. *Nature,* 348**,** 302-8.

DESHPANDE, A., KAWAI, H., METHERATE, R., GLABE, C. G. & BUSCIGLIO, J. 2009. A role for synaptic zinc in activity-dependent Abeta oligomer formation and accumulation at excitatory synapses. *J Neurosci,* 29**,** 4004-15.

DEVI, L., PRABHU, B. M., GALATI, D. F., AVADHANI, N. G. & ANANDATHEERTHAVARADA, H. K. 2006. Accumulation of amyloid precursor protein in the mitochondrial import channels of human Alzheimer's disease brain is associated with mitochondrial dysfunction. *J Neurosci,* 26**,** 9057-68.

DI LISA, F., MENABO, R., CANTON, M., BARILE, M. & BERNARDI, P. 2001. Opening of the mitochondrial permeability transition pore causes depletion of mitochondrial and cytosolic NAD+ and is a causative event in the death of myocytes in postischemic reperfusion of the heart. *J Biol Chem,* 276**,** 2571-5.

DIENEL, G. A. 2010. Astrocytes are 'good scouts': being prepared also helps neighboring neurons. *J Cereb Blood Flow Metab,* 30**,** 1893-4.

DIENEL, G. A. & HERTZ, L. 2001. Glucose and lactate metabolism during brain activation. *J Neurosci Res,* 66**,** 824-38.

DINELEY, K. T., BELL, K. A., BUI, D. & SWEATT, J. D. 2002. beta -Amyloid peptide activates alpha 7 nicotinic acetylcholine receptors expressed in Xenopus oocytes. *J Biol Chem,* 277**,** 25056-61.

DINELEY, K. T., WESTERMAN, M., BUI, D., BELL, K., ASHE, K. H. & SWEATT, J. D. 2001. Beta-amyloid activates the mitogen-activated protein kinase cascade via hippocampal alpha7 nicotinic acetylcholine receptors: In vitro and in vivo mechanisms related to Alzheimer's disease. *J Neurosci,* 21**,** 4125-33.

DINUZZO, M., MANGIA, S., MARAVIGLIA, B. & GIOVE, F. 2010. Glycogenolysis in astrocytes supports blood-borne glucose channeling not glycogen-derived lactate shuttling to neurons: evidence from mathematical modeling. *J Cereb Blood Flow Metab,* 30**,** 1895-904.

DODART, J.-C., MATHIS, C., BALES, K. R. & PAUL, S. M. 2002a. Does my mouse have Alzheimer's disease? *Genes, Brain & Behavior,* 1**,** 142-155.

DODART, J. C., BALES, K. R., GANNON, K. S., GREENE, S. J., DEMATTOS, R. B., MATHIS, C., DELONG, C. A., WU, S., WU, X., HOLTZMAN, D. M. & PAUL, S. M.

2002b. Immunization reverses memory deficits without reducing brain Abeta burden in Alzheimer's disease model. *Nat Neurosci,* 5**,** 452-7.

DODONI, G., CANTON, M., PETRONILLI, V., BERNARDI, P. & DI LISA, F. 2004. Induction of the mitochondrial permeability transition by the DNA alkylating agent N-methyl-N'-nitro-N-nitrosoguanidine. Sorting cause and consequence of mitochondrial dysfunction. *Biochim Biophys Acta,* 1658**,** 58-63.

DOLMETSCH, R. & GESCHWIND, DANIEL H. 2011. The Human Brain in a Dish: The Promise of iPSC-Derived Neurons. *Cell,* 145**,** 831-834.

DONMEZ, G., WANG, D., COHEN, D. E. & GUARENTE, L. 2010. SIRT1 suppresses beta-amyloid production by activating the alpha-secretase gene ADAM10. *Cell,* 142**,** 320-32.

DREW, S. C., MASTERS, C. L. & BARNHAM, K. J. 2009a. Alanine-2 carbonyl is an oxygen ligand in Cu2+ coordination of Alzheimer's disease amyloid-beta peptide--relevance to N-terminally truncated forms. *J Am Chem Soc,* 131**,** 8760-1.

DREW, S. C., NOBLE, C. J., MASTERS, C. L., HANSON, G. R. & BARNHAM, K. J. 2009b. Pleomorphic copper coordination by Alzheimer's disease amyloid-beta peptide. *J Am Chem Soc,* 131**,** 1195-207.

DRINGEN, R., GEBHARDT, R. & HAMPRECHT, B. 1993a. Glycogen in astrocytes: possible function as lactate supply for neighboring cells. *Brain Res,* 623**,** 208-14.

DRINGEN, R., GUTTERER, J. M. & HIRRLINGER, J. 2000. Glutathione metabolism in brain metabolic interaction between astrocytes and neurons in the defense against reactive oxygen species. *Eur J Biochem,* 267**,** 4912-6.

DRINGEN, R., SCHMOLL, D., CESAR, M. & HAMPRECHT, B. 1993b. Incorporation of radioactivity from [14C]lactate into the glycogen of cultured mouse astroglial cells. Evidence for gluconeogenesis in brain cells. *Biol Chem Hoppe Seyler,* 374**,** 343-7.

DRZEZGA, A., GRIMMER, T., RIEMENSCHNEIDER, M., LAUTENSCHLAGER, N., SIEBNER, H., ALEXOPOULUS, P., MINOSHIMA, S., SCHWAIGER, M. & KURZ, A. 2005. Prediction of individual clinical outcome in MCI by means of genetic assessment and (18)F-FDG PET. *J Nucl Med,* 46**,** 1625-32.

DRZEZGA, A., LAUTENSCHLAGER, N., SIEBNER, H., RIEMENSCHNEIDER, M., WILLOCH, F., MINOSHIMA, S., SCHWAIGER, M. & KURZ, A. 2003. Cerebral metabolic changes accompanying conversion of mild cognitive impairment into Alzheimer's disease: a PET follow-up study. *Eur J Nucl Med Mol Imaging,* 30**,** 1104-13.

DU, H., GUO, L., FANG, F., CHEN, D., SOSUNOV, A. A., MCKHANN, G. M., YAN, Y., WANG, C., ZHANG, H., MOLKENTIN, J. D., GUNN-MOORE, F. J., VONSATTEL, J. P., ARANCIO, O., CHEN, J. X. & YAN, S. D. 2008. Cyclophilin D deficiency attenuates mitochondrial and neuronal perturbation and ameliorates learning and memory in Alzheimer's disease. *Nat Med,* 14**,** 1097-105.

DU YAN, S., ZHU, Y., STERN, E. D., HWANG, Y. C., HORI, O., OGAWA, S., FROSCH, M. P., CONNOLLY, E. S., JR., MCTAGGERT, R., PINSKY, D. J., CLARKE, S., STERN, D. M. & RAMASAMY, R. 2000. Amyloid beta -peptide-binding alcohol dehydrogenase is a component of the cellular response to nutritional stress. *J Biol Chem,* 275**,** 27100-9.

DUCE, J. A., TSATSANIS, A., CATER, M. A., JAMES, S. A., ROBB, E., WIKHE, K., LEONG, S. L., PEREZ, K., JOHANSSEN, T., GREENOUGH, M. A., CHO, H. H., GALATIS, D., MOIR, R. D., MASTERS, C. L., MCLEAN, C., TANZI, R. E., CAPPAI, R., BARNHAM, K. J., CICCOTOSTO, G. D., ROGERS, J. T. & BUSH, A. I. 2010. Iron-export ferroxidase activity of beta-amyloid precursor protein is inhibited by zinc in Alzheimer's disease. *Cell,* 142**,** 857-67.

DUCKWORTH, W. C., BENNETT, R. G. & HAMEL, F. G. 1998. Insulin degradation: progress and potential. *Endocr Rev,* 19**,** 608-24.

DUFF, K. & SULEMAN, F. 2004. Transgenic mouse models of Alzheimer's disease: How useful have they been for therapeutic development? *Briefings in Functional Genomics and Proteomics,* 3**,** 47-59.

DUYCKAERTS, C., POTIER, M. C. & DELATOUR, B. 2008. Alzheimer disease models and human neuropathology: similarities and differences. *Acta Neuropathol,* 115**,** 5-38.

DWYER, D. S., VANNUCCI, S. J. & SIMPSON, I. A. 2002. Expression, regulation, and functional role of glucose transporters (GLUTs) in brain. *Int Rev Neurobiol,* 51**,** 159-88.

DYRKS, T., WEIDEMANN, A., MULTHAUP, G., SALBAUM, J. M., LEMAIRE, H. G., KANG, J., MULLER-HILL, B., MASTERS, C. L. & BEYREUTHER, K. 1988. Identification, transmembrane orientation and biogenesis of the amyloid A4 precursor of Alzheimer's disease. *EMBO J,* 7**,** 949-57.

EDBAUER, D., WINKLER, E., REGULA, J. T., PESOLD, B., STEINER, H. & HAASS, C. 2003. Reconstitution of gamma-secretase activity. *Nat Cell Biol,* 5**,** 486-8.

EDLAND, S. D., SILVERMAN, J. M., PESKIND, E. R., TSUANG, D., WIJSMAN, E. & MORRIS, J. C. 1996. Increased risk of dementia in mothers of Alzheimer's disease cases: evidence for maternal inheritance. *Neurology,* 47**,** 254-6.

EHRENKRANTZ, D., SILVERMAN, J. M., SMITH, C. J., BIRSTEIN, S., MARIN, D., MOHS, R. C. & DAVIS, K. L. 1999. Genetic epidemiological study of maternal and paternal transmission of Alzheimer's disease. *Am J Med Genet,* 88**,** 378-82.

EMBI, N., RYLATT, D. B. & COHEN, P. 1980. Glycogen synthase kinase-3 from rabbit skeletal muscle. Separation from cyclic-AMP-dependent protein kinase and phosphorylase kinase. *Eur J Biochem,* 107**,** 519-27.

ENYA, M., MORISHIMA-KAWASHIMA, M., YOSHIMURA, M., SHINKAI, Y., KUSUI, K., KHAN, K., GAMES, D., SCHENK, D., SUGIHARA, S., YAMAGUCHI, H. & IHARA, Y. 1999. Appearance of sodium dodecyl sulfate-stable amyloid beta-protein (Abeta) dimer in the cortex during aging. *Am J Pathol,* 154**,** 271-9.

ERDELYI, K., BAKONDI, E., GERGELY, P., SZABO, C. & VIRAG, L. 2005. Pathophysiologic role of oxidative stress-induced poly(ADP-ribose) polymerase-1 activation: focus on cell death and transcriptional regulation. *Cell Mol Life Sci,* 62**,** 751-9.

ERLICHMAN, J. S., HEWITT, A., DAMON, T. L., HART, M., KURASCZ, J., LI, A. & LEITER, J. C. 2008. Inhibition of monocarboxylate transporter 2 in the retrotrapezoid nucleus in rats: a test of the astrocyte-neuron lactate-shuttle hypothesis. *J Neurosci,* 28**,** 4888-96.

FALKEVALL, A., ALIKHANI, N., BHUSHAN, S., PAVLOV, P. F., BUSCH, K., JOHNSON, K. A., ENEQVIST, T., TJERNBERG, L., ANKARCRONA, M. & GLASER, E. 2006. Degradation of the amyloid beta-protein by the novel mitochondrial peptidasome, PreP. *J Biol Chem,* 281**,** 29096-104.

FALLER, P. 2009. Copper and zinc binding to amyloid-beta: coordination, dynamics, aggregation, reactivity and metal-ion transfer. *Chembiochem,* 10**,** 2837-45.

FARRIS, W., MANSOURIAN, S., CHANG, Y., LINDSLEY, L., ECKMAN, E. A., FROSCH, M. P., ECKMAN, C. B., TANZI, R. E., SELKOE, D. J. & GUENETTE, S. 2003. Insulin-degrading enzyme regulates the levels of insulin, amyloid beta-protein, and the beta-amyloid precursor protein intracellular domain in vivo. *Proc Natl Acad Sci U S A,* 100**,** 4162-7.

FARZAN, M., SCHNITZLER, C. E., VASILIEVA, N., LEUNG, D. & CHOE, H. 2000. BACE2, a beta -secretase homolog, cleaves at the beta site and within the amyloid-beta region of the amyloid-beta precursor protein. *Proc Natl Acad Sci U S A,* 97**,** 9712-7.

FERNANDEZ-FERNANDEZ, S., ALMEIDA, A. & BOLANOS, J. P. 2012. Antioxidant and bioenergetic coupling between neurons and astrocytes. *Biochem J,* 443**,** 3-11.

FERREIRA, I. L., RESENDE, R., FERREIRO, E., REGO, A. C. & PEREIRA, C. F. 2010. Multiple defects in energy metabolism in Alzheimer's disease. *Curr Drug Targets,* 11**,** 1193-206.

FINDER, V. H., VODOPIVEC, I., NITSCH, R. M. & GLOCKSHUBER, R. 2010. The recombinant amyloid-beta peptide Abeta1-42 aggregates faster and is more neurotoxic than synthetic Abeta1-42. *J Mol Biol,* 396**,** 9-18.

FLOYD, R. A. 1999. Antioxidants, oxidative stress, and degenerative neurological disorders. *Proc Soc Exp Biol Med,* 222**,** 236-45.

FONFRIA, E., MARSHALL, I. C., BOYFIELD, I., SKAPER, S. D., HUGHES, J. P., OWEN, D. E., ZHANG, W., MILLER, B. A., BENHAM, C. D. & MCNULTY, S. 2005. Amyloid beta-peptide(1-42) and hydrogen peroxide-induced toxicity are mediated by TRPM2 in rat primary striatal cultures. *J Neurochem,* 95**,** 715-23.

FORSYTH, R. J., BARTLETT, K., BURCHELL, A., SCOTT, H. M. & EYRE, J. A. 1993. Astrocytic glucose-6-phosphatase and the permeability of brain microsomes to glucose 6-phosphate. *Biochem J,* 294 (Pt 1)**,** 145-51.

FOSTER, N. L., CHASE, T. N., MANSI, L., BROOKS, R., FEDIO, P., PATRONAS, N. J. & DI CHIRO, G. 1984. Cortical abnormalities in Alzheimer's disease. *Ann Neurol,* 16**,** 649-54.

FRIEDLAND, R. P., BUDINGER, T. F., GANZ, E., YANO, Y., MATHIS, C. A., KOSS, B., OBER, B. A., HUESMAN, R. H. & DERENZO, S. E. 1983. Regional cerebral metabolic alterations in dementia of the Alzheimer type: positron emission tomography with [18F]fluorodeoxyglucose. *J Comput Assist Tomogr,* 7**,** 590-8.

FROLICH, L., BLUM-DEGEN, D., BERNSTEIN, H. G., ENGELSBERGER, S., HUMRICH, J., LAUFER, S., MUSCHNER, D., THALHEIMER, A., TURK, A., HOYER, S., ZOCHLING, R., BOISSL, K. W., JELLINGER, K. & RIEDERER, P. 1998. Brain insulin and insulin receptors in aging and sporadic Alzheimer's disease. *J Neural Transm,* 105**,** 423-38.

FRYKMAN, S., HUR, J. Y., FRANBERG, J., AOKI, M., WINBLAD, B., NAHALKOVA, J., BEHBAHANI, H. & TJERNBERG, L. O. 2010. Synaptic and endosomal localization of active gamma-secretase in rat brain. *PLoS One,* 5**,** e8948.

FUKAMI, S., WATANABE, K., IWATA, N., HARAOKA, J., LU, B., GERARD, N. P., GERARD, C., FRASER, P., WESTAWAY, D., ST GEORGE-HYSLOP, P. & SAIDO, T. C. 2002. Abeta-degrading endopeptidase, neprilysin, in mouse brain: synaptic and axonal localization inversely correlating with Abeta pathology. *Neurosci Res,* 43**,** 39-56.

FUKUI, H., DIAZ, F., GARCIA, S. & MORAES, C. T. 2007. Cytochrome c oxidase deficiency in neurons decreases both oxidative stress and amyloid formation in a mouse model of Alzheimer's disease. *Proc Natl Acad Sci U S A,* 104**,** 14163-8.

FUKUMORI, A., OKOCHI, M., TAGAMI, S., JIANG, J., ITOH, N., NAKAYAMA, T., YANAGIDA, K., ISHIZUKA-KATSURA, Y., MORIHARA, T., KAMINO, K., TANAKA, T., KUDO, T., TANII, H., IKUTA, A., HAASS, C. & TAKEDA, M. 2006. Presenilin-dependent gamma-secretase on plasma membrane and endosomes is functionally distinct. *Biochemistry,* 45**,** 4907-14.

FUKUMOTO, H., CHEUNG, B. S., HYMAN, B. T. & IRIZARRY, M. C. 2002. Beta-secretase protein and activity are increased in the neocortex in Alzheimer disease. *Arch Neurol,* 59**,** 1381-9.

FUNATO, H., ENYA, M., YOSHIMURA, M., MORISHIMA-KAWASHIMA, M. & IHARA, Y. 1999. Presence of sodium dodecyl sulfate-stable amyloid beta-protein dimers in the hippocampus CA1 not exhibiting neurofibrillary tangle formation. *Am J Pathol,* 155**,** 23-8.

FURUKAWA, A., TADA-OIKAWA, S., KAWANISHI, S. & OIKAWA, S. 2007. H2O2 accelerates cellular senescence by accumulation of acetylated p53 via decrease in the function of SIRT1 by NAD+ depletion. *Cell Physiol Biochem,* 20**,** 45-54.

GABALDON, T. & HUYNEN, M. A. 2004. Shaping the mitochondrial proteome. *Biochim Biophys Acta,* 1659**,** 212-20.

GABUZDA, D., BUSCIGLIO, J., CHEN, L. B., MATSUDAIRA, P. & YANKNER, B. A. 1994. Inhibition of energy metabolism alters the processing of amyloid precursor protein and induces a potentially amyloidogenic derivative. *J Biol Chem,* 269**,** 13623-8.

GASPARINI, L., GOURAS, G. K., WANG, R., GROSS, R. S., BEAL, M. F., GREENGARD, P. & XU, H. 2001. Stimulation of beta-amyloid precursor protein trafficking by insulin reduces intraneuronal beta-amyloid and requires mitogen-activated protein kinase signaling. *J Neurosci,* 21**,** 2561-70.

GASPARINI, L., RACCHI, M., BENUSSI, L., CURTI, D., BINETTI, G., BIANCHETTI, A., TRABUCCHI, M. & GOVONI, S. 1997. Effect of energy shortage and oxidative stress on amyloid precursor protein metabolism in COS cells. *Neurosci Lett,* 231**,** 113-7.

GAUTHIER, S., REISBERG, B., ZAUDIG, M., PETERSEN, R. C., RITCHIE, K., BROICH, K., BELLEVILLE, S., BRODATY, H., BENNETT, D., CHERTKOW, H., CUMMINGS, J. L., DE LEON, M., FELDMAN, H., GANGULI, M., HAMPEL, H., SCHELTENS, P., TIERNEY, M. C., WHITEHOUSE, P. & WINBLAD, B. 2006. Mild cognitive impairment. *Lancet,* 367**,** 1262-70.

GEGELASHVILI, M., RODRIGUEZ-KERN, A., SUNG, L., SHIMAMOTO, K. & GEGELASHVILI, G. 2007. Glutamate transporter GLAST/EAAT1 directs cell surface expression of FXYD2/gamma subunit of Na, K-ATPase in human fetal astrocytes. *Neurochem Int,* 50**,** 916-20.

GERHART, D. Z., ENERSON, B. E., ZHDANKINA, O. Y., LEINO, R. L. & DREWES, L. R. 1997. Expression of monocarboxylate transporter MCT1 by brain endothelium and glia in adult and suckling rats. *Am J Physiol,* 273**,** E207-13.

GERICKE, G. S. 2006. Reactive oxygen species and related haem pathway components as possible epigenetic modifiers in neurobehavioural pathology. *Med Hypotheses,* 66**,** 92-9.

GIACOBINI, E. 2003. Cholinergic function and Alzheimer's disease. *Int J Geriatr Psychiatry,* 18**,** S1-5.

GIANOTTI, C., NUNZI, M. G., GISPEN, W. H. & CORRADETTI, R. 1992. Phosphorylation of the presynaptic protein B-50 (GAP-43) is increased during electrically induced long-term potentiation. *Neuron,* 8**,** 843-8.

GIAUME, C., KOULAKOFF, A., ROUX, L., HOLCMAN, D. & ROUACH, N. 2010. Astroglial networks: a step further in neuroglial and gliovascular interactions. *Nat Rev Neurosci,* 11**,** 87-99.

GIBSON, G. E., HAROUTUNIAN, V., ZHANG, H., PARK, L. C., SHI, Q., LESSER, M., MOHS, R. C., SHEU, R. K. & BLASS, J. P. 2000. Mitochondrial damage in Alzheimer's disease varies with apolipoprotein E genotype. *Ann Neurol,* 48**,** 297-303.

GIBSON, G. E., PARK, L. C., ZHANG, H., SORBI, S. & CALINGASAN, N. Y. 1999. Oxidative stress and a key metabolic enzyme in Alzheimer brains, cultured cells, and an animal model of chronic oxidative deficits. *Ann N Y Acad Sci,* 893**,** 79-94.

GIBSON, G. E., SHEU, K. F. & BLASS, J. P. 1998. Abnormalities of mitochondrial enzymes in Alzheimer disease. *J Neural Transm,* 105**,** 855-70.

GLENNER, G. G. & WONG, C. W. 1984. Alzheimer's disease: initial report of the purification and characterization of a novel cerebrovascular amyloid protein. *Biochem Biophys Res Commun,* 120**,** 885-90.

GOLANSKA, E., SIERUTA, M., GRESNER, S. M., HULAS-BIGOSZEWSKA, K., CORDER, E. H., STYCZYNSKA, M., PEPLONSKA, B., BARCIKOWSKA, M. & LIBERSKI, P. P. 2008. Analysis of APBB2 gene polymorphisms in sporadic Alzheimer's disease. *Neurosci Lett,* 447**,** 164-6.

GOLDBERG, I. J., SOPRANO, D. R., WYATT, M. L., VANNI, T. M., KIRCHGESSNER, T. G. & SCHOTZ, M. C. 1989. Localization of lipoprotein lipase mRNA in selected rat tissues. *J Lipid Res,* 30**,** 1569-77.

GONG, Y., CHANG, L., VIOLA, K. L., LACOR, P. N., LAMBERT, M. P., FINCH, C. E., KRAFFT, G. A. & KLEIN, W. L. 2003. Alzheimer's disease-affected brain: presence of oligomeric A beta ligands (ADDLs) suggests a molecular basis for reversible memory loss. *Proc Natl Acad Sci U S A,* 100**,** 10417-22.

GORDON, G. R., CHOI, H. B., RUNGTA, R. L., ELLIS-DAVIES, G. C. & MACVICAR, B. A. 2008. Brain metabolism dictates the polarity of astrocyte control over arterioles. *Nature,* 456**,** 745-9.

GOTZ, J., CHEN, F., VAN DORPE, J. & NITSCH, R. M. 2001. Formation of Neurofibrillary Tangles in P301L Tau Transgenic Mice Induced by Abeta 42 Fibrils. *Science,* 293**,** 1491-1495.

GOURAS, G. K., TSAI, J., NASLUND, J., VINCENT, B., EDGAR, M., CHECLER, F., GREENFIELD, J. P., HAROUTUNIAN, V., BUXBAUM, J. D., XU, H., GREENGARD, P. & RELKIN, N. R. 2000. Intraneuronal Abeta42 accumulation in human brain. *Am J Pathol,* 156**,** 15-20.

GREENE, A. E., TODOROVA, M. T. & SEYFRIED, T. N. 2003. Perspectives on the metabolic management of epilepsy through dietary reduction of glucose and elevation of ketone bodies. *J Neurochem,* 86**,** 529-37.

GREIG, N. H., LAHIRI, D. K. & SAMBAMURTI, K. 2002. Butyrylcholinesterase: an important new target in Alzheimer's disease therapy. *Int Psychogeriatr,* 14 Suppl 1**,** 77-91.

GRUETTER, R. 2003. Glycogen: the forgotten cerebral energy store. *J Neurosci Res,* 74**,** 179-83.

GRUNDKE-IQBAL, I., IQBAL, K., QUINLAN, M., TUNG, Y. C., ZAIDI, M. S. & WISNIEWSKI, H. M. 1986. Microtubule-associated protein tau. A component of Alzheimer paired helical filaments. *J Biol Chem,* 261**,** 6084-9.

GU, Y., MISONOU, H., SATO, T., DOHMAE, N., TAKIO, K. & IHARA, Y. 2001. Distinct intramembrane cleavage of the beta-amyloid precursor protein family resembling gamma-secretase-like cleavage of Notch. *J Biol Chem,* 276**,** 35235-8.

GUO, X., WU, X., REN, L., LIU, G. & LI, L. 2011. Epigenetic mechanisms of amyloid-beta production in anisomycin-treated SH-SY5Y cells. *Neuroscience,* 194**,** 272-81.

HA, H. C. 2004. Defective transcription factor activation for proinflammatory gene expression in poly(ADP-ribose) polymerase 1-deficient glia. *Proc Natl Acad Sci U S A,* 101**,** 5087-92.

HA, H. C. & SNYDER, S. H. 1999. Poly(ADP-ribose) polymerase is a mediator of necrotic cell death by ATP depletion. *Proc Natl Acad Sci U S A,* 96**,** 13978-82.

HAASS, C. 2004. Take five--BACE and the gamma-secretase quartet conduct Alzheimer's amyloid beta-peptide generation. *EMBO J,* 23**,** 483-8.

HAASS, C., HUNG, A. Y., SCHLOSSMACHER, M. G., OLTERSDORF, T., TEPLOW, D. B. & SELKOE, D. J. 1993a. Normal cellular processing of the beta-amyloid precursor protein results in the secretion of the amyloid beta peptide and related molecules. *Ann N Y Acad Sci,* 695**,** 109-16.

HAASS, C., HUNG, A. Y., SCHLOSSMACHER, M. G., TEPLOW, D. B. & SELKOE, D. J. 1993b. beta-Amyloid peptide and a 3-kDa fragment are derived by distinct cellular mechanisms. *J Biol Chem,* 268**,** 3021-4.

HAASS, C., HUNG, A. Y. & SELKOE, D. J. 1991. Processing of beta-amyloid precursor protein in microglia and astrocytes favors an internal localization over constitutive secretion. *J Neurosci,* 11**,** 3783-93.

HAASS, C., KAETHER, C., THINAKARAN, G. & SISODIA, S. 2012. Trafficking and proteolytic processing of APP. *Cold Spring Harb Perspect Med,* 2**,** a006270.

HAASS, C., KOO, E. H., TEPLOW, D. B. & SELKOE, D. J. 1994. Polarized secretion of beta-amyloid precursor protein and amyloid beta-peptide in MDCK cells. *Proc Natl Acad Sci U S A,* 91**,** 1564-8.

HAASS, C., SCHLOSSMACHER, M. G., HUNG, A. Y., VIGO-PELFREY, C., MELLON, A., OSTASZEWSKI, B. L., LIEBERBURG, I., KOO, E. H., SCHENK, D., TEPLOW, D. B. & ET AL. 1992. Amyloid beta-peptide is produced by cultured cells during normal metabolism. *Nature,* 359**,** 322-5.

HAASS, C. & SELKOE, D. J. 2007. Soluble protein oligomers in neurodegeneration: lessons from the Alzheimer's amyloid beta-peptide. *Nat Rev Mol Cell Biol,* 8**,** 101-12.

HALLIWELL, B. 1992. Reactive oxygen species and the central nervous system. *J Neurochem,* 59**,** 1609-23.

HAMEL, F. G., MAHONEY, M. J. & DUCKWORTH, W. C. 1991. Degradation of intraendosomal insulin by insulin-degrading enzyme without acidification. *Diabetes,* 40**,** 436-43.

HAN, D., ANTUNES, F., CANALI, R., RETTORI, D. & CADENAS, E. 2003a. Voltage-dependent anion channels control the release of the superoxide anion from mitochondria to cytosol. *J Biol Chem,* 278**,** 5557-63.

HAN, D., CANALI, R., RETTORI, D. & KAPLOWITZ, N. 2003b. Effect of glutathione depletion on sites and topology of superoxide and hydrogen peroxide production in mitochondria. *Mol Pharmacol,* 64**,** 1136-44.

HAN, D., HANAWA, N., SABERI, B. & KAPLOWITZ, N. 2006. Mechanisms of liver injury. III. Role of glutathione redox status in liver injury. *Am J Physiol Gastrointest Liver Physiol,* 291**,** G1-7.

HAN, D., WILLIAMS, E. & CADENAS, E. 2001. Mitochondrial respiratory chain-dependent generation of superoxide anion and its release into the intermembrane space. *Biochem J,* 353**,** 411-6.

HAN, D., YBANEZ, M. D., AHMADI, S., YEH, K. & KAPLOWITZ, N. 2009. Redox regulation of tumor necrosis factor signaling. *Antioxid Redox Signal,* 11**,** 2245-63.

HANISCH, U. K. & KETTENMANN, H. 2007. Microglia: active sensor and versatile effector cells in the normal and pathologic brain. *Nat Neurosci,* 10**,** 1387-94.

HANSSON PETERSEN, C. A., ALIKHANI, N., BEHBAHANI, H., WIEHAGER, B., PAVLOV, P. F., ALAFUZOFF, I., LEINONEN, V., ITO, A., WINBLAD, B., GLASER, E. & ANKARCRONA, M. 2008. The amyloid beta-peptide is imported into mitochondria via the TOM import machinery and localized to mitochondrial cristae. *Proc Natl Acad Sci U S A,* 105**,** 13145-50.

HARA, M., MATSUDA, Y., HIRAI, K., OKUMURA, N. & NAKAGAWA, H. 1989. Characteristics of glucose transport in neuronal cells and astrocytes from rat brain in primary culture. *J Neurochem,* 52**,** 902-8.

HARDY, J. & ALLSOP, D. 1991. Amyloid deposition as the central event in the aetiology of Alzheimer's disease. *Trends Pharmacol Sci,* 12**,** 383-8.

HARGUS, G., COOPER, O., DELEIDI, M., LEVY, A., LEE, K., MARLOW, E., YOW, A., SOLDNER, F., HOCKEMEYER, D., HALLETT, P. J., OSBORN, T., JAENISCH, R. & ISACSON, O. 2010. Differentiated Parkinson patient-derived induced pluripotent stem cells grow in the adult rodent brain and reduce motor asymmetry in Parkinsonian rats. *Proc Natl Acad Sci U S A,* 107**,** 15921-6.

HAROLD, D., ABRAHAM, R., HOLLINGWORTH, P., SIMS, R., GERRISH, A., HAMSHERE, M. L., PAHWA, J. S., MOSKVINA, V., DOWZELL, K., WILLIAMS, A., JONES, N., THOMAS, C., STRETTON, A., MORGAN, A. R., LOVESTONE, S., POWELL, J., PROITSI, P., LUPTON, M. K., BRAYNE, C., RUBINSZTEIN, D. C., GILL, M., LAWLOR, B., LYNCH, A., MORGAN, K., BROWN, K. S., PASSMORE, P. A., CRAIG, D., MCGUINNESS, B., TODD, S., HOLMES, C., MANN, D., SMITH, A. D., LOVE, S., KEHOE, P. G., HARDY, J., MEAD, S., FOX, N., ROSSOR, M., COLLINGE, J., MAIER, W., JESSEN, F., SCHURMANN, B., VAN DEN BUSSCHE, H., HEUSER, I., KORNHUBER, J., WILTFANG, J., DICHGANS, M., FROLICH, L., HAMPEL, H., HULL, M., RUJESCU, D., GOATE, A. M., KAUWE, J. S., CRUCHAGA, C., NOWOTNY, P., MORRIS, J. C., MAYO, K., SLEEGERS, K., BETTENS, K., ENGELBORGHS, S., DE DEYN, P. P., VAN BROECKHOVEN, C., LIVINGSTON, G., BASS, N. J., GURLING, H., MCQUILLIN, A., GWILLIAM, R., DELOUKAS, P., AL-CHALABI, A., SHAW, C. E., TSOLAKI, M., SINGLETON, A. B., GUERREIRO, R., MUHLEISEN, T. W., NOTHEN, M. M., MOEBUS, S., JOCKEL, K. H., KLOPP, N., WICHMANN, H. E., CARRASQUILLO, M. M., PANKRATZ, V. S., YOUNKIN, S. G., HOLMANS, P. A., O'DONOVAN, M., OWEN, M. J. & WILLIAMS, J. 2009. Genome-wide association study identifies variants at CLU and PICALM associated with Alzheimer's disease. *Nat Genet,* 41**,** 1088-93.

HARRIS, M. E., CARNEY, J. M., COLE, P. S., HENSLEY, K., HOWARD, B. J., MARTIN, L., BUMMER, P., WANG, Y., PEDIGO, N. W., JR. & BUTTERFIELD, D. A. 1995. beta-Amyloid peptide-derived, oxygen-dependent free radicals inhibit glutamate uptake in cultured astrocytes: implications for Alzheimer's disease. *Neuroreport,* 6**,** 1875-9.

HARRIS, M. E., WANG, Y., PEDIGO, N. W., JR., HENSLEY, K., BUTTERFIELD, D. A. & CARNEY, J. M. 1996. Amyloid beta peptide (25-35) inhibits Na+-dependent glutamate uptake in rat hippocampal astrocyte cultures. *J Neurochem,* 67**,** 277-86.

HARRY, G. J., BILLINGSLEY, M., BRUININK, A., CAMPBELL, I. L., CLASSEN, W., DORMAN, D. C., GALLI, C., RAY, D., SMITH, R. A. & TILSON, H. A. 1998. In vitro techniques for the assessment of neurotoxicity. *Environ Health Perspect,* 106 Suppl 1**,** 131-58.

HARTLEY, R. S., MARGULIS, M., FISHMAN, P. S., LEE, V. M. & TANG, C. M. 1999. Functional synapses are formed between human NTera2 (NT2N, hNT) neurons grown on astrocytes. *J Comp Neurol,* 407**,** 1-10.

HAXBY, J. V., GRADY, C. L., KOSS, E., HORWITZ, B., HESTON, L., SCHAPIRO, M., FRIEDLAND, R. P. & RAPOPORT, S. I. 1990. Longitudinal study of cerebral metabolic asymmetries and associated neuropsychological patterns in early dementia of the Alzheimer type. *Arch Neurol,* 47**,** 753-60.

HE, X. Y., SCHULZ, H. & YANG, S. Y. 1998. A human brain L-3-hydroxyacyl-coenzyme A dehydrogenase is identical to an amyloid beta-peptide-binding protein involved in Alzheimer's disease. *J Biol Chem,* 273**,** 10741-6.

HELLSTRAND, E., BOLAND, B., WALSH, D. M. & LINSE, S. 2010a. Amyloid beta-Protein Aggregation Produces Highly Reproducible Kinetic Data and Occurs by a Two-Phase Process. *ACS Chem Neurosci,* 1**,** 13-8.

HELLSTRAND, E., SPARR, E. & LINSE, S. 2010b. Retardation of Abeta fibril formation by phospholipid vesicles depends on membrane phase behavior. *Biophys J,* 98**,** 2206-14.

HENDERSON, S. T. 2008. Ketone bodies as a therapeutic for Alzheimer's disease. *Neurotherapeutics,* 5**,** 470-80.

HERHOLZ, K., NORDBERG, A., SALMON, E., PERANI, D., KESSLER, J., MIELKE, R., HALBER, M., JELIC, V., ALMKVIST, O., COLLETTE, F., ALBERONI, M., KENNEDY, A., HASSELBALCH, S., FAZIO, F. & HEISS, W. D. 1999. Impairment of neocortical metabolism predicts progression in Alzheimer's disease. *Dement Geriatr Cogn Disord,* 10**,** 494-504.

HERHOLZ, K., SALMON, E., PERANI, D., BARON, J. C., HOLTHOFF, V., FROLICH, L., SCHONKNECHT, P., ITO, K., MIELKE, R., KALBE, E., ZUNDORF, G., DELBEUCK,

X., PELATI, O., ANCHISI, D., FAZIO, F., KERROUCHE, N., DESGRANGES, B., EUSTACHE, F., BEUTHIEN-BAUMANN, B., MENZEL, C., SCHRODER, J., KATO, T., ARAHATA, Y., HENZE, M. & HEISS, W. D. 2002. Discrimination between Alzheimer dementia and controls by automated analysis of multicenter FDG PET. *Neuroimage,* 17**,** 302-16.

HERRERO-MENDEZ, A., ALMEIDA, A., FERNANDEZ, E., MAESTRE, C., MONCADA, S. & BOLANOS, J. P. 2009. The bioenergetic and antioxidant status of neurons is controlled by continuous degradation of a key glycolytic enzyme by APC/C-Cdh1. *Nat Cell Biol,* 11**,** 747-52.

HERSH, L. B. & RODGERS, D. W. 2008. Neprilysin and amyloid beta peptide degradation. *Curr Alzheimer Res,* 5**,** 225-31.

HILL, E. J., JIMENEZ-GONZALEZ, C., TARCZYLUK, M., NAGEL, D. A., COLEMAN, M. D. & PARRI, H. R. 2012. NT2 derived neuronal and astrocytic network signalling. *PLoS One,* 7**,** e36098.

HITOMI, J., KATAYAMA, T., EGUCHI, Y., KUDO, T., TANIGUCHI, M., KOYAMA, Y., MANABE, T., YAMAGISHI, S., BANDO, Y., IMAIZUMI, K., TSUJIMOTO, Y. & TOHYAMA, M. 2004. Involvement of caspase-4 in endoplasmic reticulum stress-induced apoptosis and Abeta-induced cell death. *J Cell Biol,* 165**,** 347-56.

HOF, P. R., PASCALE, E. & MAGISTRETTI, P. J. 1988. K+ at concentrations reached in the extracellular space during neuronal activity promotes a Ca2+-dependent glycogen hydrolysis in mouse cerebral cortex. *J Neurosci,* 8**,** 1922-8.

HOLLINGWORTH, P., SWEET, R., SIMS, R., HAROLD, D., RUSSO, G., ABRAHAM, R., STRETTON, A., JONES, N., GERRISH, A., CHAPMAN, J., IVANOV, D., MOSKVINA, V., LOVESTONE, S., PRIOTSI, P., LUPTON, M., BRAYNE, C., GILL, M., LAWLOR, B., LYNCH, A., CRAIG, D., MCGUINNESS, B., JOHNSTON, J., HOLMES, C., LIVINGSTON, G., BASS, N. J., GURLING, H., MCQUILLIN, A., HOLMANS, P., JONES, L., DEVLIN, B., KLEI, L., BARMADA, M. M., DEMIRCI, F. Y., DEKOSKY, S. T., LOPEZ, O. L., PASSMORE, P., OWEN, M. J., O'DONOVAN, M. C., MAYEUX, R., KAMBOH, M. I. & WILLIAMS, J. 2012. Genome-wide association study of Alzheimer's disease with psychotic symptoms. *Mol Psychiatry,* 17**,** 1316-27.

HOLTZMAN, D. M., HERZ, J. & BU, G. 2012. Apolipoprotein E and apolipoprotein E receptors: normal biology and roles in Alzheimer disease. *Cold Spring Harb Perspect Med,* 2**,** a006312.

HONG, L., KO, H. W., GWAG, B. J., JOE, E., LEE, S., KIM, Y. T. & SUH, Y. H. 1998. The cDNA cloning and ontogeny of mouse alpha-synuclein. *Neuroreport,* 9**,** 1239-43.

HONG, L., KOELSCH, G., LIN, X., WU, S., TERZYAN, S., GHOSH, A. K., ZHANG, X. C. & TANG, J. 2000. Structure of the protease domain of memapsin 2 (beta-secretase) complexed with inhibitor. *Science,* 290**,** 150-3.

HONG, M. & LEE, V. M. 1997. Insulin and insulin-like growth factor-1 regulate tau phosphorylation in cultured human neurons. *J Biol Chem,* 272**,** 19547-53.

HOOPER, C., KILLICK, R. & LOVESTONE, S. 2008. The GSK3 hypothesis of Alzheimer's disease. *J Neurochem,* 104**,** 1433-9.

HOOPER, C., MARKEVICH, V., PLATTNER, F., KILLICK, R., SCHOFIELD, E., ENGEL, T., HERNANDEZ, F., ANDERTON, B., ROSENBLUM, K., BLISS, T., COOKE, S. F., AVILA, J., LUCAS, J. J., GIESE, K. P., STEPHENSON, J. & LOVESTONE, S. 2007. Glycogen synthase kinase-3 inhibition is integral to long-term potentiation. *Eur J Neurosci,* 25**,** 81-6.

HOOZEMANS, J. J., VAN HAASTERT, E. S., NIJHOLT, D. A., ROZEMULLER, A. J., EIKELENBOOM, P. & SCHEPER, W. 2009. The unfolded protein response is activated in pretangle neurons in Alzheimer's disease hippocampus. *Am J Pathol,* 174**,** 1241-51.

HORBINSKI, C. & CHU, C. T. 2005. Kinase signaling cascades in the mitochondrion: a matter of life or death. *Free Radic Biol Med,* 38**,** 2-11.

HOSAKA, S., SUZUKI, M. S. & SATO, H. 1980. Effects of cytochalasin B and colchicine on the motility and growth of Yoshida sarcoma cells in vitro. *Sci Rep Res Inst Tohoku Univ Med,* 27**,** 27-31.

HU, N. W., KLYUBIN, I., ANWYL, R. & ROWAN, M. J. 2009. GluN2B subunit-containing NMDA receptor antagonists prevent Abeta-mediated synaptic plasticity disruption in vivo. *Proc Natl Acad Sci U S A,* 106**,** 20504-9.

270

HUANG, H. C. & JIANG, Z. F. 2009. Accumulated amyloid-beta peptide and hyperphosphorylated tau protein: relationship and links in Alzheimer's disease. *J Alzheimers Dis,* 16**,** 15-27.

HUANG, H. M., CHEN, H. L., XU, H. & GIBSON, G. E. 2005. Modification of endoplasmic reticulum Ca2+ stores by select oxidants produces changes reminiscent of those in cells from patients with Alzheimer disease. *Free Radic Biol Med,* 39**,** 979-89.

HUANG, S. M., MOURI, A., KOKUBO, H., NAKAJIMA, R., SUEMOTO, T., HIGUCHI, M., STAUFENBIEL, M., NODA, Y., YAMAGUCHI, H., NABESHIMA, T., SAIDO, T. C. & IWATA, N. 2006. Neprilysin-sensitive synapse-associated amyloid-beta peptide oligomers impair neuronal plasticity and cognitive function. *J Biol Chem,* 281**,** 17941-51.

HUANG, X., ATWOOD, C. S., HARTSHORN, M. A., MULTHAUP, G., GOLDSTEIN, L. E., SCARPA, R. C., CUAJUNGCO, M. P., GRAY, D. N., LIM, J., MOIR, R. D., TANZI, R. E. & BUSH, A. I. 1999. The A beta peptide of Alzheimer's disease directly produces hydrogen peroxide through metal ion reduction. *Biochemistry,* 38**,** 7609-16.

HUGHES, R. N. 2003. Effects of glucose on responsiveness to change in young adult and middle-aged rats. *Physiol Behav,* 78**,** 529-34.

HUGHES, S. R., KHORKOVA, O., GOYAL, S., KNAEBLEIN, J., HEROUX, J., RIEDEL, N. G. & SAHASRABUDHE, S. 1998. Alpha2-macroglobulin associates with beta-amyloid peptide and prevents fibril formation. *Proc Natl Acad Sci U S A,* 95**,** 3275-80.

HUNG, A. Y. & SELKOE, D. J. 1994. Selective ectodomain phosphorylation and regulated cleavage of beta-amyloid precursor protein. *EMBO J,* 13**,** 534-42.

HURD, T. R., COSTA, N. J., DAHM, C. C., BEER, S. M., BROWN, S. E., FILIPOVSKA, A. & MURPHY, M. P. 2005. Glutathionylation of mitochondrial proteins. *Antioxid Redox Signal,* 7**,** 999-1010.

HYDEN, H. & LANGE, P. W. 1962. A kinetic study of the neuronglia relationship. *J Cell Biol,* 13**,** 233-7.

HYND, M. R., SCOTT, H. L. & DODD, P. R. 2004. Glutamate-mediated excitotoxicity and neurodegeneration in Alzheimer's disease. *Neurochem Int,* 45**,** 583-95.

IDE, T., STEINKE, J. & CAHILL, G. F., JR. 1969. Metabolic interactions of glucose, lactate, and beta-hydroxybutyrate in rat brain slices. *Am J Physiol,* 217**,** 784-92.

INARREA, P., MOINI, H., RETTORI, D., HAN, D., MARTINEZ, J., GARCIA, I., FERNANDEZ-VIZARRA, E., ITURRALDE, M. & CADENAS, E. 2005. Redox activation of mitochondrial intermembrane space Cu,Zn-superoxide dismutase. *Biochem J,* 387**,** 203-9.

INOUE, H. 2010. Neurodegenerative disease-specific induced pluripotent stem cell research. *Exp Cell Res,* 316**,** 2560-4.

INTERNATIONAL, A. S. D. 2009. World Alzheimer Report. *In:* PRINCE, M. & JACKSON, J. (eds.). Alzheimer's Disease International.

ISAAC, J. T., ASHBY, M. C. & MCBAIN, C. J. 2007. The role of the GluR2 subunit in AMPA receptor function and synaptic plasticity. *Neuron,* 54**,** 859-71.

ISHIGURO, K., SHIRATSUCHI, A., SATO, S., OMORI, A., ARIOKA, M., KOBAYASHI, S., UCHIDA, T. & IMAHORI, K. 1993. Glycogen synthase kinase 3 beta is identical to tau protein kinase I generating several epitopes of paired helical filaments. *FEBS Lett,* 325**,** 167-72.

ISRAEL, M. A. & GOLDSTEIN, L. S. 2011. Capturing Alzheimer's disease genomes with induced pluripotent stem cells: prospects and challenges. *Genome Med,* 3**,** 49.

ISRAEL, M. A., YUAN, S. H., BARDY, C., REYNA, S. M., MU, Y., HERRERA, C., HEFFERAN, M. P., VAN GORP, S., NAZOR, K. L., BOSCOLO, F. S., CARSON, C. T., LAURENT, L. C., MARSALA, M., GAGE, F. H., REMES, A. M., KOO, E. H. & GOLDSTEIN, L. S. 2012. Probing sporadic and familial Alzheimer's disease using induced pluripotent stem cells. *Nature,* 482**,** 216-20.

IVANOV, A., MUKHTAROV, M., BREGESTOVSKI, P. & ZILBERTER, Y. 2011. Lactate Effectively Covers Energy Demands during Neuronal Network Activity in Neonatal Hippocampal Slices. *Front Neuroenergetics,* 3**,** 2.

IWAI, A., MASLIAH, E., SUNDSMO, M. P., DETERESA, R., MALLORY, M., SALMON, D. P. & SAITOH, T. 1996. The synaptic protein NACP is abnormally expressed during the progression of Alzheimer's disease. *Brain Res,* 720**,** 230-4.

IWATA, N., MIZUKAMI, H., SHIROTANI, K., TAKAKI, Y., MURAMATSU, S., LU, B., GERARD, N. P., GERARD, C., OZAWA, K. & SAIDO, T. C. 2004. Presynaptic

localization of neprilysin contributes to efficient clearance of amyloid-beta peptide in mouse brain. *J Neurosci,* 24**,** 991-8.

IWATA, N., TSUBUKI, S., TAKAKI, Y., SHIROTANI, K., LU, B., GERARD, N. P., GERARD, C., HAMA, E., LEE, H. J. & SAIDO, T. C. 2001. Metabolic regulation of brain Abeta by neprilysin. *Science,* 292**,** 1550-2.

JACOBSEN, J. S., WU, C. C., REDWINE, J. M., COMERY, T. A., ARIAS, R., BOWLBY, M., MARTONE, R., MORRISON, J. H., PANGALOS, M. N., REINHART, P. H. & BLOOM, F. E. 2006. Early-onset behavioral and synaptic deficits in a mouse model of Alzheimer's disease. *Proc Natl Acad Sci U S A,* 103**,** 5161-6.

JAGUST, W., GITCHO, A., SUN, F., KUCZYNSKI, B., MUNGAS, D. & HAAN, M. 2006. Brain imaging evidence of preclinical Alzheimer's disease in normal aging. *Ann Neurol,* 59**,** 673-81.

JIANG, D., LI, X., LIU, L., YAGNIK, G. B. & ZHOU, F. 2010. Reaction rates and mechanism of the ascorbic acid oxidation by molecular oxygen facilitated by Cu(II)-containing amyloid-beta complexes and aggregates. *J Phys Chem B,* 114**,** 4896-903.

JIANG, D., LI, X., WILLIAMS, R., PATEL, S., MEN, L., WANG, Y. & ZHOU, F. 2009. Ternary complexes of iron, amyloid-beta, and nitrilotriacetic acid: binding affinities, redox properties, and relevance to iron-induced oxidative stress in Alzheimer's disease. *Biochemistry,* 48**,** 7939-47.

JIN, M., SHEPARDSON, N., YANG, T., CHEN, G., WALSH, D. & SELKOE, D. J. 2011. Soluble amyloid beta-protein dimers isolated from Alzheimer cortex directly induce Tau hyperphosphorylation and neuritic degeneration. *Proc Natl Acad Sci U S A,* 108**,** 5819-24.

JOHNSTONE, E. M., CHANEY, M. O., NORRIS, F. H., PASCUAL, R. & LITTLE, S. P. 1991. Conservation of the sequence of the Alzheimer's disease amyloid peptide in dog, polar bear and five other mammals by cross-species polymerase chain reaction analysis. *Molecular Brain Research,* 10**,** 299-305.

JOLIVALT, C. G., LEE, C. A., BEISWENGER, K. K., SMITH, J. L., ORLOV, M., TORRANCE, M. A. & MASLIAH, E. 2008. Defective insulin signaling pathway and increased glycogen synthase kinase-3 activity in the brain of diabetic mice: parallels with Alzheimer's disease and correction by insulin. *J Neurosci Res,* 86**,** 3265-74.

JONES, D. P., MODY, V. C., JR., CARLSON, J. L., LYNN, M. J. & STERNBERG, P., JR. 2002. Redox analysis of human plasma allows separation of pro-oxidant events of aging from decline in antioxidant defenses. *Free Radic Biol Med,* 33**,** 1290-300.

JOPE, R. S. & JOHNSON, G. V. 2004. The glamour and gloom of glycogen synthase kinase-3. *Trends Biochem Sci,* 29**,** 95-102.

JUN, S., GILLESPIE, J. R., SHIN, B. K. & SAXENA, S. 2009. The second Cu(II)-binding site in a proton-rich environment interferes with the aggregation of amyloid-beta(1-40) into amyloid fibrils. *Biochemistry,* 48**,** 10724-32.

KAEBERLEIN, M., MCVEY, M. & GUARENTE, L. 1999. The SIR2/3/4 complex and SIR2 alone promote longevity in Saccharomyces cerevisiae by two different mechanisms. *Genes Dev,* 13**,** 2570-80.

KAETHER, C., HAASS, C. & STEINER, H. 2006. Assembly, trafficking and function of gamma-secretase. *Neurodegener Dis,* 3**,** 275-83.

KAJIWARA, Y., AKRAM, A., KATSEL, P., HAROUTUNIAN, V., SCHMEIDLER, J., BEECHAM, G., HAINES, J. L., PERICAK-VANCE, M. A. & BUXBAUM, J. D. 2009. FE65 binds Teashirt, inhibiting expression of the primate-specific caspase-4. *PLoS One,* 4**,** e5071.

KANEMITSU, H., TOMIYAMA, T. & MORI, H. 2003. Human neprilysin is capable of degrading amyloid beta peptide not only in the monomeric form but also the pathological oligomeric form. *Neurosci Lett,* 350**,** 113-6.

KARUMBAYARAM, S., NOVITCH, B. G., PATTERSON, M., UMBACH, J. A., RICHTER, L., LINDGREN, A., CONWAY, A. E., CLARK, A. T., GOLDMAN, S. A., PLATH, K., WIEDAU-PAZOS, M., KORNBLUM, H. I. & LOWRY, W. E. 2009. Directed differentiation of human-induced pluripotent stem cells generates active motor neurons. *Stem Cells,* 27**,** 806-11.

KASISCHKE, K. A., VISHWASRAO, H. D., FISHER, P. J., ZIPFEL, W. R. & WEBB, W. W. 2004. Neural activity triggers neuronal oxidative metabolism followed by astrocytic glycolysis. *Science,* 305**,** 99-103.

272

KATAYAMA, T., IMAIZUMI, K., MANABE, T., HITOMI, J., KUDO, T. & TOHYAMA, M. 2004. Induction of neuronal death by ER stress in Alzheimer's disease. *J Chem Neuroanat,* 28**,** 67-78.

KAYED, R., PENSALFINI, A., MARGOL, L., SOKOLOV, Y., SARSOZA, F., HEAD, E., HALL, J. & GLABE, C. 2009. Annular protofibrils are a structurally and functionally distinct type of amyloid oligomer. *J Biol Chem,* 284**,** 4230-7.

KENNEDY, A. M., FRACKOWIAK, R. S., NEWMAN, S. K., BLOOMFIELD, P. M., SEAWARD, J., ROQUES, P., LEWINGTON, G., CUNNINGHAM, V. J. & ROSSOR, M. N. 1995. Deficits in cerebral glucose metabolism demonstrated by positron emission tomography in individuals at risk of familial Alzheimer's disease. *Neurosci Lett,* 186**,** 17-20.

KHAN, S. M., CASSARINO, D. S., ABRAMOVA, N. N., KEENEY, P. M., BORLAND, M. K., TRIMMER, P. A., KREBS, C. T., BENNETT, J. C., PARKS, J. K., SWERDLOW, R. H., PARKER, W. D., JR. & BENNETT, J. P., JR. 2000. Alzheimer's disease cybrids replicate beta-amyloid abnormalities through cell death pathways. *Ann Neurol,* 48**,** 148-55.

KHVOTCHEV, M., LONART, G. & SUDHOF, T. C. 2000. Role of calcium in neurotransmitter release evoked by alpha-latrotoxin or hypertonic sucrose. *Neuroscience,* 101**,** 793-802.

KHVOTCHEV, M. & SUDHOF, T. C. 2004. Proteolytic processing of amyloid-beta precursor protein by secretases does not require cell surface transport. *J Biol Chem,* 279**,** 47101-8.

KIM, D. Y., CAREY, B. W., WANG, H., INGANO, L. A., BINSHTOK, A. M., WERTZ, M. H., PETTINGELL, W. H., HE, P., LEE, V. M., WOOLF, C. J. & KOVACS, D. M. 2007. BACE1 regulates voltage-gated sodium channels and neuronal activity. *Nat Cell Biol,* 9**,** 755-64.

KIM, H. J., CHAE, S. C., LEE, D. K., CHROMY, B., LEE, S. C., PARK, Y. C., KLEIN, W. L., KRAFFT, G. A. & HONG, S. T. 2003. Selective neuronal degeneration induced by soluble oligomeric amyloid beta protein. *FASEB J,* 17**,** 118-20.

KINS, S., LAUTHER, N., SZODORAI, A. & BEYREUTHER, K. 2006. Subcellular trafficking of the amyloid precursor protein gene family and its pathogenic role in Alzheimer's disease. *Neurodegener Dis,* 3**,** 218-26.

KIRKITADZE, M. D., BITAN, G. & TEPLOW, D. B. 2002. Paradigm shifts in Alzheimer's disease and other neurodegenerative disorders: the emerging role of oligomeric assemblies. *J Neurosci Res,* 69**,** 567-77.

KIRSCHNER, D. A., INOUYE, H., DUFFY, L. K., SINCLAIR, A., LIND, M. & SELKOE, D. J. 1987. Synthetic peptide homologous to beta protein from Alzheimer disease forms amyloid-like fibrils in vitro. *Proc Natl Acad Sci U S A,* 84**,** 6953-7.

KISH, S. J., BERGERON, C., RAJPUT, A., DOZIC, S., MASTROGIACOMO, F., CHANG, L. J., WILSON, J. M., DISTEFANO, L. M. & NOBREGA, J. N. 1992. Brain cytochrome oxidase in Alzheimer's disease. *J Neurochem,* 59**,** 776-9.

KLEGERIS, A. & MCGEER, P. L. 2001. Inflammatory cytokine levels are influenced by interactions between THP-1 monocytic, U-373 MG astrocytic, and SH-SY5Y neuronal cell lines of human origin. *Neurosci Lett,* 313**,** 41-4.

KLEGERIS, A. & MCGEER, P. L. 2005. Chymotrypsin-like proteases contribute to human monocytic THP-1 cell as well as human microglial neurotoxicity. *Glia,* 51**,** 56-64.

KNOBLOCH, M., FARINELLI, M., KONIETZKO, U., NITSCH, R. M. & MANSUY, I. M. 2007. Abeta oligomer-mediated long-term potentiation impairment involves protein phosphatase 1-dependent mechanisms. *J Neurosci,* 27**,** 7648-53.

KOCH, P., TAMBOLI, I. Y., MERTENS, J., WUNDERLICH, P., LADEWIG, J., STUBER, K., ESSELMANN, H., WILTFANG, J., BRUSTLE, O. & WALTER, J. 2012. Presenilin-1 L166P mutant human pluripotent stem cell-derived neurons exhibit partial loss of gamma-secretase activity in endogenous amyloid-beta generation. *Am J Pathol,* 180**,** 2404-16.

KOFFIE, R. M., MEYER-LUEHMANN, M., HASHIMOTO, T., ADAMS, K. W., MIELKE, M. L., GARCIA-ALLOZA, M., MICHEVA, K. D., SMITH, S. J., KIM, M. L., LEE, V. M., HYMAN, B. T. & SPIRES-JONES, T. L. 2009. Oligomeric amyloid beta associates with postsynaptic densities and correlates with excitatory synapse loss near senile plaques. *Proc Natl Acad Sci U S A,* 106**,** 4012-7.

KOO, E. H., LANSBURY, P. T., JR. & KELLY, J. W. 1999. Amyloid diseases: abnormal protein aggregation in neurodegeneration. *Proc Natl Acad Sci U S A,* 96**,** 9989-90.

KOO, E. H., SISODIA, S. S., ARCHER, D. R., MARTIN, L. J., WEIDEMANN, A., BEYREUTHER, K., FISCHER, P., MASTERS, C. L. & PRICE, D. L. 1990. Precursor of amyloid protein in Alzheimer disease undergoes fast anterograde axonal transport. *Proc Natl Acad Sci U S A,* 87**,** 1561-5.

KOVACS, D. M. 2000. alpha2-macroglobulin in late-onset Alzheimer's disease. *Exp Gerontol,* 35**,** 473-9.

KREMER, A., LOUIS, J. V., JAWORSKI, T. & VAN LEUVEN, F. 2011. GSK3 and Alzheimer's Disease: Facts and Fiction. *Front Mol Neurosci,* 4**,** 17.

KRONER, Z. 2009. The relationship between Alzheimer's disease and diabetes: Type 3 diabetes? *Altern Med Rev,* 14**,** 373-9.

KRUGER, R., KUHN, W., MULLER, T., WOITALLA, D., GRAEBER, M., KOSEL, S., PRZUNTEK, H., EPPLEN, J. T., SCHOLS, L. & RIESS, O. 1998. Ala30Pro mutation in the gene encoding alpha-synuclein in Parkinson's disease. *Nat Genet,* 18**,** 106-8.

KUHN, P. H., WANG, H., DISLICH, B., COLOMBO, A., ZEITSCHEL, U., ELLWART, J. W., KREMMER, E., ROSSNER, S. & LICHTENTHALER, S. F. 2010. ADAM10 is the physiologically relevant, constitutive alpha-secretase of the amyloid precursor protein in primary neurons. *EMBO J,* 29**,** 3020-32.

KUJOTH, G. C., LEEUWENBURGH, C. & PROLLA, T. A. 2006. Mitochondrial DNA mutations and apoptosis in mammalian aging. *Cancer Res,* 66**,** 7386-9.

KUO, W. L., GEHM, B. D., ROSNER, M. R., LI, W. & KELLER, G. 1994. Inducible expression and cellular localization of insulin-degrading enzyme in a stably transfected cell line. *J Biol Chem,* 269**,** 22599-606.

KUROCHKIN, I. V. 2001. Insulin-degrading enzyme: embarking on amyloid destruction. *Trends Biochem Sci,* 26**,** 421-5.

KURT, M. A., DAVIES, D. C. & KIDD, M. 1997. Paired helical filament morphology varies with intracellular location in Alzheimer's disease brain. *Neuroscience Letters,* 239**,** 41-44.

LAFERLA, F. M. 2002. Calcium dyshomeostasis and intracellular signalling in Alzheimer's disease. *Nat Rev Neurosci,* 3**,** 862-72.

LAFON-CAZAL, M., PIETRI, S., CULCASI, M. & BOCKAERT, J. 1993. NMDA-dependent superoxide production and neurotoxicity. *Nature,* 364**,** 535-7.

LAI, A., SISODIA, S. S. & TROWBRIDGE, I. S. 1995. Characterization of sorting signals in the beta-amyloid precursor protein cytoplasmic domain. *J Biol Chem,* 270**,** 3565-73.

LAMBERT, J. C., HEATH, S., EVEN, G., CAMPION, D., SLEEGERS, K., HILTUNEN, M., COMBARROS, O., ZELENIKA, D., BULLIDO, M. J., TAVERNIER, B., LETENNEUR, L., BETTENS, K., BERR, C., PASQUIER, F., FIEVET, N., BARBERGER-GATEAU, P., ENGELBORGHS, S., DE DEYN, P., MATEO, I., FRANCK, A., HELISALMI, S., PORCELLINI, E., HANON, O., DE PANCORBO, M. M., LENDON, C., DUFOUIL, C., JAILLARD, C., LEVEILLARD, T., ALVAREZ, V., BOSCO, P., MANCUSO, M., PANZA, F., NACMIAS, B., BOSSU, P., PICCARDI, P., ANNONI, G., SERIPA, D., GALIMBERTI, D., HANNEQUIN, D., LICASTRO, F., SOININEN, H., RITCHIE, K., BLANCHE, H., DARTIGUES, J. F., TZOURIO, C., GUT, I., VAN BROECKHOVEN, C., ALPEROVITCH, A., LATHROP, M. & AMOUYEL, P. 2009. Genome-wide association study identifies variants at CLU and CR1 associated with Alzheimer's disease. *Nat Genet,* 41**,** 1094-9.

LAMBERT, M. P., BARLOW, A. K., CHROMY, B. A., EDWARDS, C., FREED, R., LIOSATOS, M., MORGAN, T. E., ROZOVSKY, I., TROMMER, B., VIOLA, K. L., WALS, P., ZHANG, C., FINCH, C. E., KRAFFT, G. A. & KLEIN, W. L. 1998. Diffusible, nonfibrillar ligands derived from Abeta1-42 are potent central nervous system neurotoxins. *Proc Natl Acad Sci U S A,* 95**,** 6448-53.

LAUDERBACK, C. M., HACKETT, J. M., HUANG, F. F., KELLER, J. N., SZWEDA, L. I., MARKESBERY, W. R. & BUTTERFIELD, D. A. 2001. The glial glutamate transporter, GLT-1, is oxidatively modified by 4-hydroxy-2-nonenal in the Alzheimer's disease brain: the role of Abeta1-42. *J Neurochem,* 78**,** 413-6.

LAUER, D., REICHENBACH, A. & BIRKENMEIER, G. 2001. Alpha 2-macroglobulin-mediated degradation of amyloid beta 1--42: a mechanism to enhance amyloid beta catabolism. *Exp Neurol,* 167**,** 385-92.

LAUREN, J., GIMBEL, D. A., NYGAARD, H. B., GILBERT, J. W. & STRITTMATTER, S. M. 2009. Cellular prion protein mediates impairment of synaptic plasticity by amyloid-beta oligomers. *Nature,* 457**,** 1128-32.

LAURIJSSENS, B., AUJARD, F. & RAHMAN, A. 2012. Animal models of Alzheimer's disease and drug development. *Drug Discovery Today: Technologies*.

LE PRINCE, G., DELAERE, P., FAGES, C., LEFRANCOIS, T., TOURET, M., SALANON, M. & TARDY, M. 1995. Glutamine synthetase (GS) expression is reduced in senile dementia of the Alzheimer type. *Neurochem Res,* 20**,** 859-62.

LEE, H. C. 2001. Physiological functions of cyclic ADP-ribose and NAADP as calcium messengers. *Annu Rev Pharmacol Toxicol,* 41**,** 317-45.

LEE, M. K., GRAHAM, S. N. & GOLD, P. E. 1988. Memory enhancement with posttraining intraventricular glucose injections in rats. *Behav Neurosci,* 102**,** 591-5.

LEISSRING, M. A., FARRIS, W., CHANG, A. Y., WALSH, D. M., WU, X., SUN, X., FROSCH, M. P. & SELKOE, D. J. 2003. Enhanced proteolysis of beta-amyloid in APP transgenic mice prevents plaque formation, secondary pathology, and premature death. *Neuron,* 40**,** 1087-93.

LEISSRING, M. A., FARRIS, W., WU, X., CHRISTODOULOU, D. C., HAIGIS, M. C., GUARENTE, L. & SELKOE, D. J. 2004. Alternative translation initiation generates a novel isoform of insulin-degrading enzyme targeted to mitochondria. *Biochem J,* 383**,** 439-46.

LEMERE, C. A., LOPERA, F., KOSIK, K. S., LENDON, C. L., OSSA, J., SAIDO, T. C., YAMAGUCHI, H., RUIZ, A., MARTINEZ, A., MADRIGAL, L., HINCAPIE, L., ARANGO, J. C., ANTHONY, D. C., KOO, E. H., GOATE, A. M. & SELKOE, D. J. 1996. The E280A presenilin 1 Alzheimer mutation produces increased A beta 42 deposition and severe cerebellar pathology. *Nat Med,* 2**,** 1146-50.

LEMKUL, J. A. & BEVAN, D. R. 2009. Perturbation of membranes by the amyloid beta-peptide--a molecular dynamics study. *FEBS J,* 276**,** 3060-75.

LESNE, S., KOH, M. T., KOTILINEK, L., KAYED, R., GLABE, C. G., YANG, A., GALLAGHER, M. & ASHE, K. H. 2006. A specific amyloid-beta protein assembly in the brain impairs memory. *Nature,* 440**,** 352-7.

LEUNG, A. W. & HALESTRAP, A. P. 2008. Recent progress in elucidating the molecular mechanism of the mitochondrial permeability transition pore. *Biochim Biophys Acta,* 1777**,** 946-52.

LEVINE, H., 3RD 1993. Thioflavine T interaction with synthetic Alzheimer's disease beta-amyloid peptides: detection of amyloid aggregation in solution. *Protein Sci,* 2**,** 404-10.

LEVY, E., CARMAN, M. D., FERNANDEZ-MADRID, I. J., POWER, M. D., LIEBERBURG, I., VAN DUINEN, S. G., BOTS, G. T., LUYENDIJK, W. & FRANGIONE, B. 1990. Mutation of the Alzheimer's disease amyloid gene in hereditary cerebral hemorrhage, Dutch type. *Science,* 248**,** 1124-6.

LI, L., SENGUPTA, A., HAQUE, N., GRUNDKE-IQBAL, I. & IQBAL, K. 2004. Memantine inhibits and reverses the Alzheimer type abnormal hyperphosphorylation of tau and associated neurodegeneration. *FEBS Lett,* 566**,** 261-9.

LI, S., HONG, S., SHEPARDSON, N. E., WALSH, D. M., SHANKAR, G. M. & SELKOE, D. 2009. Soluble oligomers of amyloid Beta protein facilitate hippocampal long-term depression by disrupting neuronal glutamate uptake. *Neuron,* 62**,** 788-801.

LI, W., WU, Y., MIN, F., LI, Z., HUANG, J. & HUANG, R. 2010. A nonhuman primate model of Alzheimer's disease generated by intracranial injection of amyloid-beta42 and thiorphan. *Metab Brain Dis,* 25**,** 277-84.

LIGURI, G., TADDEI, N., NASSI, P., LATORRACA, S., NEDIANI, C. & SORBI, S. 1990. Changes in Na+,K(+)-ATPase, Ca2(+)-ATPase and some soluble enzymes related to energy metabolism in brains of patients with Alzheimer's disease. *Neurosci Lett,* 112**,** 338-42.

LIN, H., BHATIA, R. & LAL, R. 2001. Amyloid beta protein forms ion channels: implications for Alzheimer's disease pathophysiology. *FASEB J,* 15**,** 2433-44.

LIN, M. T. & BEAL, M. F. 2006. Mitochondrial dysfunction and oxidative stress in neurodegenerative diseases. *Nature,* 443**,** 787-95.

LIN, S. J. & GUARENTE, L. 2003. Nicotinamide adenine dinucleotide, a metabolic regulator of transcription, longevity and disease. *Curr Opin Cell Biol,* 15**,** 241-6.

LIPTON, S. A. 2006. Paradigm shift in neuroprotection by NMDA receptor blockade: memantine and beyond. *Nat Rev Drug Discov,* 5**,** 160-70.

LIU, G., HUANG, W., MOIR, R. D., VANDERBURG, C. R., LAI, B., PENG, Z., TANZI, R. E., ROGERS, J. T. & HUANG, X. 2006. Metal exposure and Alzheimer's pathogenesis. *J Struct Biol,* 155**,** 45-51.

LIU, H., WANG, H., SHENVI, S., HAGEN, T. M. & LIU, R. M. 2004. Glutathione metabolism during aging and in Alzheimer disease. *Ann N Y Acad Sci,* 1019**,** 346-9.

LIU, Q., HUANG, Y., XUE, F., SIMARD, A., DECHON, J., LI, G., ZHANG, J., LUCERO, L., WANG, M., SIERKS, M., HU, G., CHANG, Y., LUKAS, R. J. & WU, J. 2009. A novel nicotinic acetylcholine receptor subtype in basal forebrain cholinergic neurons with high sensitivity to amyloid peptides. *J Neurosci,* 29**,** 918-29.

LIU, Y., LIU, F., IQBAL, K., GRUNDKE-IQBAL, I. & GONG, C. X. 2008. Decreased glucose transporters correlate to abnormal hyperphosphorylation of tau in Alzheimer disease. *FEBS Lett,* 582**,** 359-64.

LOAIZA, A., PORRAS, O. H. & BARROS, L. F. 2003. Glutamate triggers rapid glucose transport stimulation in astrocytes as evidenced by real-time confocal microscopy. *J Neurosci,* 23**,** 7337-42.

LOGAN, W. J. & SNYDER, S. H. 1972. High affinity uptake systems for glycine, glutamic and aspaspartic acids in synaptosomes of rat central nervous tissues. *Brain Res,* 42**,** 413-31.

LOMBARD, D. B., TISHKOFF, D. X. & BAO, J. 2011. Mitochondrial sirtuins in the regulation of mitochondrial activity and metabolic adaptation. *Handb Exp Pharmacol,* 206**,** 163-88.

LÓPEZ SALON, M., MORELLI, L., CASTAÑO, E. M., SOTO, E. F. & PASQUINI, J. M. 2000. Defective ubiquitination of cerebral proteins in Alzheimer's disease. *Journal of Neuroscience Research,* 62**,** 302-310.

LOVATT, D., SONNEWALD, U., WAAGEPETERSEN, H. S., SCHOUSBOE, A., HE, W., LIN, J. H., HAN, X., TAKANO, T., WANG, S., SIM, F. J., GOLDMAN, S. A. & NEDERGAARD, M. 2007. The transcriptome and metabolic gene signature of protoplasmic astrocytes in the adult murine cortex. *J Neurosci,* 27**,** 12255-66.

LOVE, S., BARBER, R. & WILCOCK, G. K. 1999. Increased poly(ADP-ribosyl)ation of nuclear proteins in Alzheimer's disease. *Brain,* 122 (Pt 2)**,** 247-53.

LOVELL, M. A., XIONG, S., XIE, C., DAVIES, P. & MARKESBERY, W. R. 2004. Induction of hyperphosphorylated tau in primary rat cortical neuron cultures mediated by oxidative stress and glycogen synthase kinase-3. *J Alzheimers Dis,* 6**,** 659-71; discussion 673-81.

LOWRY, O. H., PASSONNEAU, J. V., HASSELBERGER, F. X. & SCHULZ, D. W. 1964. Effect of Ischemia on Known Substrates and Cofactors of the Glycolytic Pathway in Brain. *J Biol Chem,* 239**,** 18-30.

LUCAS, J. J., HERNANDEZ, F., GOMEZ-RAMOS, P., MORAN, M. A., HEN, R. & AVILA, J. 2001. Decreased nuclear beta-catenin, tau hyperphosphorylation and neurodegeneration in GSK-3beta conditional transgenic mice. *EMBO J,* 20**,** 27-39.

LUE, L.-F., KUO, Y.-M., ROHER, A. E., BRACHOVA, L., SHEN, Y., SUE, L., BEACH, T., KURTH, J. H., RYDEL, R. E. & ROGERS, J. 1999. Soluble Amyloid {beta} Peptide Concentration as a Predictor of Synaptic Change in Alzheimer's Disease. *Am J Pathol,* 155**,** 853-862.

LUO, J., NIKOLAEV, A. Y., IMAI, S., CHEN, D., SU, F., SHILOH, A., GUARENTE, L. & GU, W. 2001. Negative control of p53 by Sir2alpha promotes cell survival under stress. *Cell,* 107**,** 137-48.

LUSTBADER, J. W., CIRILLI, M., LIN, C., XU, H. W., TAKUMA, K., WANG, N., CASPERSEN, C., CHEN, X., POLLAK, S., CHANEY, M., TRINCHESE, F., LIU, S., GUNN-MOORE, F., LUE, L. F., WALKER, D. G., KUPPUSAMY, P., ZEWIER, Z. L., ARANCIO, O., STERN, D., YAN, S. S. & WU, H. 2004. ABAD directly links Abeta to mitochondrial toxicity in Alzheimer's disease. *Science,* 304**,** 448-52.

MACLEAN-FLETCHER, S. & POLLARD, T. D. 1980. Mechanism of action of cytochalasin B on actin. *Cell,* 20**,** 329-41.

MAEKAWA, F., TSUBOI, T., FUKUDA, M. & PELLERIN, L. 2009. Regulation of the intracellular distribution, cell surface expression, and protein levels of AMPA receptor GluR2 subunits by the monocarboxylate transporter MCT2 in neuronal cells. *J Neurochem,* 109**,** 1767-78.

MAGISTRETTI, P. J. 2009. Role of glutamate in neuron-glia metabolic coupling. *Am J Clin Nutr,* 90**,** 875S-880S.

MAGISTRETTI, P. J. & ALLAMAN, I. 2007. Glycogen: a Trojan horse for neurons. *Nat Neurosci,* 10**,** 1341-2.

MAGISTRETTI, P. J., HOF, P. R. & MARTIN, J. L. 1986. Adenosine stimulates glycogenolysis in mouse cerebral cortex: a possible coupling mechanism between neuronal activity and energy metabolism. *J Neurosci,* 6**,** 2558-62.

MAGISTRETTI, P. J., MORRISON, J. H., SHOEMAKER, W. J., SAPIN, V. & BLOOM, F. E. 1981. Vasoactive intestinal polypeptide induces glycogenolysis in mouse cortical slices: a possible regulatory mechanism for the local control of energy metabolism. *Proc Natl Acad Sci U S A,* 78**,** 6535-9.

MAGISTRETTI, P. J. & PELLERIN, L. 1996. Cellular bases of brain energy metabolism and their relevance to functional brain imaging: evidence for a prominent role of astrocytes. *Cereb Cortex,* 6**,** 50-61.

MALANGA, M. & ALTHAUS, F. R. 2005. The role of poly(ADP-ribose) in the DNA damage signaling network. *Biochem Cell Biol,* 83**,** 354-64.

MALANGA, M., PLESCHKE, J. M., KLECZKOWSKA, H. E. & ALTHAUS, F. R. 1998. Poly(ADP-ribose) binds to specific domains of p53 and alters its DNA binding functions. *J Biol Chem,* 273**,** 11839-43.

MANCZAK, M., ANEKONDA, T. S., HENSON, E., PARK, B. S., QUINN, J. & REDDY, P. H. 2006. Mitochondria are a direct site of A beta accumulation in Alzheimer's disease neurons: implications for free radical generation and oxidative damage in disease progression. *Hum Mol Genet,* 15**,** 1437-49.

MANCZAK, M., PARK, B. S., JUNG, Y. & REDDY, P. H. 2004. Differential expression of oxidative phosphorylation genes in patients with Alzheimer's disease: implications for early mitochondrial dysfunction and oxidative damage. *Neuromolecular Med,* 5**,** 147-62.

MANNING, C. A., RAGOZZINO, M. E. & GOLD, P. E. 1993. Glucose enhancement of memory in patients with probable senile dementia of the Alzheimer's type. *Neurobiol Aging,* 14**,** 523-8.

MAO, P. & REDDY, P. H. 2011. Aging and amyloid beta-induced oxidative DNA damage and mitochondrial dysfunction in Alzheimer's disease: implications for early intervention and therapeutics. *Biochim Biophys Acta,* 1812**,** 1359-70.

MARCINKIEWICZ, M. & SEIDAH, N. G. 2000. Coordinated expression of beta-amyloid precursor protein and the putative beta-secretase BACE and alpha-secretase ADAM10 in mouse and human brain. *J Neurochem,* 75**,** 2133-43.

MARTIN, P. M., GOPAL, E., ANANTH, S., ZHUANG, L., ITAGAKI, S., PRASAD, B. M., SMITH, S. B., PRASAD, P. D. & GANAPATHY, V. 2006. Identity of SMCT1 (SLC5A8) as a neuron-specific Na+-coupled transporter for active uptake of L-lactate and ketone bodies in the brain. *J Neurochem,* 98**,** 279-88.

MASLIAH, E., ALFORD, M., DETERESA, R., MALLORY, M. & HANSEN, L. 1996a. Deficient glutamate transport is associated with neurodegeneration in Alzheimer's disease. *Ann Neurol,* 40**,** 759-66.

MASLIAH, E., IWAI, A., MALLORY, M., UEDA, K. & SAITOH, T. 1996b. Altered presynaptic protein NACP is associated with plaque formation and neurodegeneration in Alzheimer's disease. *Am J Pathol,* 148**,** 201-10.

MASLIAH, E., MALLORY, M., HANSEN, L., ALFORD, M., ALBRIGHT, T., DETERESA, R., TERRY, R., BAUDIER, J. & SAITOH, T. 1991. Patterns of aberrant sprouting in alzheimer's disease. *Neuron,* 6**,** 729-739.

MASTERS, C. L. & SELKOE, D. J. 2012. Biochemistry of amyloid beta-protein and amyloid deposits in Alzheimer disease. *Cold Spring Harb Perspect Med,* 2**,** a006262.

MASTERS, C. L., SIMMS, G., WEINMAN, N. A., MULTHAUP, G., MCDONALD, B. L. & BEYREUTHER, K. 1985. Amyloid plaque core protein in Alzheimer disease and Down syndrome. *Proc Natl Acad Sci U S A,* 82**,** 4245-9.

MATSUOKA, Y., PICCIANO, M., LA FRANCOIS, J. & DUFF, K. 2001. Fibrillar beta-amyloid evokes oxidative damage in a transgenic mouse model of Alzheimer's disease. *Neuroscience,* 104**,** 609-13.

MATTSON, M. P. 2000. Emerging neuroprotective strategies for Alzheimer's disease: dietary restriction, telomerase activation, and stem cell therapy. *Exp Gerontol,* 35**,** 489-502.

MATTSON, M. P. 2004. Pathways towards and away from Alzheimer's disease. *Nature,* 430**,** 631-9.

MATTSON, M. P. & MAGNUS, T. 2006. Ageing and neuronal vulnerability. *Nat Rev Neurosci,* 7**,** 278-94.

MAWUENYEGA, K. G., SIGURDSON, W., OVOD, V., MUNSELL, L., KASTEN, T., MORRIS, J. C., YARASHESKI, K. E. & BATEMAN, R. J. 2010. Decreased clearance of CNS beta-amyloid in Alzheimer's disease. *Science,* 330**,** 1774.

MCCORMACK, J. G., HALESTRAP, A. P. & DENTON, R. M. 1990. Role of calcium ions in regulation of mammalian intramitochondrial metabolism. *Physiol Rev,* 70**,** 391-425.

MECOCCI, P., MACGARVEY, U. & BEAL, M. F. 1994. Oxidative damage to mitochondrial DNA is increased in Alzheimer's disease. *Ann Neurol,* 36**,** 747-51.

MECOCCI, P., MACGARVEY, U., KAUFMAN, A. E., KOONTZ, D., SHOFFNER, J. M., WALLACE, D. C. & BEAL, M. F. 1993. Oxidative damage to mitochondrial DNA shows marked age-dependent increases in human brain. *Ann Neurol,* 34**,** 609-16.

MEILANDT, W. J., CISSE, M., HO, K., WU, T., ESPOSITO, L. A., SCEARCE-LEVIE, K., CHENG, I. H., YU, G. Q. & MUCKE, L. 2009. Neprilysin overexpression inhibits plaque formation but fails to reduce pathogenic Abeta oligomers and associated cognitive deficits in human amyloid precursor protein transgenic mice. *J Neurosci,* 29**,** 1977-86.

MESSIER, C. 1997. Object recognition in mice: improvement of memory by glucose. *Neurobiol Learn Mem,* 67**,** 172-5.

MESSIER, C. 2003. Diabetes, Alzheimer's disease and apolipoprotein genotype. *Exp Gerontol,* 38**,** 941-6.

MESSMER, K. & REYNOLDS, G. P. 2005. An in vitro model of inflammatory neurodegeneration and its neuroprotection. *Neurosci Lett,* 388**,** 39-44.

MHATRE, M., FLOYD, R. A. & HENSLEY, K. 2004. Oxidative stress and neuroinflammation in Alzheimer's disease and amyotrophic lateral sclerosis: common links and potential therapeutic targets. *J Alzheimers Dis,* 6**,** 147-57.

MILLER, Y., MA, B. & NUSSINOV, R. 2010. Zinc ions promote Alzheimer Abeta aggregation via population shift of polymorphic states. *Proc Natl Acad Sci U S A,* 107**,** 9490-5.

MING, G. L., BRUSTLE, O., MUOTRI, A., STUDER, L., WERNIG, M. & CHRISTIAN, K. M. 2011. Cellular reprogramming: recent advances in modeling neurological diseases. *J Neurosci,* 31**,** 16070-5.

MINOSHIMA, S., GIORDANI, B., BERENT, S., FREY, K. A., FOSTER, N. L. & KUHL, D. E. 1997. Metabolic reduction in the posterior cingulate cortex in very early Alzheimer's disease. *Ann Neurol,* 42**,** 85-94.

MIRANDA, S., OPAZO, C., LARRONDO, L. F., MUNOZ, F. J., RUIZ, F., LEIGHTON, F. & INESTROSA, N. C. 2000. The role of oxidative stress in the toxicity induced by amyloid beta-peptide in Alzheimer's disease. *Prog Neurobiol,* 62**,** 633-48.

MOECHARS, D., DEWACHTER, I., LORENT, K., REVERSE, D., BAEKELANDT, V., NAIDU, A., TESSEUR, I., SPITTAELS, K., HAUTE, C. V., CHECLER, F., GODAUX, E., CORDELL, B. & VAN LEUVEN, F. 1999. Early phenotypic changes in transgenic mice that overexpress different mutants of amyloid precursor protein in brain. *J Biol Chem,* 274**,** 6483-92.

MOORADIAN, A. D., CHUNG, H. C. & SHAH, G. N. 1997. GLUT-1 Expression in the Cerebra of Patients with Alzheimer's Disease. *Neurobiology of Aging,* 18**,** 469-474.

MOREIRA, P. I., HONDA, K., LIU, Q., SANTOS, M. S., OLIVEIRA, C. R., ALIEV, G., NUNOMURA, A., ZHU, X., SMITH, M. A. & PERRY, G. 2005. Oxidative stress: the old enemy in Alzheimer's disease pathophysiology. *Curr Alzheimer Res,* 2**,** 403-8.

MOREIRA, P. I., SANTOS, M. S., MORENO, A. M., SEICA, R. & OLIVEIRA, C. R. 2003. Increased vulnerability of brain mitochondria in diabetic (Goto-Kakizaki) rats with aging and amyloid-beta exposure. *Diabetes,* 52**,** 1449-56.

MORFINI, G. A., BURNS, M., BINDER, L. I., KANAAN, N. M., LAPOINTE, N., BOSCO, D. A., BROWN, R. H., JR., BROWN, H., TIWARI, A., HAYWARD, L., EDGAR, J., NAVE, K. A., GARBERRN, J., ATAGI, Y., SONG, Y., PIGINO, G. & BRADY, S. T. 2009. Axonal transport defects in neurodegenerative diseases. *J Neurosci,* 29**,** 12776-86.

MORGAN, K. 2011. The three new pathways leading to Alzheimer's disease. *Neuropathol Appl Neurobiol,* 37**,** 353-7.

MORITA, M., VESTERGAARD, M., HAMADA, T. & TAKAGI, M. 2010. Real-time observation of model membrane dynamics induced by Alzheimer's amyloid beta. *Biophys Chem,* 147**,** 81-6.

MOSCONI, L. 2005. Brain glucose metabolism in the early and specific diagnosis of Alzheimer's disease. FDG-PET studies in MCI and AD. *Eur J Nucl Med Mol Imaging,* 32**,** 486-510.

MOSCONI, L., DE LEON, M., MURRAY, J., E, L., LU, J., JAVIER, E., MCHUGH, P. & SWERDLOW, R. H. 2011. Reduced mitochondria cytochrome oxidase activity in adult children of mothers with Alzheimer's disease. *J Alzheimers Dis,* 27**,** 483-90.

MOSCONI, L., DE SANTI, S., LI, J., TSUI, W. H., LI, Y., BOPPANA, M., LASKA, E., RUSINEK, H. & DE LEON, M. J. 2008a. Hippocampal hypometabolism predicts cognitive decline from normal aging. *Neurobiol Aging,* 29**,** 676-92.

MOSCONI, L., DE SANTI, S., LI, Y., LI, J., ZHAN, J., TSUI, W. H., BOPPANA, M., PUPI, A. & DE LEON, M. J. 2006a. Visual rating of medial temporal lobe metabolism in mild cognitive impairment and Alzheimer's disease using FDG-PET. *Eur J Nucl Med Mol Imaging,* 33**,** 210-21.

MOSCONI, L., MISTUR, R., SWITALSKI, R., BRYS, M., GLODZIK, L., RICH, K., PIRRAGLIA, E., TSUI, W., DE SANTI, S. & DE LEON, M. J. 2009a. Declining brain glucose metabolism in normal individuals with a maternal history of Alzheimer disease. *Neurology,* 72**,** 513-20.

MOSCONI, L., MISTUR, R., SWITALSKI, R., TSUI, W. H., GLODZIK, L., LI, Y., PIRRAGLIA, E., DE SANTI, S., REISBERG, B., WISNIEWSKI, T. & DE LEON, M. J. 2009b. FDG-PET changes in brain glucose metabolism from normal cognition to pathologically verified Alzheimer's disease. *Eur J Nucl Med Mol Imaging,* 36**,** 811-22.

MOSCONI, L., PUPI, A. & DE LEON, M. J. 2008b. Brain glucose hypometabolism and oxidative stress in preclinical Alzheimer's disease. *Ann N Y Acad Sci,* 1147**,** 180-95.

MOSCONI, L., SORBI, S., DE LEON, M. J., LI, Y., NACMIAS, B., MYOUNG, P. S., TSUI, W., GINESTRONI, A., BESSI, V., FAYYAZZ, M., CAFFARRA, P. & PUPI, A. 2006b. Hypometabolism exceeds atrophy in presymptomatic early-onset familial Alzheimer's disease. *J Nucl Med,* 47**,** 1778-86.

MOSCONI, L., TSUI, W. H., RUSINEK, H., DE SANTI, S., LI, Y., WANG, G. J., PUPI, A., FOWLER, J. & DE LEON, M. J. 2007. Quantitation, regional vulnerability, and kinetic modeling of brain glucose metabolism in mild Alzheimer's disease. *Eur J Nucl Med Mol Imaging,* 34**,** 1467-79.

MUCKE, L., MASLIAH, E., YU, G. Q., MALLORY, M., ROCKENSTEIN, E. M., TATSUNO, G., HU, K., KHOLODENKO, D., JOHNSON-WOOD, K. & MCCONLOGUE, L. 2000. High-level neuronal expression of abeta 1-42 in wild-type human amyloid protein precursor transgenic mice: synaptotoxicity without plaque formation. *J Neurosci,* 20**,** 4050-8.

MUDD, L. M., WERNER, H., SHEN-ORR, Z., ROBERTS, C. T., JR., LEROITH, D., HASPEL, H. C. & RAIZADA, M. K. 1990. Regulation of rat brain/HepG2 glucose transporter gene expression by phorbol esters in primary cultures of neuronal and astrocytic glial cells. *Endocrinology,* 126**,** 545-9.

MUIRHEAD, K. E., BORGER, E., AITKEN, L., CONWAY, S. J. & GUNN-MOORE, F. J. 2010. The consequences of mitochondrial amyloid beta-peptide in Alzheimer's disease. *Biochem J,* 426**,** 255-70.

MUKHERJEE, A., SONG, E., KIHIKO-EHMANN, M., GOODMAN, J. P., JR., PYREK, J. S., ESTUS, S. & HERSH, L. B. 2000. Insulysin hydrolyzes amyloid beta peptides to products that are neither neurotoxic nor deposit on amyloid plaques. *J Neurosci,* 20**,** 8745-9.

MYLLYKANGAS, L., POLVIKOSKI, T., SULKAVA, R., VERKKONIEMI, A., CROOK, R., TIENARI, P. J., PUSA, A. K., NIINISTO, L., O'BRIEN, P., KONTULA, K., HARDY, J., HALTIA, M. & PEREZ-TUR, J. 1999. Genetic association of alpha2-macroglobulin with Alzheimer's disease in a Finnish elderly population. *Ann Neurol,* 46**,** 382-90.

NAGELE, R. G., WEGIEL, J., VENKATARAMAN, V., IMAKI, H. & WANG, K. C. 2004. Contribution of glial cells to the development of amyloid plaques in Alzheimer's disease. *Neurobiol Aging,* 25**,** 663-74.

NAHORSKI, S. R. & ROGERS, K. J. 1972. An enzymic fluorometric micro method for determination of glycogen. *Anal Biochem,* 49**,** 492-7.

NAJ, A. C., JUN, G., BEECHAM, G. W., WANG, L. S., VARDARAJAN, B. N., BUROS, J., GALLINS, P. J., BUXBAUM, J. D., JARVIK, G. P., CRANE, P. K., LARSON, E. B., BIRD, T. D., BOEVE, B. F., GRAFF-RADFORD, N. R., DE JAGER, P. L., EVANS, D., SCHNEIDER, J. A., CARRASQUILLO, M. M., ERTEKIN-TANER, N., YOUNKIN, S.

G., CRUCHAGA, C., KAUWE, J. S., NOWOTNY, P., KRAMER, P., HARDY, J., HUENTELMAN, M. J., MYERS, A. J., BARMADA, M. M., DEMIRCI, F. Y., BALDWIN, C. T., GREEN, R. C., ROGAEVA, E., ST GEORGE-HYSLOP, P., ARNOLD, S. E., BARBER, R., BEACH, T., BIGIO, E. H., BOWEN, J. D., BOXER, A., BURKE, J. R., CAIRNS, N. J., CARLSON, C. S., CARNEY, R. M., CARROLL, S. L., CHUI, H. C., CLARK, D. G., CORNEVEAUX, J., COTMAN, C. W., CUMMINGS, J. L., DECARLI, C., DEKOSKY, S. T., DIAZ-ARRASTIA, R., DICK, M., DICKSON, D. W., ELLIS, W. G., FABER, K. M., FALLON, K. B., FARLOW, M. R., FERRIS, S., FROSCH, M. P., GALASKO, D. R., GANGULI, M., GEARING, M., GESCHWIND, D. H., GHETTI, B., GILBERT, J. R., GILMAN, S., GIORDANI, B., GLASS, J. D., GROWDON, J. H., HAMILTON, R. L., HARRELL, L. E., HEAD, E., HONIG, L. S., HULETTE, C. M., HYMAN, B. T., JICHA, G. A., JIN, L. W., JOHNSON, N., KARLAWISH, J., KARYDAS, A., KAYE, J. A., KIM, R., KOO, E. H., KOWALL, N. W., LAH, J. J., LEVEY, A. I., LIEBERMAN, A. P., LOPEZ, O. L., MACK, W. J., MARSON, D. C., MARTINIUK, F., MASH, D. C., MASLIAH, E., MCCORMICK, W. C., MCCURRY, S. M., MCDAVID, A. N., MCKEE, A. C., MESULAM, M., MILLER, B. L., et al. 2011. Common variants at MS4A4/MS4A6E, CD2AP, CD33 and EPHA1 are associated with late-onset Alzheimer's disease. *Nat Genet,* 43**,** 436-41.

NAKAMURA, S., MURAYAMA, N., NOSHITA, T., ANNOURA, H. & OHNO, T. 2001. Progressive brain dysfunction following intracerebroventricular infusion of beta1–42-amyloid peptide. *Brain Research,* 912**,** 128-136.

NARITA, M., HOLTZMAN, D. M., SCHWARTZ, A. L. & BU, G. 1997. Alpha2-macroglobulin complexes with and mediates the endocytosis of beta-amyloid peptide via cell surface low-density lipoprotein receptor-related protein. *J Neurochem,* 69**,** 1904-11.

NAVARRO, A. & BOVERIS, A. 2004. Rat brain and liver mitochondria develop oxidative stress and lose enzymatic activities on aging. *Am J Physiol Regul Integr Comp Physiol,* 287**,** R1244-9.

NAVARRO, A. & BOVERIS, A. 2007. The mitochondrial energy transduction system and the aging process. *Am J Physiol Cell Physiol,* 292**,** C670-86.

NELSON, D. L. & COX, M. M. 2005. Lehninger. *Principles of Biochemistry,* 4.

NELSON, R. B., LINDEN, D. J., HYMAN, C., PFENNINGER, K. H. & ROUTTENBERG, A. 1989. The two major phosphoproteins in growth cones are probably identical to two protein kinase C substrates correlated with persistence of long-term potentiation. *J Neurosci,* 9**,** 381-9.

NEMOTO, S., TAKEDA, K., YU, Z. X., FERRANS, V. J. & FINKEL, T. 2000. Role for mitochondrial oxidants as regulators of cellular metabolism. *Mol Cell Biol,* 20**,** 7311-8.

NESTOR, P. J., FRYER, T. D., SMIELEWSKI, P. & HODGES, J. R. 2003. Limbic hypometabolism in Alzheimer's disease and mild cognitive impairment. *Ann Neurol,* 54**,** 343-51.

NEWMAN, S. F., SULTANA, R., PERLUIGI, M., COCCIA, R., CAI, J., PIERCE, W. M., KLEIN, J. B., TURNER, D. M. & BUTTERFIELD, D. A. 2007. An increase in S-glutathionylated proteins in the Alzheimer's disease inferior parietal lobule, a proteomics approach. *J Neurosci Res,* 85**,** 1506-14.

NICHOLLS, D. 2002. Mitochondrial bioenergetics, aging, and aging-related disease. *Sci Aging Knowledge Environ,* 2002**,** pe12.

NICHOLLS, D. & ATTWELL, D. 1990. The release and uptake of excitatory amino acids. *Trends Pharmacol Sci,* 11**,** 462-8.

NICKLAS, W. J., CLARK, J. B. & WILLIAMSON, J. R. 1971. Metabolism of rat brain mitochondria. Studies on the potassium ion-stimulated oxidation of pyruvate. *Biochem J,* 123**,** 83-95.

NIKOLETOPOULOU, V. & TAVERNARAKIS, N. 2012. Embryonic and induced pluripotent stem cell differentiation as a tool in neurobiology. *Biotechnol J,* 7**,** 1156-68.

NILSBERTH, C., WESTLIND-DANIELSSON, A., ECKMAN, C. B., CONDRON, M. M., AXELMAN, K., FORSELL, C., STENH, C., LUTHMAN, J., TEPLOW, D. B., YOUNKIN, S. G., NASLUND, J. & LANNFELT, L. 2001. The 'Arctic' APP mutation (E693G) causes Alzheimer's disease by enhanced Abeta protofibril formation. *Nat Neurosci,* 4**,** 887-93.

NILSSON, M. R., NGUYEN, L. L. & RALEIGH, D. P. 2001. Synthesis and purification of amyloidogenic peptides. *Anal Biochem,* 288**,** 76-82.

NISHITSUJI, K., HOSONO, T., UCHIMURA, K. & MICHIKAWA, M. 2011. Lipoprotein lipase is a novel amyloid beta (Abeta)-binding protein that promotes glycosaminoglycan-dependent cellular uptake of Abeta in astrocytes. *J Biol Chem,* 286**,** 6393-401.

NULTON-PERSSON, A. C., STARKE, D. W., MIEYAL, J. J. & SZWEDA, L. I. 2003. Reversible inactivation of alpha-ketoglutarate dehydrogenase in response to alterations in the mitochondrial glutathione status. *Biochemistry,* 42**,** 4235-42.

NUNAN, J. & SMALL, D. H. 2000. Regulation of APP cleavage by α-, β- and γ-secretases. *FEBS Letters,* 483, 6-10.

NUNOMURA, A., PERRY, G., ALIEV, G., HIRAI, K., TAKEDA, A., BALRAJ, E. K., JONES, P. K., GHANBARI, H., WATAYA, T., SHIMOHAMA, S., CHIBA, S., ATWOOD, C. S., PETERSEN, R. B. & SMITH, M. A. 2001. Oxidative damage is the earliest event in Alzheimer disease. *J Neuropathol Exp Neurol,* 60**,** 759-67.

NUNOMURA, A., PERRY, G., PAPPOLLA, M. A., WADE, R., HIRAI, K., CHIBA, S. & SMITH, M. A. 1999. RNA oxidation is a prominent feature of vulnerable neurons in Alzheimer's disease. *J Neurosci,* 19**,** 1959-64.

O'BRIEN, J., KLA, K. M., HOPKINS, I. B., MALECKI, E. A. & MCKENNA, M. C. 2007. Kinetic parameters and lactate dehydrogenase isozyme activities support possible lactate utilization by neurons. *Neurochem Res,* 32**,** 597-607.

O'CONNOR, T., SADLEIR, K. R., MAUS, E., VELLIQUETTE, R. A., ZHAO, J., COLE, S. L., EIMER, W. A., HITT, B., BEMBINSTER, L. A., LAMMICH, S., LICHTENTHALER, S. F., HEBERT, S. S., DE STROOPER, B., HAASS, C., BENNETT, D. A. & VASSAR, R. 2008. Phosphorylation of the translation initiation factor eIF2alpha increases BACE1 levels and promotes amyloidogenesis. *Neuron,* 60**,** 988-1009.

O'NUALLAIN, B., SHIVAPRASAD, S., KHETERPAL, I. & WETZEL, R. 2005. Thermodynamics of A beta(1-40) amyloid fibril elongation. *Biochemistry,* 44**,** 12709-18.

OBERHEIM, N. A., TAKANO, T., HAN, X., HE, W., LIN, J. H., WANG, F., XU, Q., WYATT, J. D., PILCHER, W., OJEMANN, J. G., RANSOM, B. R., GOLDMAN, S. A. & NEDERGAARD, M. 2009. Uniquely hominid features of adult human astrocytes. *J Neurosci,* 29**,** 3276-87.

OBERHEIM, N. A., WANG, X., GOLDMAN, S. & NEDERGAARD, M. 2006. Astrocytic complexity distinguishes the human brain. *Trends Neurosci,* 29**,** 547-53.

ODDO, S., CACCAMO, A., SHEPHERD, J. D., MURPHY, M. P., GOLDE, T. E., KAYED, R., METHERATE, R., MATTSON, M. P., AKBARI, Y. & LAFERLA, F. M. 2003. Triple-Transgenic Model of Alzheimer's Disease with Plaques and Tangles: Intracellular Aβ and Synaptic Dysfunction. *Neuron,* 39**,** 409-421.

OGAWA, M., TSUKUDA, M., YAMAGUCHI, T., IKEDA, K., OKADA, T., YANO, Y., HOSHINO, M. & MATSUZAKI, K. 2011. Ganglioside-mediated aggregation of amyloid beta-proteins (Abeta): comparison between Abeta-(1-42) and Abeta-(1-40). *J Neurochem,* 116**,** 851-7.

OGINO, K. & WANG, D. H. 2007. Biomarkers of oxidative/nitrosative stress: an approach to disease prevention. *Acta Med Okayama,* 61**,** 181-9.

OKAICHI, Y. & OKAICHI, H. 2000. Effects of glucose on scopolamine-induced learning deficits in rats performing the Morris water maze task. *Neurobiol Learn Mem,* 74**,** 65-79.

OKITA, K., MATSUMURA, Y., SATO, Y., OKADA, A., MORIZANE, A., OKAMOTO, S., HONG, H., NAKAGAWA, M., TANABE, K., TEZUKA, K., SHIBATA, T., KUNISADA, T., TAKAHASHI, M., TAKAHASHI, J., SAJI, H. & YAMANAKA, S. 2011. A more efficient method to generate integration-free human iPS cells. *Nat Methods,* 8**,** 409-12.

OLNEY, J. W., WOZNIAK, D. F. & FARBER, N. B. 1998. Glumate receptor dysfunction and Alzheimer's disease. *Restor Neurol Neurosci,* 13**,** 75-83.

OLOFSSON, A., LINDHAGEN-PERSSON, M., VESTLING, M., SAUER-ERIKSSON, A. E. & OHMAN, A. 2009. Quenched hydrogen/deuterium exchange NMR characterization of amyloid-beta peptide aggregates formed in the presence of Cu2+ or Zn2+. *FEBS J,* 276**,** 4051-60.

OPPERMANN, U. C., SALIM, S., TJERNBERG, L. O., TERENIUS, L. & JORNVALL, H. 1999. Binding of amyloid beta-peptide to mitochondrial hydroxyacyl-CoA dehydrogenase (ERAB): regulation of an SDR enzyme activity with implications for apoptosis in Alzheimer's disease. *FEBS Lett,* 451**,** 238-42.

OWEN, O. E., MORGAN, A. P., KEMP, H. G., SULLIVAN, J. M., HERRERA, M. G. & CAHILL, G. F., JR. 1967. Brain metabolism during fasting. *J Clin Invest,* 46**,** 1589-95.

OWENS, C. W. & BELCHER, R. V. 1965. A colorimetric micro-method for the determination of glutathione. *Biochem J,* 94**,** 705-11.

OZAWA, T. 1997. Genetic and functional changes in mitochondria associated with aging. *Physiol Rev,* 77**,** 425-64.

OZCANKAYA, R. & DELIBAS, N. 2002. Malondialdehyde, superoxide dismutase, melatonin, iron, copper, and zinc blood concentrations in patients with Alzheimer disease: cross-sectional study. *Croat Med J,* 43**,** 28-32.

PACHER, P. & SZABO, C. 2007. Role of poly(ADP-ribose) polymerase 1 (PARP-1) in cardiovascular diseases: the therapeutic potential of PARP inhibitors. *Cardiovasc Drug Rev,* 25**,** 235-60.

PALLAS, M., VERDAGUER, E., TAJES, M., GUTIERREZ-CUESTA, J. & CAMINS, A. 2008. Modulation of sirtuins: new targets for antiageing. *Recent Pat CNS Drug Discov,* 3**,** 61-9.

PARDRIDGE, W. M. & OLDENDORF, W. H. 1977. Transport of metabolic substrates through the blood-brain barrier. *J Neurochem,* 28**,** 5-12.

PARIHAR, M. S. & BREWER, G. J. 2007. Mitoenergetic failure in Alzheimer disease. *Am J Physiol Cell Physiol,* 292**,** C8-23.

PARK, H. J., KIM, S. S., SEONG, Y. M., KIM, K. H., GOO, H. G., YOON, E. J., MIN DO, S., KANG, S. & RHIM, H. 2006. Beta-amyloid precursor protein is a direct cleavage target of HtrA2 serine protease. Implications for the physiological function of HtrA2 in the mitochondria. *J Biol Chem,* 281**,** 34277-87.

PARKER, W. D., JR., FILLEY, C. M. & PARKS, J. K. 1990. Cytochrome oxidase deficiency in Alzheimer's disease. *Neurology,* 40**,** 1302-3.

PARPURA, V. & ZOREC, R. 2010. Gliotransmission: Exocytotic release from astrocytes. *Brain Res Rev,* 63**,** 83-92.

PARPURA-GILL, A., BEITZ, D. & UEMURA, E. 1997. The inhibitory effects of beta-amyloid on glutamate and glucose uptakes by cultured astrocytes. *Brain Res,* 754**,** 65-71.

PASTERNAK, S. H., CALLAHAN, J. W. & MAHURAN, D. J. 2004. The role of the endosomal/lysosomal system in amyloid-beta production and the pathophysiology of Alzheimer's disease: reexamining the spatial paradox from a lysosomal perspective. *J Alzheimers Dis,* 6**,** 53-65.

PATEL, J. R. & BREWER, G. J. 2003. Age-related changes in neuronal glucose uptake in response to glutamate and beta-amyloid. *J Neurosci Res,* 72**,** 527-36.

PAULA-LIMA, A. C., TRICERRI, M. A., BRITO-MOREIRA, J., BOMFIM, T. R., OLIVEIRA, F. F., MAGDESIAN, M. H., GRINBERG, L. T., PANIZZUTTI, R. & FERREIRA, S. T. 2009. Human apolipoprotein A-I binds amyloid-beta and prevents Abeta-induced neurotoxicity. *Int J Biochem Cell Biol,* 41**,** 1361-70.

PELLEGRI, G., ROSSIER, C., MAGISTRETTI, P. J. & MARTIN, J. L. 1996. Cloning, localization and induction of mouse brain glycogen synthase. *Brain Res Mol Brain Res,* 38**,** 191-9.

PELLERIN, L. 2003. Lactate as a pivotal element in neuron–glia metabolic cooperation. *Neurochemistry International,* 43**,** 331-338.

PELLERIN, L. 2008. Brain energetics (thought needs food). *Curr Opin Clin Nutr Metab Care,* 11**,** 701-5.

PELLERIN, L., BERGERSEN, L. H., HALESTRAP, A. P. & PIERRE, K. 2005. Cellular and subcellular distribution of monocarboxylate transporters in cultured brain cells and in the adult brain. *J Neurosci Res,* 79**,** 55-64.

PELLERIN, L. & MAGISTRETTI, P. J. 1994. Glutamate uptake into astrocytes stimulates aerobic glycolysis: a mechanism coupling neuronal activity to glucose utilization. *Proc Natl Acad Sci U S A,* 91**,** 10625-9.

PELLERIN, L. & MAGISTRETTI, P. J. 1997. Glutamate uptake stimulates Na+,K+-ATPase activity in astrocytes via activation of a distinct subunit highly sensitive to ouabain. *J Neurochem,* 69**,** 2132-7.

PELLERIN, L. & MAGISTRETTI, P. J. 2012. Sweet sixteen for ANLS. *J Cereb Blood Flow Metab,* 32**,** 1152-66.

PELLERIN, L., PELLEGRI, G., MARTIN, J. L. & MAGISTRETTI, P. J. 1998. Expression of monocarboxylate transporter mRNAs in mouse brain: support for a distinct role of

lactate as an energy substrate for the neonatal vs. adult brain. *Proc Natl Acad Sci U S A,* 95**,** 3990-5.

PERALVAREZ-MARIN, A., MATEOS, L., ZHANG, C., SINGH, S., CEDAZO-MINGUEZ, A., VISA, N., MOROZOVA-ROCHE, L., GRASLUND, A. & BARTH, A. 2009. Influence of residue 22 on the folding, aggregation profile, and toxicity of the Alzheimer's amyloid beta peptide. *Biophys J,* 97**,** 277-85.

PEREZ-COSTAS, E., GANDY, J. C., MELENDEZ-FERRO, M., ROBERTS, R. C. & BIJUR, G. N. 2010. Light and electron microscopy study of glycogen synthase kinase-3beta in the mouse brain. *PLoS One,* 5**,** e8911.

PERREAU, V. M., ORCHARD, S., ADLARD, P. A., BELLINGHAM, S. A., CAPPAI, R., CICCOTOSTO, G. D., COWIE, T. F., CROUCH, P. J., DUCE, J. A., EVIN, G., FAUX, N. G., HILL, A. F., HUNG, Y. H., JAMES, S. A., LI, Q. X., MOK, S. S., TEW, D. J., WHITE, A. R., BUSH, A. I., HERMJAKOB, H. & MASTERS, C. L. 2010. A domain level interaction network of amyloid precursor protein and Abeta of Alzheimer's disease. *Proteomics,* 10**,** 2377-95.

PERRONE, L., MOTHES, E., VIGNES, M., MOCKEL, A., FIGUEROA, C., MIQUEL, M. C., MADDELEIN, M. L. & FALLER, P. 2010. Copper transfer from Cu-Abeta to human serum albumin inhibits aggregation, radical production and reduces Abeta toxicity. *Chembiochem,* 11**,** 110-8.

PERRY, E. K., PERRY, R. H., BLESSED, G. & TOMLINSON, B. E. 1978. Changes in brain cholinesterases in senile dementia of Alzheimer type. *Neuropathol Appl Neurobiol,* 4**,** 273-7.

PERRY, G., CASTELLANI, R. J., HIRAI, K. & SMITH, M. A. 1998. Reactive Oxygen Species Mediate Cellular Damage in Alzheimer Disease. *J Alzheimers Dis,* 1**,** 45-55.

PETERSEN, R. C., STEVENS, J. C., GANGULI, M., TANGALOS, E. G., CUMMINGS, J. L. & DEKOSKY, S. T. 2001. Practice parameter: early detection of dementia: mild cognitive impairment (an evidence-based review). Report of the Quality Standards Subcommittee of the American Academy of Neurology. *Neurology,* 56**,** 1133-42.

PETIT-TABOUE, M. C., LANDEAU, B., DESSON, J. F., DESGRANGES, B. & BARON, J. C. 1998. Effects of healthy aging on the regional cerebral metabolic rate of glucose assessed with statistical parametric mapping. *Neuroimage,* 7**,** 176-84.

PFEIFFER-GUGLIELMI, B., FLECKENSTEIN, B., JUNG, G. & HAMPRECHT, B. 2003. Immunocytochemical localization of glycogen phosphorylase isozymes in rat nervous tissues by using isozyme-specific antibodies. *J Neurochem,* 85**,** 73-81.

PHELPS, C. H. 1972. Barbiturate-induced glycogen accumulation in brain. An electron microscopic study. *Brain Res,* 39**,** 225-34.

PHELPS, M. E., HUANG, S. C., HOFFMAN, E. J., SELIN, C., SOKOLOFF, L. & KUHL, D. E. 1979. Tomographic measurement of local cerebral glucose metabolic rate in humans with (F-18)2-fluoro-2-deoxy-D-glucose: validation of method. *Ann Neurol,* 6**,** 371-88.

PHIEL, C. J., WILSON, C. A., LEE, V. M. & KLEIN, P. S. 2003. GSK-3alpha regulates production of Alzheimer's disease amyloid-beta peptides. *Nature,* 423**,** 435-9.

PICONE, P., CARROTTA, R., MONTANA, G., NOBILE, M. R., SAN BIAGIO, P. L. & DI CARLO, M. 2009. Abeta oligomers and fibrillar aggregates induce different apoptotic pathways in LAN5 neuroblastoma cell cultures. *Biophys J,* 96**,** 4200-11.

PIEPER, A. A., VERMA, A., ZHANG, J. & SNYDER, S. H. 1999. Poly (ADP-ribose) polymerase, nitric oxide and cell death. *Trends Pharmacol Sci,* 20**,** 171-81.

PIERRE, K., CHATTON, J. Y., PARENT, A., REPOND, C., GARDONI, F., DI LUCA, M. & PELLERIN, L. 2009. Linking supply to demand: the neuronal monocarboxylate transporter MCT2 and the alpha-amino-3-hydroxyl-5-methyl-4-isoxazole-propionic acid receptor GluR2/3 subunit are associated in a common trafficking process. *Eur J Neurosci,* 29**,** 1951-63.

PIERRE, K., MAGISTRETTI, P. J. & PELLERIN, L. 2002. MCT2 is a major neuronal monocarboxylate transporter in the adult mouse brain. *J Cereb Blood Flow Metab,* 22**,** 586-95.

PILLAI, J. B., ISBATAN, A., IMAI, S. & GUPTA, M. P. 2005. Poly(ADP-ribose) polymerase-1-dependent cardiac myocyte cell death during heart failure is mediated by NAD+ depletion and reduced Sir2alpha deacetylase activity. *J Biol Chem,* 280**,** 43121-30.

PLAGEMANN, P. G. & ESTENSEN, R. D. 1972. Cytochalasin B. VI. Competitive inhibition of nucleoside transport by cultured Novikoff rat hepatoma cells. *J Cell Biol,* 55**,** 179-85.

PODLISNY, M. B., OSTASZEWSKI, B. L., SQUAZZO, S. L., KOO, E. H., RYDELL, R. E., TEPLOW, D. B. & SELKOE, D. J. 1995. Aggregation of secreted amyloid beta-protein into sodium dodecyl sulfate-stable oligomers in cell culture. *J Biol Chem,* 270**,** 9564-70.

POLLAK, N., DOLLE, C. & ZIEGLER, M. 2007. The power to reduce: pyridine nucleotides--small molecules with a multitude of functions. *Biochem J,* 402**,** 205-18.

POSTINA, R., SCHROEDER, A., DEWACHTER, I., BOHL, J., SCHMITT, U., KOJRO, E., PRINZEN, C., ENDRES, K., HIEMKE, C., BLESSING, M., FLAMEZ, P., DEQUENNE, A., GODAUX, E., VAN LEUVEN, F. & FAHRENHOLZ, F. 2004. A disintegrin-metalloproteinase prevents amyloid plaque formation and hippocampal defects in an Alzheimer disease mouse model. *J Clin Invest,* 113**,** 1456-64.

POWERS, E. T. & POWERS, D. L. 2008. Mechanisms of protein fibril formation: nucleated polymerization with competing off-pathway aggregation. *Biophys J,* 94**,** 379-91.

PRATICO, D. & DELANTY, N. 2000. Oxidative injury in diseases of the central nervous system: focus on Alzheimer's disease. *Am J Med,* 109**,** 577-85.

PROKOP, S., SHIROTANI, K., EDBAUER, D., HAASS, C. & STEINER, H. 2004. Requirement of PEN-2 for stabilization of the presenilin N-/C-terminal fragment heterodimer within the gamma-secretase complex. *J Biol Chem,* 279**,** 23255-61.

PUCHTLER, H., SWEAT, F. & LEVINE, M. 1962. On the binding of Congo Red by Amyloid. *Journal of Histochemistry & Cytochemistry,* 10**,** 355-364.

PUZZO, D., PRIVITERA, L., LEZNIK, E., FA, M., STANISZEWSKI, A., PALMERI, A. & ARANCIO, O. 2008. Picomolar amyloid-beta positively modulates synaptic plasticity and memory in hippocampus. *J Neurosci,* 28**,** 14537-45.

QIU, W. Q. & FOLSTEIN, M. F. 2006. Insulin, insulin-degrading enzyme and amyloid-beta peptide in Alzheimer's disease: review and hypothesis. *Neurobiol Aging,* 27**,** 190-8.

QIU, W. Q., WALSH, D. M., YE, Z., VEKRELLIS, K., ZHANG, J., PODLISNY, M. B., ROSNER, M. R., SAFAVI, A., HERSH, L. B. & SELKOE, D. J. 1998. Insulin-degrading enzyme regulates extracellular levels of amyloid beta-protein by degradation. *J Biol Chem,* 273**,** 32730-8.

QIU, W. Q., YE, Z., KHOLODENKO, D., SEUBERT, P. & SELKOE, D. J. 1997. Degradation of amyloid beta-protein by a metalloprotease secreted by microglia and other neural and non-neural cells. *J Biol Chem,* 272**,** 6641-6.

QUERFURTH, H. W. & LAFERLA, F. M. 2010. Alzheimer's Disease. *New England Journal of Medicine,* 362**,** 329-344.

RAFAELOFF-PHAIL, R., DING, L., CONNER, L., YEH, W. K., MCCLURE, D., GUO, H., EMERSON, K. & BROOKS, H. 2004. Biochemical regulation of mammalian AMP-activated protein kinase activity by NAD and NADH. *J Biol Chem,* 279**,** 52934-9.

RAJENDRAN, R., MINQIN, R., YNSA, M. D., CASADESUS, G., SMITH, M. A., PERRY, G., HALLIWELL, B. & WATT, F. 2009. A novel approach to the identification and quantitative elemental analysis of amyloid deposits--insights into the pathology of Alzheimer's disease. *Biochem Biophys Res Commun,* 382**,** 91-5.

RAPOPORT, S. I., HORWITZ, B., GRADY, C. L., HAXBY, J. V., DECARLI, C. & SCHAPIRO, M. B. 1991. Abnormal brain glucose metabolism in Alzheimer's disease, as measured by position emission tomography. *Adv Exp Med Biol,* 291**,** 231-48.

REBECK, G. W., HARR, S. D., STRICKLAND, D. K. & HYMAN, B. T. 1995. Multiple, diverse senile plaque-associated proteins are ligands of an apolipoprotein E receptor, the alpha 2-macroglobulin receptor/low-density-lipoprotein receptor-related protein. *Ann Neurol,* 37**,** 211-7.

REBRIN, I., KAMZALOV, S. & SOHAL, R. S. 2003. Effects of age and caloric restriction on glutathione redox state in mice. *Free Radic Biol Med,* 35**,** 626-35.

REDDY, P. H. & BEAL, M. F. 2008. Amyloid beta, mitochondrial dysfunction and synaptic damage: implications for cognitive decline in aging and Alzheimer's disease. *Trends Mol Med,* 14**,** 45-53.

REIMAN, E. M., CASELLI, R. J., CHEN, K., ALEXANDER, G. E., BANDY, D. & FROST, J. 2001. Declining brain activity in cognitively normal apolipoprotein E epsilon 4 heterozygotes: A foundation for using positron emission tomography to efficiently test treatments to prevent Alzheimer's disease. *Proc Natl Acad Sci U S A,* 98**,** 3334-9.

REIMAN, E. M., CASELLI, R. J., YUN, L. S., CHEN, K., BANDY, D., MINOSHIMA, S., THIBODEAU, S. N. & OSBORNE, D. 1996. Preclinical evidence of Alzheimer's

disease in persons homozygous for the epsilon 4 allele for apolipoprotein E. *N Engl J Med,* 334**,** 752-8.

REIMAN, E. M., CHEN, K., ALEXANDER, G. E., CASELLI, R. J., BANDY, D., OSBORNE, D., SAUNDERS, A. M. & HARDY, J. 2004. Functional brain abnormalities in young adults at genetic risk for late-onset Alzheimer's dementia. *Proc Natl Acad Sci U S A,* 101**,** 284-9.

REIMAN, E. M., UECKER, A., CASELLI, R. J., LEWIS, S., BANDY, D., DE LEON, M. J., DE SANTI, S., CONVIT, A., OSBORNE, D., WEAVER, A. & THIBODEAU, S. N. 1998. Hippocampal volumes in cognitively normal persons at genetic risk for Alzheimer's disease. *Ann Neurol,* 44**,** 288-91.

REKART, J. L., QUINN, B., MESULAM, M. M. & ROUTTENBERG, A. 2004. Subfield-specific increase in brain growth protein in postmortem hippocampus of Alzheimer's patients. *Neuroscience,* 126**,** 579-84.

RENDT, J., ERULKAR, S. & ANDREWS, P. W. 1989. Presumptive neurons derived by differentiation of a human embryonal carcinoma cell line exhibit tetrodotoxin-sensitive sodium currents and the capacity for regenerative responses. *Exp Cell Res,* 180**,** 580-4.

RIDDELL, D. R., CHRISTIE, G., HUSSAIN, I. & DINGWALL, C. 2001. Compartmentalization of beta-secretase (Asp2) into low-buoyant density, noncaveolar lipid rafts. *Curr Biol,* 11**,** 1288-93.

RIVERA, E. J., GOLDIN, A., FULMER, N., TAVARES, R., WANDS, J. R. & DE LA MONTE, S. M. 2005. Insulin and insulin-like growth factor expression and function deteriorate with progression of Alzheimer's disease: link to brain reductions in acetylcholine. *J Alzheimers Dis,* 8**,** 247-68.

ROBINET, C. & PELLERIN, L. 2010. Brain-derived neurotrophic factor enhances the expression of the monocarboxylate transporter 2 through translational activation in mouse cultured cortical neurons. *J Cereb Blood Flow Metab,* 30**,** 286-98.

ROBINSON, S. R. 2001. Changes in the cellular distribution of glutamine synthetase in Alzheimer's disease. *J Neurosci Res,* 66**,** 972-80.

ROEDER, L. M., WILLIAMS, I. B. & TILDON, J. T. 1985. Glucose transport in astrocytes: regulation by thyroid hormone. *J Neurochem,* 45**,** 1653-7.

ROQUES, B. P., NOBLE, F., DAUGE, V., FOURNIE-ZALUSKI, M. C. & BEAUMONT, A. 1993. Neutral endopeptidase 24.11: structure, inhibition, and experimental and clinical pharmacology. *Pharmacol Rev,* 45**,** 87-146.

ROSE, E. M., KOO, J. C., ANTFLICK, J. E., AHMED, S. M., ANGERS, S. & HAMPSON, D. R. 2009. Glutamate transporter coupling to Na,K-ATPase. *J Neurosci,* 29**,** 8143-55.

ROSENBERG, P. A. & DICHTER, M. A. 1985. Glycogen accumulation in rat cerebral cortex in dissociated cell culture. *J Neurosci Methods,* 15**,** 101-12.

ROZGA, M., KLONIECKI, M., DADLEZ, M. & BAL, W. 2010. A direct determination of the dissociation constant for the Cu(II) complex of amyloid beta 1-40 peptide. *Chem Res Toxicol,* 23**,** 336-40.

RYAN, C. M. & GECKLE, M. 2000. Why is learning and memory dysfunction in Type 2 diabetes limited to older adults? *Diabetes Metab Res Rev,* 16**,** 308-15.

RYDSTROM, J. 2006. Mitochondrial NADPH, transhydrogenase and disease. *Biochim Biophys Acta,* 1757**,** 721-6.

SAGAR, S. M., SHARP, F. R. & SWANSON, R. A. 1987. The regional distribution of glycogen in rat brain fixed by microwave irradiation. *Brain Res,* 417**,** 172-4.

SAGARA, J. I., MIURA, K. & BANNAI, S. 1993. Maintenance of neuronal glutathione by glial cells. *J Neurochem,* 61**,** 1672-6.

SAHOO, B., NAG, S., SENGUPTA, P. & MAITI, S. 2009. On the stability of the soluble amyloid aggregates. *Biophys J,* 97**,** 1454-60.

SAIDO, T. & LEISSRING, M. A. 2012. Proteolytic degradation of amyloid beta-protein. *Cold Spring Harb Perspect Med,* 2**,** a006379.

SAITO, T., TAKAKI, Y., IWATA, N., TROJANOWSKI, J. & SAIDO, T. C. 2003. Alzheimer's disease, neuropeptides, neuropeptidase, and amyloid-beta peptide metabolism. *Sci Aging Knowledge Environ,* 2003**,** PE1.

SALMINEN, A., KAUPPINEN, A., SUURONEN, T., KAARNIRANTA, K. & OJALA, J. 2009. ER stress in Alzheimer's disease: a novel neuronal trigger for inflammation and Alzheimer's pathology. *J Neuroinflammation,* 6**,** 41.

SANDHU, J. K., SIKORSKA, M. & WALKER, P. R. 2002. Characterization of astrocytes derived from human NTera-2/D1 embryonal carcinoma cells. *J Neurosci Res,* 68**,** 604-14.

SANG, T.-K. & JACKSON, G. R. 2005. Drosophila Models of Neurodegenerative Disease. *NeuroRX,* 2**,** 438-446.

SASTRE, M., STEINER, H., FUCHS, K., CAPELL, A., MULTHAUP, G., CONDRON, M. M., TEPLOW, D. B. & HAASS, C. 2001. Presenilin-dependent gamma-secretase processing of beta-amyloid precursor protein at a site corresponding to the S3 cleavage of Notch. *EMBO Rep,* 2**,** 835-41.

SATOH, J. & KURODA, Y. 2000. Amyloid precursor protein beta-secretase (BACE) mRNA expression in human neural cell lines following induction of neuronal differentiation and exposure to cytokines and growth factors. *Neuropathology,* 20**,** 289-96.

SATTLER, R. & TYMIANSKI, M. 2001. Molecular mechanisms of glutamate receptor-mediated excitotoxic neuronal cell death. *Mol Neurobiol,* 24**,** 107-29.

SAUVE, A. A., WOLBERGER, C., SCHRAMM, V. L. & BOEKE, J. D. 2006. The biochemistry of sirtuins. *Annu Rev Biochem,* 75**,** 435-65.

SAYRE, L. M., ZELASKO, D. A., HARRIS, P. L., PERRY, G., SALOMON, R. G. & SMITH, M. A. 1997. 4-Hydroxynonenal-derived advanced lipid peroxidation end products are increased in Alzheimer's disease. *J Neurochem,* 68**,** 2092-7.

SCHAFER, F. Q. & BUETTNER, G. R. 2001. Redox environment of the cell as viewed through the redox state of the glutathione disulfide/glutathione couple. *Free Radic Biol Med,* 30**,** 1191-212.

SCHECHTER, R., WHITMIRE, J., WHEET, G. S., BEJU, D., JACKSON, K. W., HARLOW, R. & GAVIN, J. R., 3RD 1994. Immunohistochemical and in situ hybridization study of an insulin-like substance in fetal neuron cell cultures. *Brain Res,* 636**,** 9-27.

SCHINZEL, A. C., TAKEUCHI, O., HUANG, Z., FISHER, J. K., ZHOU, Z., RUBENS, J., HETZ, C., DANIAL, N. N., MOSKOWITZ, M. A. & KORSMEYER, S. J. 2005. Cyclophilin D is a component of mitochondrial permeability transition and mediates neuronal cell death after focal cerebral ischemia. *Proc Natl Acad Sci U S A,* 102**,** 12005-10.

SCHLAEPFER, W. W. & ZIMMERMAN, U. J. 1985. Mechanisms underlying the neuronal response to ischemic injury. Calcium-activated proteolysis of neurofilaments. *Prog Brain Res,* 63**,** 185-96.

SCHMIDT, M., SACHSE, C., RICHTER, W., XU, C., FANDRICH, M. & GRIGORIEFF, N. 2009. Comparison of Alzheimer Abeta(1-40) and Abeta(1-42) amyloid fibrils reveals similar protofilament structures. *Proc Natl Acad Sci U S A,* 106**,** 19813-8.

SCHMOLL, D., FUHRMANN, E., GEBHARDT, R. & HAMPRECHT, B. 1995. Significant amounts of glycogen are synthesized from 3-carbon compounds in astroglial primary cultures from mice with participation of the mitochondrial phosphoenolpyruvate carboxykinase isoenzyme. *Eur J Biochem,* 227**,** 308-15.

SCHRAUFSTATTER, I. U., HYSLOP, P. A., HINSHAW, D. B., SPRAGG, R. G., SKLAR, L. A. & COCHRANE, C. G. 1986. Hydrogen peroxide-induced injury of cells and its prevention by inhibitors of poly(ADP-ribose) polymerase. *Proc Natl Acad Sci U S A,* 83**,** 4908-12.

SCHROETER, H., BOYD, C. S., AHMED, R., SPENCER, J. P., DUNCAN, R. F., RICE-EVANS, C. & CADENAS, E. 2003. c-Jun N-terminal kinase (JNK)-mediated modulation of brain mitochondria function: new target proteins for JNK signalling in mitochondrion-dependent apoptosis. *Biochem J,* 372**,** 359-69.

SCHUBERT, M., GAUTAM, D., SURJO, D., UEKI, K., BAUDLER, S., SCHUBERT, D., KONDO, T., ALBER, J., GALLDIKS, N., KUSTERMANN, E., ARNDT, S., JACOBS, A. H., KRONE, W., KAHN, C. R. & BRUNING, J. C. 2004. Role for neuronal insulin resistance in neurodegenerative diseases. *Proc Natl Acad Sci U S A,* 101**,** 3100-5.

SCHULZ, J. B., LINDENAU, J., SEYFRIED, J. & DICHGANS, J. 2000. Glutathione, oxidative stress and neurodegeneration. *Eur J Biochem,* 267**,** 4904-11.

SCHURR, A., PAYNE, R. S., MILLER, J. J. & RIGOR, B. M. 1997. Brain lactate is an obligatory aerobic energy substrate for functional recovery after hypoxia: further in vitro validation. *J Neurochem,* 69**,** 423-6.

SCOTT, E. M., DUNCAN, I. W. & EKSTRAND, V. 1963. Purification and properties of Glutathione Reductase of human Erythrocytes. *J Biol Chem,* 238**,** 3928-33.

SECHER, N. H. & QUISTORFF, B. 2005. Brain glucose and lactate uptake during exhaustive exercise. *J Physiol,* 568**,** 3.

SEGOVIA, G., PORRAS, A., DEL ARCO, A. & MORA, F. 2001. Glutamatergic neurotransmission in aging: a critical perspective. *Mech Ageing Dev,* 122**,** 1-29.

SELFRIDGE, J. E., E, L., LU, J. & SWERDLOW, R. H. 2013. Role of mitochondrial homeostasis and dynamics in Alzheimer's disease. *Neurobiol Dis,* 51**,** 3-12.

SELKOE, D. J. 2001. Alzheimer's disease: genes, proteins, and therapy. *Physiol Rev,* 81**,** 741-66.

SELKOE, D. J., ABRAHAM, C. R., PODLISNY, M. B. & DUFFY, L. K. 1986. Isolation of low-molecular-weight proteins from amyloid plaque fibers in Alzheimer's disease. *J Neurochem,* 46**,** 1820-34.

SERRA, J. A., DOMINGUEZ, R. O., DE LUSTIG, E. S., GUARESCHI, E. M., FAMULARI, A. L., BARTOLOME, E. L. & MARSCHOFF, E. R. 2001. Parkinson's disease is associated with oxidative stress: comparison of peripheral antioxidant profiles in living Parkinson's, Alzheimer's and vascular dementia patients. *J Neural Transm,* 108**,** 1135-48.

SESHADRI, S., FITZPATRICK, A. L., IKRAM, M. A., DESTEFANO, A. L., GUDNASON, V., BOADA, M., BIS, J. C., SMITH, A. V., CARASSQUILLO, M. M., LAMBERT, J. C., HAROLD, D., SCHRIJVERS, E. M., RAMIREZ-LORCA, R., DEBETTE, S., LONGSTRETH, W. T., JR., JANSSENS, A. C., PANKRATZ, V. S., DARTIGUES, J. F., HOLLINGWORTH, P., ASPELUND, T., HERNANDEZ, I., BEISER, A., KULLER, L. H., KOUDSTAAL, P. J., DICKSON, D. W., TZOURIO, C., ABRAHAM, R., ANTUNEZ, C., DU, Y., ROTTER, J. I., AULCHENKO, Y. S., HARRIS, T. B., PETERSEN, R. C., BERR, C., OWEN, M. J., LOPEZ-ARRIETA, J., VARADARAJAN, B. N., BECKER, J. T., RIVADENEIRA, F., NALLS, M. A., GRAFF-RADFORD, N. R., CAMPION, D., AUERBACH, S., RICE, K., HOFMAN, A., JONSSON, P. V., SCHMIDT, H., LATHROP, M., MOSLEY, T. H., AU, R., PSATY, B. M., UITTERLINDEN, A. G., FARRER, L. A., LUMLEY, T., RUIZ, A., WILLIAMS, J., AMOUYEL, P., YOUNKIN, S. G., WOLF, P. A., LAUNER, L. J., LOPEZ, O. L., VAN DUIJN, C. M. & BRETELER, M. M. 2010. Genome-wide analysis of genetic loci associated with Alzheimer disease. *JAMA,* 303**,** 1832-40.

SEUBERT, P., VIGO-PELFREY, C., ESCH, F., LEE, M., DOVEY, H., DAVIS, D., SINHA, S., SCHLOSSMACHER, M., WHALEY, J., SWINDLEHURST, C. & ET AL. 1992. Isolation and quantification of soluble Alzheimer's beta-peptide from biological fluids. *Nature,* 359**,** 325-7.

SHAH, S., LEE, S. F., TABUCHI, K., HAO, Y. H., YU, C., LAPLANT, Q., BALL, H., DANN, C. E., 3RD, SUDHOF, T. & YU, G. 2005. Nicastrin functions as a gamma-secretase-substrate receptor. *Cell,* 122**,** 435-47.

SHANKAR, G. M., BLOODGOOD, B. L., TOWNSEND, M., WALSH, D. M., SELKOE, D. J. & SABATINI, B. L. 2007. Natural oligomers of the Alzheimer amyloid-beta protein induce reversible synapse loss by modulating an NMDA-type glutamate receptor-dependent signaling pathway. *J Neurosci,* 27**,** 2866-75.

SHANKAR, G. M., LI, S., MEHTA, T. H., GARCIA-MUNOZ, A., SHEPARDSON, N. E., SMITH, I., BRETT, F. M., FARRELL, M. A., ROWAN, M. J., LEMERE, C. A., REGAN, C. M., WALSH, D. M., SABATINI, B. L. & SELKOE, D. J. 2008. Amyloid-beta protein dimers isolated directly from Alzheimer's brains impair synaptic plasticity and memory. *Nat Med,* 14**,** 837-42.

SHANKAR, G. M. & WALSH, D. M. 2009. Alzheimer's disease: synaptic dysfunction and Abeta. *Mol Neurodegener,* 4**,** 48.

SHI, Y., KIRWAN, P., SMITH, J., ROBINSON, H. P. & LIVESEY, F. J. 2012. Human cerebral cortex development from pluripotent stem cells to functional excitatory synapses. *Nat Neurosci,* 15**,** 477-86, S1.

SHIPTON, O. A., LEITZ, J. R., DWORZAK, J., ACTON, C. E., TUNBRIDGE, E. M., DENK, F., DAWSON, H. N., VITEK, M. P., WADE-MARTINS, R., PAULSEN, O. & VARGAS-CABALLERO, M. 2011. Tau protein is required for amyloid {beta}-induced impairment of hippocampal long-term potentiation. *J Neurosci,* 31**,** 1688-92.

SHOFFNER, J. M. 1997. Oxidative phosphorylation defects and Alzheimer's disease. *Neurogenetics,* 1**,** 13-9.

SHOJI, M., GOLDE, T. E., GHISO, J., CHEUNG, T. T., ESTUS, S., SHAFFER, L. M., CAI, X. D., MCKAY, D. M., TINTNER, R., FRANGIONE, B. & ET AL. 1992. Production of the

Alzheimer amyloid beta protein by normal proteolytic processing. *Science,* 258**,** 126-9.

SHULMAN, R. G., HYDER, F. & ROTHMAN, D. L. 2001. Cerebral energetics and the glycogen shunt: neurochemical basis of functional imaging. *Proc Natl Acad Sci U S A,* 98**,** 6417-22.

SHULMAN, R. G., ROTHMAN, D. L., BEHAR, K. L. & HYDER, F. 2004. Energetic basis of brain activity: implications for neuroimaging. *Trends Neurosci,* 27**,** 489-95.

SIMPSON, I. A., CHUNDU, K. R., DAVIES-HILL, T., HONER, W. G. & DAVIES, P. 1994. Decreased concentrations of GLUT1 and GLUT3 glucose transporters in the brains of patients with Alzheimer's disease. *Ann Neurol,* 35**,** 546-551.

SIMS, N. R., BLASS, J. P., MURPHY, C., BOWEN, D. M. & NEARY, D. 1987. Phosphofructokinase activity in the brain in Alzheimer's disease. *Ann Neurol,* 21**,** 509-10.

SIMS, N. R., BOWEN, D. M. & DAVISON, A. N. 1981. [14C]acetylcholine synthesis and [14C]carbon dioxide production from [U-14C]glucose by tissue prisms from human neocortex. *Biochem J,* 196**,** 867-76.

SIMS, N. R., BOWEN, D. M., NEARY, D. & DAVISON, A. N. 1983. Metabolic processes in Alzheimer's disease: adenine nucleotide content and production of 14CO2 from [U-14C]glucose in vitro in human neocortex. *J Neurochem,* 41**,** 1329-34.

SINHA, S., ANDERSON, J. P., BARBOUR, R., BASI, G. S., CACCAVELLO, R., DAVIS, D., DOAN, M., DOVEY, H. F., FRIGON, N., HONG, J., JACOBSON-CROAK, K., JEWETT, N., KEIM, P., KNOPS, J., LIEBERBURG, I., POWER, M., TAN, H., TATSUNO, G., TUNG, J., SCHENK, D., SEUBERT, P., SUOMENSAARI, S. M., WANG, S., WALKER, D., ZHAO, J., MCCONLOGUE, L. & JOHN, V. 1999. Purification and cloning of amyloid precursor protein beta-secretase from human brain. *Nature,* 402**,** 537-40.

SISODIA, S. S. 1992. Beta-amyloid precursor protein cleavage by a membrane-bound protease. *Proc Natl Acad Sci U S A,* 89**,** 6075-9.

SKEBERDIS, V. A., LAN, J., ZHENG, X., ZUKIN, R. S. & BENNETT, M. V. 2001. Insulin promotes rapid delivery of N-methyl-D- aspartate receptors to the cell surface by exocytosis. *Proc Natl Acad Sci U S A,* 98**,** 3561-6.

SLUNT, H. H., THINAKARAN, G., VON KOCH, C., LO, A. C., TANZI, R. E. & SISODIA, S. S. 1994. Expression of a ubiquitous, cross-reactive homologue of the mouse beta-amyloid precursor protein (APP). *J Biol Chem,* 269**,** 2637-44.

SMALL, G. W., ERCOLI, L. M., SILVERMAN, D. H., HUANG, S. C., KOMO, S., BOOKHEIMER, S. Y., LAVRETSKY, H., MILLER, K., SIDDARTH, P., RASGON, N. L., MAZZIOTTA, J. C., SAXENA, S., WU, H. M., MEGA, M. S., CUMMINGS, J. L., SAUNDERS, A. M., PERICAK-VANCE, M. A., ROSES, A. D., BARRIO, J. R. & PHELPS, M. E. 2000. Cerebral metabolic and cognitive decline in persons at genetic risk for Alzheimer's disease. *Proc Natl Acad Sci U S A,* 97**,** 6037-42.

SMALL, G. W., MAZZIOTTA, J. C., COLLINS, M. T., BAXTER, L. R., PHELPS, M. E., MANDELKERN, M. A., KAPLAN, A., LA RUE, A., ADAMSON, C. F., CHANG, L. & ET AL. 1995. Apolipoprotein E type 4 allele and cerebral glucose metabolism in relatives at risk for familial Alzheimer disease. *JAMA,* 273**,** 942-7.

SMILLIE, K. J. & COUSIN, M. A. 2011. The Role of GSK3 in Presynaptic Function. *Int J Alzheimers Dis,* 2011**,** 263673.

SMITH, C. D., CARNEY, J. M., STARKE-REED, P. E., OLIVER, C. N., STADTMAN, E. R., FLOYD, R. A. & MARKESBERY, W. R. 1991. Excess brain protein oxidation and enzyme dysfunction in normal aging and in Alzheimer disease. *Proc Natl Acad Sci U S A,* 88**,** 10540-3.

SMITH, M. A., HARRIS, P. L., SAYRE, L. M. & PERRY, G. 1997. Iron accumulation in Alzheimer disease is a source of redox-generated free radicals. *Proc Natl Acad Sci U S A,* 94**,** 9866-8.

SMITH, M. A., NUNOMURA, A., ZHU, X., TAKEDA, A. & PERRY, G. 2000. Metabolic, metallic, and mitotic sources of oxidative stress in Alzheimer disease. *Antioxid Redox Signal,* 2**,** 413-20.

SMITH, R. P., HIGUCHI, D. A. & BROZE, G. J., JR. 1990. Platelet coagulation factor XIa-inhibitor, a form of Alzheimer amyloid precursor protein. *Science,* 248**,** 1126-8.

SNYDER, S. W., LADROR, U. S., WADE, W. S., WANG, G. T., BARRETT, L. W., MATAYOSHI, E. D., HUFFAKER, H. J., KRAFFT, G. A. & HOLZMAN, T. F. 1994.

Amyloid-beta aggregation: selective inhibition of aggregation in mixtures of amyloid with different chain lengths. *Biophys J,* 67**,** 1216-28.

SOLANO, D. C., SIRONI, M., BONFINI, C., SOLERTE, S. B., GOVONI, S. & RACCHI, M. 2000. Insulin regulates soluble amyloid precursor protein release via phosphatidyl inositol 3 kinase-dependent pathway. *FASEB J,* 14**,** 1015-22.

SOMMERFIELD, A. J., DEARY, I. J., MCAULAY, V. & FRIER, B. M. 2003. Moderate hypoglycemia impairs multiple memory functions in healthy adults. *Neuropsychology,* 17**,** 125-32.

SORBI, S., BIRD, E. D. & BLASS, J. P. 1983. Decreased pyruvate dehydrogenase complex activity in Huntington and Alzheimer brain. *Ann Neurol,* 13**,** 72-8.

SORG, O. & MAGISTRETTI, P. J. 1992. Vasoactive intestinal peptide and noradrenaline exert long-term control on glycogen levels in astrocytes: blockade by protein synthesis inhibition. *J Neurosci,* 12**,** 4923-31.

SOTELO, C. & PALAY, S. L. 1968. The fine structure of the lateral vestibular nucleus in the rat : I. Neurons and Neuroglial Cells. *J Cell Biol,* 36**,** 151-79.

SPILLANTINI, M. G., DIVANE, A. & GOEDERT, M. 1995. Assignment of human alpha-synuclein (SNCA) and beta-synuclein (SNCB) genes to chromosomes 4q21 and 5q35. *Genomics,* 27**,** 379-81.

STEFANATOS, R. & SANZ, A. 2011. Mitochondrial complex I: a central regulator of the aging process. *Cell Cycle,* 10**,** 1528-32.

STEVENS, B. 2008. Neuron-astrocyte signaling in the development and plasticity of neural circuits. *Neurosignals,* 16**,** 278-88.

STOLTENBERG, M., BUSH, A. I., BACH, G., SMIDT, K., LARSEN, A., RUNGBY, J., LUND, S., DOERING, P. & DANSCHER, G. 2007. Amyloid plaques arise from zinc-enriched cortical layers in APP/PS1 transgenic mice and are paradoxically enlarged with dietary zinc deficiency. *Neuroscience,* 150**,** 357-69.

STONE, W. S., COTTRILL, K. L., WALKER, D. L. & GOLD, P. E. 1988. Blood glucose and brain function: interactions with CNS cholinergic systems. *Behav Neural Biol,* 50**,** 325-34.

STORZ, P. 2006. Reactive oxygen species-mediated mitochondria-to-nucleus signaling: a key to aging and radical-caused diseases. *Sci STKE,* 2006**,** re3.

STRELTSOV, V. A., VARGHESE, J. N., MASTERS, C. L. & NUTTALL, S. D. 2011. Crystal structure of the amyloid-beta p3 fragment provides a model for oligomer formation in Alzheimer's disease. *J Neurosci,* 31**,** 1419-26.

STRUBLE, R. G., ALA, T., PATRYLO, P. R., BREWER, G. J. & YAN, X. X. 2010. Is brain amyloid production a cause or a result of dementia of the Alzheimer's type? *J Alzheimers Dis,* 22**,** 393-9.

SUEMORI, I. 1975. Experimental study of dibutyryl cyclic AMP; its metabolic effects observed in anesthetized human subjects. *Tohoku J Exp Med,* 117**,** 111-8.

SUH, S. W., AOYAMA, K., MATSUMORI, Y., LIU, J. & SWANSON, R. A. 2005. Pyruvate administered after severe hypoglycemia reduces neuronal death and cognitive impairment. *Diabetes,* 54**,** 1452-8.

SUH, Y. H. & CHECLER, F. 2002. Amyloid precursor protein, presenilins, and alpha-synuclein: molecular pathogenesis and pharmacological applications in Alzheimer's disease. *Pharmacol Rev,* 54**,** 469-525.

SUNRAM-LEA, S. I., FOSTER, J. K., DURLACH, P. & PEREZ, C. 2002. The effect of retrograde and anterograde glucose administration on memory performance in healthy young adults. *Behav Brain Res,* 134**,** 505-16.

SURESHBABU, N., KIRUBAGARAN, R., THANGARAJAH, H., MALAR, E. J. & JAYAKUMAR, R. 2010. Lipid-induced conformational transition of amyloid beta peptide fragments. *J Mol Neurosci,* 41**,** 368-82.

SUZUKI, A., STERN, S. A., BOZDAGI, O., HUNTLEY, G. W., WALKER, R. H., MAGISTRETTI, P. J. & ALBERINI, C. M. 2011. Astrocyte-neuron lactate transport is required for long-term memory formation. *Cell,* 144**,** 810-23.

SWANSON, R. A. 1992a. Astrocyte glutamate uptake during chemical hypoxia in vitro. *Neurosci Lett,* 147**,** 143-6.

SWANSON, R. A. 1992b. Physiologic coupling of glial glycogen metabolism to neuronal activity in brain. *Can J Physiol Pharmacol,* 70 Suppl**,** S138-44.

SWANSON, R. A., MORTON, M. M., SAGAR, S. M. & SHARP, F. R. 1992. Sensory stimulation induces local cerebral glycogenolysis: Demonstration by autoradiography. *Neuroscience,* 51**,** 451-461.

SWERDLOW, R. H. & KHAN, S. M. 2004. A "mitochondrial cascade hypothesis" for sporadic Alzheimer's disease. *Med Hypotheses,* 63**,** 8-20.

SWERDLOW, R. H., PARKS, J. K., CASSARINO, D. S., MAGUIRE, D. J., MAGUIRE, R. S., BENNETT, J. P., JR., DAVIS, R. E. & PARKER, W. D., JR. 1997. Cybrids in Alzheimer's disease: a cellular model of the disease? *Neurology,* 49**,** 918-25.

TABERNERO, A., GIAUME, C. & MEDINA, J. M. 1996. Endothelin-1 regulates glucose utilization in cultured astrocytes by controlling intercellular communication through gap junctions. *Glia,* 16**,** 187-95.

TABERNERO, A., MEDINA, J. M. & GIAUME, C. 2006. Glucose metabolism and proliferation in glia: role of astrocytic gap junctions. *J Neurochem,* 99**,** 1049-61.

TAKAHASHI, K. & YAMANAKA, S. 2006. Induction of pluripotent stem cells from mouse embryonic and adult fibroblast cultures by defined factors. *Cell,* 126**,** 663-76.

TAKASHIMA, A., NOGUCHI, K., SATO, K., HOSHINO, T. & IMAHORI, K. 1993. Tau protein kinase I is essential for amyloid beta-protein-induced neurotoxicity. *Proc Natl Acad Sci U S A,* 90**,** 7789-93.

TAKUMA, K., YAO, J., HUANG, J., XU, H., CHEN, X., LUDDY, J., TRILLAT, A. C., STERN, D. M., ARANCIO, O. & YAN, S. S. 2005. ABAD enhances Abeta-induced cell stress via mitochondrial dysfunction. *FASEB J,* 19**,** 597-8.

TAMAGNO, E., PAROLA, M., BARDINI, P., PICCINI, A., BORGHI, R., GUGLIELMOTTO, M., SANTORO, G., DAVIT, A., DANNI, O., SMITH, M. A., PERRY, G. & TABATON, M. 2005. Beta-site APP cleaving enzyme up-regulation induced by 4-hydroxynonenal is mediated by stress-activated protein kinases pathways. *J Neurochem,* 92**,** 628-36.

TANZI, R. E., MOIR, R. D. & WAGNER, S. L. 2004. Clearance of Alzheimer's Abeta peptide: the many roads to perdition. *Neuron,* 43**,** 605-8.

TAYLOR, E. R., HURRELL, F., SHANNON, R. J., LIN, T. K., HIRST, J. & MURPHY, M. P. 2003. Reversible glutathionylation of complex I increases mitochondrial superoxide formation. *J Biol Chem,* 278**,** 19603-10.

TERRY, A. V., JR. & BUCCAFUSCO, J. J. 2003. The cholinergic hypothesis of age and Alzheimer's disease-related cognitive deficits: recent challenges and their implications for novel drug development. *J Pharmacol Exp Ther,* 306**,** 821-7.

TERWEL, D., MUYLLAERT, D., DEWACHTER, I., BORGHGRAEF, P., CROES, S., DEVIJVER, H. & VAN LEUVEN, F. 2008. Amyloid activates GSK-3beta to aggravate neuronal tauopathy in bigenic mice. *Am J Pathol,* 172**,** 786-98.

THANNICKAL, V. J. & FANBURG, B. L. 2000. Reactive oxygen species in cell signaling. *Am J Physiol Lung Cell Mol Physiol,* 279**,** L1005-28.

THORNS, V., MALLORY, M., HANSEN, L. & MASLIAH, E. 1997. Alterations in glutamate receptor 2/3 subunits and amyloid precursor protein expression during the course of Alzheimer's disease and Lewy body variant. *Acta Neuropathol,* 94**,** 539-48.

TIETZE, F. 1969. Enzymic method for quantitative determination of nanogram amounts of total and oxidized glutathione: Applications to mammalian blood and other tissues. *Analytical Biochemistry,* 27**,** 502-522.

TIEU, K., PERIER, C., VILA, M., CASPERSEN, C., ZHANG, H. P., TEISMANN, P., JACKSON-LEWIS, V., STERN, D. M., YAN, S. D. & PRZEDBORSKI, S. 2004. L-3-hydroxyacyl-CoA dehydrogenase II protects in a model of Parkinson's disease. *Ann Neurol,* 56**,** 51-60.

TOMITSUKA, E., HIRAWAKE, H., GOTO, Y., TANIWAKI, M., HARADA, S. & KITA, K. 2003. Direct evidence for two distinct forms of the flavoprotein subunit of human mitochondrial complex II (succinate-ubiquinone reductase). *J Biochem,* 134**,** 191-5.

TOUGU, V., KARAFIN, A., ZOVO, K., CHUNG, R. S., HOWELLS, C., WEST, A. K. & PALUMAA, P. 2009. Zn(II)- and Cu(II)-induced non-fibrillar aggregates of amyloid-beta (1-42) peptide are transformed to amyloid fibrils, both spontaneously and under the influence of metal chelators. *J Neurochem,* 110**,** 1784-95.

TOWNSEND, M., SHANKAR, G. M., MEHTA, T., WALSH, D. M. & SELKOE, D. J. 2006. Effects of secreted oligomers of amyloid beta-protein on hippocampal synaptic plasticity: a potent role for trimers. *Journal of Physiology-London,* 572**,** 477-492.

TRETTER, L. & ADAM-VIZI, V. 2000. Inhibition of Krebs cycle enzymes by hydrogen peroxide: A key role of [alpha]-ketoglutarate dehydrogenase in limiting NADH production under oxidative stress. *J Neurosci,* 20**,** 8972-9.

TURNER, A. J., ISAAC, R. E. & COATES, D. 2001. The neprilysin (NEP) family of zinc metalloendopeptidases: genomics and function. *Bioessays,* 23**,** 261-9.

TURNER, D. A. & ADAMSON, D. C. 2011. Neuronal-astrocyte metabolic interactions: understanding the transition into abnormal astrocytoma metabolism. *J Neuropathol Exp Neurol,* 70**,** 167-76.

TURNER, R. S., SUZUKI, N., CHYUNG, A. S., YOUNKIN, S. G. & LEE, V. M. 1996. Amyloids beta40 and beta42 are generated intracellularly in cultured human neurons and their secretion increases with maturation. *J Biol Chem,* 271**,** 8966-70.

UEDA, K., FUKUSHIMA, H., MASLIAH, E., XIA, Y., IWAI, A., YOSHIMOTO, M., OTERO, D. A., KONDO, J., IHARA, Y. & SAITOH, T. 1993. Molecular cloning of cDNA encoding an unrecognized component of amyloid in Alzheimer disease. *Proc Natl Acad Sci U S A,* 90**,** 11282-6.

UEMURA, E. & GREENLEE, H. W. 2001. Amyloid beta-peptide inhibits neuronal glucose uptake by preventing exocytosis. *Exp Neurol,* 170**,** 270-6.

UL-HAQ, Z., KHAN, W., KALSOOM, S. & ANSARI, F. L. 2010. In silico modeling of the specific inhibitory potential of thiophene-2,3-dihydro-1,5-benzothiazepine against BChE in the formation of beta-amyloid plaques associated with Alzheimer's disease. *Theor Biol Med Model,* 7**,** 22.

UMEGAKI, H., USHIDA, C., IKARI, H., OGAWA, O., NAKAMURA, A., SUZUKI, Y., ENDO, H., AKATSU, H., YAMAMOTO, T. & IGUCHI, A. 2002. Plasma insulin and glucose levels in elderly female subjects with Alzheimer's disease. *Geriatrics & Gerontology International,* 2**,** 75-79.

UNGER, J. W., LIVINGSTON, J. N. & MOSS, A. M. 1991. Insulin receptors in the central nervous system: localization, signalling mechanisms and functional aspects. *Prog Neurobiol,* 36**,** 343-62.

VAN DAM, D. & DE DEYN, P. P. 2011. Animal models in the drug discovery pipeline for Alzheimer's disease. *Br J Pharmacol,* 164**,** 1285-300.

VANNUCCI, S. J., KOEHLER-STEC, E. M., LI, K., REYNOLDS, T. H., CLARK, R. & SIMPSON, I. A. 1998. GLUT4 glucose transporter expression in rodent brain: effect of diabetes. *Brain Res,* 797**,** 1-11.

VANNUCCI, S. J., MAHER, F. & SIMPSON, I. A. 1997. Glucose transporter proteins in brain: delivery of glucose to neurons and glia. *Glia,* 21**,** 2-21.

VARADARAJAN, S., YATIN, S., AKSENOVA, M. & BUTTERFIELD, D. A. 2000. Alzheimer's amyloid beta-peptide-associated free radical oxidative stress and neurotoxicity. *J Struct Biol,* 130**,** 184-208.

VASSAR, R., BENNETT, B. D., BABU-KHAN, S., KAHN, S., MENDIAZ, E. A., DENIS, P., TEPLOW, D. B., ROSS, S., AMARANTE, P., LOELOFF, R., LUO, Y., FISHER, S., FULLER, J., EDENSON, S., LILE, J., JAROSINSKI, M. A., BIERE, A. L., CURRAN, E., BURGESS, T., LOUIS, J. C., COLLINS, F., TREANOR, J., ROGERS, G. & CITRON, M. 1999. Beta-secretase cleavage of Alzheimer's amyloid precursor protein by the transmembrane aspartic protease BACE. *Science,* 286**,** 735-41.

VEKRELLIS, K., YE, Z., QIU, W. Q., WALSH, D., HARTLEY, D., CHESNEAU, V., ROSNER, M. R. & SELKOE, D. J. 2000. Neurons regulate extracellular levels of amyloid beta-protein via proteolysis by insulin-degrading enzyme. *J Neurosci,* 20**,** 1657-65.

VELLIQUETTE, R. A., O'CONNOR, T. & VASSAR, R. 2005. Energy inhibition elevates beta-secretase levels and activity and is potentially amyloidogenic in APP transgenic mice: possible early events in Alzheimer's disease pathogenesis. *J Neurosci,* 25**,** 10874-83.

VENDEMIALE, G., GRATTAGLIANO, I. & ALTOMARE, E. 1999. An update on the role of free radicals and antioxidant defense in human disease. *Int J Clin Lab Res,* 29**,** 49-55.

VERGUN, O. 2007. Studies elucidating the mechanisms of calcium induced mitochondrial depolarization in individual isolated brain mitochondria. *Biochemistry (Moscow) Supplement Series A: Membrane and Cell Biology,* 1**,** 38-44.

VERKHRATSKY, A. & BUTT, A. 2013. Neuroglia: Definition, Classification, Evolution, Numbers, Development. *Glial Physiology and Pathophysiology.* John Wiley & Sons, Ltd.

VILCHEZ, D., ROS, S., CIFUENTES, D., PUJADAS, L., VALLES, J., GARCIA-FOJEDA, B., CRIADO-GARCIA, O., FERNANDEZ-SANCHEZ, E., MEDRANO-FERNANDEZ, I.,

DOMINGUEZ, J., GARCIA-ROCHA, M., SORIANO, E., RODRIGUEZ DE CORDOBA, S. & GUINOVART, J. J. 2007. Mechanism suppressing glycogen synthesis in neurons and its demise in progressive myoclonus epilepsy. *Nat Neurosci,* 10**,** 1407-13.

VIRAG, L. & SZABO, C. 2002. The therapeutic potential of poly(ADP-ribose) polymerase inhibitors. *Pharmacol Rev,* 54**,** 375-429.

VOLTERRA, A. & MELDOLESI, J. 2005. Astrocytes, from brain glue to communication elements: the revolution continues. *Nat Rev Neurosci,* 6**,** 626-40.

VOLTERRA, A., TROTTI, D., TROMBA, C., FLORIDI, S. & RACAGNI, G. 1994. Glutamate uptake inhibition by oxygen free radicals in rat cortical astrocytes. *J Neurosci,* 14**,** 2924-32.

VON ROTZ, R. C., KOHLI, B. M., BOSSET, J., MEIER, M., SUZUKI, T., NITSCH, R. M. & KONIETZKO, U. 2004. The APP intracellular domain forms nuclear multiprotein complexes and regulates the transcription of its own precursor. *J Cell Sci,* 117**,** 4435-48.

VOSSEL, K. A., ZHANG, K., BRODBECK, J., DAUB, A. C., SHARMA, P., FINKBEINER, S., CUI, B. & MUCKE, L. 2010. Tau reduction prevents Abeta-induced defects in axonal transport. *Science,* 330**,** 198.

WAAGEPETERSEN, H. S., QU, H., SONNEWALD, U., SHIMAMOTO, K. & SCHOUSBOE, A. 2005. Role of glutamine and neuronal glutamate uptake in glutamate homeostasis and synthesis during vesicular release in cultured glutamatergic neurons. *Neurochem Int,* 47**,** 92-102.

WALLS, A. B., SICKMANN, H. M., BROWN, A., BOUMAN, S. D., RANSOM, B., SCHOUSBOE, A. & WAAGEPETERSEN, H. S. 2008. Characterization of 1,4-dideoxy-1,4-imino-d-arabinitol (DAB) as an inhibitor of brain glycogen shunt activity. *J Neurochem,* 105**,** 1462-70.

WALLS, K. C., COSKUN, P., GALLEGOS-PEREZ, J. L., ZADOURIAN, N., FREUDE, K., RASOOL, S., BLURTON-JONES, M., GREEN, K. N. & LAFERLA, F. M. 2012. Swedish Alzheimer mutation induces mitochondrial dysfunction mediated by HSP60 mislocalization of amyloid precursor protein (APP) and beta-amyloid. *J Biol Chem,* 287**,** 30317-27.

WALSH, D. M., KLYUBIN, I., FADEEVA, J. V., CULLEN, W. K., ANWYL, R., WOLFE, M. S., ROWAN, M. J. & SELKOE, D. J. 2002. Naturally secreted oligomers of amyloid [beta] protein potently inhibit hippocampal long-term potentiation in vivo. *Nature,* 416**,** 535-539.

WALSH, D. M., LOMAKIN, A., BENEDEK, G. B., CONDRON, M. M. & TEPLOW, D. B. 1997. Amyloid beta-protein fibrillogenesis. Detection of a protofibrillar intermediate. *J Biol Chem,* 272**,** 22364-72.

WALSH, D. M., THULIN, E., MINOGUE, A. M., GUSTAVSSON, N., PANG, E., TEPLOW, D. B. & LINSE, S. 2009. A facile method for expression and purification of the Alzheimer's disease-associated amyloid beta-peptide. *FEBS J,* 276**,** 1266-81.

WALTER, J., FLUHRER, R., HARTUNG, B., WILLEM, M., KAETHER, C., CAPELL, A., LAMMICH, S., MULTHAUP, G. & HAASS, C. 2001. Phosphorylation regulates intracellular trafficking of beta-secretase. *J Biol Chem,* 276**,** 14634-41.

WALTON, H. S. & DODD, P. R. 2007. Glutamate-glutamine cycling in Alzheimer's disease. *Neurochem Int,* 50**,** 1052-66.

WANG, H. & DOERING, L. C. 2012. Induced pluripotent stem cells to model and treat neurogenetic disorders. *Neural Plast,* 2012**,** 346053.

WANG, H., SHIMOJI, M., YU, S. W., DAWSON, T. M. & DAWSON, V. L. 2003. Apoptosis inducing factor and PARP-mediated injury in the MPTP mouse model of Parkinson's disease. *Ann N Y Acad Sci,* 991**,** 132-9.

WANG, J., DICKSON, D. W., TROJANOWSKI, J. Q. & LEE, V. M. 1999. The levels of soluble versus insoluble brain Abeta distinguish Alzheimer's disease from normal and pathologic aging. *Exp Neurol,* 158**,** 328-37.

WANG, R., MESCHIA, J. F., COTTER, R. J. & SISODIA, S. S. 1991. Secretion of the beta/A4 amyloid precursor protein. Identification of a cleavage site in cultured mammalian cells. *J Biol Chem,* 266**,** 16960-4.

WANG, X., PEREZ, E., LIU, R., YAN, L. J., MALLET, R. T. & YANG, S. H. 2007. Pyruvate protects mitochondria from oxidative stress in human neuroblastoma SK-N-SH cells. *Brain Res,* 1132**,** 1-9.

292

WATSON, G. S. & CRAFT, S. 2004. Modulation of memory by insulin and glucose: neuropsychological observations in Alzheimer's disease. *Eur J Pharmacol,* 490**,** 97-113.

WATSON, G. S., PESKIND, E. R., ASTHANA, S., PURGANAN, K., WAIT, C., CHAPMAN, D., SCHWARTZ, M. W., PLYMATE, S. & CRAFT, S. 2003. Insulin increases CSF Abeta42 levels in normal older adults. *Neurology,* 60**,** 1899-903.

WAVRANT-DEVRIEZE, F., RUDRASINGHAM, V., LAMBERT, J. C., CHAKRAVERTY, S., KEHOE, P., CROOK, R., AMOUYEL, P., WU, W., HOLMANS, P., RICE, F., PEREZ-TUR, J., FRIGARD, B., MORRIS, J. C., CARTY, S., COTTEL, D., TUNSTALL, N., LOVESTONE, S., PETERSEN, R. C., CHARTIER-HARLIN, M. C., GOATE, A., OWEN, M. J., WILLIAMS, J. & HARDY, J. 1999. No association between the alpha-2 macroglobulin I1000V polymorphism and Alzheimer's disease. *Neurosci Lett,* 262**,** 137-9.

WEIDEMANN, A., EGGERT, S., REINHARD, F. B., VOGEL, M., PALIGA, K., BAIER, G., MASTERS, C. L., BEYREUTHER, K. & EVIN, G. 2002. A novel epsilon-cleavage within the transmembrane domain of the Alzheimer amyloid precursor protein demonstrates homology with Notch processing. *Biochemistry,* 41**,** 2825-35.

WEIDEMANN, A., KONIG, G., BUNKE, D., FISCHER, P., SALBAUM, J. M., MASTERS, C. L. & BEYREUTHER, K. 1989. Identification, biogenesis, and localization of precursors of Alzheimer's disease A4 amyloid protein. *Cell,* 57**,** 115-26.

WENDER, R., BROWN, A. M., FERN, R., SWANSON, R. A., FARRELL, K. & RANSOM, B. R. 2000. Astrocytic glycogen influences axon function and survival during glucose deprivation in central white matter. *J Neurosci,* 20**,** 6804-10.

WERTKIN, A. M., TURNER, R. S., PLEASURE, S. J., GOLDE, T. E., YOUNKIN, S. G., TROJANOWSKI, J. Q. & LEE, V. M. 1993. Human neurons derived from a teratocarcinoma cell line express solely the 695-amino acid amyloid precursor protein and produce intracellular beta-amyloid or A4 peptides. *Proc Natl Acad Sci U S A,* 90**,** 9513-7.

WICHTERLE, H. & PRZEDBORSKI, S. 2010. What can pluripotent stem cells teach us about neurodegenerative diseases? *Nat Neurosci,* 13**,** 800-4.

WIESINGER, H., HAMPRECHT, B. & DRINGEN, R. 1997. Metabolic pathways for glucose in astrocytes. *Glia,* 21**,** 22-34.

WILD-BODE, C., FELLERER, K., KUGLER, J., HAASS, C. & CAPELL, A. 2006. A basolateral sorting signal directs ADAM10 to adherens junctions and is required for its function in cell migration. *J Biol Chem,* 281**,** 23824-9.

WILLE, H., PRUSINER, S. B. & COHEN, F. E. 2000. Scrapie infectivity is independent of amyloid staining properties of the N-terminally truncated prion protein. *J Struct Biol,* 130**,** 323-38.

WILLEM, M., GARRATT, A. N., NOVAK, B., CITRON, M., KAUFMANN, S., RITTGER, A., DESTROOPER, B., SAFTIG, P., BIRCHMEIER, C. & HAASS, C. 2006. Control of peripheral nerve myelination by the beta-secretase BACE1. *Science,* 314**,** 664-6.

WILLIAMS, K. J., FLESS, G. M., PETRIE, K. A., SNYDER, M. L., BROCIA, R. W. & SWENSON, T. L. 1992. Mechanisms by which lipoprotein lipase alters cellular metabolism of lipoprotein(a), low density lipoprotein, and nascent lipoproteins. Roles for low density lipoprotein receptors and heparan sulfate proteoglycans. *J Biol Chem,* 267**,** 13284-92.

WOBUS, A. M. & BOHELER, K. R. 2005. Embryonic stem cells: prospects for developmental biology and cell therapy. *Physiol Rev,* 85**,** 635-78.

WOEHRLING, E. K., HILL, E. J. & COLEMAN, M. D. 2007. Development of a neurotoxicity test-system, using human post-mitotic, astrocytic and neuronal cell lines in co-culture. *Toxicol In Vitro,* 21**,** 1241-6.

WOEHRLING, E. K., HILL, E. J. & COLEMAN, M. D. 2010. Evaluation of the importance of astrocytes when screening for acute toxicity in neuronal cell systems. *Neurotox Res,* 17**,** 103-13.

WOLFE, M. S., XIA, W., OSTASZEWSKI, B. L., DIEHL, T. S., KIMBERLY, W. T. & SELKOE, D. J. 1999. Two transmembrane aspartates in presenilin-1 required for presenilin endoproteolysis and gamma-secretase activity. *Nature,* 398**,** 513-7.

WONG-RILEY, M., ANTUONO, P., HO, K.-C., EGAN, R., HEVNER, R., LIEBL, W., HUANG, Z., RACHEL, R. & JONES, J. 1997. Cytochrome oxidase in Alzheimer's disease:

Biochemical, histochemical, and immunohistochemical analyses of the visual and other systems. *Vision Research,* 37**,** 3593-3608.

WONG-RILEY, M. T. 1989. Cytochrome oxidase: an endogenous metabolic marker for neuronal activity. *Trends Neurosci,* 12**,** 94-101.

WOODS, S. C., SEELEY, R. J., BASKIN, D. G. & SCHWARTZ, M. W. 2003. Insulin and the blood-brain barrier. *Curr Pharm Des,* 9**,** 795-800.

WRAY, S., SELF, M., LEWIS, P. A., TAANMAN, J. W., RYAN, N. S., MAHONEY, C. J., LIANG, Y., DEVINE, M. J., SHEERIN, U. M., HOULDEN, H., MORRIS, H. R., HEALY, D., MARTI-MASSO, J. F., PREZA, E., BARKER, S., SUTHERLAND, M., CORRIVEAU, R. A., D'ANDREA, M., SCHAPIRA, A. H., UITTI, R. J., GUTTMAN, M., OPALA, G., JASINSKA-MYGA, B., PUSCHMANN, A., NILSSON, C., ESPAY, A. J., SLAWEK, J., GUTMANN, L., BOEVE, B. F., BOYLAN, K., STOESSL, A. J., ROSS, O. A., MARAGAKIS, N. J., VAN GERPEN, J., GERSTENHABER, M., GWINN, K., DAWSON, T. M., ISACSON, O., MARDER, K. S., CLARK, L. N., PRZEDBORSKI, S. E., FINKBEINER, S., ROTHSTEIN, J. D., WSZOLEK, Z. K., ROSSOR, M. N. & HARDY, J. 2012. Creation of an open-access, mutation-defined fibroblast resource for neurological disease research. *PLoS One,* 7**,** e43099.

WRIGHT, C. I., GEULA, C. & MESULAM, M. M. 1993. Neurological cholinesterases in the normal brain and in Alzheimer's disease: relationship to plaques, tangles, and patterns of selective vulnerability. *Ann Neurol,* 34**,** 373-84.

WYSS-CORAY, T. 2006. Inflammation in Alzheimer disease: driving force, bystander or beneficial response? *Nat Med,* 12**,** 1005-15.

XI, J., LIU, Y., LIU, H., CHEN, H., EMBORG, M. E. & ZHANG, S. C. 2012. Specification of midbrain dopamine neurons from primate pluripotent stem cells. *Stem Cells,* 30**,** 1655-63.

XU, Y., OLA, M. S., BERKICH, D. A., GARDNER, T. W., BARBER, A. J., PALMIERI, F., HUTSON, S. M. & LANOUE, K. F. 2007. Energy sources for glutamate neurotransmission in the retina: absence of the aspartate/glutamate carrier produces reliance on glycolysis in glia. *J Neurochem,* 101**,** 120-31.

YAGI, T., ITO, D., OKADA, Y., AKAMATSU, W., NIHEI, Y., YOSHIZAKI, T., YAMANAKA, S., OKANO, H. & SUZUKI, N. 2011. Modeling familial Alzheimer's disease with induced pluripotent stem cells. *Hum Mol Genet,* 20**,** 4530-9.

YAN, S. D., FU, J., SOTO, C., CHEN, X., ZHU, H., AL-MOHANNA, F., COLLISON, K., ZHU, A., STERN, E., SAIDO, T., TOHYAMA, M., OGAWA, S., ROHER, A. & STERN, D. 1997. An intracellular protein that binds amyloid-beta peptide and mediates neurotoxicity in Alzheimer's disease. *Nature,* 389**,** 689-95.

YAN, S. D., SHI, Y., ZHU, A., FU, J., ZHU, H., ZHU, Y., GIBSON, L., STERN, E., COLLISON, K., AL-MOHANNA, F., OGAWA, S., ROHER, A., CLARKE, S. G. & STERN, D. M. 1999. Role of ERAB/L-3-hydroxyacyl-coenzyme A dehydrogenase type II activity in Abeta-induced cytotoxicity. *J Biol Chem,* 274**,** 2145-56.

YAN, X. X., XIONG, K., LUO, X. G., STRUBLE, R. G. & CLOUGH, R. W. 2007. beta-Secretase expression in normal and functionally deprived rat olfactory bulbs: inverse correlation with oxidative metabolic activity. *J Comp Neurol,* 501**,** 52-69.

YANG, A. J., CHANDSWANGBHUVANA, D., MARGOL, L. & GLABE, C. G. 1998. Loss of endosomal/lysosomal membrane impermeability is an early event in amyloid Abeta1-42 pathogenesis. *J Neurosci Res,* 52**,** 691-8.

YANG, F., UEDA, K., CHEN, P., ASHE, K. H. & COLE, G. M. 2000. Plaque-associated alpha-synuclein (NACP) pathology in aged transgenic mice expressing amyloid precursor protein. *Brain Res,* 853**,** 381-3.

YANG, T. & SAUVE, A. A. 2006. NAD metabolism and sirtuins: metabolic regulation of protein deacetylation in stress and toxicity. *AAPS J,* 8**,** E632-43.

YAO, J., DU, H., YAN, S., FANG, F., WANG, C., LUE, L. F., GUO, L., CHEN, D., STERN, D. M., GUNN MOORE, F. J., XI CHEN, J., ARANCIO, O. & YAN, S. S. 2011. Inhibition of amyloid-beta (Abeta) peptide-binding alcohol dehydrogenase-Abeta interaction reduces Abeta accumulation and improves mitochondrial function in a mouse model of Alzheimer's disease. *J Neurosci,* 31**,** 2313-20.

YAO, J., IRWIN, R. W., ZHAO, L., NILSEN, J., HAMILTON, R. T. & BRINTON, R. D. 2009. Mitochondrial bioenergetic deficit precedes Alzheimer's pathology in female mouse model of Alzheimer's disease. *Proc Natl Acad Sci U S A,* 106, 14670-5.

YAP, L. P., GARCIA, J. V., HAN, D. & CADENAS, E. 2009. The energy-redox axis in aging and age-related neurodegeneration. *Adv Drug Deliv Rev,* 61**,** 1283-98.

YEUNG, F., HOBERG, J. E., RAMSEY, C. S., KELLER, M. D., JONES, D. R., FRYE, R. A. & MAYO, M. W. 2004. Modulation of NF-kappaB-dependent transcription and cell survival by the SIRT1 deacetylase. *EMBO J,* 23**,** 2369-80.

YING, W. 2006. NAD+ and NADH in cellular functions and cell death. *Front Biosci,* 11**,** 3129-48.

YING, W. 2008. NAD+/NADH and NADP+/NADPH in cellular functions and cell death: regulation and biological consequences. *Antioxid Redox Signal,* 10**,** 179-206.

YING, W., CHEN, Y., ALANO, C. C. & SWANSON, R. A. 2002. Tricarboxylic acid cycle substrates prevent PARP-mediated death of neurons and astrocytes. *J Cereb Blood Flow Metab,* 22**,** 774-9.

YOO, A. S., CHENG, I., CHUNG, S., GRENFELL, T. Z., LEE, H., PACK-CHUNG, E., HANDLER, M., SHEN, J., XIA, W., TESCO, G., SAUNDERS, A. J., DING, K., FROSCH, M. P., TANZI, R. E. & KIM, T. W. 2000. Presenilin-mediated modulation of capacitative calcium entry. *Neuron,* 27**,** 561-72.

YOUNG, E., CESENA, T., MEIRI, K. F. & PERRONE-BIZZOZERO, N. I. 2002. Changes in protein kinase C (PKC) activity, isozyme translocation, and GAP-43 phosphorylation in the rat hippocampal formation after a single-trial contextual fear conditioning paradigm. *Hippocampus,* 12**,** 457-64.

YU, N., MARTIN, J. L., STELLA, N. & MAGISTRETTI, P. J. 1993. Arachidonic acid stimulates glucose uptake in cerebral cortical astrocytes. *Proc Natl Acad Sci U S A,* 90**,** 4042-6.

YU, S. W., WANG, H., POITRAS, M. F., COOMBS, C., BOWERS, W. J., FEDEROFF, H. J., POIRIER, G. G., DAWSON, T. M. & DAWSON, V. L. 2002. Mediation of poly(ADP-ribose) polymerase-1-dependent cell death by apoptosis-inducing factor. *Science,* 297**,** 259-63.

YUKIOKA, F., MATSUZAKI, S., KAWAMOTO, K., KOYAMA, Y., HITOMI, J., KATAYAMA, T. & TOHYAMA, M. 2008. Presenilin-1 mutation activates the signaling pathway of caspase-4 in endoplasmic reticulum stress-induced apoptosis. *Neurochem Int,* 52**,** 683-7.

ZHANG, F., WANG, S., GAN, L., VOSLER, P. S., GAO, Y., ZIGMOND, M. J. & CHEN, J. 2011. Protective effects and mechanisms of sirtuins in the nervous system. *Prog Neurobiol,* 95**,** 373-95.

ZHANG, H., GO, Y. M. & JONES, D. P. 2007a. Mitochondrial thioredoxin-2/peroxiredoxin-3 system functions in parallel with mitochondrial GSH system in protection against oxidative stress. *Arch Biochem Biophys,* 465**,** 119-26.

ZHANG, S., LIN, Y., KIM, Y. S., HANDE, M. P., LIU, Z. G. & SHEN, H. M. 2007b. c-Jun N-terminal kinase mediates hydrogen peroxide-induced cell death via sustained poly(ADP-ribose) polymerase-1 activation. *Cell Death Differ,* 14**,** 1001-10.

ZHANG, X. M., CAI, Y., XIONG, K., CAI, H., LUO, X. G., FENG, J. C., CLOUGH, R. W., STRUBLE, R. G., PATRYLO, P. R. & YAN, X. X. 2009. Beta-secretase-1 elevation in transgenic mouse models of Alzheimer's disease is associated with synaptic/axonal pathology and amyloidogenesis: implications for neuritic plaque development. *Eur J Neurosci,* 30**,** 2271-83.

ZHAO, W. Q. & ALKON, D. L. 2001. Role of insulin and insulin receptor in learning and memory. *Mol Cell Endocrinol,* 177**,** 125-34.

ZHOU, Q., LAM, P. Y., HAN, D. & CADENAS, E. 2008. c-Jun N-terminal kinase regulates mitochondrial bioenergetics by modulating pyruvate dehydrogenase activity in primary cortical neurons. *J Neurochem,* 104**,** 325-35.

ZHOU, Q., LAM, P. Y., HAN, D. & CADENAS, E. 2009. Activation of c-Jun-N-terminal kinase and decline of mitochondrial pyruvate dehydrogenase activity during brain aging. *FEBS Lett,* 583**,** 1132-40.

ZHU, X., LEE, H. G., CASADESUS, G., AVILA, J., DREW, K., PERRY, G. & SMITH, M. A. 2005. Oxidative imbalance in Alzheimer's disease. *Mol Neurobiol,* 31**,** 205-17.

ZHU, X., LEE, H. G., PERRY, G. & SMITH, M. A. 2007. Alzheimer disease, the two-hit hypothesis: an update. *Biochim Biophys Acta,* 1772**,** 494-502.

ZHU, X., RAINA, A. K., LEE, H. G., CASADESUS, G., SMITH, M. A. & PERRY, G. 2004. Oxidative stress signalling in Alzheimer's disease. *Brain Res,* 1000**,** 32-9.

ZIEGLER, G. A. & SCHULZ, G. E. 2000. Crystal structures of adrenodoxin reductase in complex with NADP+ and NADPH suggesting a mechanism for the electron transfer of an enzyme family. *Biochemistry,* 39**,** 10986-95.

Appendices

Appendix 1. Mini-PROTEAN Tetra Cell (Electrophoresis) protocol (Bio-rad)

Section 4
Reagent Preparation and Stock Solutions

4.1 Volumes Required Per Gel

The volumes listed are required to completely fill a gel cassette. Amounts may be adjusted depending on the application (with or without comb, with or without stacking gel, etc.).

Gel Thickness (mm)	Volume (ml)
0.5	2.8
0.75	4.2
1.0	5.6
1.5	8.4

Note: 10 ml of monomer solution is sufficient for two stacking gels of any thickness.

4.2 SDS-PAGE (Laemmli)[1] Buffer System

Stock Solutions and Buffers

1. Acrylamide/Bis (30% T, 2.67% C)

87.6 g	acrylamide	(29.2 g/100 ml)
2.4 g	N'N'-bis-methylene-acrylamide	(0.8 g/100 ml)

   Make to 300 ml with deionized water. Filter and store at 4°C in the dark (30 days maximum).
   or use:
   Preweighed acrylamide/bis, 37.5:1 mixture (30%T, 2.67% C)
   (Bio-Rad catalog #161-0125, 150 g)
   30% acrylamide/bis solution, 37.5:1 mixture (30%T, 2.67% C)
   (Bio-Rad catalog #161-0158, 500 ml)
   (Bio-Rad catalog #161-0159, 2 x 500 ml)

2. 10% (w/v) SDS
   Dissolve 10 g SDS in 90 ml water with gentle stirring and bring to 100 ml with deionized water. Alternatively, 10% SDS solution (250 ml) can be used (Bio-Rad catalog #161-0416).

3. 1.5 M Tris-HCl, pH 8.8

27.23 g	Tris base (18.15 g/100 ml)
80 ml	deionized water

   Adjust to pH 8.8 with 6 N HCl. Bring total volume to 150 ml with deionized water and store at 4°C. Alternatively, 1.5 M Tris-HCl, pH 8.8 (1 L) premixed buffer can be used (Bio-Rad catalog #161-0798).

4. 0.5 M Tris-HCl, pH 6.8

6 g	Tris base
60 ml	deionized water

   Adjust to pH 6.8 with 6 N HCl. Bring total volume to 100 ml with deionized water and store at 4°C. Alternatively, 0.5 M Tris-HCl, pH 6.8 (1 L) premixed buffer can be used (Bio-Rad catalog #161-0799).

5. Sample Buffer (SDS Reducing Buffer)

3.55 ml	deionized water
1.25 ml	0.5 M Tris-HCl, pH 6.8
2.5 ml	glycerol
2.0 ml	10% (w/v) SDS
0.2 ml	0.5% (w/v) Bromophenol Blue
9.5 ml	Total volume

Store at room temperature.

Use: Add 50 µl β-mercaptoethanol to 950 µl sample buffer prior to use. Dilute the sample at least 1:2 with sample buffer and heat at 95°C for 4 minutes.

6. 10x Electrode (Running) Buffer, pH 8.3 (makes 1 L)

30.3 g	Tris base
144.0 g	glycine
10.0 g	SDS

Dissolve and bring total volume up to 1,000 ml with deionized water. Do not adjust pH with acid or base. Store at 4°C. If precipitation occurs, warm to room temperature before use. Alternatively, electrophoresis running buffer 10x Tris/glycine/SDS, 5 L cube (Bio-Rad catalog #161-0772) can be used.

Use: Dilute 50 ml of 10x stock with 450 ml deionized water for each electrophoresis run. Mix thoroughly before use.

7. 10% (w/v) APS (fresh daily)
    100 mg   ammonium persulfate
    Dissolve in 1 ml of deionized water.

Gel Formulations (10 ml)

1. Prepare the monomer solution by mixing all reagents except the TEMED and 10% APS. Degas the mixture for 15 minutes.

Percent Gel	DDI H$_2$O (ml)	30% Degassed Acrylamide/Bis (ml)	Gel Buffer* (ml)	10% w/v SDS (ml)
4%	6.1	1.3	2.5	0.1
5%	5.7	1.7	2.5	0.1
6%	5.4	2.0	2.5	0.1
7%	5.1	2.3	2.5	0.1
8%	4.7	2.7	2.5	0.1
9%	4.4	3.0	2.5	0.1
10%	4.1	3.3	2.5	0.1
11%	3.7	3.7	2.5	0.1
12%	3.4	4.0	2.5	0.1
13%	3.1	4.3	2.5	0.1
14%	2.7	4.7	2.5	0.1
15%	2.4	5.0	2.5	0.1
16%	2.1	5.3	2.5	0.1
17%	1.7	5.7	2.5	0.1

* Resolving Gel Buffer – 1.5 M Tris-HCl, pH 8.8

* Stacking Gel Buffer – 0.5 M Tris-HCl, pH 6.8

2. Immediately prior to pouring the gel, add:

For 10 ml monomer solution:
Resolving gel: 50 µl 10% APS and
                        5 µl TEMED
Stacking gel: 50 µl 10% APS and
                        10 µl TEMED
Swirl gently to initiate polymerization.

Note: Prepare any desired volume of monomer solution by using multiples of the 10 ml recipe. The volumes of APS and TEMED must be adjusted accordingly.

Warning: The catalyst concentration is very important! Webbing and incomplete well formulation can result from inaccurate catalyst concentration.

4.3 Discontinuous Native PAGE (Ornstein-Davis)[2]

Stock Solutions and Buffers

1. Acrylamide/Bis (30% T, 2.67% C)

    87.6 g   acrylamide (29.2 g/100 ml)
    2.4 g   N'N'-bis-methylene-acrylamide (0.8 g/100 ml)

    Make to 300 ml with deionized water. Filter and store at 4°C in the dark (30 days maximum).
    or, use:
    Preweighed acrylamide/bis, 37.5:1 mixture
    (Bio-Rad catalog #161-0125, 150 g)
    30% acrylamide/bis solution, 37.5:1 mixture
    (Bio-Rad catalog #161-0158, 500 ml)
    (Bio-Rad catalog #161-0159, 2 x 500 ml)

2. 1.5 M Tris-HCl, pH 8.8

    27.23 g   Tris base (18.15 g/100 ml)
    80 ml   deionized water

    Adjust to pH 8.8 with 6 N HCl. Bring total volume up to 150 ml with deionized water and store at 4°C. Alternatively, 1.5 M Tris-HCl, pH 8.8 (1 L) premixed buffer can be used (Bio-Rad catalog #161-0798).

3. 0.5 M Tris-HCl, pH 6.8

    6 g   Tris base
    60 ml   deionized water

    Adjust to pH 6.8 with 6 N HCl. Bring total volume up to 100 ml with deionized water and store at 4°C. Alternatively, 0.5 M Tris-HCl, pH 6.8 (1 L) premixed buffer can be used (Bio-Rad catalog #161-0799).

4. Sample Buffer

    5.55 ml   deionized water
    1.25 ml   0.5 M Tris-HCl, pH 6.8
    3.0 ml   glycerol
    0.2 ml   0.5% (w/v) Bromophenol Blue
    10.0 ml   Total volume

    Store at room temperature.
    Use: Dilute the sample at least 1:2 with sample buffer and heat at 95°C for 4 minutes.

5. 10x Electrode (Running) Buffer, pH 8.3

> 30.3 g   Tris base (15 g/L)
> 144.1 g   glycine (72 g/L)

Bring total volume up to 1,000 ml with deionized water. Do not adjust pH. Alternatively, electrophoresis running buffer 10x Tris/Glycine, 1 L (Bio-Rad catalog #161-0734) can be used.

Usage: Dilute 100 ml of 10x stock with 900 ml deionized water for each electrophoresis run.

Gel Formulations (10 ml)

1. Prepare the monomer solution by mixing all reagents except the TEMED and 10% APS. Degas the mixture for 15 minutes.

Percent Gel	30% Degassed DDI H_2O (ml)	Acrylamide/Bis (ml)	Gel Buffer* (ml)
4%	6.2	1.3	2.5
5%	5.8	1.7	2.5
6%	5.5	2.0	2.5
7%	5.2	2.3	2.5
8%	4.8	2.7	2.5
9%	4.5	3.0	2.5
10%	4.2	3.3	2.5

* Resolving Gel Buffer – 1.5 M Tris-HCl, pH 8.8

* Stacking Gel Buffer – 0.5 M Tris-HCl, pH 6.8

2. Immediately prior to pouring the gel, add:

50 ml APS and
TEMED (5 µl for resolving gels; 10 µl TEMED for stacking gels)
Swirl gently to initiate polymerization.
Note: Prepare any desired volume of monomer solution by using multiples of the 10 ml recipe. The volumes of APS and TEMED must be adjusted accordingly.

|	Aβ(1-42) / DMSO	Aβ(1-42) / HEPES	Aβ(1-42) / F12	Aβ(1-40) / HEPES
6h	>0.05	>0.05	>0.05	>0.05
24h	<0.0001	>0.05	<0.05	>0.05
48h	<0.0001	>0.05	<0.0001	>0.05
72h	<0.0001	>0.05	<0.0001	>0.05
96h	<0.0001	>0.05	<0.01	>0.05

Appendix 2   Two-way ANOVA followed by Bonferroni post-test (Graphpad Prism). Aggregation of 20μM Aβ(1-42) and Aβ(1-40) preparations using ThT fluorescence.

|	Aβ(1-42) / DMSO	Aβ(1-42) / HEPES	Aβ(1-42) / F12	Aβ(1-40) / HEPES
6h	<0.001	>0.05	<0.0001	>0.05
24h	<0.0001	>0.05	<0.0001	<0.01
48h	<0.0001	>0.05	<0.0001	>0.05
72h	<0.0001	<0.001	<0.0001	>0.05
96h	<0.0001	<0.05	<0.001	>0.05

Appendix 3   Two-way ANOVA followed by Bonferroni post-test (Graphpad Prism). Aggregation of 2µM Aβ(1-42) and Aβ(1-40) preparations using ThT fluorescence.

	Aβ(1-42) / DMSO	Aβ(1-42) / HEPES	Aβ(1-42) / F12	Aβ(1-40) / HEPES
6h	>0.05	>0.05	>0.05	>0.05
24h	>0.05	>0.05	>0.05	>0.05
48h	>0.05	>0.05	>0.05	>0.05
72h	<0.05	>0.05	>0.05	>0.05
96h	>0.05	>0.05	<0.05	>0.05

Appendix 4   Two-way ANOVA followed by Bonferroni post-test (Graphpad Prism). Aggregation of 0.2μM Aβ(1-42) and Aβ(1-40) preparations using ThT fluorescence.
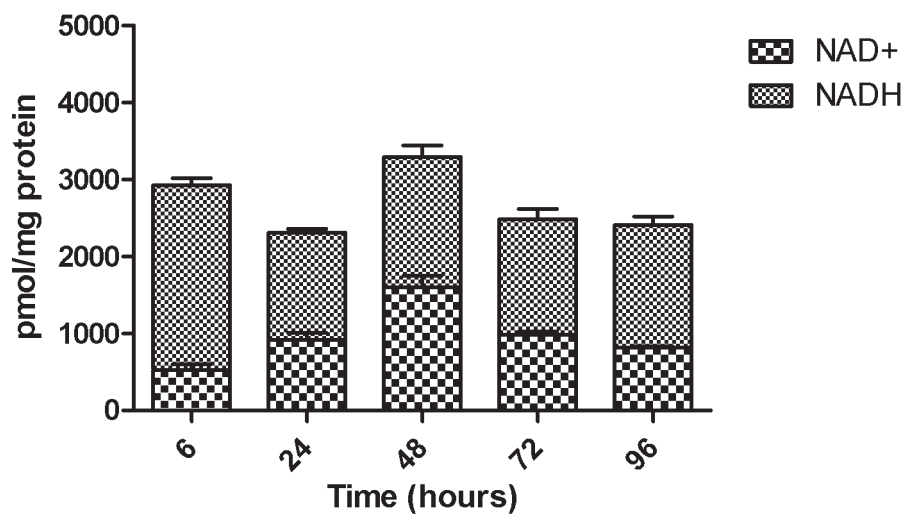
Appendix 5 NAD+ and NADH inside control NT2.N/A cultures.
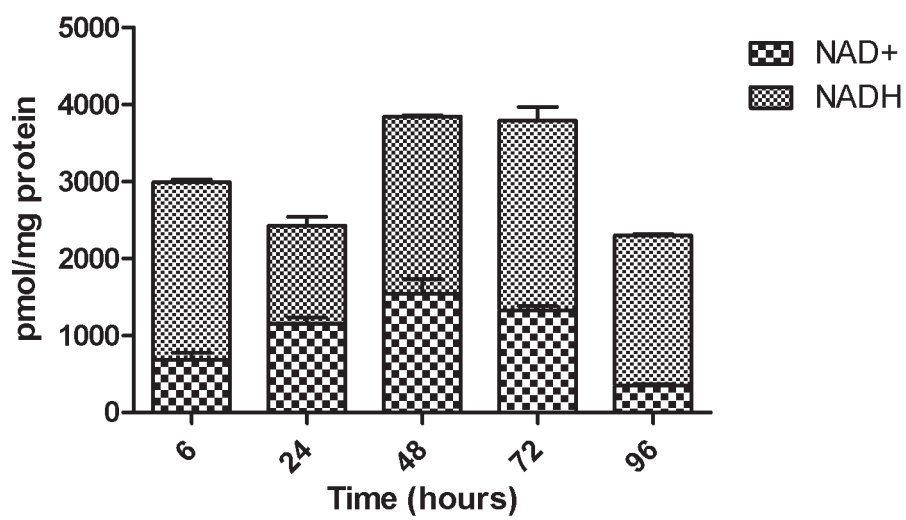
Appendix 6 NAD+ and NADH levels inside the cells following treatment of NT2.N/A with 2µM Aβ.

Appendix 7. CellTiter-Glo® Luminescent Cell Viability Assay (ATP)

Aston University

Illustration removed for copyright restrictions

Page removed for copyright restrictions.

Appendix 8. Gene table for Human Alzheimer's Disease RT² Profiler™ PCR Array

| Symbol	Well	Fold Difference	T-TEST	Fold Up- or Down-Regulation
		Test Sample /Control Sample	p value	Test Sample /Control Sample
A2M	A01	2.29	0.0319	2.29
ABCA1	A02	0.75	0.4299	-1.34
ACHE	A03	0.87	0.6613	-1.15
ADAM9	A04	1.75	0.0123	1.75
APBA1	A05	1.18	0.6563	1.18
APBA3	A06	0.82	0.4701	-1.22
APBB1	A07	1.00	0.9942	-1.00
APBB2	A08	3.50	0.0306	3.50
APH1A	A09	1.22	0.2494	1.22
APLP1	A10	1.33	0.7060	1.33
APLP2	A11	1.53	0.4551	1.53
APOA1	A12	0.45	0.4840	-2.22
APOE	B01	0.89	0.8389	-1.13
APP	B02	1.27	0.5442	1.27
NAE1	B03	1.18	0.5426	1.18
BACE1	B04	2.32	0.0318	2.32
BACE2	B05	1.10	0.7037	1.10
BCHE	B06	0.30	0.0487	-3.29
BDNF	B07	1.34	0.6582	1.34
CASP3	B08	0.99	0.9686	-1.01
CASP4	B09	4.76	0.0222	4.76
CDC2	B10	0.51	0.2628	-1.98
CDK5	B11	1.70	0.1146	1.70
CDKL1	B12	1.80	0.4642	1.80
CHAT	C01	1.11	0.8317	1.11
CLU	C02	0.87	0.6690	-1.15
CTSB	C03	1.15	0.3800	1.15
CTSC	C04	1.01	0.9690	1.01
CTSD	C05	0.65	0.2725	-1.54
CTSG	C06	0.44	0.4181	-2.26
CTSL1	C07	1.40	0.7344	1.40
EP300	C08	1.77	0.3431	1.77
ERN1	C09	0.45	0.2607	-2.20
GAP43	C10	10.13	0.0433	10.13
GNAO1	C11	1.86	0.1740	1.86
GNAZ	C12	1.66	0.0180	1.66
GNB1	D01	1.10	0.7504	1.10
GNB2	D02	1.07	0.8499	1.07
GNB4	D03	1.18	0.4869	1.18
GNB5	D04	1.00	0.9925	-1.00
GNG10	D05	1.02	0.9263	1.02
GNG11	D06	0.79	0.6561	-1.27
GNG3	D07	1.57	0.1256	1.57

GNG4	D08	1.76	0.2165	1.76
GNG5	D09	1.06	0.6924	1.06
GNG7	D10	0.68	0.0893	-1.48
GNG8	D11	**2.27**	**0.0184**	**2.27**
GNGT1	D12	1.02	0.9623	1.02
GNGT2	E01	0.42	0.2975	-2.39
GSK3A	E02	0.79	0.5520	-1.27
GSK3B	E03	**3.41**	**0.0458**	**3.41**
HSD17B10	E04	1.01	0.9243	1.01
IDE	E05	**3.23**	**0.0038**	**3.23**
IL1A	E06	0.92	0.8771	-1.09
INS	E07	1.12	0.9042	1.12
INSR	E08	1.56	0.2286	1.56
LPL	E09	**3.54**	**0.0454**	**3.54**
LRP1	E10	0.90	0.7607	-1.11
LRP6	E11	1.65	0.1952	1.65
LRP8	E12	1.02	0.9547	1.02
MAP2	F01	1.73	0.1401	1.73
MAPT	F02	1.67	0.1709	1.67
MPO	F03	0.42	0.3312	-2.36
NCSTN	F04	1.11	0.8218	1.11
PKP4	F05	0.86	0.5506	-1.16
PLAT	F06	1.44	0.2120	1.44
PLAU	F07	1.00	0.9993	1.00
PLG	F08	0.33	0.1175	-3.02
PRKCA	F09	1.00	0.9987	1.00
PRKCB	F10	1.00	0.9940	1.00
PRKCD	F11	0.63	0.2562	-1.59
PRKCE	F12	**2.12**	0.0897	**2.12**
PRKCG	G01	0.84	0.7726	-1.20
PRKCI	G02	1.61	0.0949	1.61
PRKCQ	G03	0.99	0.9796	-1.01
PRKCZ	G04	1.03	0.8931	1.03
PSEN1	G05	1.17	0.6064	1.17
PSEN2	G06	0.77	0.3168	-1.30
SERPINA3	G07	1.52	0.5953	1.52
SNCA	G08	**2.13**	**0.0165**	**2.13**
SNCB	G09	0.86	0.7436	-1.17
UBQLN1	G10	1.15	0.6545	1.15
UQCRC1	G11	0.71	0.0768	-1.41
UQCRC2	G12	0.88	0.3827	-1.14
B2M	H01	1.00	0.9789	-1.00
HPRT1	H02	0.65	**0.0241**	-1.53
RPL13A	H03	1.09	0.6664	1.09
GAPDH	H04	0.88	0.2542	-1.14
ACTB	H05	1.60	**0.0174**	1.60
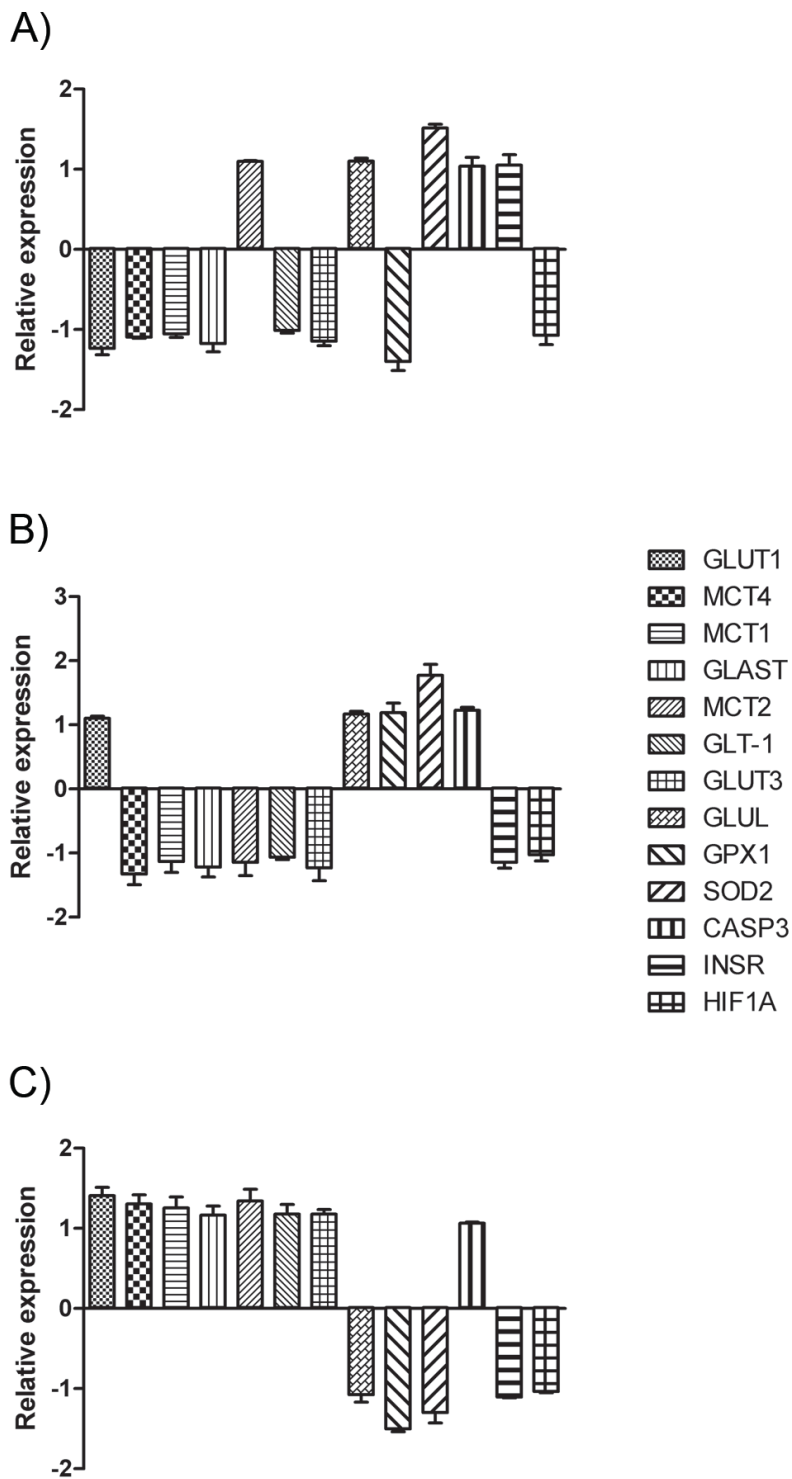
Appendix 9   Gene expression in NT2.N/A cultures following treatment with 20µM Aβ(1-42) for A) 48h, B) 72h, C) 96h. Results are expressed as the average fold change ± SEM (n=3) and considered significant above 2-fold change.
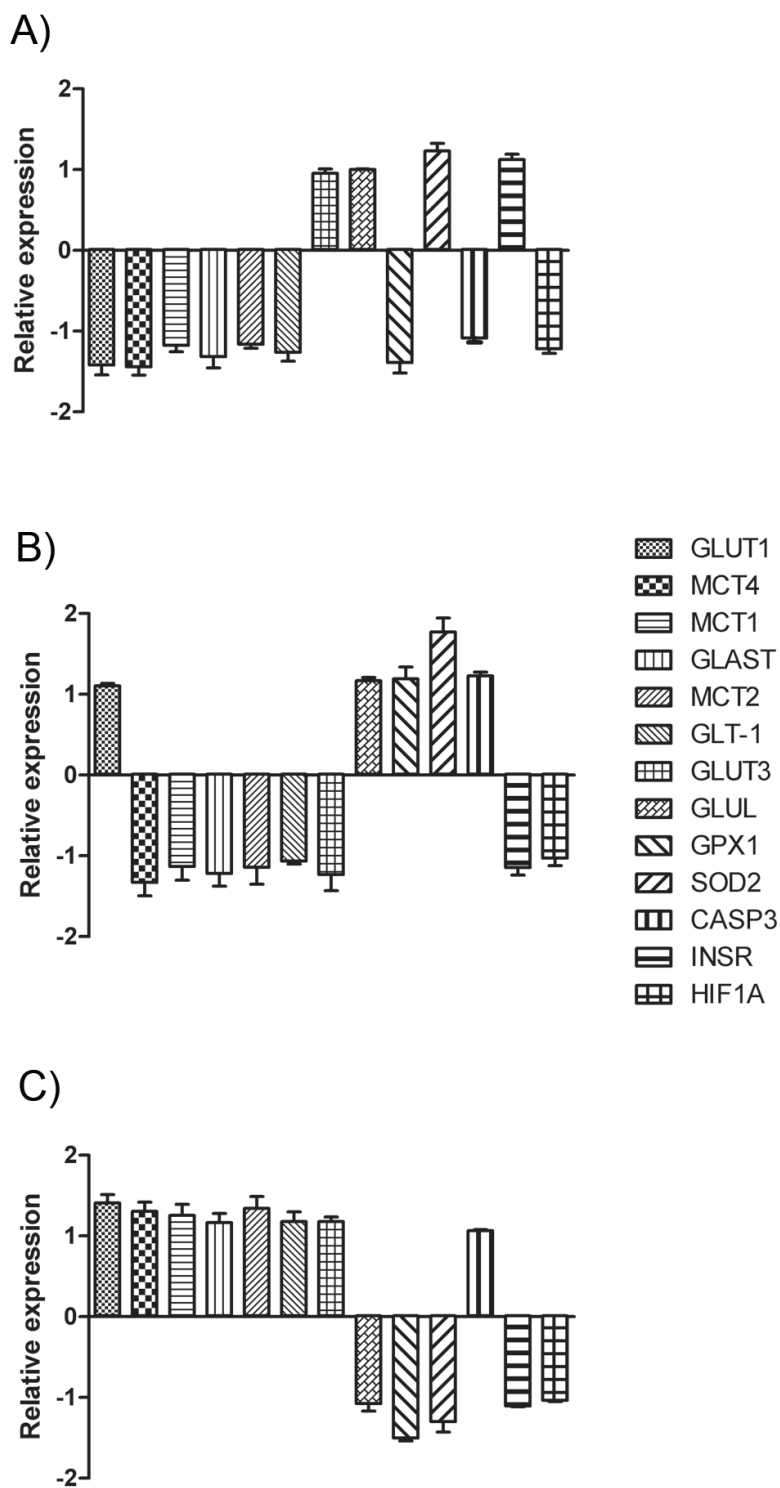
Appendix 10 Gene expression in NT2.N/A cultures following treatment with 2μM Aβ(1-42) for A) 48h, B) 72h, C) 96h. Results are expressed as the average fold change ± SEM (n=3) and considered significant above 2-fold change.
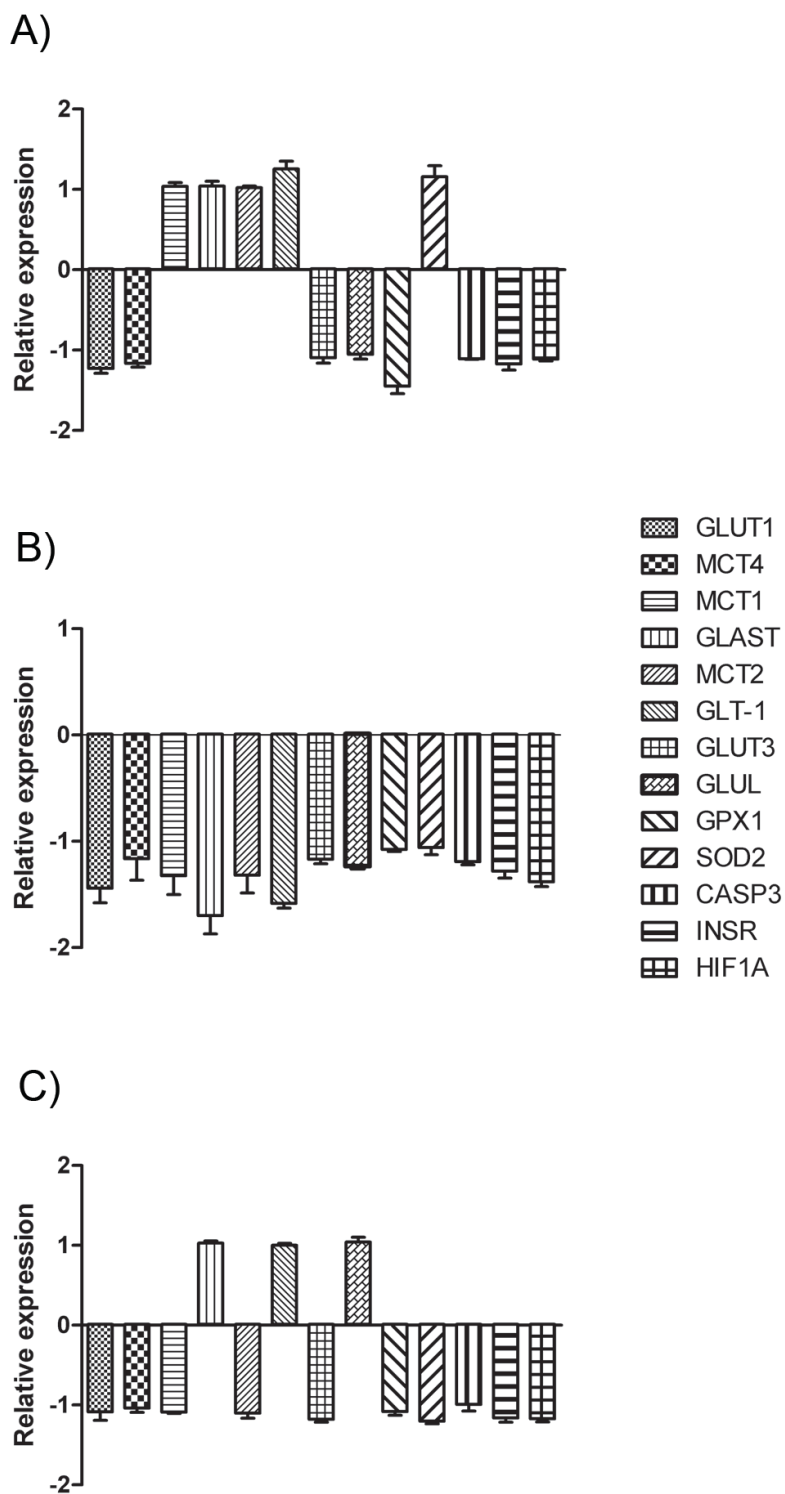
Appendix 11 Gene expression in NT2.N/A cultures following treatment with 0.2μM Aβ(1-42) for A) 48h, B) 72h, C) 96h. Results are expressed as the average fold change ± SEM (n=3) and considered significant above 2-fold change.